Origin and morphogenesis of the murine spleen

Sally Burn

PhD by Research

University of Edinburgh

2007

Declaration

This thesis has been entirely composed by me. The experiments were performed solely by me except where stated. The work has not been submitted for any other degree or professional qualification.

Sally Burn, April 2007

Acknowledgments

The first person to thank is Bob Hill, my supervisor, for being eternally optimistic. Thanks also in addition Bob for efficiently helping me to remove wholly entirely superfluous and unnecessary words, phrases, and paragraphs, and to help and assist in enabling me to say things, concepts, and general ideas succinctly and concisely, without the need for over-clarification and repetition and repetition or needless prolongation of sentences.

On a day-to-day lab basis, thanks must go to Laura Lettice, who knows everything lab-related. Thank you also for: nutrients during the write-up meltdown implosion experience, gossip, and the most fantastic pink birthday ever! ☺ Big thanks as well to Marit Boot, my partner in gut culture crime, who also did the initial work on how to get guts to enjoy being in culture. Thanks for your words of wisdom during the write-up process, and for humouring me when I jammed an eyelash into a gut – "to see what might happen". Now if only I'd removed all the mascara first…

Finishing off the lab-related acknowledgments, thanks go to Carlo DeAngelis (OPT magic and gut culture dissection assistance) and Rob Watson (for introducing me to the world of guts during my MSc). On the transgenic side of things, thank you to Paul Devenney for his microinjection wizardry and similarly thanks to Simon Heaney and Brendan Doe for theirs. Thank you to Janice and the rest of the Transgenic Unit for feeding the kids. Likewise, thanks to the staff of the BRF for feeding my other mice. Thank you to Peter Hohenstein/Dirk-Jan Kleinjan for the *gl-Cre* mice and Ian Jackson/Alan Hart for the *Rwhs* mice. I'd also like to thank Peter and Nick (Hastie) for waiting around for me and being so understanding during my protracted "proof-reading and getting around to handing it in!" period. Thank you.

So that just about covers my words for the lab, other than to say thanks to the rest of C3 for entertainment, reagents, and general chit-chat. All my bench-mates have been fantastic too, especially Lee. Special big-up to all office-mates, past and present, especially those who experienced the West Wing "office" – Pam, Heather, Karen, Carol. Around the rest of the building thanks go to Technical Services for providing clean things, Stephen and Stuart for sequencing, and Paul Perry for making the microscopes work. Also, Paul and Sandy for easing thesis printing traumas.

Non-work mentions go to the student population of the HGU, particularly the Midori Club, and of course that human elite: those who inhabited 2F2, 21 West Maitland Street (Andy, Joel, Anne, James, Hannah, Matthias – though clearly not all at once). Hannah: you are still my flatmate, and a fantastic one at that. Thanks for keeping an eye on me and cheering me up. ☺ Anne: you are now in Houston. Ha, ha,

bet that's sweaty. You were a great flatmate and are a brilliant friend and I hope to get over there to see you soon. Go you big red fire-engine.

Outside of science (what?! Such a place exists?!) I'd like to thank the following for keeping me cheery and reminding me that even though that PCR may have failed for the *n*th time, there is still dancing to be done and good times to be had: Amy (provider of cakes!), Debbie (Egg partner extraordinaire!), Neil, Nicci and the rest of the Nottingham contingent. Special thanks go to Nat for services to keeping me sane and de-frazzling me more times than I'd care to remember. And finally, "gorangutan"-sized thanks to Venkat for psychotherapy and words of wisdom during the write-up period from an old person who's already been there. Sometime around 1792 I think. I can't believe you read it all so quickly; I owe you. Also, as an addendum: thank you so much for helping with the printing – you star! ☺

Last, but so unbelievably least, are my parents. I'm biased, but I think they're the best in the world. Thanks firstly for putting up with my extended education, and secondly for being so supportive at every stage of it. I know you think I never take your advice to "go home!", but I do sometimes listen and you're both such a big help. ☺ Thank you Mam for teaching me the ultimate wisdom: that any work-based disappointment can be instantly eased by purchasing shoes, bags, and other such pretty things. Thank you Dad for your wonderful words of encouragement and advice. I was particularly inspired by your insightful comments in the last weeks before I handed in: "think of your thesis as being like a nice chocolate. You put it in your mouth a good few months ago and it tasted really nice and you liked it, but now it's worked its way through and it's just hanging around somewhere near your bowels. You just need that final push to get rid of it". Crude, yes, but oh so true and it strangely motivated me....

Whoops, gone over the word limit again.

"Tell me your secrets
And ask me your questions
Oh let's go back to the start...
...I was just guessing
At numbers and figures
Pulling your puzzles apart
Questions of science
Science and progress
Do not speak as loud as my heart"
- The Scientist (Coldplay)

Abstract

Between E9.5 and E12.5 of mouse embryonic development the gut undergoes a series of changes such that it is transformed from a midline endodermal tube to an asymmetric patterned system. The need to understand the processes underlying this patterning cannot be underestimated as gut defects are the most common human congenital malformations.

This thesis establishes methods to investigate early spleen development in the mouse embryo. An expression analysis of early *Nkx2-5* expression is reported, along with the finding that *Nkx2-5* may be the earliest marker of splenic precursors in the mouse. Expression of *Nkx2-5* is also shown for the first time to overlap considerably with that of *Bapx1* (*Nkx3-2*) - a major gut development gene upstream of *Nkx2-5*. An *in silico* analysis of the evolutionary conserved regions upstream of *Nkx2-5* is presented along with the establishment and analysis of stable transgenic reporter lines expressing *LacZ* under the control of an *Nkx2-5* gut regulatory sequence (*NGRS*). *NGRS* confers spleen, posterior stomach, and pyloric sphincter expression, with very little of the cardiac expression associated with endogenous *Nkx2-5*. This enhancer is thus ideal for gut studies, providing a tool for directing gut-specific expression and genetic manipulations. *NGRS* was also found not to require *Bapx1* for its activity. Finally, *NGRS* is demonstrated to have the potential to mark abnormal spleen development, in a previously unreported splenic mutant: the *Rwhs* mutant.

Potential uses for *NGRS* are explored; two different strategies to generate a gut-specific tamoxifen-inducible lineage tracing system are reported. These were unsuccessful and, consequently, an alternative approach was taken to marking and following spleen development, using *NGRS-LacZ* in an organ culture system. Data generated from these experiments shed some light on how the E11.5 spleen develops, providing evidence for migration of splenic precursors along the stomach, and suggesting that an inhibitory "anchor" effect is normally exerted by the posterior spleno-pancreatic mesenchyme, disruption of which permits precocious spleen development. Attempts to investigate the existence of a spleen cell chemoattractant in the anterior stomach are also reported.

Finally, an analysis of the role of Wnt signalling in development of the spleno-pancreatic region is presented. A preliminary report of ectopic *Wnt3* and *Wnt8a* expression in the abnormal posterior stomach of the *Bapx1* $^{-/-}$ gut was investigated and found not to be supported. However, analysis of wild type guts revealed that canonical Wnt signalling is active in the developing spleen at E11.5, E12.5 and E14.5. A subsequent expression screen revealed that a number of *Wnt* and *Fzd* genes are expressed in the E14.5 spleen.

Table of contents

List of figures

List of tables

Abbreviations

°C	Degrees Celsius
µl	Microlitres
µg	Micrograms
µM	Micromolar
AIP	Anterior Intestinal Portal
AP	Alkaline Phosphatase
AP	Anterior-posterior
AR	Activating Region
ASD	Atrial Septal Defect
ASMP	Anterior Splanchnic Mesodermal Plate
AV	Atrioventricular
BAT-gal	β-catenin Activated Transgene -galactosidase
BCIP	5-Bromo-4-chloro-3-indolyl-phosphate, 4-toluidine salt
bp	Base Pair
BRF	Biomedical Research Facility
BSA	Bovine Serum Albumin
CIP	Calf Intestinal Phosphatase
CIP	Caudal Intestinal Portal
dATP	Deoxyadenosine Triphosphate
dCTP	Deoxycytidine Triphosphate
dGTP	Deoxyguanosine Triphosphate
dH_2O	Deionised water
DEPC	Diethylpyrocarbonate
DIG	Digoxygenin
DMEM	Dulbecco's Modified Eagle's Medium
DMF	N,N-dimethylformamide
DMSO	Dimethyl sulphoxide
dNTP	Deoxynucleotide
DORV	Double outlet in/of the right ventricle
dpc	days post coitum
dTTP	Deoxythymidine Triphosphate
DV	Dorsal-ventral
E	Embryonic Day
ECR	Evolutionary Conserved Region
EM	Epithelial-mesenchymal

ENS	Enteric Nervous System
ER	Oestrogen Receptor
ERT	Oestrogen Receptor (human), Tamoxifen inducible
ERT2	Oestrogen Receptor (human), Tamoxifen inducible 2
ERTM	Oestrogen Receptor (mouse), Tamoxifen inducible
ES	Embryonic Stem
EtOH	Ethanol
F	Forward
FCS	Foetal Calf Serum
Fzd	Frizzled
g	Grams
GDNF	Glial cell Derived Neurotrophic Factor
GFP	Green Fluorescent Protein
GI	Gastrointestinal
HGU	Human Genetics Unit
HPRT	Hypoxanthine Guanine Phosphoribosyltransferase
hr	Hour
ICC	Interstitial Cell of Cajal
IPTG	Isopropyl-β-d-thiogalactopyranoside
IR	Inhibitory Region
kb	Kilobase
l	Litres
LBD	Ligand Binding Domain
LPM	Lateral Plate Mesoderm
LR	Left-right
M	Molar
MAdCAM-1	Mucosal Addressin Cell Adhesion Molecule-1
Mb	Megabase
MCS	Multiple Cloning Site
MeOH	Methanol
min	Minute
ml	Millilitres
Mm	Millimolar
NBT	Nitroblue Tetrazolium chloride
ng	Nanograms
NGRS	*Nkx2.5* Gut Regulatory Sequence
nt	Nucleotide
OHT	4-hydroxytamoxifen
OPT	Optical Projection Tomography

PBS	Phosphate Buffered Saline
PCR	Polymerase Chain Reaction
PFA	Paraformaldehyde
R	Reverse
R26R	ROSA26 reporter
rpm	Revolutions per minute
RT	Reverse Transcriptase
RT	Room Temperature
RT-PCR	Reverse Transcription PCR (Polymerase Chain Reaction)
sFRP	Secreted Frizzled-Related Protein
SMP	Splanchnic Mesothelial Plate
t0	Time = 0 hours
t24	Time = 24 hours
t48	Time = 48 hours
TGU	Transgenic Unit
U	Unit (of enzyme activity)
UTR	Untranslated region
UV	Ultraviolet
VSD	Ventricular Septal Defect
ZRS	ZPA (Zone of Polarising Activity) Regulatory Sequence

CHAPTER 1

Introduction

"The student of Nature wonders the more and is astonished the less, the more conversant he becomes with her operations; but of all of the perennial miracles she offers to his inspection, perhaps the most worthy of admiration is the development of a plant or of an animal from its embryo"
– Thomas Henry Huxley

1.1 Introduction to thesis

"Compared to readily accessible organs such as the limb, or to organs such as the heart and pancreas that are the focus of resourceful charities, the gut has been left behind. However, it is clear... that the many fascinating developmental, evolutionary, and medical aspects of the gut will continue to attract much attention and generate pertinent information"

(Stainier, 2005)

The gastrointestinal (GI) tract is a conserved feature of multicellular animals; its derivate organs are essential for a variety of processes including digestion, respiration, haematopoiesis, and immunity. Some aspects of the patterning of the gut organ primordia and of the subsequent processes of organogenesis are well understood; there are, however, gaps in our knowledge of how this essential system develops. The need to fill these gaps cannot be underestimated as gut defects present a major disease burden and are the most common human congenital malformations (de Santa et al., 2002). Congenital gut defects cause considerable perinatal morbidity and can prove lethal.

The early development of the gut provides an opportunity to view an unparalleled array of fundamental morphogenetic processes. In the 72-hour-period between E9.5 (embryonic day 9.5) and E12.5 of mouse development the gut undergoes a series of complex and rapid changes; as a result the midline uniform gut tube is transformed into an asymmetric patterned system containing the primordia of the accessory organs.

Important developmental phenomena such as epithelial-mesenchymal (EM) interaction, axial patterning, cell migration, and budding morphogenesis are documented in the gut. Many major developmental molecules have been shown to be required for gut development; information collected about their roles in the gut is extremely important as many of these factors also have roles in other aspects of vertebrate development. Yet there still remain many unanswered questions about early gut development, particularly with regard to the spleen. This thesis describes attempts through a variety of methods to provide information on, and tools for, the further study of early spleen and, to a lesser extent, pyloric sphincter development in the mouse embryo.

1.2 Overview of gut development

1.2.1 Early gut development

The GI tract and its accessory organs develop from a sheet, and subsequently a tube, of endoderm lying along the anterior-posterior (AP) axis of the embryo (for an excellent primer see (Roberts, 1999)). The anterior end of this endodermal sheet folds back on itself ventrally at the start of mouse somitogenesis (~E8.0), thus forming the foregut pocket with the anterior intestinal portal (AIP) at its leading edge. The AIP elongates such that folding continues in a posterior direction until ~E8.5 when the AIP reaches the yolk stalk (umbilicus) and meets the caudal intestinal portal (CIP) which has travelled from the posterior of the embryo. The CIP invaginates at a later stage than the AIP (at ~E8.5). The enclosed space posterior to the CIP constitutes the hindgut pocket.

Convergence of the AIP and CIP is aided by turning of the mouse embryo at E8.5-9.0. Apart from the turning, the process of gut folding shows evolutionary conservation and is remarkably similar between mouse and chick, though *Xenopus* gut folding is somewhat different (Grapin-Botton and Melton, 2000). Closure of the gut tube is complete once the AIP and CIP make contact. The ventral part of the completed gut tube is composed of endodermal cells which migrated with the AIP and CIP, whereas the dorsal portion is comprised of midline endoderm which remained relatively static. The lateral walls of the tube arise from folding of the endoderm which underlies the lateral plate mesoderm (LPM); this is again facilitated by turning.

Following closure of the tube, the multipotent stem cells within the gut endoderm differentiate and become organised into the major organ precursors. The endodermal component of the stomach, pancreas, intestine, lungs, liver, bladder and thyroid all originate from this tube. Correct development of the gut is hence essential for numerous vital processes.

The majority of the gut tube lies posterior to the branchial arches and becomes surrounded by splanchnic mesoderm, derived from the LPM (Hogan and Zaret, 2002; Funayama et al., 1999). This splanchnic mesoderm undergoes differentiation into

mesenchyme which plays signalling roles during gut morphogenesis. The splanchnic mesoderm and the mesenchyme derived from it are the main tissues of interest in this thesis. The region of gut tube that is focussed upon encompasses the stomach, pyloric sphincter, pancreatic buds, and spleen. The development of these organs is described in **Sections 1.3-1.6**. **Figure 1.1** depicts the stages of interest in mammalian gut development.

1.2.2 Axial patterning and EM interactions in the gut

The gut tube is patterned along four axes: AP (cranial-caudal), dorsal-ventral (DV), left-right (LR), and radial. AP patterning of the gut is one of the first steps in polarising the symmetrical embryo. Initial AP patterning of the endoderm is established by the late primitive streak stage, and refined at later stages (E8.5-12.5) through the combinatorial action of transcription factors and signalling molecules whose expression patterns are regionalised within the endoderm and/or mesenchyme (Hogan and Zaret, 2002). Accordingly, EM (epithelial-mesenchymal) interactions specify regions between which morphological and gene expression differences emerge. These distinct regions give rise later in development to different organs. Genes that exhibit such differential expression patterns include members of the *Nkx, Hox,* and *Pax* families.

EM interactions are a fundamental feature of morphogenesis across a range of tissues and many examples exist in the developing gut. *Sonic hedgehog* (*Shh*) and *Indian hedgehog* (*Ihh*), for instance, have overlapping expression domains within the developing posterior stomach epithelium, from where they are secreted to act on mesodermal/mesenchymal targets including *Bmp4* (Bitgood and McMahon, 1995). Both factors induce smooth muscle differentiation in the target splanchnic mesoderm tissue, and are essential for murine GI tract organogenesis (Apelqvist et al., 1997; Ramalho-Santos et al., 2000; Litingtung et al., 1998). Loss of *Shh* expression causes gut defects the length of the gut tube: the stomach epithelium is transformed to an intestinal phenotype, duodenal stenosis and imperforate anus occur, and pancreatic development,

gut rotation, and enteric nervous system (ENS) development are all disrupted (Ramalho-Santos et al., 2000). Endodermal Shh also induces *Hoxd-13* expression in the splanchnic mesoderm, and both Bmp4 and Hoxd-13 act to modulate the action of Shh (Roberts et al., 1998). Bmp4 counteracts Shh-induced mesodermal proliferation, whilst Hoxd-13 signals back to direct the hindgut endoderm towards a region-specific epithelial fate – a second level of EM interaction. Recombination experiments reveal the inductive nature of the mesenchyme as it can induce a fate specific to its indigenous region in epithelium taken from a different part of the gut (Yasugi, 1993). Such EM interactions are central to gut development (reviewed in (Fukuda and Yasugi, 2005)).

A gut *Hox* code functions to specify and regionalise the mesenchyme along the AP axis. The formation of many morphological and functional boundaries within the gut appears to be dictated by the regional subsets of *Hox* genes expressed in the mesenchyme which pattern the underlying epithelium through EM interactions (Roberts et al., 1995b; Kawazoe et al., 2002).

The DV axis is the second axis to be patterned. The accessory organs of the gut (thyroid, lungs, liver, and pancreas) emerge following budding morphogenesis of the gut tube along the DV axis. Ventral specification of the gut is required for these budding events, though the pancreas also possesses a dorsal bud. Budding morphogenesis is one of the fundamental common processes of the "morphogenetic code" of development (Hogan, 1999).

Differentiation along the LR axis provides the third level of axial pattering. The organs of the adult GI tract are positioned asymmetrically along the body's LR axis, and establishment of this asymmetry is essential for correct organ development (discussed further in **Section 1.9**). The first indication of gut asymmetry is the bulging of the stomach to the left between E9.5 and E10.5.

The final level of gut patterning occurs along a radial axis. In cross-section, the fully developed gut tube contains a series of distinct tissue morphologies across the radial axis – i.e. from the serosa through to the lumen. The gut epithelium is regenerated and repatterned along this radial axis throughout adult life.

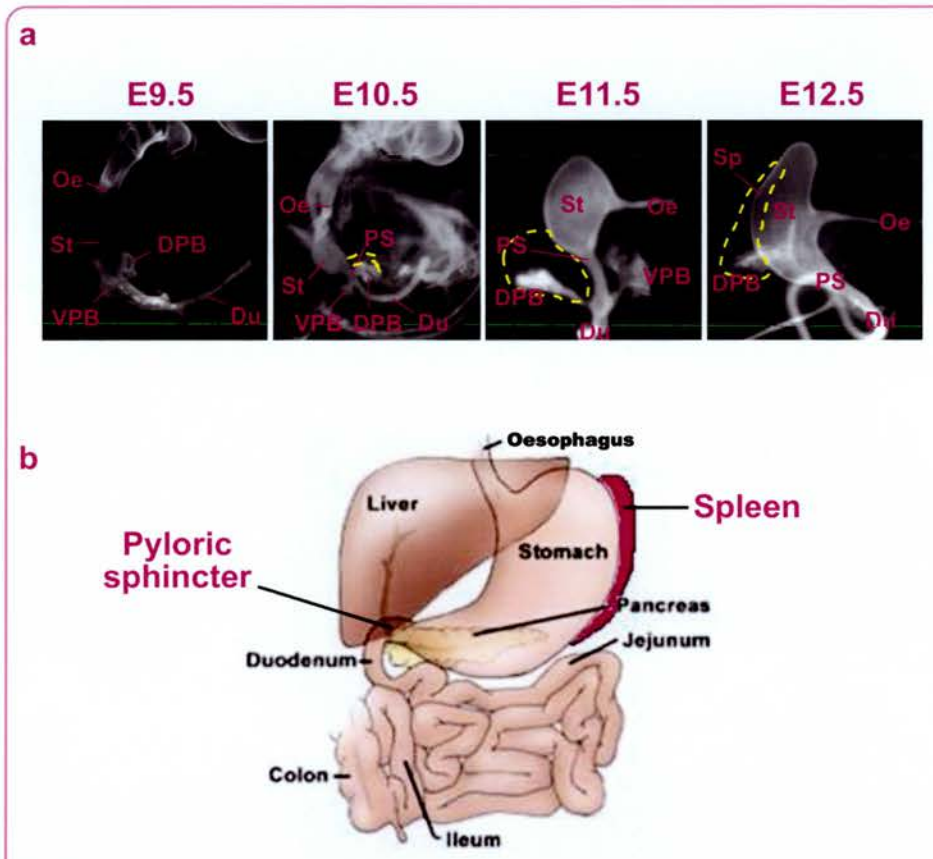

Figure 1.1 **Development of the mammalian gut**

a) Optical projection tomography (OPT) images of gut development in mouse embryos (courtesy of Robert Watson). The gut tubes are stained with an antibody against E-cadherin (an epithelial marker) to aid visualisation and are shown either within the context of the embryo (E9.5, E10.5) or as dissected guts (E11.5, E12.5).
At E9.5 the gut tube follows the curve of the embryo but is itself relatively uniform. The pancreatic buds (**DPB**, **VPB**) bulge out slightly along the dorsal-ventral axis. No constrictions are visible between gut regions. By E10.5, however, the pyloric sphincter (**PS**) constriction can be detected. The oesophagus is located at the anterior tip of the stomach at E10.5, but has shifted posteriorly onto the inner curvature by E11.5. The gut has a more familiar appearance by E12.5 and from this point growth becomes the predominant developmental force. Spleen growth occurs in close proximity to that of the mesenchyme surrounding the dorsal pancreatic bud; the putative splenic mesenchyme (E10.5, E11.5) and developing spleen (E12.5) are denoted by a dashed yellow line.
Oe: oesophagus, **St**: stomach, **DPB**: dorsal pancreatic bud, **VPB**: ventral pancreatic bud, **Du**: duodenum, **PS**: pyloric sphincter, **Sp**: spleen

b) The layout of the adult human gastrointestinal tract.

1.3 The stomach

1.3.1 Development of the stomach

The stomach is an evolutionary adaptation of the gut tube that frees the organism from having to continually feed, instead permitting storage of food during digestion. The primitive chordate *Amphioxus* does not possess a stomach, nor do some primitive fish such as the hagfish (Smith et al., 2000a). The stomach is one of the first morphologically distinct regions to develop from the uniform endodermal gut tube. It is first distinguishable at ~E9.5 as a bulge in the posterior foregut. The mechanism underlying this bulging is unknown, though perhaps some insight can be drawn from *Drosophila* in which organ shape is determined by orientated cell division (Baena-Lopez et al., 2005). Alternatively, increased cell proliferation may facilitate this bulging. However, recent evidence from our lab has indicated that the main mechanism is actually regulated *decreased* proliferation, as this creates the constrictions which demarcate the gut regions (Watson et al., 2007). Thus constriction events appear to be the major mechanism for AP patterning of the gut at E9.5-10.5. Thereafter, between E10.5 and E12.5, controlled outgrowth is most important (Watson et al., 2007).

The anterior of the stomach is closed and the posterior leads into the duodenum, through the pyloric sphincter. The concave surface of the stomach is termed the 'lesser curvature'; the oesophagus enters through this surface. The 'greater curvature' refers to the convex edge of the stomach; the spleen is nearest to this curvature. The surfaces and axes of the developing stomach are illustrated later in this thesis, in **Figure 4.2**.

The murine stomach can be functionally and morphologically divided into two regions: the anterior/proximal stomach (fundus), and the posterior/distal stomach (antrum/pylorus). The former is lined with folds of stratified squamous epithelium and gastric glands; the latter features villi, mucosal glands and a simpler epithelial lining. Regional epithelial differentiation initiates in the stomach at ~E12.5 and is the result of signalling from the overlying mesenchyme – another example of EM interaction (Hogan and Zaret, 2002). A reciprocal example of EM interaction is the differentiation of

splanchnic mesoderm into smooth muscle which is dependent on signals from the underlying endoderm.

The stomach wall is radially patterned into three smooth muscle layers: the longitudinal (outer), circular (middle), and muscularis mucosae (inner) layers (Smith et al., 2000a; Hogan and Zaret, 2002). An additional highly cellular submucosa layer lies between the middle and inner layers, and a mesothelial layer (the serosa) forms the final barrier with the coelomic cavity. The circular layer forms first, at E11.0-13.0, followed by the longitudinal muscle at E15.0 in the proximal stomach and at birth in the distal stomach (Hogan and Zaret, 2002). The muscularis mucosae layer does not form fully until after birth, though a thin layer of smooth muscle pertaining to this layer can be detected at E18.5 (Watson et al., 2007).

1.3.2 Genes implicated in stomach development

A number of genes have been implicated in the development of the mammalian stomach including *Bapx1* (*Nkx3-2*), *Fgf10, Tgfa, Shh,* and *Gli3* (Fukuda and Yasugi, 2005; Kim et al., 2005b). Hedgehog signalling underlies many aspects of stomach patterning. A putative hedgehog target is *Nr2f2* (*COUP-TFII*), which is expressed in both the mesenchyme and epithelium (Takamoto et al., 2005). Conditional (*Bapx1-Cre* directed) loss of this gene from the mesenchyme causes major stomach patterning defects along both the AP and radial axes. These defects are reminiscent of those seen when hedgehog signalling is inhibited: the stomach is reduced in size, and epithelial and circular smooth muscle differentiation is adversely affected, as is the distribution of ENS neurons. The presence of epithelial defects following ablation of *Nr2f2* specifically from the mesenchyme demonstrates the importance of EM interactions in stomach patterning.

Barx1 is also expressed in the stomach mesenchyme and is another important stomach development gene. Expression commences at E9.5 in the presumptive stomach region of the gut (Tissier-Seta et al., 1995). This expression is maintained in the stomach mesenchyme until E16.5 and also appears to mark the splenic mesenchyme at E11.5. No

expression is detected elsewhere in the gut. *Barx1* loss causes a shrunken stomach phenotype with disorganisation and infolding of the epithelial lining, resulting in failure of lumen formation (Kim et al., 2005a). An intestinal epithelium marker, *Cdx2*, becomes ectopically expressed in the abnormal stomach epithelium. Conversely, the endogenously expressed genes *Sfrp1* and *Sfrp2* are down-regulated in the mesenchyme. The secreted protein products of these genes normally negatively regulate Wnt signalling in the endoderm/epithelium. Thus mesenchymal Barx1 normally regulates the specification of the stomach epithelium through inhibition of canonical Wnt signalling in the latter tissue – a further example of EM interaction.

1.4 The pyloric sphincter

1.4.1 Development of the pyloric sphincter

The pyloric sphincter demarcates the boundary between the stomach and duodenum and acts to slow the passage of food, thus allowing adequate digestion and mixing. A reasonable amount of data has been published on the structure, function, and innervation of the neonatal and adult pyloric sphincter across a range of species. There is, however, little known about the origin and embryonic development of this tissue.

In humans, the pyloric sphincter is a ring of thickened circular muscle, covered by the folds of the mucosa layer (Gray and Carter, 1998). The earliest identification of a pyloric sphincter structure has been made at day 32[1] of human embryonic development when the anterior duodenum is noted to be dilated (Bourdelat et al., 1992). The circular and longitudinal muscle layers have noticeably thickened by day 40[2], pre-empting the final structure: a thickened circular muscle ring populated by bundles of fibres from the outer longitudinal layer. Smooth muscle α-actin and desmin can be detected in these

[1] Carnegie stage 14; comparable to mouse stage E11.5
[2] Carnegie stage 16; comparable to mouse stage E12.5

fibres (Bourdelat et al., 1992). The pyloric sphincter of the guinea pig shows a similar anatomy (Cai and Gabella, 1984).

The murine pyloric sphincter constriction is first detectable at E10.5 (personal observation). The identity of the muscle populating the sphincter is unclear. Smooth muscle α-actin is not detectable at high levels in the sphincter until E18.5 (S. Burn, MSc (Res) thesis, University of Edinburgh, 2003). The late appearance of smooth muscle may be reconcilable with the fact that the pyloric sphincter does not function as a classical sphincter; it remains open much of the time, acting as a constriction rather than a controlled opening (Schulze-Delrieu and Shirazi, 1983). It is, however, unlikely that *de novo* smooth muscle formation would occur so late in development. The late appearance of smooth muscle markers may thus be explained by a report in the guinea pig that the pyloric sphincter is actually a "funnel" of stomach muscle which hangs into the duodenum (Cai and Gabella, 1984). One further possibility is that the sphincter is populated by muscle cells from elsewhere. Indeed, it has recently been reported that the anal sphincter is populated by somitic muscle cells which migrate from the hind limb (Valasek et al., 2005). In addition to the unknown origins of the pyloric sphincter, there is also little consensus in the literature as to what actually constitutes the sphincter. In rat, for example, it has been reported to actually comprise two connected muscle loops (the proximal and distal sphincters) (Kudo et al., 1998).

1.4.2 Genes implicated in pyloric sphincter development

Although differences exist between gut development in mouse and chick (particularly the existence of a two chambered stomach in chick), they have enough in common to merit comparative studies (Smith et al., 2000a). Both species have a glandular anterior stomach, with non-glandular morphology in the posterior. Expression patterns also show conservation, for example: *Wnt5a* and *Bmp4* are expressed in the anterior stomach, whilst the posterior stomach is characterised by expression/increased expression of *Six2, Barx1,* and *Bmpr1b* (Smith et al., 2000a). The pyloric sphincter of

both organisms is marked by *Nkx2-5* expression and a similar – albeit broader - expression domain is noted in *Xenopus* (Smith et al., 2000a). The sphincter itself can also be found in amphibians and some fish, though not in primitive fish such as the hagfish or in *Amphioxus* (Smith et al., 2000a).

Pyloric sphincter development has been well characterised in chick due to the ability to ectopically express genes, or dominant-negative forms of genes, in specific cells/tissues using viral constructs. These findings are summarised in **Figure 1.2** and details are provided in the figure legend (Roberts et al., 1998; Smith and Tabin, 1999; Smith et al., 2000b; Nielsen et al., 2001; Moniot et al., 2004; Theodosiou and Tabin, 2005). A central aspect of this patterning is the differential regulation of *Bmp4* along the gut due to inhibition by Bapx1 in the gizzard (Nielsen et al., 2001). Formation of the pyloric sphincter from the gizzard is therefore induced by Bmp4 secreted from the adjacent duodenal mesenchyme in response to endodermal Shh (Smith and Tabin, 1999). Accordingly, the Bmp4 receptor gene *Bmpr1b* is specifically expressed in the gizzard (Smith et al., 2000b). The mesoderm becomes thinner in the sphincter than in the gizzard due to increased apoptosis and decreased proliferation in the Bmp4/Bmpr1b-selected gizzard mesoderm (Smith et al., 2000b).

Bmp4 is also necessary and sufficient for pyloric *cNkx2-5* expression (Smith and Tabin, 1999). The *cNkx2-5* expression domain specifically marks the pyloric sphincter mesoderm, overlapping that of mesodermal *Bmpr1b* in the gizzard, and bordering that of duodenal *Bmp4* (Smith and Tabin, 1999). Ectopic *Bmp4* or *Bmpr1b* expression directly induces ectopic *cNkx2-5* in the mesoderm of the gizzard, but not the duodenum, pointing to the gizzard as the origin of the sphincter (Smith and Tabin, 1999; Smith et al., 2000b). The endoderm underlying this ectopic *cNkx2-5* expression develops features of the pyloric sphincter (e.g. bulbous microvilli); mesodermal *cNkx2-5* is necessary and sufficient for epithelial pyloric sphincter formation (Smith et al., 2000b). This is yet another example of the importance of EM interactions during gut development.

Most recently it has been discovered that mesenchymal *Sox9* is also required for correct pyloric sphincter development in chick, as it is both necessary and sufficient to specify the epithelial component (Moniot et al., 2004; Theodosiou and Tabin, 2005).

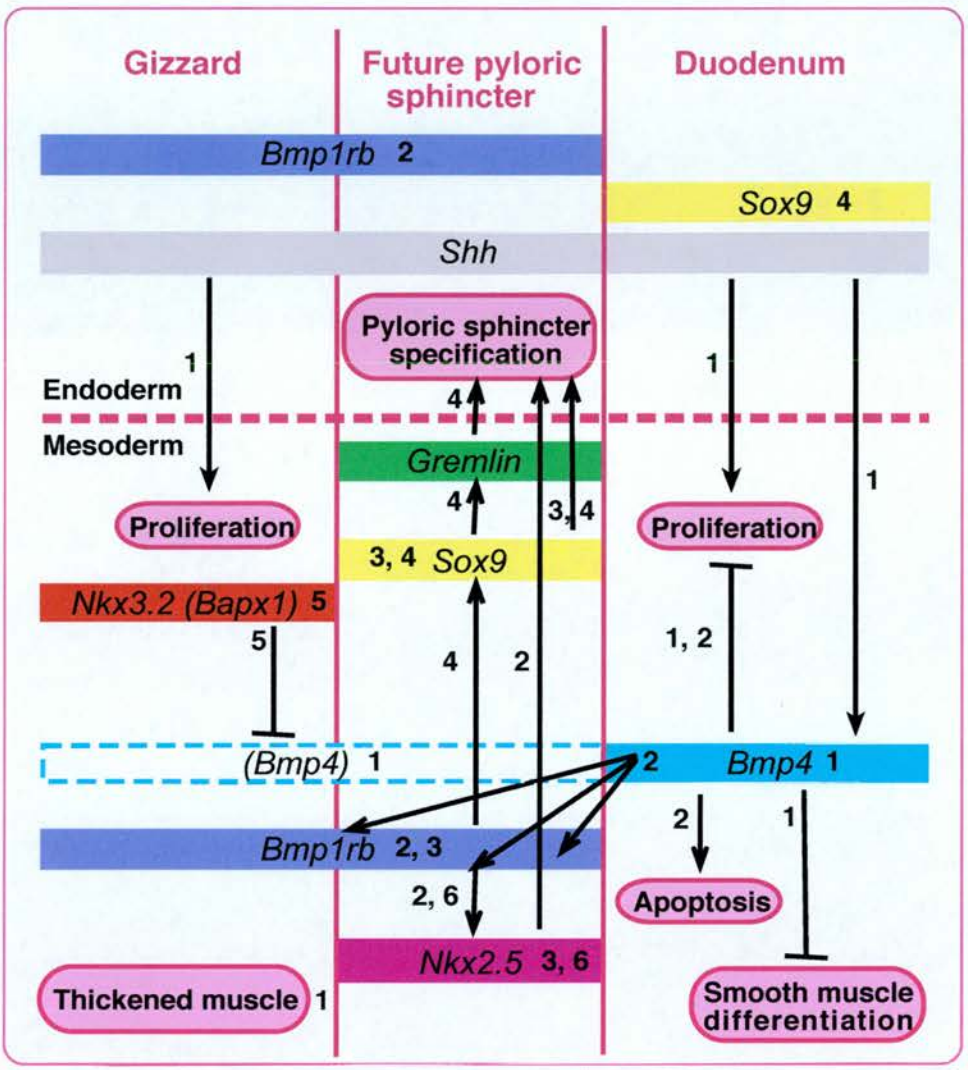

Figure 1.2 **Regulation of pyloric sphincter development in chick**

Differential regulation of *Bmp4* along the gut tube produces differential patterns of muscle growth and differentiation. *Bmp4* is not expressed in the gizzard (posterior stomach chamber), due to inhibition by Bapx1 (Nkx3.2); however, Bmp4 protein secreted from the neighbouring duodenum induces formation of the pyloric sphincter from the gizzard. *cNkx2.5* expression specifically marks the pyloric sphincter mesoderm; Bmp4 is both necessary and sufficient for this expression. Ectopic *cNkx2.5* expression (induced by *Bmp4* or *BMPR1B*) can only be induced in the mesoderm of the gizzard, but not the duodenum, pointing to the gizzard as the origin of the sphincter. Mesodermal *cNkx2.5* is both necessary and sufficient for epithelial pyloric sphincter formation. Mesodermal *Sox9* is also required for correct pyloric sphincter development in chick, as it is necessary and sufficient to specify the epithelial component. Sox9 positively controls expression of *Gremlin*, a modulator of the BMP pathway which may relay signals from mesodermal Sox9 to the underlying epithelium. Details are provided in **Section 1.4.2** of the main text.

References: **1**) Roberts *et al.*, 1998, **2**) Smith *et al.*, 2000, **3**) Theodosiou and Tabin, 2005, **4**) Moniot *et al.*, 2004, **5**) Nielsen *et al.*, 2001, **6**) Smith and Tabin, 1999

Once again this effect is realised through EM signalling. The mesodermal *Sox9* expression is controlled by BMP signalling; in turn, Sox9 itself positively controls the expression of *Grem1* (*Gremlin*), a modulator of the BMP pathway (Moniot et al., 2004). Grem1 is a diffusible factor and thus may relay signals from mesodermal Sox9 to the underlying epithelium. *Sox9* and *Nkx2-5* are independently regulated by BMP signalling; no interaction has been detected between these genes at the transcriptional level, though their products may interact to specify the sphincter epithelium (Theodosiou and Tabin, 2005). Misexpression of either gene in the gizzard mesoderm produces the same phenotype as misexpression of both (i.e. transformation of the underlying epithelium to a pyloric sphincter phenotype). *Nkx2-5* and *Sox9* may therefore perform partially redundant roles in pyloric sphincter formation in chick.

Development of the pyloric sphincter in mice is less understood, though it is already apparent that it is regulated differently to in chick. Data from our lab indicates that *Shh* is not expressed in the posterior stomach epithelium of mice (Hill lab, unpublished data), whereas it is in chick. Conversely, whilst *Bmp4* is not expressed in the chick gizzard, it appears to be expressed at low levels throughout the stomach in mice (Hill lab, unpublished data). Also, murine *Bapx1* does not appear to act upstream of *Bmp4*, as *Bmp4* expression is not increased in *Bapx1*$^{-/-}$ guts (Hill lab, unpublished data). *Nkx2-5* expression is lost in these mutants guts, but a relationship between these two homeobox genes does not appear to be maintained in chick, as ectopic *Bapx1* expression does not affect *Nkx2-5* gut expression (Nielsen et al., 2001).

There are however some shared features of mouse and chick pyloric sphincter development, mainly in the molecules involved and their expression patterns. *Bapx1* is expressed in the posterior stomach mesenchyme (Akazawa et al., 2000; Nielsen et al., 2001) and mesenchymal *Nkx2-5* expression marks the pyloric sphincter in both species (Lints et al., 1993b; Tanaka et al., 1998b; Buchberger et al., 1996). *Bmpr1b* expression in the posterior stomach is also conserved (Smith et al., 2000a). Beyond expression data, however, virtually nothing is known about the genetics of murine pyloric sphincter development. The one piece of information available is that *Hoxd* genes may play a role in patterning the pyloric sphincter, as deletion of the *Hoxd* complex results in abnormal

cell differentiation in the pyloric region of the stomach epithelium (Zakany and Duboule, 1999). The need for mouse mutants with pyloric sphincter defects is thus a major one.

1.4.3 Pyloric stenosis and other human defects

Pyloric stenosis is one of the most common congenital abnormalities in humans, affecting ~3/1000 live births (Carter and Evans, 1969). It is this clinical importance that makes the quest for knowledge about the origins and development of the pyloric sphincter so important. Pyloric stenosis (also known as hypertrophic pyloric stenosis) is characterised by morphological abnormalities of the sphincter region, leading to obstruction and manifesting as severe vomiting in the neonate (de Santa et al., 2002). Both muscle and neural development are affected. The circular and longitudinal smooth muscle layers are hypertrophic, with the enteric nerves in the former layer being enlarged and lacking in nitric oxide synthase (NOS) activity, and those in the latter being shortened (Vanderwinden et al., 1992; Abel, 2000). The Interstitial Cells of Cajal (ICCs) are largely absent from affected sphincters (Vanderwinden et al., 1996). This may explain the lack of coordination observed between the sphincter and stomach muscle contractions, as the "pacemaker" action of the ICCs normally regulates gut motility.

There is some evidence that pyloric stenosis may be a result of developmental immaturity of the muscle layers. The distribution of desmin[3] in hypertrophic neonatal pyloric sphincters is comparable to that found during normal foetal development, whereas desmin is not detected in normal, age-matched tissue (Guarino et al., 2000). This excess of desmin may affect the organisation of the muscle and prevent correct co-ordination of contraction and relaxation. *Transforming growth factor-α (Tgfa), epidermal growth factor (Egf),* and *Egf-receptor (Egfr)* are other genes inappropriately overexpressed in the circular and longitudinal muscle layers of pyloric stenosis patients,

[3] A cytoskeletal protein found in intermediate filaments of the muscle

and these may promote smooth muscle overgrowth (Shima and Puri, 1999; Shima et al., 2000).

Although no major candidate gene for pyloric stenosis has been identified, there is a definite genetic component, with a family history being present in ~12% of cases (Hulka et al., 1997). Mutations in the nitric oxide synthase gene (*Nos1*) or its promoter may confer susceptibility to pyloric stenosis in some families (Chung et al., 1996; Saur et al., 2004). The mouse *Nos1* knockout has pyloric stenosis, as well as a grossly enlarged stomach (also seen in human pyloric stenosis) and hypertrophic circular muscle layer (Huang et al., 1993). The mouse model of phenylketonuria (the *hph-1* mouse) also displays transient pyloric stenosis and has thus been the subject of studies into the underlying muscular changes involved (Abel, 2000; Abel et al., 2004). *Hph1* mice are deficient for tetrahydrobiopterin which is a cofactor for phenylalanine hydroxylase and also, intriguingly, NOS. Human phenylketonuria has been associated with pyloric stenosis in cases when the phenylketonuria is left untreated (Johnson et al., 1978).

There also appears to be some association between pyloric stenosis and duplication of the proximal region of chromosome 9q, although the significance of this has been disputed (Yamamoto et al., 1988; Chung et al., 1993). Inheritance is complex, and a multifactorial sex-modified[4] threshold model seems likely, though multiple interacting loci may also be responsible (Carter and Evans, 1969; Carter et al., 1980; Chakraborty, 1986; Mitchell and Risch, 1993). Simple autosomal dominant inheritance has also been reported in one large family (Fried et al., 1981). Pyloric stenosis can also occur in conjunction with other congenital malformations, sometimes as part of a syndrome. In a survey of 13 patients with right-sided congenital diaphragmatic hernia, for example, Khwaja and colleagues found that three of these also suffered from pyloric stenosis (Khwaja et al., 1989).

It is unclear whether pyloric stenosis develops postnatally or if an existing perinatal form precedes postnatal detection. An incident of perinatal occurrence has however been reported (de Santa et al., 2002). The pyloric sphincter constriction is also malformed, expanded, or lost during embryonic development in mice with mutations in

[4] Males are affected more than females by 5:1, particularly first-born males.

Bapx1, Sox11, and the gene affected by the Dominant hemimelia mutation (Akazawa et al., 2000; Sock et al., 2004)(unpublished data, Hill lab). These mutants are discussed in **Section 1.9.4**.

1.5 The spleen

1.5.1 Development of the spleen

"To anyone looking over the literature on the development of the mammalian spleen the necessity for more work on the finer details of the process is evident"

(Thiel and Downey, 1921) ...

... 85 years on from this seminal paper the later stages of spleen development - such as differentiation of the various cell types within the spleen - are well studied, but questions about the very earliest stages have remained unanswered until recently. Many details are still unknown due to a deficit of early splenic markers and mutations affecting early spleen development. Insights cannot be gained from lower organisms as the spleen is a vertebrate-specific organ.

The common description of the earliest spleen rudiment is that of a condensation of mesenchyme lying dorsal to the developing stomach, within the left-side of the dorsal mesogastrium[5] at ~E10.5-11.0 (marked in yellow in **Figure 1.1a**) (Thiel and Downey, 1921; Green, 1967; Brendolan et al., 2005; Brendolan et al., 2007). This putative splenic mesenchyme underlies the Splanchnic Mesothelial Plate (SMP), a structure which plays a key role in spleen development (Hecksher-Sorensen et al., 2004). The SMP is discussed in detail in **Section 1.9.3**. The condensed mesenchyme expresses a number of markers expressed in later spleen development (see below), thus implicating it as the source of splenic precursor cells (Hecksher-Sorensen et al., 2004). The events prior to condensation are unclear, although there may be some initial contribution of cells from

[5] The sheet of mesenchyme connecting the stomach with the dorsal body wall

the overlying thickened coelomic epithelium (peritoneum) (Thiel and Downey, 1921). The origin (pre-E10.5) of the condensed mesenchyme is the first question that our lab is interested in, the second being how the mesenchyme then develops into a recognisable elongated spleen form (from E11.5).

To address the first question, spleen development must be traced back further than E10.5, to discover when and where splenic precursors are first identifiable. *Xenopus* splenic precursors appear to be initially located on both sides of the embryo; the left-side pool preferentially develops into the spleen (Patterson et al., 2000). If a comparable situation were to exist in mammals then defects in this system could provide a mechanism for asplenia and polysplenia. Both of these developmental abnormalities are reported in humans and are of clinical importance given their association with other LR asymmetry defects, including cardiac disorders (Bartram et al., 2005).

The second question concerns what happens to the splenic mesenchyme following condensation. The details of how this patch of tissue undergoes the transition from lying at the posterior of the stomach to becoming an elongated structure along the AP length of the stomach are unclear. This change occurs within a ~24 hour window, between E11.5-12.5. Most studies agree that there is a single initial patch of splenic mesenchyme at ~E11.5, and that a single elongated spleen structure extends from this region by ~E12.5. However there are also exceptions, such as the description that the spleen develops inside the omentum[6] as two thickenings extending from the lower left and upper right areas of the omentum (Godin et al., 1999). It is also clear that the spleen is formed in a posterior-to-anterior manner, such that the anterior limit of an E12.0 spleen will be somewhere between that seen at E11.5 and E12.5. But the mechanism for this development is far from clear. Migration of the splenic precursor cells up towards the anterior stomach is conceivable, though equally possible is that the posterior of the spleen is derived from the E11.5 condensed mesenchyme whilst the remainder is composed of cells contributed by the underlying stomach mesenchyme in a posterior-to-anterior manner. Experimental distinction between these models will be difficult, and is addressed in **Chapter 4**.

[6] The part of the peritoneal membrane surrounding the gut

1.5.2 Genes implicated in spleen development

The condensed splenic mesenchyme lies dorsal to the dorsal pancreatic bud, and expresses a range of genes known to mark the spleen at later stages: *Bapx1, Nkx2-5, Hox11 (Tlx1), Capsulin (Pod1/Tcf21), Wt1,* and *Pbx1* (Hecksher-Sorensen et al., 2004; Roberts et al., 1994; Lu et al., 1998; Rackley et al., 1993; Brendolan et al., 2005). Loss of most of these genes results in asplenia, with the exception of *Nkx2-5*, loss of which proves lethal before spleen development initiates (Lettice et al., 1999b; Lyons et al., 1995; Roberts et al., 1994; Lu et al., 2000; Herzer et al., 1999; Brendolan et al., 2005). *Sox11*$^{-/-}$, *Nkx2-3*$^{-/-}$, and *Dh* homozygous mutant mice are also asplenic (Sock et al., 2004; Pabst et al., 1999; Green, 1967).

The first gene shown to be required for spleen development was *Hox11* (*Tlx-1*), loss of which causes a spleen-specific phenotype (Roberts et al., 1994; Dear et al., 1995; Roberts et al., 1995a). The earliest report indicated that *Hox11* is required for initiation of spleen development (Roberts et al., 1994). However, a later study showed that *Hox11* is in fact required for cell survival, as *Hox11* loss halts proliferation (and may to a lesser extent promote apoptosis[7]) of the splenic mesenchyme leading to regression of the spleen anlage between E13.0-13.5 (Dear et al., 1995; Kanzler and Dear, 2001). Splenic cells do persist beyond this time, albeit in a disorganised tissue into which haematopoietic cells do not migrate (Kanzler and Dear, 2001). Incomplete separation of the dorsal mesogastrium (splenic precursor region) from the stomach has also been reported (Roberts et al., 1995a). *Hox11*$^{-/-}$ cells cannot contribute to spleen development in chimaeras, indicating a cell-autonomous action of Hox11 in spleen development, and are in fact actively excluded from chimaeric spleens (Kanzler and Dear, 2001). It is possible that the excluded splenic cells instead contribute to the enlarged stomach – and perhaps pancreas – seen in these mutants (Roberts et al., 1995a).

Homozygous loss of *Capsulin* also causes asplenia, due to apoptosis of the splenic primordium at E12.5 (Lu et al., 2000). A similar apoptotic fate occurs in *Wt1*$^{-/-}$

[7] This has, however, been disputed. Roberts and colleagues detected no increase in cell death at the site of normal spleen development (Roberts et al., 1995a).

spleens from E13.5, demonstrating a requirement for *Wt1* in maintenance of the spleen primordium (Herzer et al., 1999). Thus *Capsulin, Wt1*, and *Hox11* are all required for spleen cell survival but not for the initial development of the spleen primordium (Lu et al., 2000; Herzer et al., 1999; Dear et al., 1995).

Expression of *Capsulin, Wt1, Hox11,* and *Nkx2-5* overlaps in the E10.5 dorsal mesenchyme, implicating it as the spleen primordium (Hecksher-Sorensen et al., 2004). Marking of cells at this early stage in mouse development is of particular importance as the splenic mesenchyme is not yet so intimately associated with the stomach. *Hox11* is strongly expressed in this splanchnic mesenchyme and is regarded as the earliest marker of the presumptive spleen (Roberts et al., 1994). However, recent evidence suggests that *Nkx2-5* is the earliest marker of splenic precursors in *Xenopus* (Patterson et al., 2000). Strong *Nkx2-5* expression is also seen in the putative splenic mesenchyme of the mouse at E10.5 ((Hecksher-Sorensen et al., 2004), **Section 2.2.2** of this thesis).

Hox11 and *Nkx2-5* expression is lost from the E11-12.5 condensing splenic mesenchyme of $Pbx1^{-/-}$ mutants (Brendolan et al., 2005). *Hox11* is a direct target of Pbx1 and is positively regulated by the synergistic action of Pbx1 with Hox11 itself in splenic mesenchyme cells. $Pbx1^{-/-}$ mice are asplenic by E13.5, due to splenic agenesis which occurs as a result of decreased proliferation following normal establishment of the spleen primordium (Brendolan et al., 2005). A hypoplastic spleen is present at E11.0-12.5 and this maintains *Bapx1* and *Capsulin* expression, though *Wt1* expression is lost in addition to that of *Hox11* and *Nkx2-5* (Brendolan et al., 2005). The loss of *Wt1* may be an effect of *Hox11* loss, as *Wt1* expression is significantly reduced in $Hox11^{-/-}$ mutants (Koehler et al., 2000). It should be, however, noted that this relationship has been disputed in another study in which *Wt1* expression was maintained in the E12.5 $Hox11^{-/-}$ spleen (Herzer et al., 1999). This contradiction may however simply be a result of differing genetic backgrounds as the mutant spleen in the latter study appears to still be relatively intact by E12.5.

Splanchnic mesoderm development prior to E11.0 is apparently normal in $Pbx1^{-/-}$ mutants (Brendolan et al., 2005). *Bapx1* is not downstream of *Pbx1* in the spleen development hierarchy, as *Bapx1* loss causes a defect of the splenic mesenchyme at an

earlier stage than the splenic agenesis caused by *Pbx1* loss, and *Bapx1* expression is intact in the *Pbx1*$^{-/-}$ spleen (Hecksher-Sorensen et al., 2004; Brendolan et al., 2005). However, it is unlikely that a single, linear spleen development genetic cascade exists. The authors of the *Pbx1*$^{-/-}$ spleen agenesis paper propose instead that Pbx1 plays a central role in spleen development by regulating both the essential *Bapx1*- and *Capsulin (Pod1)*- dependent spleen development pathways via control of their downstream targets, *Hox11* and *Nkx2-5* (Brendolan et al., 2005). *Pbx1* also plays a role later in spleen development by promoting proliferation of the spleen at E13.5 (Brendolan et al., 2005).

A summary of the genetic pathways underlying spleen development is provided in **Figure 1.3**.

1.5.3 Functions of the spleen

"To the left of your stomach, a deep violet-red,
A filter's at work filling blood cells with dread:
The red blood cell graveyard! It's not Halloween.
I'm talking about that blood basher, the spleen.*"*

- Allan Wolf, The Blood-Hungry Spleen

Following the initial establishment and growth of the splenic primordium (the stages with which this thesis is concerned), haematopoietic stem cells migrate from the developing liver into the spleen by E12.5-13.0 and the spleen itself commences haematopoietic cell production at E14.5 (Godin et al., 1999; Bertrand et al., 2006). Correct development of the foetal spleen is dependent on interaction between the stromal and haematopoietic cells; for example, the stroma drives macrophage commitment (Bertrand et al., 2006). Cell differentiation occurs throughout the rest of foetal spleen development such that the spleen becomes populated by a range of specialised cell types.

The adult spleen is the biggest lymphoid organ in the mammalian body and acts as the largest filter of blood (Mebius and Kraal, 2005). In addition to the removal of old

a

Mutant	Expression lost	Expression retained
Bapx1 (Nkx3.2) -/-	Hox11 [1, 2] Nkx2.5 [3]	Pbx1 [4] Pod1 [4]
Pbx1 -/-	Hox11 [4] Nkx2.5 [4] Wt1 [4]	Pod1 [4] Bapx1 [4]
Hox11 -/-	Wt1 (decreased) [5]	Pbx1 [6] Nkx2.5 [4] Wt1 [4]
Pod1 (Capsulin) -/-	Nkx2.5 [4]	Bapx1 [4] Pbx1 [7] Hox11 [7]
Wt1 -/-		Hox11 [6]

b

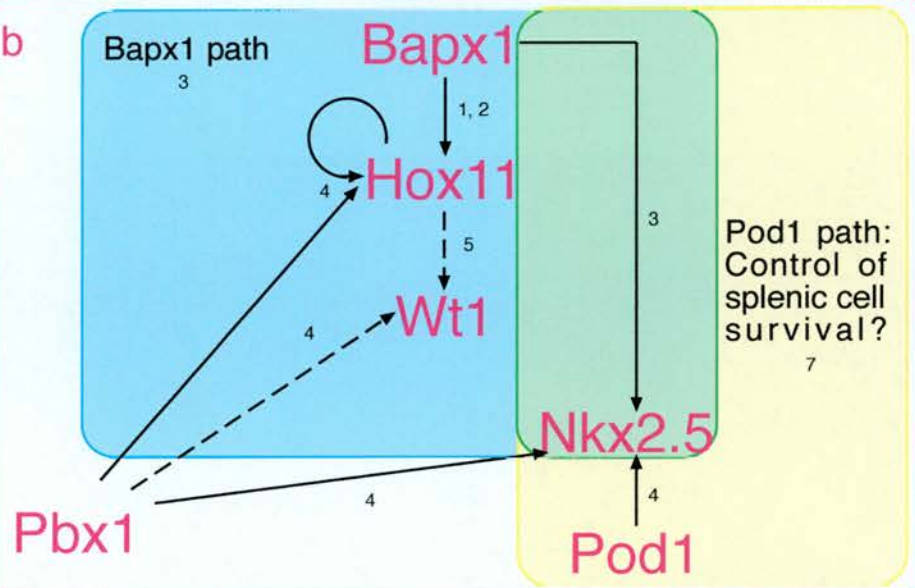

Figure 1.3 The genetic regulation of murine spleen development

a) A table of expression data from published asplenic mutants

b) The possible regulatory pathways underlying spleen development. Two major pathways are predicted to exist, based on the available data: the Bapx1 and the Pod1 (Capsulin) pathways. Both of these factors regulate Nkx2.5 expression. Pbx1 may act as a master regulator as it can act on the downstream targets of both pathways.

References: 1) Lettice et al., 1999, 2) Akazawa et al., 2000, 3) Watson et al., 2007, 4) Brendolan et al., 2005, 5) Koehler et al., 2000, 6) Herzer et al., 1999, 7) Lu et al., 2000

erythrocytes from the blood, the spleen also recycles iron and plays an important role in both innate and adaptive immunity. The spleen is arranged as a network of branching arterial vessels, and comprises two main components: the red and the white pulp. The red pulp acts as a filter to take old or damaged erythrocytes out of circulation, and consists of macrophages, plasma cells and stroma cells. The white pulp contains lymphocytes, including B and T cells which undergo activation and maturation in this tissue. Lymphocytes are white blood cells which play crucial roles in the immune response; these enter the spleen through the marginal sinus, which is located between the white pulp and the marginal zone. The marginal zone is populated by naïve B cells, specialised macrophages and other cell types, including the sinus-lining non-lymphoid cells which express the *mucosal addressin cell adhesion molecule-1 (Madcam1)* gene and are thought to regulate passage of lymphocytes and antigens into the white pulp from the blood (Tanaka et al., 1996).

A reservoir of haematopoietic stem cells is maintained in the adult spleen and this can be used to supplement those produced by the bone marrow in response to disease or trauma. More recently, it has been discovered that the spleen also contains non-lymphoid stem cells which have the potential to differentiate into fully functional pancreatic islet and ductal epithelial cells (Kodama et al., 2003)[8]. These adult stem cells can also differentiate into other cell types (osteoblast-like cells), and this capacity may be a result of persistent *Hox11* expression (Kodama et al., 2005).

The existence of splenic stem cells may shed some light on the association between splenectomies and the development of diabetes in certain disease situations (Kodama et al., 2005). It may also provide an explanation for how functional ectopic islets develop specifically in the spleen of *PTF1-p48* deficient mice which undergo defective pancreatic development (Krapp et al., 1998). Similarly, cells from the regressing spleen primordium in *Hox11* null mice relocate to the pancreatic mesenchyme (Kanzler and Dear, 2001). These facts are particularly interesting given the close relationship of the spleen and dorsal pancreatic mesoderm during development. These

[8] There has, however, been some debate over whether spleen cells can truly contribute to the recovered pancreatic islets (Chong et al., 2006; Nishio et al., 2006; Suri et al., 2006; Faustman et al., 2006).

tissues undergo major developmental changes in close proximity to one another between E10.5-12.5; the mesenchyme of the spleen and that overlying the dorsal pancreas are contiguous at these stages. A common origin could explain the presence of splenic stem cells which are capable of differentiation into pancreatic islet cells. The spleno-pancreatic mesenchyme is, however, of unknown origin; it is not detectable at E9.5 yet is by E10.5. The thickened splanchnic mesothelium of the SMP is a candidate precursor tissue as defects of this tissue cause disruption of the spleno-pancreatic region (Green, 1967; Hecksher-Sorensen et al., 2004). The earlier, broader paraaortic splanchnopleura/aorta-gonad-mesonephros (P-Sp/AGM) region mesoderm is another candidate as cells from this tissue are multipotent and so the persistence of undifferentiated P-Sp/AGM cells in the spleen could serve as an explanation for the range of fates that splenic stem cells can adopt in the laboratory (Kodama et al., 2005).

1.5.4 Defects of the human spleen

Development of the spleen is almost always abnormal in individuals with heterotaxia (defects in LR asymmetric development) (Bartram et al., 2005). Any defect in LR asymmetric development is of clinical note as congenital heart disease - due to abnormal cardiac asymmetry - is often also present. Spleen abnormalities associated with heterotaxia mainly take the form of polysplenia or asplenia and are usually sporadic. Familial cases occur more rarely and mostly show autosomal recessive inheritance (Bartram et al., 2005). Though most commonly found in individuals with defects in asymmetric patterning of other organs, spleen defects may also occur in isolation. The occurrence of "polyasplenia" (with either associated anomalies or in isolation) is ~1/24,000-40,000 (Aylsworth, 2001). "Polyasplenia" encompasses both poly- and asplenia and reflects the view held by some that they are part of the same spectrum of disorders.

Polysplenia is a result of bilateral left-handedness, such that spleen tissue can be present on both sides of the body. The form that this tissue takes varies and includes

multi-lobed spleens, clusters of small spenuli, and mixtures of small and large spleens; these multiple spleens are actually most commonly (64-75% of cases) only located on the right side of the body, despite the label of "bilateral left-handedness" (Bartram et al., 2005). Malformations associated with polysplenia include a bilaterally symmetrical liver, bilaterally bilobed lungs, an absent gallbladder, a right-sided stomach, and a reduced pancreas (in up to 50% of cases) (Bartram et al., 2005). Polysplenia does not, however, present any major health challenges in isolation

Asplenia is regarded as bilateral right-handedness (dextro-isomerism) and results in a total absence of splenic tissue. Defects associated with asplenia include bilaterally trilobed lungs, an enlarged bilaterally symmetrical liver, and a variety of cardiac defects (Bartram et al., 2005). Congenital heart disease is present in up to 99% of asplenic individuals[9] (Aylsworth, 2001). In addition to the characteristic cardiac defects, congenital asplenia (Ivemark syndrome) shows an association with other gut abnormalities, including situs inversus/heterotaxia and intestinal malrotation, and can prove fatal through sepsis associated with lack of a spleen (Mishalany et al., 1982; Phoon and Neill, 1994). Experiments in mice have shown that the main issue associated with absence of the spleen (either congenitally or by splenectomy) is a lack of B-1a cells (Wardemann et al., 2002). These specialised B cells provide the body's main source of antibodies and form part of the immune response to bacterial and viral infection.

There is an intriguing predominance of asplenic male sufferers, echoing the situation seen with pyloric stenosis (Mishalany et al., 1982). Whilst polysplenia is equally common between the sexes, there is also a male predominance of individuals with a single right-sided spleen (Bartram et al., 2005). The presence of a single spleen on the right side of the body is a rarer occurrence than poly- or asplenia (Bartram et al., 2005). If splenic precursors do initially exist bilaterally then preferential survival of those on the right - perhaps in response to an abnormally sided inductive signal - could serve as an explanation for this condition. The three types of spleen defect show overlapping associated defects, suggesting a common developmental basis. Individuals

[9] This may be an overestimate as patients are reported on the basis of their cardiac defects, whereas isolated asplenia may escape medical attention

with a single right-sided spleen have the most in common with asplenic individuals; this may support the notion that splenic precursors are originally located bilaterally, and if bilateral right-handedness is inappropriately induced the result is asplenia or, more rarely, survival of precursors on the right-hand side.

1.6 The pancreas

1.6.1 Development of the pancreas

The pancreas is a vertebrate-specific derivate of the gut tube which plays roles in digestion and hormonal regulation (Slack, 1995). Two distinct cell populations exist in the differentiated pancreatic endoderm: exocrine (secrete enzymes into the intestine) and endocrine (release hormones into the bloodstream). The pancreas is not of direct relevance to this thesis, but its development is so intertwined with that of the spleen that it merits a brief discussion. As mentioned in the previous section, the splenic and pancreatic primordia both emerge in the dorsal mesogastrium. Whilst the spleen is entirely mesenchymal, the pancreas is an endodermal organ with associated pancreatic mesenchyme. This dorsal pancreatic mesenchyme is indistinguishable from the splenic mesenchyme at E10.5, and these two tissues remain in contact throughout much of development (personal observations). Adult splenic stem cells retain the potential to differentiate into functional pancreatic islet cells (Kodama et al., 2003).

The endodermal component of the pancreas initially takes the form of two buds – dorsal and ventral – which emerge from the posterior foregut (for an in-depth review see (Slack, 1995)). It is the dorsal pancreatic bud which is closely associated with the spleen whilst the ventral bud lies in closer contact with the hepatic duct and duodenum. These two buds undergo branching morphogenesis and fuse following gut rotation.

The pancreatic mesenchyme can be first detected as an accumulation of mesodermal cells which appears between the dorsal aorta and dorsal endoderm at the 22-25 somite stage, just before and/or concomitant with leftward growth of the gut

(personal observations and (Wessells and Cohen, 1967)). This splanchnic mesenchyme gathers around the dorsal pancreatic bud and promotes growth and differentiation of the pancreatic epithelium through EM interactions (Kim and Hebrok, 2001; Edlund, 2002). One prime example of these interactions is the requirement of mesenchymal *Fgf10* for the differentiation and branching morphogenesis of the pancreatic epithelium (Bhushan et al., 2001).

1.6.2 Genes implicated in pancreas development

Many other genes, in addition to *Fgf10*, are also known to play essential roles in pancreatic development. The homeobox gene *Pdx1*, for example, is expressed in the pancreatic endoderm and is essential for pancreatic development (Jonsson et al., 1994; Ahlgren et al., 1996). Conversely, exclusion of endodermal *Shh* expression from the pancreas is essential for correct pancreatic (and spleen) mesenchyme development (Apelqvist et al., 1997). Genes required for pancreatic budding include *Onecut1 (Hnf-6, OC-1), P48 (Ptf1a), Hes1,* and *Isl1*; genes required for the establishment of endocrine cells include *NeuroD* and *Ngn3*; endocrine differentiation genes include *Pax4, Pax6, Nkx2-2, Nkx6-1* and *Nkx6-2* (reviewed in (Grapin-Botton and Melton, 2000; Collombat et al., 2006)). The spleen differentiation gene *Hox11* is also expressed in the pancreatic mesenchyme from E12.5 (when expression is contiguous with that in the spleen) to E14.5 (Kanzler and Dear, 2001).

The homeobox gene *Hex* is responsible for specification of the ventral pancreas (Bort et al., 2004). The morphogenetic mechanism of this gene's action is particularly interesting: controlling proliferation and consequently the position of the pancreatic endoderm so that these cells escape the influence of the cardiogenic mesoderm, which induces a liver fate. Control of organ position appears to be a central theme in pancreas development, as the pancreatic primordium must also become physically separated from the splenic mesenchyme if correct pancreatic development is to occur. Prolonged interaction with the spleen – either *in vitro* or in the *Bapx1*$^{-/-}$ mouse – results in

metaplastic transformation of the pancreas into ectopic gut-like structures (Asayesh et al., 2006).

1.7 Gut development genes

The search for genes expressed during gut development is of utmost importance, as gut abnormalities are the most common human congenital defect, and many occur in familial and syndromic forms, suggesting a genetic basis (de Santa et al., 2002). A number of genes and gene families known to play roles in gut development have been discussed in the previous sections, and many more undoubtedly exist given the complexity of gut morphogenesis. Indeed, a recent study of the expression of nearly every known and predicted transcription factor gene during murine gut organogenesis showed that around 1000 transcription factor genes are expressed in the developing gut (small intestine or stomach) between E11.0-17.0 (Choi et al., 2006).

Members of the *Hedgehog, Hox, Fgf, Bmp, Sox,* and *Pax* gene families have essential functions in gut development, often across a range of vertebrate species. The *Nkx* gene family has also been mentioned a number of times in the discussion thus far. *Nkx* genes play key roles in development of many regions of the GI tract, and a number are essential for murine spleen development. Homologues also play roles in invertebrate gut development. These facts, along with the central role of *Nkx2-5* – and *Bapx1 (Nkx3-2)* - in this thesis, merit the *Nkx* genes a section of their own; this follows next.

1.8 Nkx genes in development

1.8.1. Identification of the NK gene family in Drosophila melanogaster

NK/Nkx genes regulate many aspects of mesodermal patterning, and a number of these are expressed in the invertebrate and vertebrate developing gut. Members of the *NK/Nkx* gene family encode homeobox-containing proteins, implying a role in transcriptional regulation. Homeoboxes – also known as homeodomains - are a common feature of developmental transcription factors, and are thought to facilitate sequence-specific DNA binding, allowing regulation of target genes (Gehring, 1987). It was by probing the *Drosophila melanogaster* genome for a homeodomain-encoding sequence that the first invertebrate *NK* genes (*NK-1, NK-2, NK-3,* and *NK-4*) were identified by Kim & Nirenberg (hence "*NK*") in 1989 (Kim and Nirenberg, 1989). The NK-2, -3, and -4 homeobox amino acid sequences show 59-66% homology to one another – greater than to any other known *Drosophila* homeodomain - whereas that of NK-1 has greater homology with non-NK factors. On the basis of these findings, *NK-1* was put into a class of its own (*NK-1*), whilst *NK-2, -3*, and *-4* became known as *NK-2* genes (Harvey, 1996). Vertebrate homologues of both classes have since been identified across a range of phyla and species, although, as will become apparent throughout this discussion, the naming of these genes often does not reflect their ancestral links. The four original *Drosophila* NK genes have also now been renamed with reference to their mutant phenotypes: *NK-1* is referred to as *slouch* (*slou*), *NK-2* as *ventral nervous system defective (vnd)*, *NK-3* as *bagpipe* (*bap*), and *NK-4* as *tinman* (*tin*). The roles and mutant phenotypes of *bap* and *tin* are discussed in **Section 1.8.2**.

Proteins encoded by *NK-2* group genes share not only overall homeodomain homology, but also an NK-2-specific tyrosine at amino acid 54 of the domain (Harvey, 1996). This residue is conserved from sponge to human, and is thought to be involved in binding preferentially to a CAAG core motif as opposed to the classical TAAT homeodomain binding site (Harvey, 1996; Damante et al., 1996). A further subdivision

of the *NK-2* class of genes is made on the presence (Type I) or absence (Type II) of an NK2-Specific domain (NK2-SD), C-terminal to the homeodomain (Harvey, 1996). The function of this domain is unknown. Most NK-2 proteins – including Bap and the vertebrate Tin homologues – are Type I but Tin is a Type II protein. Given the particularly high similarity between the *tin* and *bap* homeodomain sequences, as well as their genomic proximity, it is possible that *tin* arose from a duplication of the ancestral *bap* gene and subsequently lost this domain.

The four original *Drosophila NK* genes share similarity not only in their homeodomain-encoding sequences, but also in genomic location. Whilst *NK-2/vnd* resides on the X chromosome, *NK-1/slou, NK-3/bap,* and *NK-4/tin* are clustered on the third chromosome, in the 93E1-5 region of the right arm (Kim and Nirenberg, 1989). An approximately 180kb genomic region including this section also contains three other homeobox genes (*ladybird early (lbl), ladybird late (lbe), C15*), and the six genes are collectively known as the 93DE gene cluster - the second largest cluster of physically linked homeobox genes in the *Drosophila* genome (Jagla et al., 2001). Distinct vertebrate homologues exist for most of these genes and this, along with the degree of divergence seen between the homeodomain sequences within the cluster, strongly suggests that the cluster is not the result of a recent genomic duplication.

A unifying feature of the genes in the 93DE cluster is that they encode proteins containing an N-terminal "TN" domain, similar to the Eh1 repression domain found in transcriptional repressors of the Engrailed family (Smith and Jaynes, 1996; Harvey, 1996; Jagla et al., 2001). Negative regulation of target genes may thus be a shared trait of the 93DE gene products. On the basis of TN domain and homeobox similarity, the two most similar genes in the 93DE complex are *tin* and *bap* (Jagla et al., 2001).

In addition to the two classes of *NK2* genes already discussed, a Type III class also exists, members of which have neither the NK2-SD nor the TN domain (Harvey, 1996). This class includes *NK2* genes from flatworms and *C.elegans*, vertebrate *Nkx5-1* genes, and *NK1*-type genes. Only one gene is known to have the NK2-SD but not the TN domain: *Nkx2-9*, a murine gene involved in neural development (Pabst et al., 1998).

The six 93DE cluster genes are involved in regulating progressive mesoderm specification, through a cascade of interactions under the initial control of *tin* (Jagla et al., 2001; Azpiazu and Frasch, 1993). *Tin* is required for the specification of the dorsal mesoderm to cardiac, somatic, and visceral fates (Azpiazu and Frasch, 1993; Bodmer, 1993). Subsequent activation of *bap* by Tin is required for the specification of visceral muscle precursors (Azpiazu and Frasch, 1993). The other 93DE genes are then activated by Tin to control the downstream specification of other mesodermal cell types.

1.8.2 Tin and bap are required for visceral mesoderm formation

Tin is alternatively named *mesoderm specific homeobox-containing gene 2* (*msh2*) (Bodmer et al., 1990), reflecting the essential role Tin plays in specifying the *Drosophila* dorsal mesoderm to become either cardiac or visceral muscle (Bodmer, 1993). *Tin* is the first of the 93DE cluster genes to be expressed and this expression occurs at an early point during mesoderm formation, downstream of maternal *dorsal* and zygotic *twist* and *snail* (Bodmer et al., 1990). Expression is initially found in all the mesodermal cells of the segmented embryo, but then becomes restricted to the dorsal mesoderm (Bodmer et al., 1990). The specific activation of *tin* in the dorsal mesoderm requires binding by - and the synergistic action of – activating Smad proteins and inhibitory autoregulatory Tin (Xu et al., 1998a). Activation of *tin* in the dorsal mesoderm is also dependent on *decapentaplegic* (*dpp*) expression in the dorsal ectoderm (Frasch, 1995).

Tin expression is essential for correct patterning of the dorsal mesoderm and the resulting specification of the component cells to cardiac, visceral, and somatic (body wall) muscle fates (Azpiazu and Frasch, 1993; Bodmer, 1993). *Tin* mutants lack a heart, visceral mesoderm, and the midgut muscles normally derived from this latter tissue. Exogenous expression of *tin* rescues these tissues, although no ectopic cardiac tissue is generated indicating that the role of *tin* is in patterning of the mesoderm rather than as a

master cardiac development gene (Bodmer, 1993). Recent work has shown that the cardiac role of *tin* is, more specifically, to allow cells to adopt a fully functional myocardial fate (including post-embryonic maturation) over an inflow tract fate (Zaffran et al., 2006).

Both *tin* and the downstream mesoderm specification gene *bap* possess dpp-responsive elements which drive their dorsal mesoderm expression (Xu et al., 1998c). Activation of *bap* by Tin specifically in the dorsal mesoderm is dependent on dpp from the ectoderm overlying this region (Staehling-Hampton et al., 1994). Expression of *bap* is stimulated by Tin within eleven segments of the dorsal-most region of the mesodermal *tin* expression domain (Azpiazu and Frasch, 1993). As *bap* is expressed only within sections of the *tin* expression domain there are presumably other genes involved in establishing this segmented pattern; these may take the form of epidermal segmentation genes, as the anterior borders of the *bap* expression segments perfectly match the epidermal parasegments (Azpiazu and Frasch, 1993). Within the segments, an interplay between Hedgehog and Wingless creates differences in *bap* expression: Hedgehog promotes *bap* expression in the anterior, whilst Wingless (via induction of *sloppy paired*) suppresses expression in the posterior (Azpiazu et al., 1996b; Lee and Frasch, 2000).

Both Tin and Bap are required for visceral mesoderm formation. More specifically, both are required for the specification of the segmentally positioned *bap*-expressing cells to develop into the somatic and visceral mesoderm (Azpiazu and Frasch, 1993). The *bap*-expressing cells rearrange such that each segment elongates along the AP axis of the embryo and the cells begin to surround the midgut endoderm. A ventral subset of the cells in each segment adopts a columnar morphology and, when AP elongation is complete, the patches of columnar cells connect, forming the visceral mesoderm (Azpiazu and Frasch, 1993). The midgut musculature subsequently develops from this tissue after the formation of the midgut constrictions. *Tin* mutants, however, lack these constrictions. Formation of the midgut constrictions is also known to be dependent on dpp-mediated transduction of signals from the visceral mesoderm to the underlying endoderm, as formation is disrupted in *Dpp* mutants (Panganiban et al.,

1990). Correct visceral mesoderm development also appears be required for migration of the midgut endoderm as this process is disrupted in *tin* mutants (Azpiazu and Frasch, 1993; Bodmer, 1993). It should be noted that whilst the midgut is severely affected in *tin* mutants, the proventriculus, foregut, and hindgut develop apparently normally (Azpiazu and Frasch, 1993).

Visceral mesoderm differentiation is disrupted in *bap* mutants such that the visceral mesoderm suffers segmental disruptions (~70% of cells are missing); the tissue that is present does not have columnar morphology (Azpiazu and Frasch, 1993). The mesodermal defects appear to be specific to the midgut, even though *bap* is also expressed in the foregut and hindgut mesoderm. The derivative midgut musculature fails to form and some precursor cells are transformed into body wall musculature or gonadal mesoderm (Azpiazu and Frasch, 1993). As in *tin* mutants, the midgut constrictions are also absent in *bap* mutant embryos and midgut endoderm migration is retarded (Azpiazu and Frasch, 1993). Whilst capable of rescuing visceral mesoderm development in *bap* null embryos, ectopic *bap* expression cannot achieve this in *tin* null mutants, indicating an essential upstream role for tin in visceral development (Park et al., 1998a). There is no requirement for *bap* in Tin-mediated cardiac development (Azpiazu and Frasch, 1993).

A couple of Bap target genes have been identified. *Vimar* is expressed in the mid/hindgut visceral mesoderm progenitors and this expression is dependent on Bap (Lo and Frasch, 1998). Another target is *biniou* (*bin*) which is an essential regulator of visceral mesoderm development and is required for differentiation of the circular and longitudinal midgut muscle layers (Zaffran et al., 2001). Murine homologues of *tin (Nkx2-5), bap (Bapx1/Nkx3-2)*, and *bin (FoxF1)* are all expressed in the gut splanchnic mesoderm at E9.5 (data presented in **Section 2.2.1**; (Hecksher-Sorensen et al., 2004; Mahlapuu et al., 2001b)). *FoxF1* is required for correct patterning of the mouse oesophagus and trachea, both foregut-derivatives (Mahlapuu et al., 2001a). *Xenopus FoxF1* is also required for normal gut mesoderm differentiation, but acts upstream of *Xbap* in this process (Tseng et al., 2004).

1.8.3 Vertebrate Nkx *genes*

The 93DE *NK* cluster is essential for mesoderm specification. Clustering of related developmentally important genes is a well documented feature of the *Drosophila* genome, most notably the *Hox* complexes, which also happen to reside on the right arm of chromosome 3 (Kaufman et al., 1980). In the 17 years since the first identification of the *NK* genes many vertebrate *Nkx* genes have been isolated and found to play key roles in the development of the heart, nervous system, and – most importantly for this thesis – the gut. The 93DE *NK* cluster is present in *Amphioxus* as a series of three "mini" clusters scattered along one chromosome: the first contains the orthologues of *tin* and *bap*, the second contains two orthologues of *slou*, and the third contains the *C15* and *Lbx* orthologues (Luke et al., 2003). During vertebrate evolution this series of three clusters has been duplicated and sections lost such that the human genome contains four dispersed clusters. The *tin* orthologue *NKX2-6* and the *bap* orthologue *NKX3-1* lie in extremely close proximity to one another on 8p, and the respective *lbx* and *C15* orthologues *LBX2* and *TLX2* lie very close on 2p (Luke et al., 2003). These occurrences suggest selection for their linkage, potentially on the basis of coregulation. Similarly, a near-full complement of genes is retained on 10q, where orthologues of *tin (NKX2-3), Lbx (LBX1), C15 (TLX1),* and *slou (NKX1-2)* can be found in the same order in which they lie in the amphioxus genome (Luke et al., 2003). Finally, *NKX2-5* (*tin*) and *TLX3* (*Tlx*) are both on chromosome 5q, and *NKX3-2* (*bap*) and *NKX1-1* (*slou*) co-reside on 4p (Luke et al., 2003).

1.8.4 Nkx2-5

1.8.4.1 Similarities to tin

Many homologues of the *Drosophila NK-2* genes can be found across a range of vertebrate genomes, highlighting their developmental importance. These homologues tend to share high homeodomain sequence identity with either *NK2/vnd* (vertebrate *Nkx2* genes) or *NK3/bap* (vertebrate *Nkx3* genes) (Harvey, 1996). Despite this nomenclature, a number of the vertebrate *Nkx2* genes are functionally equivalent to *tin*. It should also be noted that when greater weighting is given to putatively important homeodomain residues these *Nkx2* genes show greater similarity to *tin* and *bap* than *vnd* (Lints et al., 1993b). *Nkx2-5/CSX* is regarded as the major vertebrate *tin* homologue on the basis of its expression (in pharyngeal endoderm and during early cardiogenesis) and function (it is essential for cardiac development across a range of species) (Harvey, 1996). The *tin* cardiac expression pattern is highly conserved in vertebrate *Nkx2-5* genes: expression initiates in splanchnic mesoderm-derived myocardial progenitor cells, and is maintained during differentiation into the heart tube (Harvey, 1996).

Rescue experiments in *Drosophila* using chimaeric Tin proteins - containing various regions of vertebrate Nkx2 proteins - have shown that the cardiac and visceral specification function of the Tin homeodomain has been conserved during evolution, even if the cardiac specification role is not utilised in mice (more on this later) (Ranganayakulu et al., 1998; Park et al., 1998a; Lyons et al., 1995). The divergent regions outside of the homeodomain confer specificity as full-length vertebrate *Nkx2-5* cannot functionally substitute for Tin in *Drosophila* cardiac development (Park et al., 1998a; Ranganayakulu et al., 1998). Visceral mesoderm formation and downstream *bap* expression are, however, rescued. The inability to rescue cardiac specification is probably a consequence of fine-tuning for roles in vertebrate cardiac differentiation, and this being too divergent from the arthropod heart development program. The only full-length vertebrate *tin* homologue able to rescue *Drosophila* cardiac-specific gene expression is zebrafish *Nkx2-3* (Park et al., 1998a). The reason for this is not entirely

clear as of all the zebrafish *tin* homologues *Nkx2-3* shows the weakest heart expression; nor does it share any greater sequence or structural similarity with *tin* than any other vertebrate homologues. The ability of this poorly expressed cardiac gene to rescue heart development - and of other predominantly heart-expressed *Nkx* genes to rescue only visceral development - may allude to the fact that common developmental mechanisms are shared between organs, but that these become interchanged and placed under different regulation during evolution.

Chimaeric protein studies also showed that the cardiogenic domain is located in the N-terminal first 52 amino acids of Tin, as full-length murine Nkx2-5 can rescue *Drosophila* heart development when it is engineered to contain this region (Ranganayakulu et al., 1998). This domain may have been lost during vertebrate evolution, may have diverged to respond to different upstream factors or have different functions, or may have arisen in *Drosophila* following the vertebrate-invertebrate evolutionary split.

Two pieces of evidence from these substitution assays suggest that, despite the marginally closer identity of vertebrate *tin* homologues with *bap* in the homeodomain and NK2-SD sequences, the vertebrate *tin* homologues are functionally most related to *tin*. Firstly, whilst the full-length Tin homologues *Nkx2-5, ZNkx2-7,* and *XNkx2-3* can rescue visceral mesoderm in *tin* mutants, *bap* cannot (Park et al., 1998a). Secondly, this ability appears to be due to a *tin*-like function, as *Nkx2-5* cannot rescue visceral mesoderm in *bap* mutant embryos (Ranganayakulu et al., 1998).

It is plausible that the ancestral role of *tin* was in visceral mesoderm development, and that the cardiac functions evolved independently in the vertebrate and invertebrate lineages. This would fit with the previous suggestion that *tin* may have arisen from duplication of an ancestral *bap* gene and then diverged. Such divergence in sequence and function might explain the differences in heart development between arthropods and vertebrates, and the inability of full-length vertebrate *tin* homologues to rescue heart development in *tin* mutants. The ability of the *tin* homologues' homeodomains to rescue cardiac specification may demonstrate that this conserved domain can be put to multiple uses depending on its genomic context and the selection

of factors with which it associates. Indeed, zebrafish *Nkx2-5* (predominantly expressed in the heart) can rescue pharyngeal muscle development in the *C.elegans ceh-22* (*Nkx2-5/tin* homologue) mutant, supporting the notion of a conserved mechanism underlying vertebrate/insect heart and nematode pharyngeal development (Haun et al., 1998). The nematode pharyngeal muscle develops from foregut visceral mesoderm, and is not only involved in circulation (in place of a cardiac heart), but also in feeding. It has been postulated that the cardiac and gut lineages evolved from an ancestral coelomic structure expressing *tin*-like genes in early multicellular organisms (the "gastroderm") (Bishopric, 2005). Cardiac mesoderm and pharyngeal mesoderm remain the main sites of expression associated with vertebrate *tin* homologues.

1.8.4.2 Differences to tin

The likening of *Nkx2-5/CSX* to *tin* is based on similarities in expression and function, but there are also some important differences in both of these aspects. Most notably, an essential role cannot be demonstrated for *Nkx2-5* in gut development, due to the early lethality of knockout mice (Lyons et al., 1995). Another major difference is that whilst *tin* is essential for specification of the cardiac precursors destined to form the heart tube, *Nkx2-5* loss causes only a differentiation defect which does not become lethal until E9-10, after the beating heart tube has been successfully established (Lyons et al., 1995; Biben et al., 2000; Jay et al., 2004). Commitment of cells to a cardiac lineage is not affected and the linear tube forms normally; it does not, however, express the earliest marker of ventricular differentiation, nor does it undergo looping morphogenesis at E8.25-8.5 (Lyons et al., 1995). Looping of the heart tube is essential for physical separation of the atrial and ventricular chambers and is thought to be under LR control. It should be noted at this juncture that in a further *Nkx2-5* knockout study in which the entire coding sequence was removed – thus ensuring a true null allele – cardiac looping did occur and embryos died slightly later, between E9.5-11.5 (Tanaka et al., 1999a). The reason for this difference is unclear, as other aspects of the reported knockout phenotype

were recapitulated. Null embryos in all published studies have been severely retarded in growth and development, and exhibit pericardial oedema and distension of the veins; it is these factors which appear to cause the embryonic lethality (Lyons et al., 1995). Embryos homozygous for the completely null *Nkx2-5* allele also have major yolk sac defects (Tanaka et al., 1999a).

Interpretation of the differential effect of *tin* and *Nkx2-5* loss on heart development is of course complicated by the differences between vertebrate and arthropod heart development: a ventral complex chambered heart arising from the LPM, versus a dorsal mesoderm-derived tube composed of four rows of cells, respectively (Bodmer and Venkatesh, 1998).

Redundancy between vertebrate *tin* homologues could also serve as an explanation for the less severe cardiac defect. Three members of the vertebrate *Nkx2* family that are very closely related at the sequence level are *Nkx2-3, Nkx2-5*, and *Nkx2-6* (Harvey, 1996). These three genes also show overlapping spatio-temporal expression patterns in a range of vertebrate organisms (see **Table 1.1** and references therein) and loss of function studies have suggested that functional redundancy may indeed exist between them (Lyons et al., 1995; Pabst et al., 1999; Tanaka et al., 2000).

1.8.4.3 Murine Nkx2-5 *expression*

Murine *Nkx2-5* is located on chromosome 17, in the vicinity of the t-locus (Himmelbauer et al., 1994). *Nkx2-5* transcripts and Nkx2-5 protein are detectable within the cardiac crescent from E7.5, in the resulting linear heart tube at E9.0, in the subsequently looped heart tube at E9.5, and in the atrial and ventricular myocardium throughout development and into adulthood (Lints et al., 1993b; Lints et al., 1993a; Komuro and Izumo, 1993; Tanaka et al., 1998a; Kasahara et al., 1998). In addition to the main body of the heart, *Nkx2-5* is expressed in the precursors of the outflow tract which is derived from a secondary heart field, dorsal to the heart (Stanley et al., 2002). Nkx2-5 associates with Tbx5, Tbx20, and Gata4 to promote cardiac differentiation (Hiroi et al.,

2001; Stennard et al., 2003; Durocher et al., 1997), and overexpression during embryonic development results in major heart defects and lethality between E14.5 and birth (Kasahara et al., 2001). *Nkx2-5* is also an early marker of the heart primordia in human, chick, zebrafish and *Xenopus* (Shiojima et al., 1996; Schultheiss et al., 1995; Chen and Fishman, 1996; Tonissen et al., 1994).

Nkx2-5 expression can also be detected in the pharyngeal endoderm precursor region from E8.5-9.5 (Lints et al., 1993b). This may be relevant to cardiac development, as the pharyngeal endoderm is thought to secrete the heart inducer. The pharyngeal-derived thyroid primordium also expresses *Nkx2-5*, as does the developing tongue (Lints et al., 1993b; Kasahara et al., 1998). *Nkx2-5* expression overlaps with that of *Nkx2-3* in the pharyngeal endoderm, *Nkx2-1* in the thyroid, and *Nkx2-6* in the pharyngeal pouches and tongue (Harvey, 1996). Expression can also be detected in a subset of the cranial skeletal muscles, and *Nkx2-5* has been shown to have a role in skeletal myoblast differentiation *in vitro* (Riazi et al., 2005). The full *Nkx2-5* expression pattern is the result of complex regulation; an array of cardiac, thyroid, pharyngeal, and gut enhancers lie upstream of *Nkx2-5* (Schwartz and Olson, 1999). These are discussed in **Chapter 2.**

1.8.4.4 Nkx2-5 *in gut development*

The expression of *tin* in the developing *Drosophila* gut is an evolutionary conserved feature of its homologues: *ceh-22* is expressed in the nematode pharynx (feeding muscle), and *Nkx2-5* expression is present in the developing gut of mouse, chick, and *Xenopus* (Lints et al., 1993b; Buchberger et al., 1996; Tonissen et al., 1994). On the basis of its expression pattern, murine *Nkx2-5* does not appear to be active in gut muscle development, but does appear to be central to other aspects of gut morphogenesis. Nkx2-5 protein is detectable in the E11.5 stomach, E12.5 spleen, and E13.5 dorsal mesentery, with a few positive cells detectable in the E12.5 and E15.5 liver (Kasahara et al., 1998). Expression also rings the distal stomach at E11.5 and E14.5, marking the developing pyloric sphincter (Hecksher-Sorensen et al., 2004; Kasahara et

al., 1998; Lints et al., 1993b). No expression has been detected in the neonatal or adult stomach.

A similar pyloric sphincter expression pattern is noted during chick development. *cNkx2-5* is expressed in the developing gut from stage 18, when it overlaps with *cNkx-2.3* in the mesodermal midgut in which *cNkx-2.3* is more caudally expressed (Buchberger et al., 1996). These domains become increasingly distinct during development until *cNkx2-5* marks only the pyloric sphincter, whilst *cNkx-2.3* is expressed throughout the midgut and hindgut with highest expression abutting the posterior limit of *cNkx2-5* expression. Repression of endogenous *cNkx2-5* activity using a retroviral dominant-negative construct shifts the boundary of *cNkx2-5* expression anteriorly into the gizzard and proventricular mesoderm, and also expands the anterior limit of *cNkx2-3* expression into the gizzard and proventriculus (Smith et al., 2000b). *cNkx2-5* is both necessary and sufficient for development of the epithelial component of the pyloric sphincter (Smith et al., 2000b).

The requirement for *Nkx2-5* in gut development cannot be assessed using any of the published *Nkx2-5* homozygous knockout mice, as these not only die by 9-10dpc (days post coitum), but are also severely growth retarded and so do not develop beyond the 24 somite stage (Lyons et al., 1995). A ventricular-specific knockout has been generated by crossing *Nkx2-5* "floxed" allele mice with mice harbouring a ventricular myocyte-specific Cre, and these survive into adulthood when they present with heart defects similar to those in human *NKX2-5* mutants (Pashmforoush et al., 2004). If a suitable gut mesenchyme-specific Cre line were available then this might provide a way of circumventing the issue of early embryonic lethality. This is discussed further in **Chapter 3**.

1.8.4.5 Nkx2-5 *in spleen development*

Nkx2-5 is a marker of the developing spleen, and this splenic expression has been seen to connect with the distal stomach expression - or the aforementioned dorsal

mesentery expression domain - perhaps suggesting a common mesenchymal origin (Lints et al., 1993b). At E12.5 nearly all cells in the spleen produce Nkx2-5, as do a handful of cells in the neonatal spleen (Kasahara et al., 1998). Embryonic *Nkx2-5* expression appears to reside in the splenic stroma as opposed to the haematopoietic cells, but is not found in stromal cells from other haematopoietic tissues (Lints et al., 1993b). Splenic expression persists into adulthood (Lints et al., 1993b).

Expression of *Nkx2-5* in the spleen is dependent on *Capsulin* and *Pbx1* at E12-12.5, but not on *Hox11* (Brendolan et al., 2005). Brendolan and colleagues also suggest that splenic *Nkx2-5* expression is not affected by *Bapx1* loss – a finding contradictory to evidence from our lab. It should be noted, however, that the *Bapx1*$^{-/-}$ mutants in the Brendolan study are not those generated by and used in our lab's work, but those obtained from Drs W. Zimmer and R. Schwartz. These mutant mice do not appear to have as severe a spleen phenotype as they still possess splenic tissue by E12.5 (Brendolan et al., 2005). Research in our lab supports the dependence of *Nkx2-5* expression on Bapx1, and the requirement for *Bapx1* in spleen development.

The earliest reported origin of the spleen is a patch of condensed mesenchyme lying dorsal to the stomach, close to the pancreas, on the left side of the body cavity at around E10.5-11.0 (reviewed in (Brendolan et al., 2007) and references therein). This tissue is marked by *Nkx2-5* expression from E10.5-12.5 (Lints et al., 1993b; Hecksher-Sorensen et al., 2004). Expression of splenic markers has not been traced earlier than this stage, at which the putative splenic mesenchyme is already located on the left-side of the gut. In *Xenopus*, however, bilateral expression of *XNkx2-5* has been observed in two patches of splenic precursor tissue, one on either side of the body (Patterson et al., 2000).

XNkx2-5 has been implicated in the establishment of asymmetry in the heart and spleen, acting downstream of the left-side-expressed *Pitx2*, and the handedness of gut looping is also correlated with *XNkx2-5* expression (Patterson et al., 2000). *XNkx2-5*-marked splenic precursor cells are initially located on both sides of the embryo, but only the left side cells form the spleen. This loss of right-sided *XNkx2-5*-marked splenic tissue is not due to migration to the left-side or due to loss of these right-side cells by

apoptosis. Instead, the right-hand cells lose *XNkx2-5* expression and their ability to react to spleen induction signals, presumably adopting a different developmental fate (Patterson et al., 2000). Explant studies showed this *XNkx2-5* downregulation to be due to a local signal. If cells competent to become spleen tissue were to initially exist on both sides of the embryo in other vertebrate species, then this might provide a possible explanation for polysplenia. Indeed, mutations in human *NKX2-5* can cause defects in LR visceral asymmetry, including polysplenia (Watanabe et al., 2002).

1.8.4.6 Nkx2-5 *in LR asymmetry*

Murine *Nkx2-5* is intimately associated with the development of LR asymmetry. The homeobox gene *Pitx2* is required for LR asymmetry in the embryo and is itself asymmetrically expressed, on the left side of the LPM and in its derivative organs (Yoshioka et al., 1998; Lu et al., 1999; Lin et al., 1999). Early *Pitx2* expression in the LPM is initiated by Nodal signalling, but maintenance of late (eight somite pair stage through to E10.5) expression in specific organ primordia is achieved through binding of Nkx2-5 to a high-affinity binding site in the *Pitx2* left side-specific enhancer (ASE) (Shiratori et al., 2001). Transgenic embryos in which this enhancer drives *LacZ* exhibit X-gal staining specifically in the left-side of the E10.5 anterior gut dorsal mesentery and heart. Specific mutation of the ASE Nkx2-5 binding site ablates this late expression. The ASE is evolutionary conserved, and can be found in *Xenopus* (Shiratori et al., 2001). Transgenic mouse embryos in which *LacZ* is driven by the *Xenopus* ASE display X-gal staining in most of the endogenous ASE locations, including the E10.5 dorsal mesentery of the anterior gut.

In addition to the above role in maintaining asymmetric gene expression, *Nkx2-5* is also itself under control of the LR asymmetry cascade. *Nkx2-5* is expressed in the left-side mesenchyme of the gut at E10.5, and this expression is ablated when the LR asymmetry gene *Bapx1* is lost (Jacob Hecksher-Sorensen, PhD thesis, University of Edinburgh, 2001).

1.8.4.7 NKX2-5 *mutations – cardiac phenotypes*

Human *NKX2-5* (*CSX*) is located at 5q34-25 and shares 100% identity with murine *Nkx2-5* in its homeodomain (Shiojima et al., 1996). Like *Nkx2-5*, *NKX2-5* is expressed during cardiac development and also in the adult heart (Shiojima et al., 1996). Many *NKX2-5* mutations have been reported. All affected individuals have cardiac defects, and so are detected and reported with respect to these, often with no mention of whether gut defects were investigated. A number of cases of associated gut defects have, however, been described.

A range of cardiac defects are found in patients with *NKX2-5* mutations (Schott et al., 1998; Benson et al., 1999; Hosoda et al., 1999; Zhu et al., 2000; Goldmuntz et al., 2001; Gutierrez-Roelens et al., 2002; Ikeda et al., 2002; Watanabe et al., 2002; McElhinney et al., 2003; Sarkozy et al., 2005; Gutierrez-Roelens et al., 2006). The most common are atrial septal defect (ASD) and AV (atrioventricular) conduction block. Other common phenotypes include left ventricular hypertrophy, ventricular septal defect (VSD), pulmonary valve stenosis/atresia, and mirror-image arch branching. Less frequent effects include sub valvular aortic stenosis, and the presence of a double outlet (outflow tract) in the right ventricle (DORV). Many of these malformations are commonly associated with defects in LR asymmetry, particularly ASD, VSD, and DORV (Ramsdell, 2005). Accordingly, many of these defects also overlap with those associated with asplenia and polysplenia. For example, DORV is found in ~82% of asplenia cases, and AV conduction block is present in ~22% of polysplenic individuals (Bartram et al., 2005).

All reported *NKX2-5* mutations are heterozygous; this is in contrast to the situation in mouse in which both copies of the gene must be non-functional to cause a phenotype. When survival permits reproduction, the human mutations are transmitted in an autosomal dominant fashion. Multiple mutations (up to 14) can be present in one individual; these are usually of a somatic origin and are specific to the diseased tissue (Reamon-Buettner and Borlak, 2004). Multiple mutations have also been detected in

Down's syndrome patients with cardiac abnormalities (Reamon-Buettner and Borlak, 2004).

A correlation between genotype and phenotype is not obvious from the mutations reported thus far, although it has been proposed that missense mutations in the homeodomain and nonsense/frameshift mutations confer the most severe AV block (Hirayama-Yamada et al., 2005). Reported functional effects include reduction/loss of DNA binding affinity, reduction/loss of transactivation ability, loss of homodimerisation ability, and dominant-negative reduction of transactivation by the wild type protein through homodimerisation (Kasahara et al., 2000). Expression of a mutant Nkx2-5 which cannot bind DNA, on a wild type background from embryonic stages and into adulthood, also causes progressive heart failure in mice, most notably due to AV conduction block (Kasahara et al., 2001).

The reason for the difference in severity between mouse and human *Nkx2-5/NKX2-5* loss is unclear. Heterozygous loss of murine *Nkx2-5* has produced no obvious effect in two studies (Lyons et al., 1995; Tanaka et al., 1999a). This may be indicative of functional redundancy between murine cardiac (*Nkx*) genes. Yet as the homozygous null phenotype is so severe it also seems that there is an essential requirement for *Nkx2-5* during early cardiogenesis. This requirement appears to be even more profound during human development as a mutant phenotype is produced by the functional loss of just one copy of *NKX2-5* and no homozygous mutants have been recorded. Of course, an element of detection bias may exist if only the most severely affected heterozygotes require medical treatment. This may corroborate with findings from two more recent studies which showed that *Nkx2-5* haploinsufficieny can occur in mice, with the result that heterozygous knockout mice can have cardiac development phenotypes; such occurrences are, however, rare or difficult to detect (Biben et al., 2000; Jay et al., 2004).

1.8.4.8 NKX2-5 *mutations – gut phenotypes*

Four deletions have been reported that result in total loss of the NKX2-5 homeodomain (Watanabe et al., 2002; Hirayama-Yamada et al., 2005; Konig et al., 2006). One of these deletions removes seven nucleotides (nucleotides 215-221) resulting in a frameshift from residue 72 and subsequent loss of the homeodomain and truncation at amino acid 172 (Watanabe et al., 2002). This was associated with a number of cardiac abnormalities typical of *NKX2-5* mutations, but also a range of gut defects. One of the members of the affected family had cardiac abnormalities and also presented with a midline liver, gut malrotation and polysplenia – all suggestive of fundamental defects in the development of gut asymmetry. This heterotaxy was specific to the gut as the heart and lung were correctly positioned. Furthermore, one of the offspring of this individual had pyloric stenosis in addition to heart defects, and thus both the gut tissues in which *Nkx2-5* is developmentally expressed were abnormal in individuals with this mutation. This may be the first evidence that *NKX2-5* plays an essential role in the development of the spleen and pyloric sphincter. Intriguingly, an association between pyloric stenosis and congenital heart defects (of unknown aetiology) has been proposed, though this does not seem to be major (Mehta and Ambalavanan, 1997). These two birth defects also occur together in a number of syndromes.

The loss of the homeodomain in the above mutation is particularly interesting given that such loss is predicted to prevent dimerisation, and that positive autoregulation of/by Nkx2-5 is proposed to exist in the murine gut (Tanaka et al., 1999c). This homeodomain-less protein may also be exerting a dominant-negative effect as a heterozygous 2.2Mb 5q35 deletion – which totally removes the *NKX2-5* gene - confers only heart defects, and not any reported gut abnormalities (Baekvad-Hansen et al., 2006). It would thus appear that simple loss of one copy of *NKX2-5* is compatible with normal gut development, though of course interacting loci could modulate this situation. The link between *Nkx2-5* haploinsufficieny and cardiac defects in heterozygous knockout mice - discussed earlier - was significantly affected by genetic background

(Biben et al., 2000; Jay et al., 2004); a similar caveat may therefore apply to human gut defects.

Why gut defects have only been seen in two affected individuals is an interesting issue. It may of course be that the gut defects were the effect of a second mutated gene, either directly or through interplay with *NKX2-5*. Another hypothesis is that gut defects may be a more prevalent component of the *NKX2-5* mutant phenotype but that they simply go undetected. Although pyloric stenosis would require medical attention, polysplenia often goes undiagnosed as it does not present any major health issues. The role of *NKX2-5/Nkx2-5* in gut development is thus a very interesting, yet poorly understood, area of research.

In addition to heart and gut abnormalities, thyroid dysgenesis has also been reported in four *NKX2-5* missense mutation patients (Dentice et al., 2006). Consequently, thyroid development was re-examined in *Nkx2-5*$^{-/-}$ embryos and found to be disrupted due to a reduction (<50%) in the number of precursor cells in the thyroid buds (Dentice et al., 2006).

1.8.5 Bapx1 (Nkx3-2)

1.8.5.1 Bapx1 *in vertebrate development*

The sequences of the *bap* homeodomain, TN, and NK-2 domains are well conserved in the vertebrate homologue *Bapx1* (*Nkx3-2*), as are aspects of *bap* function and expression (Tribioli et al., 1997). One novel aspect of *Bapx1* function is its role in regulating patterning of the mammalian middle ear (Tucker et al., 2004). This is an evolutionary adaptation of the role of *Bapx1* in jaw development in non-mammalian vertebrates (Miller et al., 2003). *Bapx1* also plays an important role in skeletal patterning and development of the basal skull (Lettice et al., 1999b) – another function not associated with fly *bap*. Bapx1 promotes somitic chondrogenesis through its action as a

transcriptional repressor, and a chondrogenic *Bapx1/Sox9* positive autoregulatory loop is established and maintained in response to Shh/BMP signals (Murtaugh et al., 2001; Zeng et al., 2002). In addition, *Bapx1* plays roles in limb development in chick (Provot et al., 2006; Church et al., 2005). Murine *Bapx1* is also expressed in the proliferative zone of the limb bud, though no limb defects have been observed in mice deficient for *Bapx1* (Lettice et al., 1999b).

1.8.5.2 Bapx1 *mutants*

A number of *Bapx1* knockout mouse lines have been generated, and the resulting phenotypes are fairly consistent (Lettice et al., 1999b; Tribioli and Lufkin, 1999; Akazawa et al., 2000). In the first report, Lettice and colleagues engineered an insertion mutation by placing the *neomycin*-resistance cassette into the first exon of *Bapx1* (Lettice et al., 1999b). Skeletal and spleen development were disrupted in mice homozygous for this allele (discussed in **Section 1.8.5.5**), and these died neonatally due to respiratory problems. There was however the possibility that the mutants expressed a weak allele of *Bapx1*, as a spliced transcript (corresponding to the 3' coding region) was detected at low-levels. This interpretation is supported by the existence of a slightly more severe array of skeletal defects in the null mice generated in two further studies (described below), though it should be noted that the majority of the phenotypes observed are shared between all three lines.

Akazawa and colleagues produced a total null allele by replacing the entire *Bapx1* coding sequence with a cassette including *LacZ*, thus allowing analysis of expression in heterozygotes (Akazawa et al., 2000). Expression was observed in previously reported regions of endogenous *Bapx1* expression, and the gut expression was confirmed to be solely mesenchymal. Major expression occurred in the E13.5 mesenchymal spleen and this persisted in the red pulp, capsule, and central arterioles of the adult spleen. The adult gut also expressed *LacZ* in the muscle layers of the stomach, pyloric sphincter, and – to a lesser extent – duodenum. The homozygous knockout mice

exhibited asplenia, gastroduodenal malformations, and neonatal lethal skeletal dysplasia. In the third study, Tribioli and Lufkin generated a similar null allele – removing nearly all the *Bapx1* coding sequence - and observed comparable effects in homozygous mutants (Tribioli and Lufkin, 1999).

Based on the murine *Bapx1* knockout phenotypes, mutations in human *BAPX1* might be expected to produce similar effects. Intriguingly, axial skeleton defects show some association with poly- and asplenia in humans (Aylsworth, 2001). However, whilst the genomic region in which *BAPX1* resides has been associated with inherited skeletal disorders, *BAPX1* itself has not been reported to be mutated in any human diseases. Despite this lack of disease-causing mutations, *BAPX1* has however been implicated in a human disorder: oculo-auriculo-vertebral spectrum (OAVS) (Fischer et al., 2006b). OAVS is the second most common craniofacial birth defect, and comprises a range of developmental anomalies – often unilaterally - including ear malformation, vertebral defects, and facial abnormalities. *Bapx1*-deficient mice exhibit the first two of these phenotypes (Tucker et al., 2004; Lettice et al., 1999b). The cause of OAVS is not, however, due to simple loss of *BAPX1* expression, but instead attributed to a strong allelic expression imbalance (Fischer et al., 2006b). This imbalance is dependent on histone deacetylation – i.e. epigenetic *BAPX1* dysregulation. This imbalance appears to predispose to OAVS, as a similar imbalance is also observed in unaffected relatives of patients but not in unrelated unaffected controls. Gut defects were not however detected in this study, nor are they a known component of OAVS, though anal atresia and tracheo-oeosophageal fistula have been seen in two OAVS sufferers (aetiology unknown) (B. Horsthemke, personal communication).

1.8.5.3 Bapx1 *in gut development*

Like *Bap*, *Bapx1* is essential for correct visceral mesoderm development; it does not, however, share *Bap*'s role in controlling midgut muscle development (Akazawa et al., 2000; Tribioli and Lufkin, 1999). Nor does the other mammalian *Bap*-like gene,

Nkx-3.1, perform this role, suggesting that the function of *bap* in midgut musculature development has not been retained in mammals. This is not to say that it has not been conserved in vertebrates, as the role appears to have been delegated to a third, amphibian-specific homologue: *XNkx-3.3/zax* (Lettice et al., 2001).

1.8.5.4 Bapx1*: a target and promoter of the LR asymmetry pathway in the gut*

One striking difference between the expression pattern of *bap* and *Bapx1* is that whilst the former is expressed in a bilaterally symmetrical manner, the vertebrate homologue exhibits LR asymmetric expression and serves as a link between gut development and the signalling pathway that establishes LR asymmetry (Schneider et al., 1999; Hecksher-Sorensen et al., 2004). This is discussed in more detail in **Section 1.9**.

Human, mouse, chick, and *Xenopus BAPX1/Bapx1/XbapI* are expressed in the splanchnic mesoderm from which the visceral musculature is derived (Tribioli and Lufkin, 1997; Tribioli et al., 1997; Schneider et al., 1999; Newman et al., 1997). The role of *Bapx1* (*cNkx3-2*) has been well studied in chick. c*Nkx3-2* is initially expressed on the left-side of the anterior LPM - overlapping the left-side marker *Pitx2* - due to promotion by the left-side genetic pathway headed by Shh and repression on the right-side by Fgf8 (Schneider et al., 1999). Expression then shifts to a more bilateral state in the anterior gut mesoderm and becomes restricted to the gizzard, with no expression in the flanking proventriculus or duodenum; expression then becomes strongest in the distal-most portion of the gizzard, bordering the pyloric sphincter from which it is absent (Schneider et al., 1999; Nielsen et al., 2001). Ectopic *cNkx3-2* expression in the proventricular mesoderm is sufficient to induce a gizzard phenotype in the underlying epithelium (Nielsen et al., 2001). This proventricular misexpression also affects the mesoderm itself and causes inappropriate thickening such that the normally left-sided bulge of the proventriculus is at the midline or flipped to the right. This disruption of

normal asymmetry may be the result of the inappropriate bilateral expression of ectopic *cNkx3-2* in the presumptive stomach mesoderm when it ought to be only left-sided.

The requirement for *cNkx3-2* in avian gut development has been assessed using a "reverse-function" mutant, so called because cNkx3-2 was transformed from a transcriptional repressor into an activator (Nielsen et al., 2001). This reversal of function (specifically in the endogenous gizzard mesoderm expression site) produced a reduced stomach with a thin muscle layer, as seen with ectopic *Bmp4* expression in the gizzard (Nielsen et al., 2001). This suggests that cNkx3-2 may normally inhibit *Bmp4* in the gizzard, and is supported by the presence of ectopic *Bmp4* (and *Wnt5a*) expression in this tissue. The role of *cNkx3-2* in chick gut development thus appears to be in regulating muscle thickness.

The initially left-sided expression in chick is the reverse of the situation in mouse, in which *Bapx1* is expressed on the right-side of the LPM at E8.5 (Schneider et al., 1999). However, by E9.5 expression is roughly symmetric (Lettice et al., 2001). By E10.5, expression has shifted to the left of the embryo, in the splenic mesenchyme underlying the splanchnic mesothelial plate (SMP) and in the lateral-most part of the SMP (Lettice et al., 2001). Despite the differences in early asymmetric expression between mammalian and avian *Bapx1*, both genes are under the control of the LR signalling pathway, as shown by disruption of these expression patterns in embryos with altered LR asymmetry (Schneider et al., 1999) [10]. Following establishment of LR asymmetry, *Bapx1* expression is maintained during gut organogenesis in the mesoderm overlying the stomach, midgut, and splenic primordium, and is downregulated at E16.5 (Tribioli et al., 1997).

[10] More specifically, following ectopic expression of chick asymmetry factors, and in the *inv* (*inversion of turning*) mouse mutant which has complete *situs inversus* (Yokoyama et al., 1993)

1.8.5.5 Effects of Bapx1 *loss in the gut*

A major aspect of the mouse *Bapx1*-loss phenotype is abnormal morphogenesis of the stomach-duodenal region (Akazawa et al., 2000). *Bapx1* regulates the shape of the stomach and duodenum by controlling regional cell proliferation rates (Watson et al., 2007). More specifically, *Bapx1* is required to downregulate proliferation in the endoderm of the duodenum and therefore maintain the narrow diameter of this section of the gut tube; thus in *Bapx1*$^{-/-}$ mutants inappropriate proliferation occurs and so the duodenum becomes abnormally wide (Watson et al., 2007). This widened duodenum is indistinguishable from the posterior stomach as early as E10.5 and thus *Bapx1* is required for specifying the AP boundary in this region. The mutant duodenum also folds back and fuses with the stomach by ~E12.5, and may branch ectopically. A further aspect of the *Bapx1*$^{-/-}$ phenotype is that the dorsal pancreatic bud remains at the midline and develops along an axis almost parallel to the stomach, as opposed to lying perpendicular to it (Hecksher-Sorensen et al., 2004).

The pyloric sphincter constriction is absent in *Bapx1*$^{-/-}$ mutants and the abnormally shaped stomach does not narrow before meeting the region where the sphincter would normally be located (Akazawa et al., 2000; Watson et al., 2007). The abnormal pyloric region is still, however, populated by normally differentiated smooth muscle cells; this indicates that the role of *bap* in midgut musculature development has not been retained by *Bapx1* (Akazawa et al., 2000). Some aspects of duodenal morphology are observable in the enlarged posterior stomach (Watson et al., 2007). The stomach villi appear to be transformed to an elongated duodenal phenotype. Additionally, the circular muscle layer is thinner, the longitudinal layer develops precociously, and the muscularis mucosa layer is absent in the posterior stomach of E18.5 *Bapx1*$^{-/-}$ mutants – all characteristics of the duodenum (Watson et al., 2007). However, given that the duodenum is already expanded, and thus indistinguishable from the posterior stomach, by E10.5 it would seem that the abnormal foregut-midgut tissue seen at E18.5 is not the result of transformation of stomach to duodenal tissue, but rather

due to the "transformed" stomach tissue actually being expanded duodenal tissue in the first place. This expanded duodenal tissue does, however, take on expression of some stomach-specific markers[11].

Although *Bapx1* and *Nkx2-5* expression do not overlap within the established pyloric sphincter[12], their domains do show some slight overlap in the SMP at E10.5 (Hecksher-Sorensen et al., 2004). This is also the point at which the pyloric sphincter is thought to begin developing and thus at which its absence is first conspicuous. Loss of the pyloric sphincter is associated with loss of pyloric *Nkx2-5* expression at E12.5 in *Bapx1*$^{-/-}$ mice (Watson et al., 2007). This suggests that *Bapx1* may regulate *Nkx2-5*. Alternatively, loss of this pyloric marker could simply be a consequence of a sphincter cell deficiency due to absence of another Bapx1-mediated mechanism. A role for *Nkx2-5* in pyloric sphincter development has been demonstrated in chick (Smith et al., 2000b). However, the hierarchy of *Nkx* genes in the chick gut appears to be different to that in the mouse: *Nkx2-5* expression – along with that of *Nkx2-3*, *Pitx2,* and *Pdx1* - is not affected by ectopic *Bapx1* expression in chick (Nielsen et al., 2001).

1.8.5.6 Bapx1 *in spleen development*

As with *bap* inactivation, loss of *Bapx1* expression causes abnormalities in the visceral mesoderm. However, whilst gut muscle development is disrupted in the *Drosophila* mutants, mice null for *Bapx1* show other visceral abnormalities including disrupted spleen development (Lettice et al., 1999b; Tribioli and Lufkin, 1999; Akazawa et al., 2000). This role in spleen development is an evolutionary adaptation as the spleen is a vertebrate-specific organ.

---

[11] SOX2, a marker of the stomach epithelium, is expressed, whilst the duodenal markers *Shh* and alkaline phosphatase activity are absent (Watson et al., 2007).

[12] *Nkx3.2* is expressed anterior to the pyloric sphincter but not within the constriction itself. *Nkx2-5* is expressed at a more posterior level, including in the pyloric sphincter constriction

The coelomic splanchnic mesothelium and underlying mesenchymal cells which condense to form the spleen express *Bapx1* at E10.5; these precursors appear to be absent from *Bapx1*$^{-/-}$ mutants at E11.5 - the point at which spleen development would normally be observed (Tribioli and Lufkin, 1999). It has alternatively been reported that some spleen precursors are still present at E14.5, and form a sparse splenic "scaffold" which fails to condense and subsequently regresses (Akazawa et al., 2000). The loss of this scaffold and the mesenchymal cells therein has been attributed to failure of lymphocytes to home to the region, perhaps due to loss of interactions with splenic mesenchyme (Akazawa et al., 2000). Our observation is that fatty mesentery tissue is present in place of the spleen, and ectopic intestine-like cysts are present in the splenic region in approximately half of the *Bapx1*$^{-/-}$ mutants (discussed in **Section 1.9.4.1**) (Asayesh et al., 2006). Bapx1 may normally promote maintenance of the spleen through *Hox11*, as this splenic marker is not expressed at E12.0 or E14.5 in *Bapx1*$^{-/-}$ mutants (Lettice et al., 1999b; Akazawa et al., 2000).

1.8.6 Other vertebrate Nkx *genes*

Vertebrate homologues exist for all of the genes in the *Drosophila* 93DE *NK* cluster, with multiple homologues existing for some within a single species. Vertebrate *Nkx* genes also exist which have no direct homologue in the 93DE cluster (murine *Nkx5-1/Hmx3*, *Nkx5-2/Hmx2*)[13] (Bober et al., 1994). Details of the vertebrate *Nkx* genes are summarised in **Table 1.1**.

[13] *Drosophila Hmx* has since been identified in the 90B5 region of chromosome 3 (Wang et al., 2000b)

Gene	Species	Expression, gain/loss of function phenotype, interactions	References
Nkx1-1 (sax2)	Zebrafish	Midbrain, hindbrain, spinal cord	(Bae et al., 2004)
	Mouse	Murine homologue of *NK1* (see *Nkx1-2*)	(Bober et al., 1994)
Nkx1-2 (sax1)	Zebrafish	Neuroectoderm, **anus**	(Bae et al., 2004)
	Chick	Neural plate, spinal cord	(Spann et al., 1994)
	Mouse	Posterior CNS. Formerly named *Nkx1-1*	(Schubert et al., 1995)
Nkx2-1	Xenopus	Forebrain, thyroid, lung	(Small et al., 2000)
	Mouse (*Ttf1*) (*T/EBP*)	Forebrain	(Price, 1993)
		Knockout: no thyroid gland; lung and brain defects; no pituitary gland; lethal by birth	(Kimura et al., 1996)
		Knockout: **foregut septation between oesophagus and trachea fails**, lungs do not undergo branching morphogenesis; lethal postnatally (respiratory insufficiency)	(Minoo et al., 1999)
	Human	Heterozygous loss of function mutations (5 patients) cause hypothyroidism, choreoathetosis (involuntary movements due to basal ganglia defects), lung problems	(Krude et al., 2002)
Nkx2-2	Mouse	Forebrain	(Price, 1993)
		Dorsal pancreatic bud endoderm from E9.5 **Null mice develop diabetes due to incomplete β-cell differentiation**	(Sussel et al., 1998)
		Maintains *Nkx6-1* expression in β-cells - necessary for their full differentiation	(Sander et al., 2000)
Nkx2-3	Xenopus	**Embryonic small intestine and posterior stomach**	(Smith et al., 2000a)
		Early heart; pharyngeal endoderm; **adult intestine, spleen,** heart	(Evans et al., 1995)
		Cardiac overexpression causes a functional enlarged heart (myocardial hyperplasia)	(Cleaver et al., 1996)
		Suppression by dominant-negative form is lethal - cardiac differentiation blocked	(Grow and Krieg, 1998)
	Zebrafish	Pharyngeal and **gut endoderm; mid/hindgut epithelium**; not in heart	(Lee et al., 1996)
	Chicken	Differentiated myocardial cells, branchial arches, **mid/hindgut mesoderm – anterior limit meets posterior of pyloric sphincter *Nkx2-5*; adult mid/hindgut**	(Buchberger et al., 1996)
	Mouse	**E9.5 gut mesenchyme posterior to stomach**; pharyngeal epithelium, branchial arches, tongue epithelium, jaw; not in heart	(Pabst et al., 1997)
		Highly expressed in adult spleen *Knockout*: **Asplenia or reduced spleens, delayed villus formation; postnatal lethality from intestinal malabsorption in majority of mutants**	(Pabst et al., 1999)
Nkx2-4	Xenopus	Ventral diencephalon	(Small et al., 2000)
	Mouse	Forebrain	(Price, 1993)
Nkx2-5	Xenopus	Heart, pharyngeal endoderm, **gut**	(Tonissen et al., 1994)
		Cardiac overexpression causes a functional enlarged heart (myocardial hyperplasia)	(Cleaver et al., 1996)
		Suppression by dominant-negative form is lethal - cardiac differentiation blocked	(Grow and Krieg, 1998)

	Zebrafish	Cardiac precursors from gastrulation (more akin to *Drosophila* than vertebrate); initiates cardiogenic differentiation; no expression detected in non-cardiac tissues Overexpression causes enlarged heart; higher levels randomize cardiac looping	(Chen and Fishman, 1996)
		Cardiac primordia, heart tube; transient low expression in pharyngeal endoderm	(Lee et al., 1996)
	Chicken	Cardiac primordia, heart tube; cardiac muscle; pharyngeal endoderm & ectoderm	(Schultheiss et al., 1995)
		Precardiac mesoderm, adult heart; precedes cardiac *Nkx2-3*; branchial arches; **pyloric sphincter, mid/hindgut mesoderm; becomes restricted to pyloric sphincter**	(Buchberger et al., 1996)
	Mouse	Myocardiogenic progenitors; heart, anterior endoderm (an inducer of cardiac precursors); thyroid primordium, **stomach, spleen**; adult heart, **spleen**, tongue	(Lints et al., 1993b)
		Heart primordia from E7.5; E12.5 heart, pharyngeal endoderm, **distal stomach, spleen,** subset of cranial skeletal muscles, E15.5 tongue	(Tanaka et al., 1998a)
		Protein: Cardiac cells from 7.8dpc; **E11.5 & E13.5 stomach; throughout E12.5 spleen, some expression in neonatal spleen**; tongue, subset of cranial muscles	(Kasahara et al., 1998)
		Knockout: null embryos die by E9-10 as *Nkx2-5* required for looping morphogenesis, though not for specification of cardiac lineage	(Lyons et al., 1995)
	Human	Foetal and adult heart	(Shiojima et al., 1996)
Nkx2-6	Mouse (*Tlx*)	E8.5-10.5 heart, pharyngeal endoderm; E14.5 heart, tongue, hypothalamus	(Tanaka et al., 1998a)
		E8-8.5 myocardium, foregut/pharyngeal endoderm, E9.5 outflow tract; **ventral hindgut endoderm from E9.5; foregut-midgut junction from E9.5-11 – includes the proximal region of the common bile and dorsal pancreatic ducts**	(Biben et al., 1998)
		Knockout: Homozygous mutant mice are viable and fertile; no obvious phenotype. *Nkx2-5* expression domain expanded in pharynx.	(Tanaka et al., 2000)
	Human	Mutation in homeodomain associated with failure of outflow tract septation	(Heathcote et al., 2005)
Nkx2-7	Zebrafish	Heart – prior to *Nkx2-5*; endoderm that gives rise to pharyngeal & **gut endoderm** – prior to *Nkx2-3, Nkx2-5*. Similar pattern to murine *Nkx2-6*	(Lee et al., 1996)
Nkx2-8	Chicken	Heart tube - undetectable after looping; pharyngeal pouches	(Reecy et al., 1997)
Nkx2-9	Mouse	Ventral CNS domains, neural tube structures	(Pabst et al., 1998)
		Homozygous mutant mice are viable and fertile; abnormal spinal accessory nerve	(Pabst et al., 2003)
Nkx3-1	Xenopus (*koza*)	Somitic muscle, myocardium of heart, cement gland; may regulate cell proliferation; regulated by hedgehog signalling	(Newman and Krieg, 2002)
	Mouse (*Bax*)	Developing prostatic buds (neonate), adult prostate gland; androgen-dependent	(Bieberich et al., 1996)
		Somites, dorsal aorta, tongue, tooth buds, urogenital sinus, kidney arteries	(Tanaka et al., 1999b)
		Knockout: mice are viable and fertile; defects in prostate and minor salivary glands	(Schneider et al., 2000)
	Human	Adult prostate; androgen regulated	(He et al., 1997)
Nkx3-2/	Xenopus	**Midgut musculature**, facial cartilage (*Xbap*)	(Newman et al., 1997)

Bapx1	Chicken	**Left LPM, then bilaterally in gizzard mesoderm; not in proventriculus, pyloric sphincter, or duodenum** **Negatively regulates *Bmp4* & *Wnt5a* in gizzard** **Essential for normal stomach development & gut LR asymmetry**	(Nielsen et al., 2001)
		Asymmetric expression in left LPM, then becomes more bilateral. Target of LR signalling; downstream of left-side *Shh* and inhibited on right by Fgf8	(Schneider et al., 1999)
	Mouse	Lateral plate & **splanchnic mesoderm**, skeleton, branchial arches (mandible)	(Tribioli et al., 1997)
		Asymmetric expression in right LPM, then becomes more bilateral. Stomach mesoderm at E9.5. Target of LR signalling	(Schneider et al., 1999)
		Controls development of axial skeleton, skull, & **spleen**	(Lettice et al., 1999b)
		Expression highest in right LPM at E8.5; bilateral by E9.5 **E10.5 dorsal pancreatic mesenchyme, associated with spleen development.** **Role in patterning gut mesoderm, but not in gut musculature** E10.5 limb mesenchyme, 1st branchial arch, sclerotome	(Lettice et al., 2001)
		Null: **Asplenia, gastroduodenal malformation**, and lethal skeletal dysplasia	(Akazawa et al., 2000)
		Activated by Pax1 & Pax6 to induce chondrogenic differentiation in sclerotome	(Rodrigo et al., 2003)
		Regulates patterning of the middle ear	(Tucker et al., 2004)
	Human	Limb & skeletal mesenchymal condensations, **LPM/splanchnic mesoderm (ventral stomach, patches in hindgut)**. Maps to region associated with skeletal disorders	(Tribioli and Lufkin, 1997)
		Allelic imbalance of *BAPX1* implicated in oculo-auriculo-vertebral spectrum (OAVS) - ear malformation, vertebral defects, and facial abnormalities.	(Fischer et al., 2006b)
Nkx3-3	Xenopus (*zax*)	**Midgut musculature (at level of future stomach),** pharyngeal endoderm	(Newman and Krieg, 1999; Lettice et al., 2001)
Nkx5-1 (Hmx3)	Mouse	E10.5 otic vesicle, neural tube, dorsal root ganglia; E11.5-14.5 ear, head/branchial arch mesenchyme, cranial ganglia, optic cup; **E13.5 myenteric ganglia of stomach**	(Bober et al., 1994)
		LacZ knock-in: **E10.5 stomach (muscle), E12.5 oesophagus**, trachea, atria of heart	(Wang et al., 2000b);
Nkx5-2 (Hmx2)	Mouse	CNS and inner ear from E13.5; colocalises with *Nkx5-1*	(Rinkwitz-Brandt et al., 1995)
Nkx6-1	Zebrafish	Motoneurons; downstream of Hh	(Cheesman et al., 2004)
	Chicken	**Foregut endoderm; can be induced by Pdx1 in anterior endoderm**	(Pedersen et al., 2005)
	Mouse	Subset of motor neurons	(Qiu et al., 1998)
		Pancreatic β-cells	(Rudnick et al., 1994)
		Downstream of *Nkx2-2* in pancreatic epithelium from E10.5 ***Knockout*: Loss of β-cell precursors in null mice**	(Sander et al., 2000)

		E9.5 dorsal pancreatic bud, E10.5 ventral pancreatic epithelium	(Alanentalo et al., 2006)
		E12.5 anterior stomach mesenchyme; pancreatic epithelium at E12.5, E16.5	(Nelson et al., 2005)
		Pdx1 dependent	(Pedersen et al., 2005)
Nkx6-2	Chicken	**Epithelium of pancreas, caudal stomach and rostral duodenum**	(Pedersen et al., 2005)
	Mouse	Neural tube from E8.5	(Vallstedt et al., 2001)
		Knockout: mice are viable and fertile with no observable mutant phenotype	(Cai et al., 2001)
		Dorsal and ventral pancreatic buds at E9.5 - down regulated at E16.5; E10.5 stomach and duodenum endoderm/epithelium, restricted to glandular (posterior) stomach epithelium from E12.5, anterior to pyloric sphincter	(Alanentalo et al., 2006)
Nkx6-3	Chicken	**Transiently in pancreatic endoderm; later in caudal stomach, rostral duodenum**	(Pedersen et al., 2005)
	Mouse	**E12.5 and E16.5 posterior stomach and duodenal epithelium**	(Nelson et al., 2005)
		Central nervous system (hindbrain); **duodenal and glandular stomach endoderm from E10.5, restricted by E12.5 to region spanning pyloric sphincter**	(Alanentalo et al., 2006)

***Table 1.1* - Vertebrate developmentally expressed *Nkx* genes**
Details of *Nkx* gene expression patterns, interactions and mutations are provided in this table. The information is not exhaustive, as homologues may also be present in other species, but is based on current knowledge.

1.8.6.1 Other vertebrate Nkx *genes in gut development*

A number of other *Nkx* genes are expressed in the developing gut. A common feature of these genes is that they are involved in patterning of the gut along the DV axis. Most of the organ primordia of the GI tract are formed by budding morphogenesis of the gut tube along the DV axis, and these endodermal gut derivatives often express *Nkx* genes or underlie *Nkx*-expressing mesoderm. Examples include the thyroid (*Nkx2-1, Nkx2-5*), lungs (*Nkx2-1*), and pancreas (endodermal *Nkx2-2, Nkx2-6, Nkx6-1, Nkx6-2;* mesenchymal *Nkx2-5, Nkx3-2*) (see **Table 1.1** for references). *Nkx2-5*, *Nkx3-2* and *Nkx5-1* are expressed in the E10.5 gut mesoderm, with the first two of these genes also being splenic markers ((Hecksher-Sorensen et al., 2004; Wang et al., 2000b); Weidong Wang, personal communication).

The spleen is a hub of *Nkx* gene activity. *Nkx2-3, Nkx2-5, Nkx3-2,* and *Hox11* are all expressed during spleen development (Pabst et al., 1999; Lints et al., 1993b; Lettice et al., 1999b; Roberts et al., 1994; Roberts et al., 1995a). *Hox11* (*Tlx1*) is one of the three murine homologues of *Drosophila C15/93Bal/311*, the other two being *Tlx2 (Hox11L1)* and *Tlx3 (Hox11L2)* (Kennedy et al., 1991; Dear et al., 1993; Dear and Rabbitts, 1994). *Hox11*-null mice are asplenic (Roberts et al., 1994; Dear et al., 1995).

A further splenic *Nkx* gene is *Nkx2-3*. This *tin*-like gene is expressed in the gut mesenchyme at a level posterior to the stomach from E9.5; intestinal mesenchyme represents the predominant expression site both during development and in adulthood (Pabst et al., 1997). Loss of *Nkx2-3* leads to abnormal development of the spleen and small intestine, and in ≥30% of births results in postnatal lethality due to intestinal malabsorption (Pabst et al., 1999; Wang et al., 2000a). *Nkx2-3* is also expressed in mesenchymal (stromal) cells of the developing spleen, and in the adult spleen (Pabst et al., 1999). *Nkx2-3*$^{-/-}$ mice have a variable spleen defect in addition to a decrease in the number and size of Peyer's patches – another secondary lymphoid organ (Wang et al., 2000a). Surviving postnatal mutants have an abnormal T cell-dependent immune response (Wang et al., 2000a). Spleen abnormalities range from a severe reduction in the size of the organ (and the number of lymphatic cells

therein) and disorganisation, to full asplenia (20-36% of births) (Pabst et al., 1999; Pabst et al., 2000; Wang et al., 2000a).

The splenic disorganisation in *Nkx2-3*$^{-/-}$ mice is a result of stromal rather than haematopoietic defects, as bone marrow reconstitution cannot rescue the mutant spleen phenotypes (Tarlinton et al., 2003). Abnormal lymphocyte homing causes the reduction in certain cell types in the spleen. Nkx2-3 can activate transcription of *Madcam1*, expression of which is lost in the knockout mice, apparently leading to the failure of lymphocyte homing in the spleen (Pabst et al., 2000; Wang et al., 2000a). The sinus-lining non-lymphoid cells which normally express *Madcam1* are thought to regulate passage of lymphocytes and antigens into the white pulp from the blood (Tanaka et al., 1996).

1.8.7 An Nkx *code?*

The overlapping expression patterns, functions, and DNA-binding specificities of Nkx gene family members, coupled with null phenotypes less severe than predicted, is suggestive of genetic redundancy. Specific combinations of Nkx genes in particular regions may be required for the specification of developmental fates, and form an "Nkx code". Examples may include heart (*Nkx2-3, Nkx2-5, Nkx2-6*), pharynx (*Nkx2-5, Nkx2-3, Nkx2-6*), gut (*Nkx2-2, Nkx2-5, Nkx2-3, Nkx2-6, Bapx1*), and spleen (*Nkx2-3, Nkx2-5, Bapx1, Hox11*) codes. An overview of *Nkx* gene expression in the gut is provided in **Figure 1.4**.

Mice null for *Nkx2-5* provide no insight into the role of this gene in gut development as they die before gut morphogenesis initiates (Lyons et al., 1995). Many human mutants have been identified, but of these only two have gut abnormalities (Watanabe et al., 2002). Is this lack of gut defects indicative of functional redundancy between *Nkx* genes in the gut? An extremely interesting – and ambitious - approach to this problem would be to generate gut-specific knockouts of *Nkx2-2, 2.3, 2.5, 2.6*, and *Bapx1*, and to examine the ensuing mutant gut phenotypes both in isolation and in the various compound mutants.

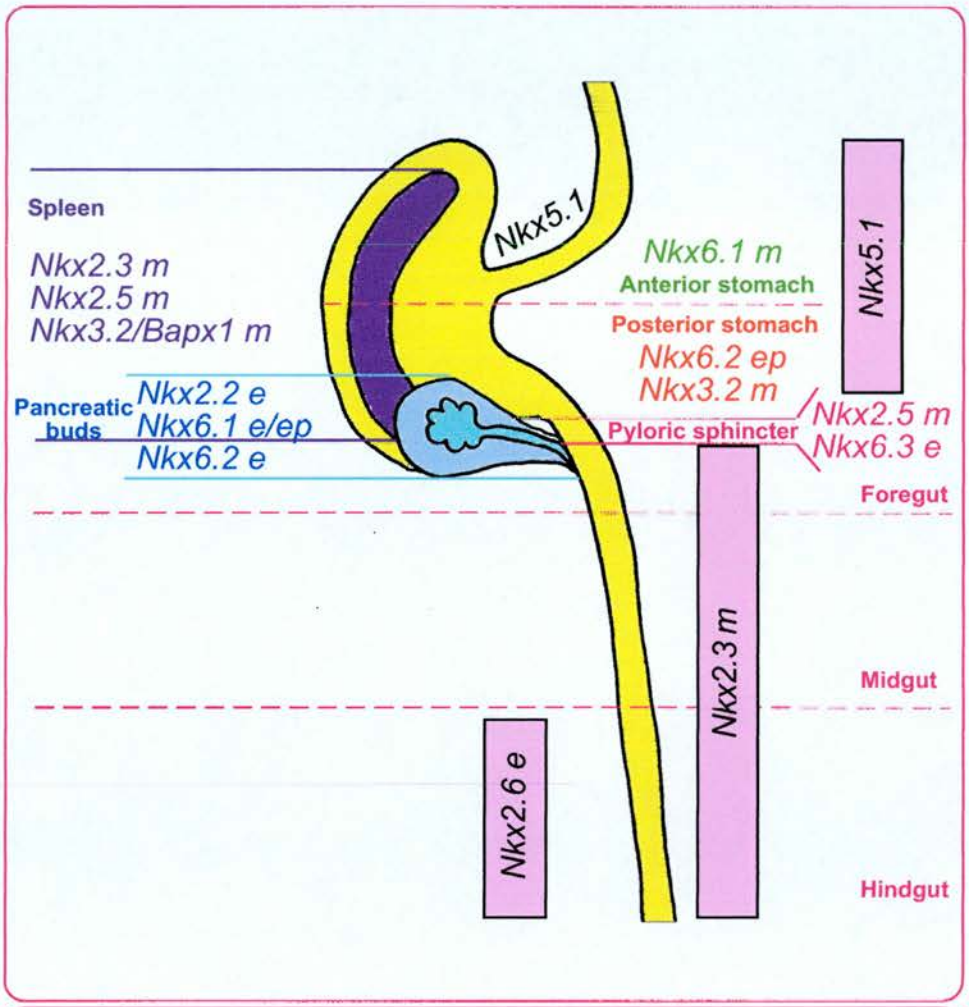

***Figure 1.4 Nkx* genes in gut development: an *Nkx* gut code?**

A number of *Nkx* genes are expressed in the developing mouse gut, across a range of tissue types. This schematic shows a stylised E12.5 gut and is overlaid with the names of genes expressed around this time. It should of course be noted that these expression patterns differ at earlier and later developmental stages. The tissue type in which expression has been detected is denoted after the gene name by **"e"** (endoderm), **"m"** (mesenchyme), or **"ep"** (epithelium), when this information is known. Broad expression domains are denoted by pink boxes. Only the dorsal pancreatic bud (**blue**) is illustrated, but expressed genes are listed for both buds. The spleen is shown in **purple**.

References: see **Table 1.1**

Another point to note about the Nkx2 gene family is that the same gene may have different functions or expression in different species (e.g. cardiac expression of *Nkx2-3* in chick and *Xenopus*, but not in mouse and zebrafish). This may be due to homologues being placed under the control of different regulatory cascades within different species. Indeed, whilst *tin/Nkx2-5* and *bap/Bapx1* are both players in gut development in *Drosophila*, chick, and mouse, their hierarchical order of activity appears to have changed. *Tin* is upstream of *bap* in fly, no relationship has been noted in chick, and *Bapx1* is upstream of *Nkx2-5* in mouse (Azpiazu and Frasch, 1993; Nielsen et al., 2001; Watson et al., 2007).

1.9 Role of LR asymmetry in gut development

1.9.1 LR asymmetry in general development

Many aspects of vertebrate development require morphological asymmetry. Normal left-right (LR) asymmetry is termed *situs solitus*; both mouse and human mutants exist with complete mirror-image reversal of this arrangement (*situs inversus*). Not all reversals are complete though, and thus a spectrum of intermediate defects (*situs ambiguus*) exists, including heterotaxy (discordance between asymmetry of different organs), isomerism (one side is duplicated), and isolated abnormalities in normally asymmetric organs (for an excellent primer see (Aylsworth, 2001)). Heterotaxia can be caused by mutations in single genes, and estimates of its occurrence range between 1 in 6,000-20,000 live births, and in 0.03-1.1% of foetuses once abortions and stillbirths are taken into account (Belmont et al., 2004; Bartram et al., 2005).

There are four stages in the establishment of LR asymmetry (reviewed in (Hamada et al., 2002)):

1) **Breaking of symmetry**[14] and subsequent initiation of LR polarity relative to the DV and AP axes, mediated by the node (located at the midline, at the anterior tip of the primitive streak). This is followed by...
2) **Transmission of LR positional signals** from the node to LPM[15], inducing...
3) **Asymmetric gene expression** of signalling molecules in the LPM (e.g. *Nodal, Lefty2*; both transiently expressed in the left LPM[16]), thus initiating...
4) **Asymmetric organ morphogenesis**. Three main mechanisms appear to exist: directional tube looping (e.g. heart, gut), differential lobation (e.g. lungs, liver), and regression of one side of the primordia (e.g. blood vessels). How factors (e.g. *Pitx2*) involved in this stage exert control is unknown but this may be through regulation of differential cell proliferation, migration, and adhesion.

The importance of LR asymmetry in development is alluded to by the conservation within the chordate phyla of mechanisms and genes involved in at least the first three stages (reviewed in (Boorman and Shimeld, 2002)). However, whilst most of the components of the asymmetry pathway are conserved between mouse and chicken, some have adopted different roles. Most notably, the chick right-side determinant Fgf8 promotes left-side gene expression in mouse; also, whilst Shh promotes expression of left-side determinants in chick, its mode of action in mouse is suppression of these on the right side of the LPM (Meyers and Martin, 1999).

Whilst quite a lot is known about the first three stages of LR asymmetry establishment, the final stage is less understood, i.e. how organ primordia interpret asymmetric gene expression and translate this into asymmetric morphogenesis. This is addressed with respect to the gut in the next section.

---

[14] Possibly by nodal flow (cilia in node rotate such that a leftward flow of extra-embryonic fluid is established, potentially allowing leftward flow of an unknown left-side determinant molecule), though it remains contentious whether this is truly the symmetry breaking event (Tabin, 2005)
[15] Either by relay through signaling cascades or by diffusion of molecules
[16] Mice with loss of these genes have LR asymmetry defects, and mutations have also been detected in the human homologues in individuals with laterality disorders (Hamada et al., 2002; Peeters and Devriendt, 2006)

1.9.2 Role of LR asymmetry in gut development

LR asymmetry is essential for correct gut patterning in vertebrates. The mechanisms for establishing gut LR asymmetry vary across species: for example, gut rotation is essential in mammals, whereas the avian stomach becomes asymmetric due to differential growth (reviewed in (Schneider et al., 1999)). The *Xenopus* gut tube becomes asymmetric (loops) through differential rates of elongation of the left and right sides, such that the left becomes concave and the right convex (Muller et al., 2003). *Xenopus* gut tube concavity (slow elongation) correlates with and is induced by *Pitx2* expression (Muller et al., 2003).

In normal asymmetric morphology (*situs solitus*) the stomach and spleen are located to the left of the midline; this is illustrated in **Figure 1.5**, along with deviations from the normal state. As described in **Section 1.5.4** asplenia (bilateral right-sidedness) and polysplenia (bilateral left-sidedness) are common in individuals with *situs ambiguus*, and often occur in conjunction with abnormal sidedness of other normally asymmetric organs (Bartram et al., 2005). Many mouse mutants have also been documented which have defects in gut LR asymmetry. Mutation or loss of genes involved in all four stages of LR asymmetry establishment underlies many of these phenotypes. The final stage of the process – LR asymmetric morphogenesis of organ primordia – is least understood. However, recent work in our lab has shed some light on how this is controlled. This is discussed in the following section.

1.9.3 The SMP

In 1967, Green described a transient thickening of the mesothelium (epithelium) which has a columnar structure and covers the spleno-pancreatic mesoderm (Green, 1967). She termed this the Anterior Splanchnic Mesodermal Plate (ASMP) and suggested that it is required for correct development of the gut. Nearly 40 years later, workers in our lab further characterised this layer as a physical feature of the mesoderm which acts as an organiser, mediating transduction of signals from

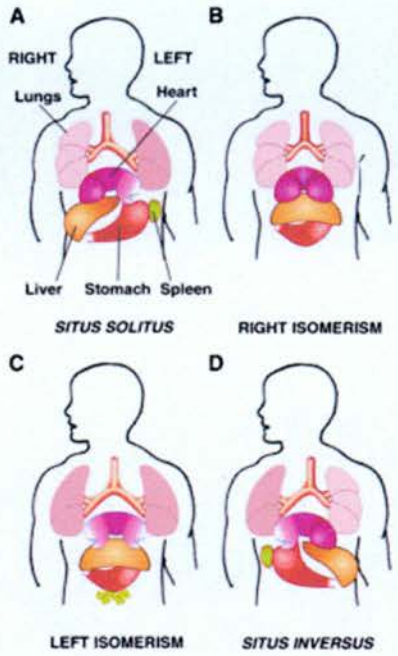

Figure 1.5: **LR asymmetric development is required for correct organ placement.**

A: the normal arrangement of organs in the adult human - *situs solitus.*
B,C,D: abnormalities of this arrangement.

Whilst asymmetry is largely similar in the mouse, some differences do exist. In human the left lung is bilobed and the right trilobed; in mice the left lung has one large lobe and the right is comprised of four smaller lobes.

Figure taken from (Capdevila et al. 2000)

the LR pathway to gut organ primordia (Hecksher-Sorensen et al., 2004). The Splanchnic Mesodermal Plate (SMP) directs spleen and pancreatic laterality by inducing leftward growth of the spleno-pancreatic mesenchyme. The SMP is itself under control of the LR pathway as its growth is regulated by *Bapx1*, which is asymmetrically expressed (Schneider et al., 1999).

The SMP takes the form of a distinct columnar epithelial layer (Hecksher-Sorensen et al., 2004). It is first detectable at E9.5 as a bilateral layer of thickened splanchnic mesoderm surrounding the endoderm of the midline stomach and dorsal pancreatic bud; few mesenchymal cells lie between it and the endoderm. The SMP initiates leftward lateral growth in response to the LR asymmetry pathway, and by E10.5 the underlying mesenchyme and endodermal dorsal pancreatic bud bulge to the left (Hecksher-Sorensen et al., 2004). At this latter stage the SMP appears as a triangle shape in cross-sections of the gut, capping the left-dorsal aspect of the gut at

the foregut-midgut boundary (from the posterior stomach to the pancreatic buds). The SMP is a transient feature of the gut, as it is lost by E11.5. Development of the SMP between E9.5 and E10.5 is depicted in **Figure 1.6**.

The transition between the bilateral and asymmetric (left-sided) states of the SMP occurs over a 24-hour-period, between E9.5-10.5. The left-side undergoes lateral growth and maintains its thickened columnar epithelial morphology, whilst the cells on the right remain at the midline and lose their elongated appearance in a ventral-to-dorsal manner (Hecksher-Sorensen et al., 2004). The right-side cells eventually become indistinguishable from the underlying mesenchyme or adjacent gut mesothelial lining. The SMP is 50-60μm thick and is noticeably distinct from the unorganised, more loosely arranged mesenchymal cells that lie between it and the gut endoderm.

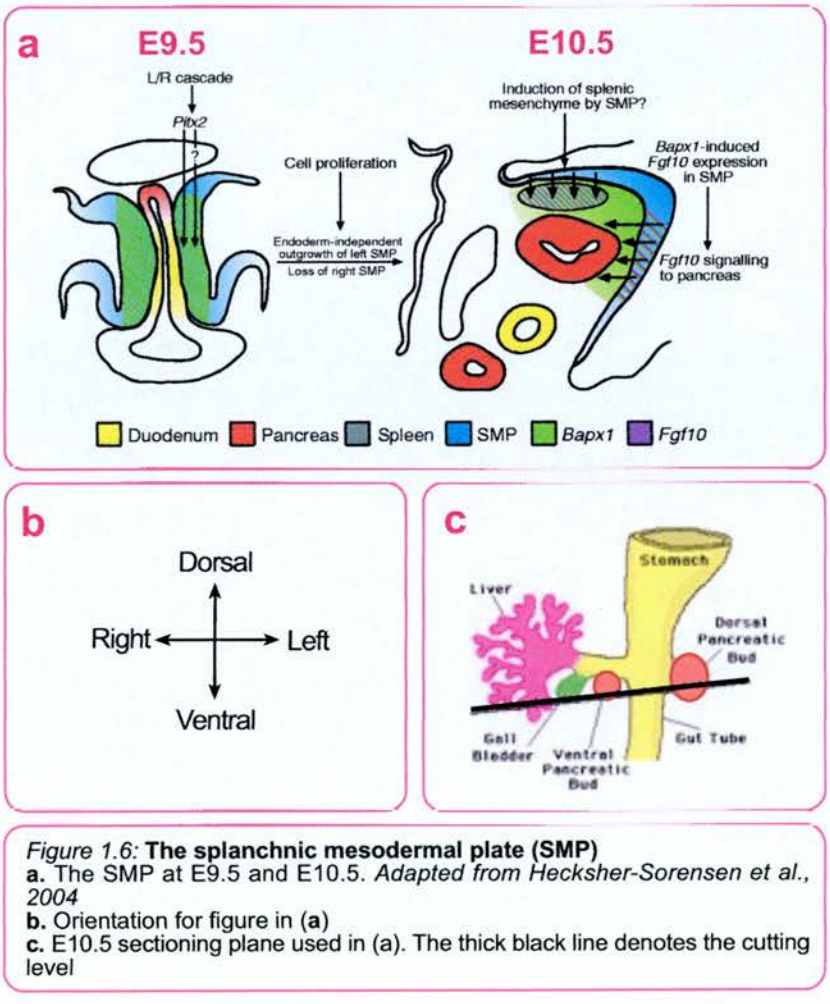

Figure 1.6: **The splanchnic mesodermal plate (SMP)**
a. The SMP at E9.5 and E10.5. *Adapted from Hecksher-Sorensen et al., 2004*
b. Orientation for figure in (**a**)
c. E10.5 sectioning plane used in (a). The thick black line denotes the cutting level

A similar highly organised columnar epithelial layer flanks the initially symmetrical endodermal gut tube in the developing zebrafish gut and is autonomously (independent of the endoderm) required for correct gut looping (Horne-Badovinac et al., 2003). This structure is derived from the LPM, as is the murine SMP, though whether these epithelial layers are homologous is not clear. Certainly, the processes of asymmetric morphogenesis in which they are involved differ. The SMP grows out to the left, and the underlying gut mesenchyme and dorsal pancreatic endoderm seem to follow in its wake (Hecksher-Sorensen et al., 2004). In zebrafish, however, the LPM appears to actively push the underlying gut endoderm to adopt an asymmetric position (Horne-Badovinac et al., 2003). The left and right sides of the LPM undergo asymmetric, yet coordinated, tissue migration and thus adopt an asymmetrical morphology and position with the result that the gut tube is forced to adopt a leftward bend. It should of course be noted at this juncture that only tentative comparisons can be drawn between fish and mammalian gut development as many aspects of the final gut pattern are different. Finally, as mentioned previously, there is also evidence in *Xenopus* that asymmetric differences exist in the thickness and structure of the endodermal epithelium between the left and right sides during midgut looping (Muller et al., 2003).

1.9.3.1 The SMP in spleen development

The thickened columnar epithelium of the SMP was first documented in 1921 by Thiel & Downey who thought it may participate in spleen development by contributing cells to the underlying mesenchyme, with which it is continuous and yet distinct from (Thiel and Downey, 1921). They described the columnar epithelium as being a condensed region of mesenchyme, rather than distinct epithelium *per se*.

The earliest report of splenic precursors has been in the E10.5 SMP region. The dorsal mesenchyme underlying the SMP expresses *Hox11, Capsulin, Wt1*, and *Nkx2-5*, thus implicating this patch of cells as the origin of the splenic mesenchyme (Hecksher-Sorensen et al., 2004). This putative splenic mesenchyme is not detectable at E9.5 but instead emerges over the next 24 hours as the SMP undergoes leftward lateral growth; whether the mesenchyme is *de novo* - perhaps derived from the SMP

itself - or has migrated from another location is unclear. The SMP itself does not express splenic marker genes – or at least not at a high level – but does exist in tight association with this splenic primordium.

A characteristic of the SMP is that the cells within it proliferate at a high rate (Hecksher-Sorensen et al., 2004). This may drive the outward growth required for asymmetric pancreatic morphology and spleen formation, thus linking these two developmental events. Spleen and pancreatic laterality have been shown to be associated in *Xenopus* (Patterson et al., 2000). High proliferation and the resultant outgrowth of the SMP may also provide a space into which mesenchymal cells from elsewhere can migrate. Alternatively, the mesenchymal splenic precursor cells may themselves be the product of SMP proliferation. A similar conclusion was reached in 1921, when Thiel & Downey proposed that proliferation of the coelomic epithelium resulted in "crowding" of some of the resulting cells into the underlying mesenchyme during spleen development in pig (Thiel and Downey, 1921). Holyoke found that the coelomic epithelium overlying the site of human spleen development is in a similar state of active proliferation (Holyoke, 1936). Even if there is no direct contribution from the thickened epithelium to the underlying splenic mesenchyme, there is a distinct possibility that essential EM interactions may occur between these layers.

1.9.3.2 The SMP and LR asymmetric gene expression

The SMP exhibits LR asymmetric gene expression and leftward growth in response to upstream LR signalling cascades. Asymmetric gene expression is established in the morphologically symmetrical SMP by E9.5, as *Pitx2* and *Barx1* are predominantly left-sided at this stage (Hecksher-Sorensen et al., 2004). *Invs* (inversion of body turning) homozygous mutants have *situs inversus* and the SMP is transposed onto the right side of the embryo, demonstrating its dependence on the genetic establishment of LR asymmetry (Hecksher-Sorensen et al., 2004).

Bapx1 expression is bilateral in the SMP at E9.5, and is then wholly left-sided in the tip of the SMP and underlying mesenchyme by E10.5 (Hecksher-Sorensen et al., 2004). *Bapx1* conveys LR information to the SMP, which relays this on to the

underlying mesenchyme and endoderm; thus the SMP itself is essential for downstream LR gut patterning (Hecksher-Sorensen et al., 2004). Leftward growth of the pancreas is dependent on the SMP. Conversely, the lateral growth of the SMP is autonomous and does not require involvement of the pancreatic endoderm – as demonstrated by normal SMP outgrowth in *Fgf10*-deficient mutants which have no gut endoderm in the spleno-pancreatic region (Hecksher-Sorensen et al., 2004).

Fgf9, Fgf10, Fgf11, and *Fgf13* are all expressed in the E10.5 SMP-associated mesenchyme (Hecksher-Sorensen et al., 2004). *Fgf9* is specifically expressed in the lateral tip of the SMP and the underlying dorsal mesenchyme; *Fgf10* is detected in the ventral SMP and associated mesenchyme. One hypothesis is that secretion of these growth factors may encourage the leftward growth of the SMP. This may be substantiated by the expression of the gene encoding a high affinity FGF9 receptor - *Fgfr3* - in the extreme tip of the SMP (Hecksher-Sorensen et al., 2004).

1.9.4 SMP mutants

Two mouse mutant strains exist in which SMP development is disturbed and the spleen fails to form: the *Bapx1*$^{-/-}$ and *Dh* mutants (Hecksher-Sorensen et al., 2004; Green, 1967). Pancreatic laterality is also defective in these mutants. The loss of the distinctive SMP structure and the subsequent failure of leftward growth in these mutants may indicate that the rigid structure of the SMP somehow guides this outgrowth. Credence may be given to this idea by the accumulation of f-actin around the thickened SMP epithelium during normal development, as actin filaments have been proposed to play a role in tissue outgrowth (Hecksher-Sorensen et al., 2004; Quinlan et al., 2004).

1.9.4.1 Bapx1 *knockout mice*

Knocking out *Bapx1* results in adverse effects on splanchnic mesoderm derivatives in the spleno-pancreatic region, and this was discussed fully in **Section 1.8.5.5**. The mesenchyme surrounding the posterior stomach and duodenum is

abnormal, and mice are born with gut and pancreatic morphological abnormalities. Additionally, mutants do not have a spleen or a pyloric sphincter constriction.

The SMP is defective in *Bapx1*$^{-/-}$ mutants; its shape is altered and leftward growth is inferior to that in wild type embryos (Hecksher-Sorensen et al., 2004). *Bapx1* thus regulates leftward growth of the SMP and underlying mesenchyme and appears to act as a link between the LR asymmetry pathway and asymmetric organ morphogenesis. Expression of *Fgf10* in the SMP is greatly downregulated in the *Bapx1*$^{-/-}$ SMP at E10.5 (Hecksher-Sorensen et al., 2004). Wild type *Fgf10* expression normally resides in the ventral SMP and underlying mesenchyme at E10.5, to the left of the dorsal pancreatic bud. Given that FGF10 can act as a chemoattractant (Park et al., 1998b), it is plausible that the dorsal pancreas grows towards this, i.e. producing leftward movement of the bud and surrounding mesenchyme. Indeed, *Fgf10* is already known to be required for early pancreatic morphogenesis, although this is due to its role in maintaining proliferation in the pancreatic epithelium (Bhushan et al., 2001). *Fgf9* expression is also reduced in the SMP of *Bapx1*$^{-/-}$ mutants at E10.5 (Hecksher-Sorensen et al., 2004).

The *Bapx1*$^{-/-}$ mutant gut provides an excellent opportunity to examine the interrelationship between spleen and pancreas development, demonstrating that highly coordinated interactions between these tissues are necessary for their correct development (Asayesh et al., 2006). The splenic and pancreatic tissues do not correctly separate in the *Bapx1*$^{-/-}$ mutant and thus the pancreas remains in prolonged contact with the spleen, resulting in a metaplastic transformation such that these tissues develop into ectopic gut-like structures in ~50% of mutant embryos[17]. These structures are first detectable at ~E14-14.5 as cyst-like outgrowths from the dorsal pancreatic endoderm into the mesenchyme where the spleen would normally develop. Markers of pancreatic endoderm are lost from these cysts which appear to adopt an intestinal epithelium phenotype. The cysts can induce the surrounding mesenchyme to adopt intestinal – versus spleen – mesenchyme characteristics; this may be due to the ectopic activation of Shh signalling observed in the transformed pancreatic epithelium. *Shh* is normally excluded from the developing pancreas;

[17] Apoptosis occurs in the disorganised splenic mesenchyme of the remaining ~50% of mutants (Asayesh et al., 2006).

ectopic expression induces a mixed pancreatic-intestinal phenotype (Apelqvist et al., 1997).

Ectopic gut structures can also be induced from wild-type pancreatic epithelium co-cultured with *Bapx1*$^{-/-}$ splenic mesenchyme, suggesting that it is this latter tissue which mediates the transformations (Asayesh et al., 2006). Further co-culture experiments demonstrated that it is indeed the splenic mesenchyme which induces cyst development, but not as a result of being *Bapx1*-deficient. Wild type splenic mesenchyme also induces cyst formation when co-cultured with wild type pancreatic epithelium, as the normally precise spatially and temporally controlled interactions between these two tissues are disrupted. *Bapx1*$^{-/-}$ splenic mesenchyme therefore induces cyst formation not through some inherent quality *per se*, but by being left in close apposition with the pancreas during development. This may be due to short-range signalling from the splenic mesenchyme (possibly via Activin A) (Asayesh et al., 2006).

The transformation in the *Bapx1*$^{-/-}$ mutant also explains the failure of spleen development. The mutant splenic mesenchyme becomes established and expresses splenic markers such as *Pbx1* and *Capsulin*; however, this mesenchyme then fails to condense and instead persists as loosely organised cells (Brendolan et al., 2005; Asayesh et al., 2006). Normal separation of the condensed splenic mesenchyme from the pancreas therefore fails, and so these cells remain adjacent to the dorsal pancreatic bud (Asayesh et al., 2006). This apposition of the pancreas and spleen is likely related to the observation that leftward growth of the SMP fails in *Bapx1*$^{-/-}$ mutants (Hecksher-Sorensen et al., 2004).

1.9.4.2 The dominant hemimelia mutation

The dominant hemimelia *(Dh)* mutation arose spontaneously and is characterised by skeletal and hindlimb abnormalities, most noticeable as an alteration in the number of digits (Green, 1967; Morin et al., 1999). The limb defects have been attributed to disruption of EM interactions and anterior mesenchyme formation in the limb bud (Lettice et al., 1999a). Major gut defects are also present in both *Dh/+* and *Dh/Dh* mutants, though these are more severe in the latter. The spleen is absent in

Dh mutants and this appears to be due to a deficit of the SMP, which is thinner or absent by E9.5 (Green, 1967; Hecksher-Sorensen et al., 2004). Unorganised mesenchyme is found in place of the specialised SMP cells. The leftward growth of the SMP and underlying spleno-pancreatic mesenchyme normally observed between E9.5 and E10.5 does not occur; this may be attributable to loss of inductive (leftward growth) signals from the SMP to the underlying spleno-pancreatic mesenchyme. Indeed, *Fgf9* and *Fgf10* are both downregulated in *Dh* mutants (Hecksher-Sorensen et al., 2004).

Overall the gut is smaller (smaller stomach; shorter, thinner digestive tract) in *Dh* mutants than in wild type embryos (Green, 1967). Again, this is more pronounced in the homozygous mutants, who have a particularly small stomach and pancreas. Additional phenotypes in both classes of *Dh* mutant include misplacement of the vitelline vein with respect to the duodenum, and abnormal development of the kidneys and female genitourinary system. The primary tissue affected is the splanchnic mesoderm, and all the defects are predicted to stem from the disrupted development of this tissue. The *Dh* mutant phenotype also extends to another area of the spleno-pancreatic region: the pyloric sphincter, which is widened or absent (Hill lab, unpublished data).

The genetic defect underlying the *Dh* phenotype is unknown though the affected gene resides on chromosome 1 (Hill et al., 1987). Past candidates for this gene include *En-1* and *Gli2*, but these have since been discounted (Higgins et al., 1992; Hughes et al., 1997). More recently our lab has focused on *Inhbb* as a possible candidate (unpublished).

1.9.4.3 Other SMP mutants?

The *Bapx1*$^{-/-}$ and *Dh* mutants are the only currently known SMP mutants. An SMP mutant would by definition possess defects in the spleen, pancreas, and possibly the pyloric sphincter. One possible candidate mutant is therefore the *Sox11* knockout mouse. Within the developing gut, *Sox11* is expressed in the oesophagus, stomach, and pancreas (Hargrave et al., 1997). *Sox11* is predominantly expressed in the mesenchyme surrounding the pancreatic buds at E9.5-10.5, though some

expression can be detected in the epithelium (Lioubinski et al., 2003). By E12.5 *Sox11* is restricted to the pancreatic epithelium. Expression of *LacZ* knocked into the *Sox11* locus also revealed contiguous expression in the mesenchyme of the spleen and stomach at E14.5 (Sock et al., 2004). Loss of *Sox11* causes asplenia and an expanded pyloric sphincter phenotype (Sock et al., 2004). As the pancreas is also affected (by hypoplasia) it is therefore possible that *Sox11* may play an important role in the SMP. Indeed, *Sox11* expression is present in the SMP at E10.5, in a dorsal region overlapping the prospective spleno-pancreatic mesenchyme (Lioubinski et al., 2003). Loss of the splenic primordium is already obvious at E13.5, suggesting a defect of mesenchymal versus haematopoietic development (Sock et al., 2004). Additional abnormalities in *Sox11*-deficient mice include lung and (caudal) stomach hypoplasia, persistent gut herniation, skeletal and craniofacial defects, and failure of closure of the abdominal wall and eyelids. A number of cardiac defects are also present, and it is these that are the likely cause of the lethal cyanosis at birth.

If other SMP mutants do exist, then analysis of their defects may provide pertinent information on development of this tissue and its derivatives. Genetic markers of the region and tools to examine its development will be essential for this task, along with as much knowledge as possible of what constitutes normal development. This thesis reports efforts to achieve these goals.

1.10 Aims of thesis

The mutant phenotypes discussed in the previous section demonstrate that correct development of the spleno-pancreatic mesenchyme is of utmost significance. Gaining a better understanding of the processes underlying this development is thus extremely important. This thesis is concerned with a number of problems relating to spleen morphogenesis, and these are summarised in the following aims:

1) ***To gain a better insight into the role of the homeobox gene Nkx2-5 in gut development, particularly with reference to the spleen.*** Areas of interest are: when *Nkx2-5* expression initiates in the developing gut; how *Nkx2-5* expression relates to that of *Bapx1*; whether an upstream regulatory region confers gut expression and, if so, whether this can be used a) for **Aim (2)** below, and b) to direct a gut-specific knockout of *Nkx2-5*. These initial lines of investigation form the basis of the studies reported in **Chapters 2 and 3**.

2) ***To characterise a suitable marker of splenic precursors in order to facilitate identification of these cells during normal and mutant spleen development.*** The main stage of interest is early spleen development and the aim is thus to ascertain whether splenic precursors can be identified at an earlier stage than that already published (i.e. E10.5 dorsal mesenchyme underlying the SMP), and whether these can be marked throughout development. This work is presented in **Chapter 2**.

3) ***To develop Aim (2) and produce an inducible lineage tracing system which will allow marking of splenic precursors at a specific time-point.*** Such an approach is

necessary if one is to accurately follow spleen development. Attempts to produce such a system are detailed in **Chapter 3**.

4) ***To build on Aim (2) and develop a system for marking splenic precursors in gut organ culture.*** Major morphogenetic changes occur in the splenic primordium between E10.5 and E12.5 and it is not possible to observe these occurring *in utero*. As such, explant culture may provide the tool for observing these changes. This work is presented in **Chapter 4**.

5) ***To use the above system to manipulate spleen development and thus gain insights into how normal splenogenesis proceeds.*** This is also reported in **Chapter 4**.

The overall aim can therefore be summarised as providing insights into early spleen development. **Chapter 5** also contains data pertaining to this central aim, albeit not encompassed by the specific aims listed above.

CHAPTER 2

Nkx2-5 as a marker of the developing spleen

"It is the mystery and beauty of organic form that sets the problem for us"
– Ross Harrison, embryologist (1913)

2.1 Introduction

The origin and early development of the mammalian spleen is something of an enigma. The earliest recognisable splenic primordium is a condensation of mesenchyme at the posterior dorsal aspect of the stomach at E11.5 (Thiel and Downey, 1921). Splenic markers such as *Hox11* are expressed in this tissue and are also detected in the dorsal mesenchyme underlying the SMP at E10.5, suggesting this to be the splenic precursor region (Hecksher-Sorensen et al., 2004). The E10.5 putative splenic mesenchyme is already located on the left of the body cavity. There is, however, evidence in *Xenopus* that splenic precursors initially exist on both sides of the embryo, but only the left-side pool develops into the spleen (Patterson et al., 2000). Both populations express *Nkx2-5*, which is a marker of the developing spleen in both *Xenopus* and mammals (Patterson et al., 2000; Lints et al., 1993b). It does not necessarily follow that such an arrangement occurs during mammalian development, particularly as multiple aspects of *Xenopus* gut development differ to those in mammals; however, it is conceivable that disruption of an initially bilateral system could explain mammalian polysplenia and/or asplenia. The potential existence of splenic precursors on both sides of the mouse embryo is thus worthy of investigation.

The (putative splenic) mesenchyme underlying the SMP at E10.5 is of unknown origin. Twenty-four hours earlier, at E9.5, very few if any mesenchymal cells can be seen between the bilateral SMP and the endodermal gut tube (Hecksher-Sorensen et al., 2004). Mesenchyme populates the region concomitant with leftward SMP growth. This could be due to migration of mesenchyme from elsewhere in the embryo, or it may be a result of cellular contribution from the highly proliferative SMP (Hecksher-Sorensen et al., 2004).

A further mystery is how the condensed splenic mesenchyme observed at E11.5, lying adjacent to the posterior stomach, adopts the characteristic elongated spleen shape by E12.5. There is thus a need for methods which reliably and specifically mark splenic mesenchyme. This chapter reports investigations into the value of *Nkx2-5* in answering such questions. Endogenous *Nkx2-5* expression is examined in **Section 2.2**, whilst the remainder of the chapter is concerned with an *Nkx2-5* gut-specific upstream regulatory sequence.

2.2 *Nkx2-5* expression in the SMP

Nkx2-5 is expressed in two domains in the SMP at E10.5: dorsal (relating to the putative splenic mesenchyme) and ventral (Hecksher-Sorensen et al., 2004). Expression has not, however, been traced to an earlier point in gut development. An analysis of *Nkx2-5* expression was thus undertaken to investigate whether *Nkx2-5*-expressing cells could be detected prior to E10.5 in the developing gut.

The second motivation for this study was to ascertain whether expression of *Nkx2-5* overlaps significantly with that of *Bapx1 (Nkx3-2)*, a major gut development gene. *Bapx1* is required for correct SMP development and its loss causes a variety of defects in the spleno-pancreatic region, including an expanded pyloric sphincter and asplenia (Akazawa et al., 2000; Hecksher-Sorensen et al., 2004; Watson et al., 2007). *Nkx2-5* is normally expressed in both of these affected tissues, but this expression is lost in the *Bapx1*$^{-/-}$ mutant gut as is the earlier expression in the mesenchyme underlying the defective SMP at E10.5 (Jacob Hecksher-Sorensen, PhD thesis, University of Edinburgh, 2001)[18]. The effects of *Bapx1* on gut development may be mediated through *Nkx2-5*. It is also possible, of course, that Nkx2-5 performs non-essential functions in the gut and that its absence is coincidental to the other effects of *Bapx1* loss. Unfortunately, these two alternative hypotheses cannot be tested by engineering loss of *Nkx2-5*, as *Nkx2-5* homozygous null mice die from defects in heart looping by ~E9.0-10.0 (Lyons et al., 1995).

Regardless of the downstream details, it does appear that *Bapx1* is upstream of *Nkx2-5* in gut development; there are however a number of intriguing facets to this relationship. Firstly, it does not appear to be an evolutionary conserved relationship: reversal of chick *Bapx1* function does not affect *cNkx2-5* expression, whilst the relationship is completely reversed in *Drosophila* as *tin* activates *bap* (Nielsen et al., 2001; Azpiazu and Frasch, 1993). Secondly, overlapping expression has not been identified in the early developing mouse gut. Expression of both genes coincides in the spleen later in development but does not fully overlap in the pyloric sphincter.

[18] A recent study reported that *Nkx2-5* expression is not lost from the *Bapx1*$^{-/-}$ splenic mesenchyme (Brendolan et al., 2005). This is contradictory to data from our lab. However, the *Bapx1*$^{-/-}$ mutants used in this study were not those generated by and studied in our lab; these mice do not appear to have as severe a spleen phenotype as they still possess splenic tissue at E12.5.

Given that both the pyloric sphincter and spleen *Nkx2-5* expression domains are lost in the *Bapx1*$^{-/-}$ mutant, and that the *Bapx1*$^{-/-}$ phenotype manifests in early gut development (between E9.5 and E10.5), it might be expected that they share an expression domain at an early stage in gut development when these two tissues share a common ancestor. In the E10.5 SMP, the two *Nkx2-5* expression domains are largely exclusive to that of *Bapx1*, which is expressed in the tip of the SMP. *Nkx2-5* expression therefore needs to be examined at earlier stages to ascertain whether significant overlap with *Bapx1* occurs. If such overlap does exist then this may infer direct regulation of *Nkx2-5* by Bapx1. The alternative is of course that *Nkx2-5* may be dependent on *Bapx1* indirectly via another *Bapx1*-dependent gene or feature of the SMP.

To establish a point of early expressional overlap, *in situ* hybridisation was performed with an RNA probe complementary to *Nkx2-5* on whole E9.5 and E10.5 CD1 mouse embryos, with E12.5 CD1 guts and E9.5 hearts used as control tissues. Sufficient data on *Bapx1* expression at E9.5 and E10.5 already existed in the lab (Hecksher-Sorensen et al., 2004). The sectioning angles used in order to visualise the characteristic SMP shape are depicted in **Figure 2.1**, as these do not relate to standard planes.

2.2.1 Nkx2-5 expression in the SMP at E9.5

Detection of *Nkx2-5* expression in the ~E9.5 SMP is shown in **Figure 2.2a i-ii**. Expression was detected at previously reported sites (pharyngeal endoderm, heart), and also bilaterally throughout the SMP. At the level of the posterior stomach, expression is only detected in the ventral aspect of the SMP (**Figure 2.2a i**). This expression is specific to the thickened SMP structure and is not found in the gut endoderm. At a more caudal level, *Nkx2-5* expression is detected throughout the SMP (**Figure 2.2a ii**). Signal was also detected in the putative liver precursor region, which lies ventral to the gut endoderm. This may simply be a background signal, although there are reports of *Nkx2-5* detection in the developing liver (Kasahara *et al.*, 1998; Stanley *et al.*, 2002).

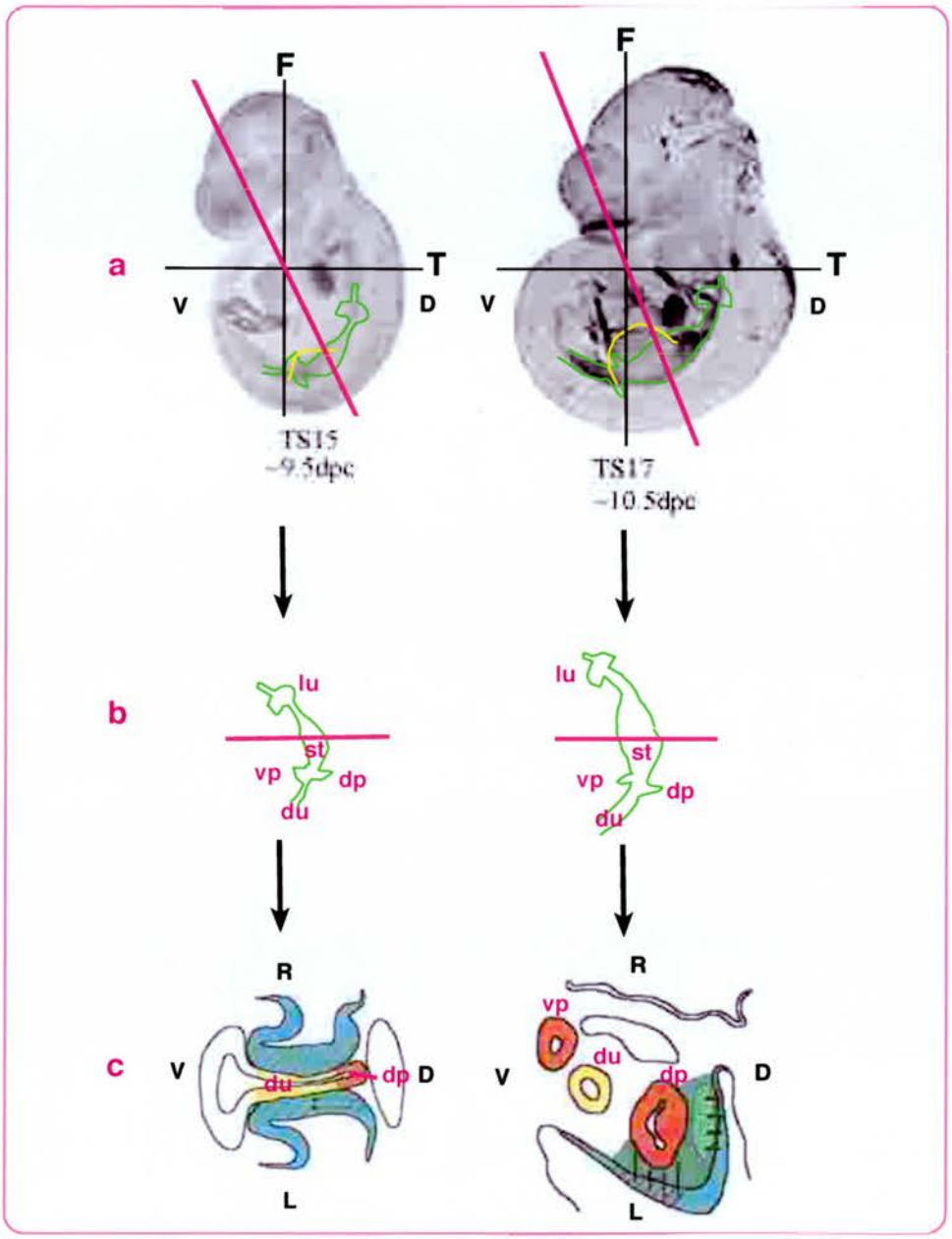

Figure 2.1 **Sectioning planes used to analyse gut (SMP) development at E9.5 and E10.5**

a: Planes used to section embryos. The sectioning planes used to study the gut (SMP) at E9.5 and E10.5 are indicated by pink lines. The standard transverse (**T**) and frontal (**F**) planes are depicted by black lines. The gut tube is illustrated in green and the forelimb bud is outlined in yellow.
b: Sectioning angles superimposed on illustrations of the developing gut
c: Graphic of the resulting sections through the gut (SMP) (NB: images are, however, presented so that dorsal lies at the top of the page in this thesis)
D: dorsal, **V**: ventral, **lu**: lung buds, **st**: stomach, **dp**: dorsal pancreatic bud, **vp**: ventral pancreatic bud, **L**: left, **R**: right

As signal was relatively low when detected with NBT/BCIP, *Nkx2-5* detection was also performed using Fast Red and confocal microscopy (**Figure 2.2a iii**). Fast Red has been found in our lab to be better suited to the detection of low-level expression in the SMP than NBT/BCIP when analysed using laser scanning confocal microscopy. Again, expression was noted in the heart and throughout the SMP. The embryos analysed by this method were at a slightly later stage (~E9.75) than those stained with NBT/BCIP, as the SMP had already begun to bulge to the left. Gut mesenchyme can be first detected between the dorsal aorta and dorsal pancreatic bud at this stage, and was also shown to express *Nkx2-5*. On the basis of what we know of how the SMP develops, and of the position of this tissue, it is likely that this mesenchyme relates to the putative splenic mesenchyme which underlies the SMP at E10.5. This E10.5 mesenchyme also expresses *Nkx2-5* (see below), along with a selection of other splenic markers (Hecksher-Sorensen et al., 2004). The ~E9.75 *Nkx2-5*-expressing mesenchyme may therefore represent the earliest occurrence of splenic precursors. The origin of the marked mesenchyme is unknown; one suggestion is that the thickened mesothelium of the highly proliferative SMP may contribute cells to the underlying splenic mesenchyme (discussed in **Chapter 1**). This may be evidenced by the expression of the splenic marker *Nkx2-5* in both the SMP at E9.5-9.75 and in the mesenchyme at ~E9.75.

Expression was also examined at the later stage (~E9.75) using NBT/BCIP. The gut shown exhibits an expression pattern intermediate between those seen at E9.5 and E10.5 (**Figure 2.2a iv**). *Nkx2-5* expression is localised to both sides of the thickened SMP, though far more so on the outgrowing left-side. Between E9.5 and E10.5 this thickened morphology is lost from the right-side; loss of *Nkx2-5* expression from the right-side SMP may thus precede this physical change. Expression was not detected in the right-side underlying mesenchyme, but was found in the mesenchyme underlying the left-side *Nkx2-5*-positive SMP. This left-side SMP/mesenchyme domain might be related to the E10.5 ventral expression domain (see **Figure 2.2c**).

A puzzling aspect of the E9.5-9.75 *Nkx2-5* expression pattern is that it appears to include the gut endoderm, at the level of the pancreatic buds. This is unexpected as *Nkx2-5* and *Nkx* genes in general are expressed in mesodermal or

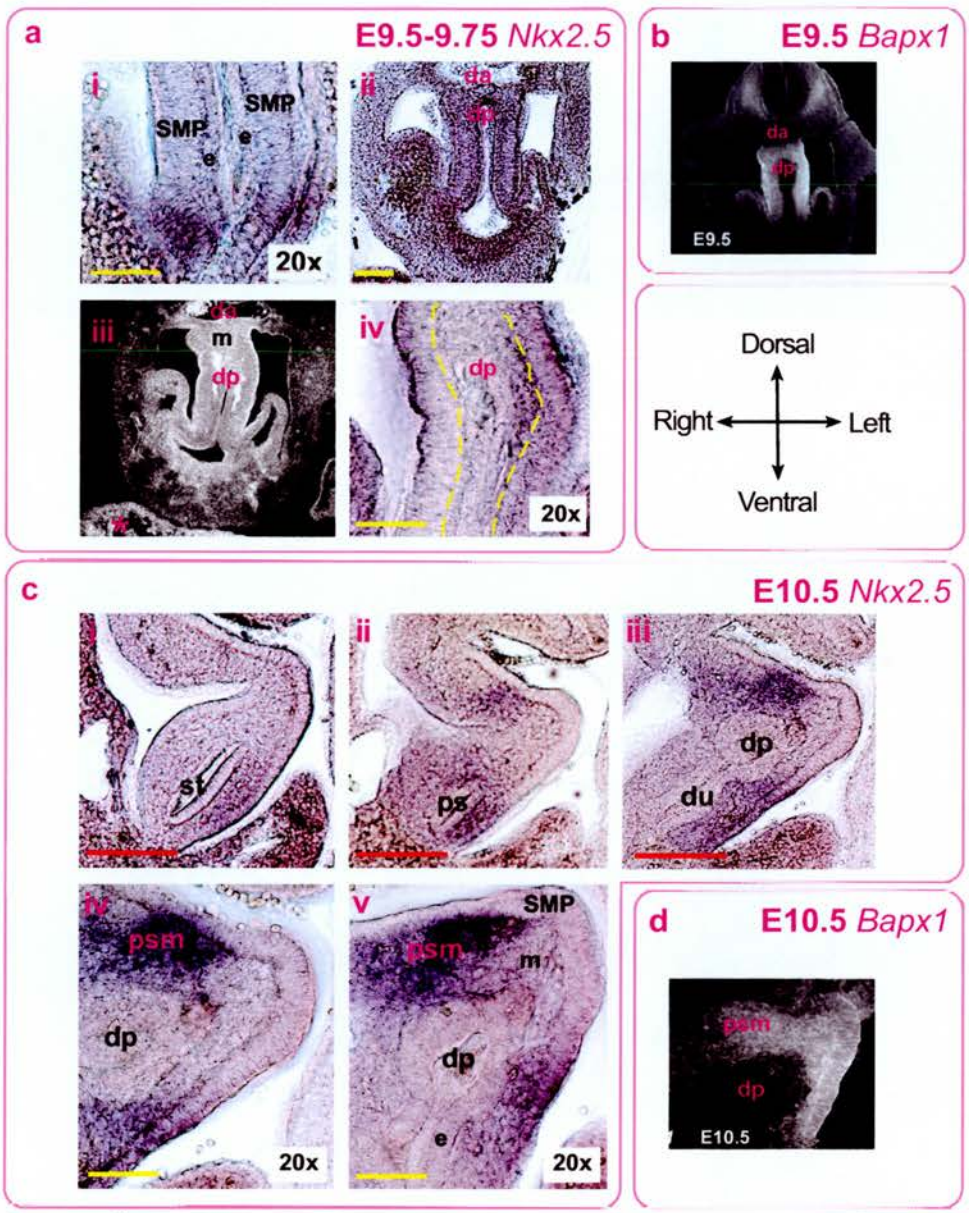

***Figure 2.2: In situ* hybridisation analysis of *Nkx2.5* expression in the E9.5-10.5 gut.**
a. i) Expression in the ventral SMP at the posterior stomach level at ~E9.5. **ii)** *Nkx2.5* is expressed throughout the SMP at the pancreatic bud level. **iii)** At ~E9.75, *Nkx2.5* is expressed throughout the SMP and in the emerging dorsal spleno-pancreatic mesenchyme. Cardiac expression is also present (*). **iv)** At a slightly later stage expression resembles the E10.5 ventral expression domain (SMP: **yellow**). Vibratome sections: 70μm (**i-iii**), 150μm (**iv**). **Yellow scale bars** represent 100μm.
b. *Bapx1* expression in the E9.5 SMP.
c. i) At E10.5 *Nkx2.5* is expressed in a left-ventral region of the mesenchyme and SMP at the level of the posterior stomach. **ii)** Expression rings the presumptive pyloric sphincter, and is now in the dorsal mesenchyme. **iii)** *Nkx2.5* is expressed in two distinct regions at the level of the dorsal pancreatic bud. **iv-v)** 20x magnifications of the SMP and underlying mesenchyme. Vibratome sections: 80 μm. **Red scale bars:** 200μm, **yellow bars**: 100μm.
d. *Bapx1* expression in the E10.5 SMP tip and underlying mesenchyme

b & d are from *Hecksher-Sorensen et al., 2004* and show Fast Red detection of expression visualised by confocal microscopy, as does **a-iii.** All other images show NBT/BCIP signal detection and were obtained using standard microscopy. All images were obtained at 10x magnification, unless otherwise stated. **da**: dorsal aorta, **dp**: dorsal pancreatic bud, **du**: duodenum, **e**: endoderm, **m**: mesenchyme, **ps**: pyloric sphincter, **psm**: putative splenic mesenchyme, **SMP**: splanchnic mesothelial plate, **st**: stomach,

mesenchymal tissues, and *Nkx2-5* expression at later stages of gut development is mesenchyme-specific. It is perhaps significant then that *Nkx2-5* is expressed in the E8.0 foregut endoderm (Lints et al., 1993b). The endodermal expression observed here could thus be related to this earlier expression. Alternatively, this may be an experimental artefact. Endodermal expression did not persist beyond ~E9.75 (**Figure 2.2c**).

Nkx2-5 expression in the developing gut has previously been regarded as a left-sided event. However, the expression observed at E9.5-9.75 shows that *Nkx2-5* expression is initially bilateral in the mammalian gut, mirroring the situation in *Xenopus* spleen development (Patterson et al., 2000). *Nkx2-5* may therefore be the earliest marker of the mammalian spleen and as such is a promising candidate for a genetic marker of this tissue.

2.2.2 Nkx2-5 expression in the SMP at E10.5

Expression of *Nkx2-5* has been observed in two discrete domains within the E10.5 SMP and underlying mesenchyme (Hecksher-Sorensen et al., 2004). The subtleties of this expression pattern had not, however, been fully investigated. This experiment was thus repeated and the presence of two distinct domains was confirmed (**Figure 2c**). These two expression domains encompass cells from the SMP and/or underlying mesenchyme, but not the endoderm.

Figure 2.2c i-iii shows three sections through the SMP from an E10.5 embryo, proceeding in an anterior-posterior direction, with high magnification images of the SMP provided in **iv-v**. At the posterior stomach level (**i**) *Nkx2-5* expression is detectable only in the mesenchyme to the left of the endodermal stomach, in a ventral region underlying the SMP. Expression is also present in the SMP. At the level of the stomach-duodenal boundary (**ii**) the ventral domain surrounds the endodermal gut tube suggesting that, in addition to being expressed in the developing pyloric sphincter structure, *Nkx2-5* may also be a marker of the pyloric sphincter rudiment. The ventral expression is located on both sides of the gut

tube, and thus may be the direct derivative of the bilateral *Nkx2-5* expression observed at E9.5-9.75. The dorsal *Nkx2-5* expression domain also becomes apparent at the stomach-duodenal boundary level. The dorsal domain corresponds to a region of mesenchyme abutting the SMP in which the early splenic markers *Hox11*, *Capsulin*, and *Wt1* are expressed (Hecksher-Sorensen et al., 2004). The dorsal *Nkx2-5* expression may be *de novo* at E10.5, or it may correspond to an earlier domain: the mesenchymal expression that lies dorsal to the dorsal pancreatic bud at ~E9.75. Moving down the gut tube to the pancreatic bud level (**iii**), the dorsal expression appears to intensify. The ventral domain is restricted at this level to a patch of expression on the left of the SMP/underlying mesenchyme, and includes cells from both these tissue types (**iv, v**).

The data presented here supports the existence of two distinct *Nkx2-5* expression domains in the E10.5 spleno-pancreatic mesenchyme, suggesting either a division of the single E9.5-9.75 expression domain, or the refinement of this domain and concomitant *de novo* appearance of a second domain.

2.2.3 Nkx2-5 expression overlaps that of Bapx1

Expression of *Bapx1* in the SMP at E9.5 and E10.5 is shown in **Figure 2.2b, d**. Significant expressional overlap occurs between *Nkx2-5* and *Bapx1* in the bilateral SMP at ~E9.5 (e.g. compare **Figure 2.2 a iii** with **Figure 2.2b**). There is therefore now a known point when the opportunity for direct regulatory interaction exists: E9.5. Perhaps more crucially, it has now also been demonstrated that two markers of spleen development (*Bapx1*, *Nkx2-5*) are expressed in a bilateral manner in the SMP as early as E9.5.

By E10.5 the *Bapx1* and *Nkx2-5* expression domains are largely exclusive, with *Bapx1* expression localising to the SMP tip and underlying mesenchyme, flanked by the two *Nkx2-5* expression domains. One could imagine that the two *Nkx2-5* domains are directly related to the E9.5 *Nkx2-5*-positive SMP (and the

emerging dorsal mesenchyme), whilst the *Nkx2-5*-negative mesenchyme is derived from the *Bapx1*-positive SMP tip.

Many aspects of the *Bapx1*$^{-/-}$ phenotype are manifest by E10.5 and *Nkx2-5* expression is lost from the mutant SMP region by this time (Jacob Hecksher-Sorensen, PhD thesis, University of Edinburgh, 2001). The obvious next question is therefore whether *Nkx2-5* expression is absent from the *Bapx1*$^{-/-}$ SMP at E9.5. This question has not been answered during my studies as - despite numerous attempts with a variety of different *Nkx2-5* probes and protocols - expression in the gut was often too weak to reliably detect in wild type controls.

2.3 Characterising a gut regulatory element upstream of *Nkx2-5*

2.3.1 Modular control of Nkx2-5 expression

Expression of *Nkx2-5* and *Bapx1* overlaps completely in the wild type SMP at E9.5, and *Nkx2-5* expression is lost in the *Bapx1*$^{-/-}$ mutant gut. The possibility thus exists that Bapx1 may directly regulate *Nkx2-5*. Regulatory interaction between *NK* genes is a central feature of *Drosophila* mesoderm development, and examples also exist of dependence of vertebrate *Nkx* genes on other family members (see **Chapter 1**). Direct regulation of *Nkx2-5* by Bapx1 would most likely be mediated through interaction with a regulatory region located in the genomic vicinity of *Nkx2-5*. A number of such enhancer elements are known to exist in the genomic landscape around *Nkx2-5*; control of the *Nkx2-5* expression pattern is modular, with different regulatory regions required for different components of the overall pattern (Schwartz and Olson, 1999).

Non-coding *Nkx2-5* regulatory sequences are found in a range of vertebrate species and also in *Drosophila*. The *Drosophila tin-D* enhancer is located 3' to *tin* and drives expression in the dorsal mesoderm (Yin et al., 1997). Activation of *tin* by *tin-D* occurs in response to dpp - facilitated by Smad proteins - and Tin itself (Xu et

al., 1998b). Binding sites for Smad and BMP (the vertebrate Dpp orthologue) proteins are also a functional feature of murine and chick *Nkx2-5* enhancer sequences (Liberatore et al., 2002; Lien et al., 2002; Brown, III et al., 2004; Lee et al., 2004).

The regulatory landscape around murine *Nkx2-5* has been well studied, due to the essential role this gene plays in heart development. As such, many of the published enhancer regions have been analysed with respect to cardiac expression, with elements conferring non-cardiac aspects of the *Nkx2-5* expression pattern not being investigated in depth. A review of the *Nkx2-5* enhancer elements discovered in the mouse genome is presented in **Appendix Table 1**, and these findings are summarised in **Figure 2.3**. This schematic is an updated version of that of Schwartz and Olson (1999), as this is largely in agreement with my interpretation of the available expression data (Schwartz and Olson, 1999). The regulatory regions presented in the schematic are predicted on the basis of data from a number of studies.

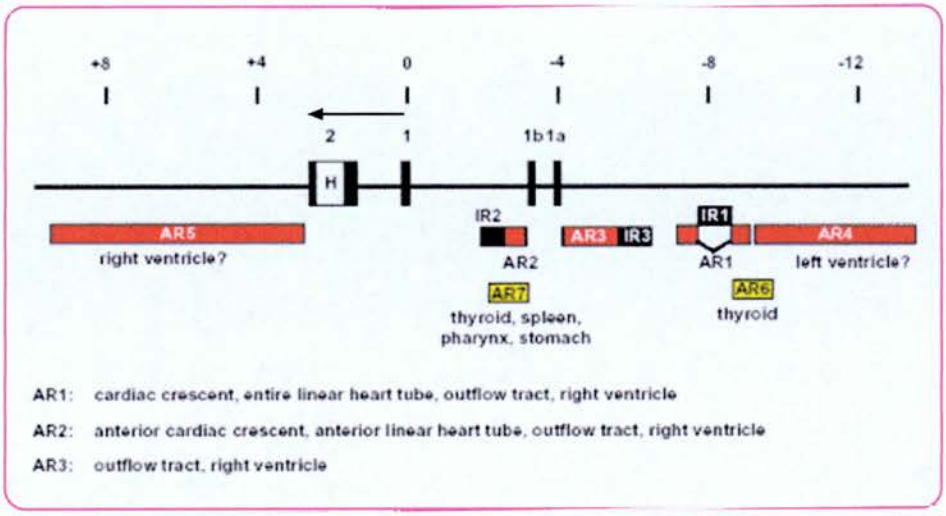

Figure 2.3* The regulatory elements in the genomic neighbourhood of *Nkx2.5

The gut regulatory region used in this chapter (*NGRS*) is equivalent to AR7. *Nkx2.5* has two upstream exons (exon 1a, 1b), which may rarely be spliced into *Nkx2.5* transcripts (*Reecy et al., 1999; Tanaka et al., 1999b*). The arrow indicates the direction of transcription. Compiled from references cited in the main text, and adapted from *Schwartz & Olson, 1999.*

One upstream region has been identified which can confer reporter gene expression in the distal stomach and spleen from E10.5 and E11.5, respectively (Searcy et al., 1998; Lien et al., 1999; Reecy et al., 1999; Tanaka et al., 1999c; Lien et al., 2002). In **Figure 2.3**, this gut regulatory region is equivalent to the proposed AR7 (Activating Region 7) that confers thyroid, pharynx, stomach, and spleen expression. The AR7 itself encompasses two other putative elements: the AR2 (outflow tract, basal right ventricle) and the IR2 (Inhibiting Region 2), which inhibits cardiac expression. Hence this model can explain the findings of both Reecy *et al.* (1999) and Searcy *et al.* (1998), which at first appear contradictory (Reecy et al., 1999; Searcy et al., 1998). The Reecy data shows that nucleotides -1627 to -3512 upstream of the *Nkx2-5* translational start point confer AR7 activity without associated cardiac expression, which is predicted by inclusion of the IR2; the Searcy study found that nucleotides -2776 to -3299 confer both AR7 and cardiac expression, and this is explained by the lack of a complete IR2. Gut expression may be conferred solely by the AR2, but this element alone has associated cardiac activity and so must be kept in association with the IR2 to minimise cardiac expression. The gut-specificity of the AR2 is supported by the fact that it is histone acetylated specifically in the stomach at E12.5 (Chi et al., 2005). Furthermore, the AR2 sequence is conserved down to *Xenopus*, and the *Xenopus* "AR2" sequence can drive gut expression in transgenic mice (Sparrow et al., 2000).

2.3.2 An upstream Nkx2-5 Gut Regulatory Sequence (NGRS)

The putative *Nkx2-5* upstream gut enhancer region discussed above could be of value to the study of gut development and the role of *Nkx2-5* therein. This genomic region has only been investigated from a cardiac perspective and, as such, a detailed analysis of the expression conferred in the developing gut has not been published. Expression is reported in the spleen and "posterior stomach", but it is not clear how this relates to endogenous *Nkx2-5* expression. Nor has it been shown how early in spleen development this enhancer marks splenic cells. I therefore cloned a 1956bp genomic region comparable to the AR7 and used it to drive *LacZ* expression,

in conjunction with the heterologous *β-globin* promoter, in transient transgenic mouse embryos (Sally Burn, MSc (Res) thesis, University of Edinburgh, 2002). The cloning strategy is illustrated in **Figure 2.4**, and details are provided in the **Appendix**. *Nkx2-5* regulatory regions have been studied in conjunction with both exogenous promoters and the *Nkx2-5* promoter. In the study using an exogenous (*hsp68*) promoter, cardiac expression was less than in studies of comparable regions used in conjunction with the endogenous promoter (Lien et al., 1999). The use of the *β-globin* promoter here may therefore be beneficial.

A similar genomic region had previously been demonstrated to drive transgene expression in the thyroid, ventral pharynx, spleen primordium, and distal stomach at E12.5-13.5, with only minor cardiac expression in the inflow and outflow tracts at E9.5 and E13.5 (Reecy et al., 1999). This expression pattern was recapitulated with my construct at E12.5, and the "distal stomach" expression was shown to be around the pyloric sphincter. Expression was also found in the spleen and mesenchyme overlying the dorsal pancreas, whilst cardiac expression was minimal. This cloned element is herein referred to as the *Nkx2-5* Gut Regulatory Sequence (***NGRS***) and the *LacZ* reporter construct as ***NGRS-LacZ***.

The preliminary indication from this experiment was that the *NGRS* might be a valuable tool for marking pyloric sphincter and spleen cells for lineage tracing purposes. The element also had the potential to direct a gut-specific *Nkx2-5* knockout given its minimal cardiac expression at E12.5. A more in depth characterisation was therefore undertaken to assess its usefulness. If the *NGRS* were to be used in lineage tracing studies then it would need to be shown that the E12.5 gut expression was not simply *de novo*, but instead related to earlier stages in gut development. Cardiac expression would also need to be minimal throughout development. These issues could be examined to an extent using transient transgenics but a stably expressing line would be ultimately required to fully investigate the element. The *in silico* characterisation of the *NGRS*, generation of stable transgenic lines, and an in depth expression analysis are discussed in the following sections.

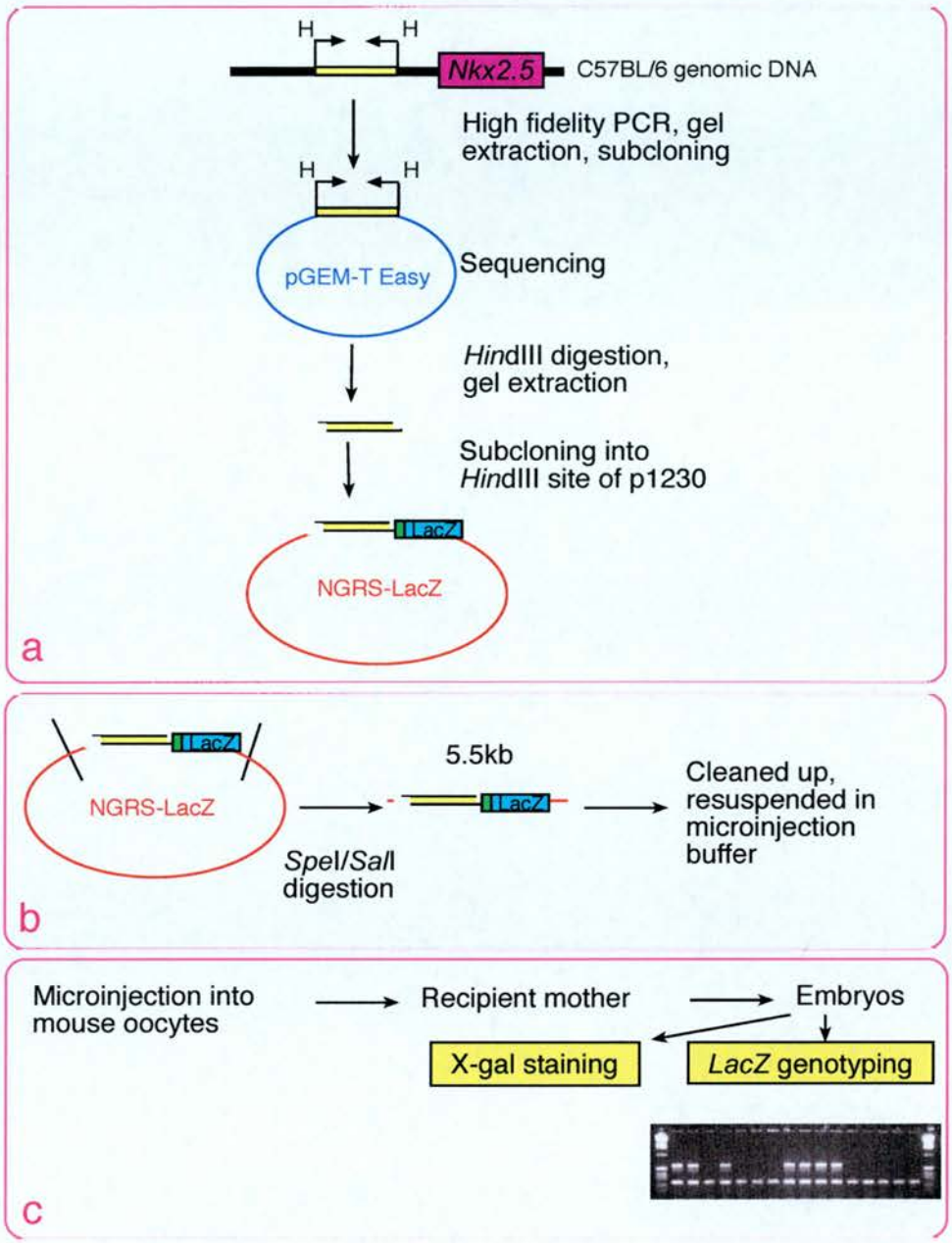

Figure 2.4 Cloning of the NGRS and generation of NGRS-LacZ transient transgenic embryos

a) Isolation of the 1956nt *NGRS* (yellow) and cloning of the *NGRS-LacZ* construct. H: *Hin*dIII recognition site; green box: β-*globin* promoter.
b) Preparation of a ~5.5kb fragment for microinjection. This step was performed each time transient transgenic embryos were needed.
c) Microinjection and embryo analysis. A typical *LacZ/Myo* genotyping PCR is shown in which the upper (600bp) band is *LacZ*, and the lower (250bp) band is *Myo*.

2.3.3 In silico analysis of NGRS

Non-coding regions of the genome might be expected to be free of evolutionary constraints, as they are "non-functional" and thus their base composition is irrelevant. However, it has become increasingly apparent that the genome is littered with regions of DNA that have been highly conserved through evolution and which perform essential regulatory functions. Such regions can be identified by comparing the genomic landscape between multiple species and identifying regions of high sequence homology, most commonly 70% identity over 100bp of ungapped sequence (Dermitzakis et al., 2005). The insinuation is that if a non-coding sequence shows high identity between species then it has been specifically conserved and thus must perform a function – though conservation across a range of species is not a mandatory prerequisite for functional enhancers (Hill, 2004). Further analysis often reveals highly conserved binding sites for transcription factors, the nature of which can offer insights into the roles of the associated gene. An analysis of the evolutionary conservation of, and sequence motifs within, the *NGRS* was hence undertaken.

The ECR (Evolutionary Conserved Region) browser programme (Ovcharenko et al., 2004) was used in conjunction with the rVISTA 2.0 tool (Loots and Ovcharenko, 2004) to analyse the region upstream of *Nkx2-5*. Two distinct ECRs were identified within the *NGRS* region (**Figure 2.5**). Given their genomic locations, the proximal ECR is most likely the IR2 element, and the distal ECR the AR2 element. The 3' half of this distal element shares high sequence identity with the ~300bp *Xenopus* sequence which drives AR2-type expression in transgenic mice (Sparrow et al., 2000).

Conserved transcription factor binding sites, previously reported in the AR2, were confirmed during the *in silico* analysis presented here: 6 GATA , 4 Smad, 1 HNF-3, and 1 Nkx2-5 sites (Sparrow et al., 2000; Lien et al., 2002). In addition to confirming published sites, the ECR analysis revealed conserved binding sites for *Nkx2-2, Nkx2-5*, and *Nkx6-1* in the IR2. A manual search for consensus binding sequences also showed that four high affinity *Bapx1* sites (Kim et al., 2003) exist in the murine *NGRS* (two in the AR2, two in the IR2).

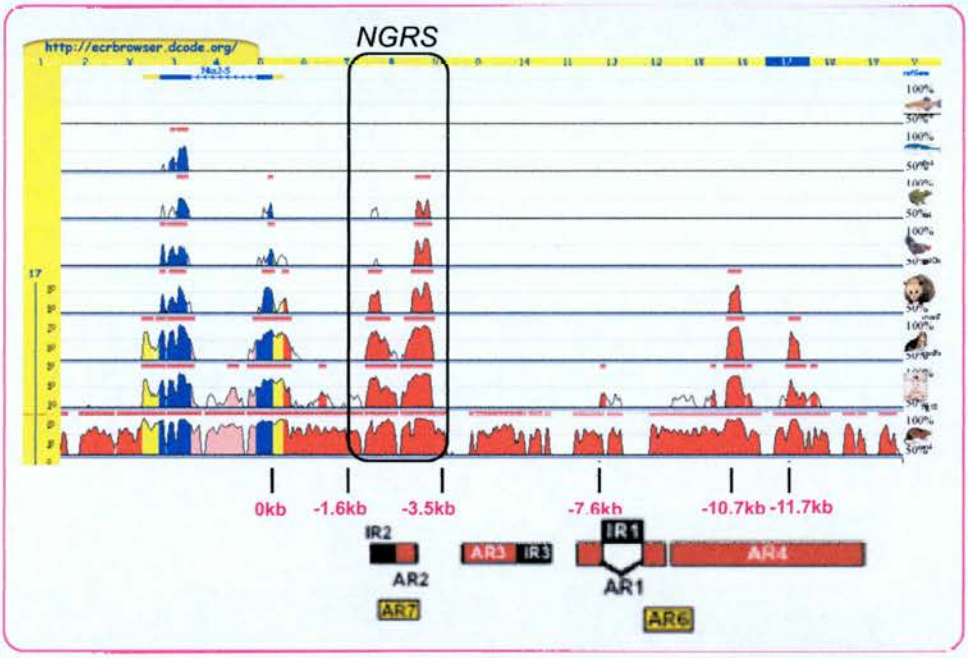

Figure 2.5 **The evolutionary conserved regions (ECRs) upstream of *Nkx2.5***

The *NGRS* region of the mouse genome was aligned with the genomes of (from top to bottom) fugu, zebrafish, *Xenopus*, chick, opossum, dog, human, and rat. Evolutionary conserved regions were then detected using the ECRBrowser program. The parameters for ECR detection were 70% identity over 100bp of ungapped sequence. The vertical axis for each species represents percent sequence identity, from 50 to 100%. The results were output as a smooth graph (smoothed version of a Pip-plot). Shading within the peaks indicates the type of sequence: red – intergenic element, blue – coding exon, yellow – untranslated region (UTR), pale pink - intron. Synteny is indicated by the blue line along the bottom of each alignment.
The cloned NGRS region is outlined by a black box; two distinct ECR peaks are present in this region. The ECRs upstream of *Nkx2.5* are aligned with the proposed activating and inhibitory regulatory regions presented in **Figure 2.3**. The approximate distances of the main ECRs from the translational start point of *Nkx2.5* are written in pink.

2.3.4 Generation and analysis of transient transgenic NGRS-LacZ embryos

2.3.4.1 Generation of transient transgenic embryos

The *NGRS* appeared to be a good marker of the developing spleen and pyloric sphincter on the basis of the expression observed at E12.5. The next obvious question was whether this expression can be traced to an earlier stage in development, or whether it is *de novo*, therefore limiting the use of the *NGRS* as a tool. Three microinjection sessions were undertaken to generate transient transgenic embryos carrying the *NGRS-LacZ* construct used previously, in which *LacZ* is driven by the *NGRS* and the *β-globin* promoter. Embryos were genotyped by polymerase chain reaction (PCR) using primers against *LacZ* and *Myogenin*; the former identifies embryos carrying the transgene, the latter confirms the integrity of the DNA. The results of the microinjections are summarised in **Table 2.1**.

Session	Stage	Number of recipients	Number of embryos	Number transgenic (PCR)	X-gal staining
1	E9.5	4	11	1	None
2	E9.5	n/a	7	0	None
3	E10.5	2	17	3	3/3 - described in **Section 2.3.4.2**

***Table 2.1* – Results of *NGRS-LacZ* microinjection sessions to generate transient transgenic embryos**

Transgenic embryos were identified by PCR for *LacZ*. Many of the embryos from the first session were runted and reabsorptions had occurred. One of the embryos from the third session showed retarded growth; this was one of the three transgenic embryos.
n/a: not available

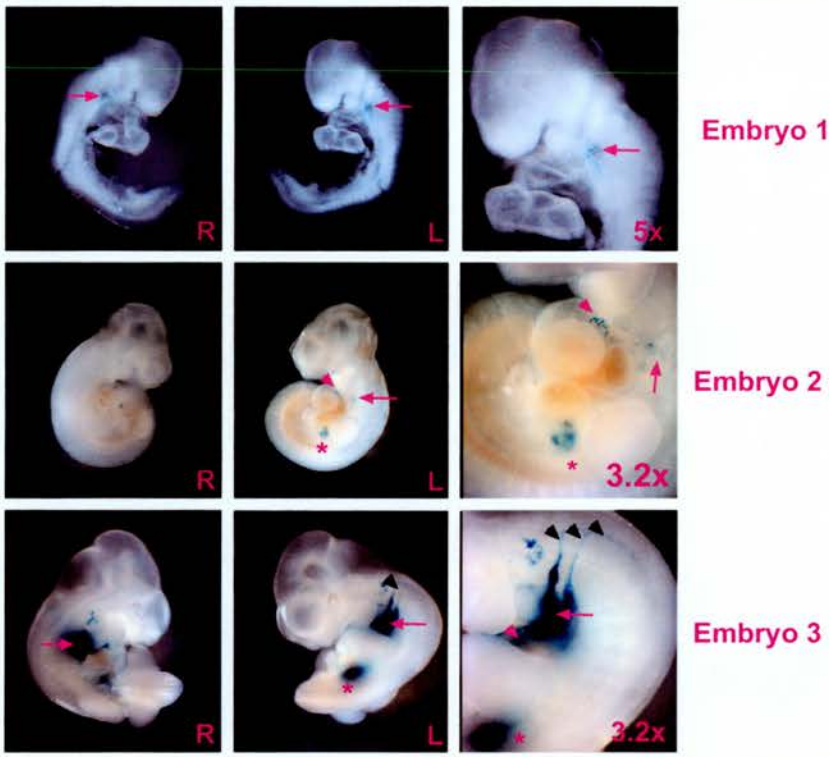

Figure 2.6 **X-gal detection of *NGRS-LacZ* expression in E10.5 transient transgenic embryos**

Right (**R**) and left (**L**) side photos are at 2.5x magnification; the third column of images is at increased magnification. **Embryo 1** is developmentally retarded; **Embryo 2** shows mosaic expression; **Embryo 3** shows strong expression. Note the left-sided gut expression in Embryos 2 & 3. **Pink arrow**: pharyngeal endoderm expression; **pink arrowhead**: cardiac outflow tract expression; **pink asterisk**: gut expression; **black arrowhead**: expression in nerves.

2.3.4.2 NGRS-LacZ expression analysis

Transgene expression in the three E10.5 transient transgenic embryos was examined by whole mount X-gal staining (**Figure 2.6**). Expression was present in the runted embryo (**Embryo 1**) in the pharyngeal endoderm. The other two embryos showed expression in the pharyngeal endoderm, outflow tract, and gut. The outflow tract expression was minimal, and the gut expression left-sided. Ectopic expression was noted in the presumptive facial nerves of **Embryo 3**.

Embryos 2 & 3 were examined in more detail by sectioning (**Figure 2.7**). **Embryo 2** exhibited milder staining and so was cut into thick slices on a vibratome; the strongly stained **Embryo 3** was examined using thinner microtome sections. Three representative sections through the gut are shown for each embryo, progressing in an anterior-posterior direction. **Embryo 2** was mosaic for transgene expression, whereas **Embryo 3** expressed *LacZ* in all cells within positive tissues. The pharyngeal endoderm expression was localised to the thyroid primordium (**Figure 2.7a-iv**).

The left-sided gut expression was localised to the SMP. In **Embryo 2**, gut expression commenced in the ventral SMP and mesenchyme surrounding the exit of the posterior stomach (**Figure 2.7a-i**), with some expression also apparent in the dorsal mesenchyme - a staining pattern reminiscent of endogenous *Nkx2-5* expression. Expression continued in these tissues to the level of the pancreatic buds (**Figure 2.7a-ii, iii**). The finer sectioning technique employed for **Embryo 3** revealed that the most anterior gut expression is in the dorsal mesenchyme, perhaps relating to the dorsal mesogastrium or the putative splenic mesenchyme (**Figure 2.7b-i**). Expression then spread throughout the more posterior mesenchyme and SMP (**Figure 2.7b-ii, iii**). It should be noted that whilst **Figure 2.7 b-ii** appears to depict some endodermal expression, this was not noted in other sections and may be an artefact of the sectioning process (c.f. **Figure 2.7b-iii**). The presence of staining throughout the mesenchyme underlying the SMP is in contrast to the two distinct domains of endogenous *Nkx2-5* expression. The entirety of the SMP itself was also stained, as opposed to just the ventral region marked by *Nkx2-5* expression. Strong

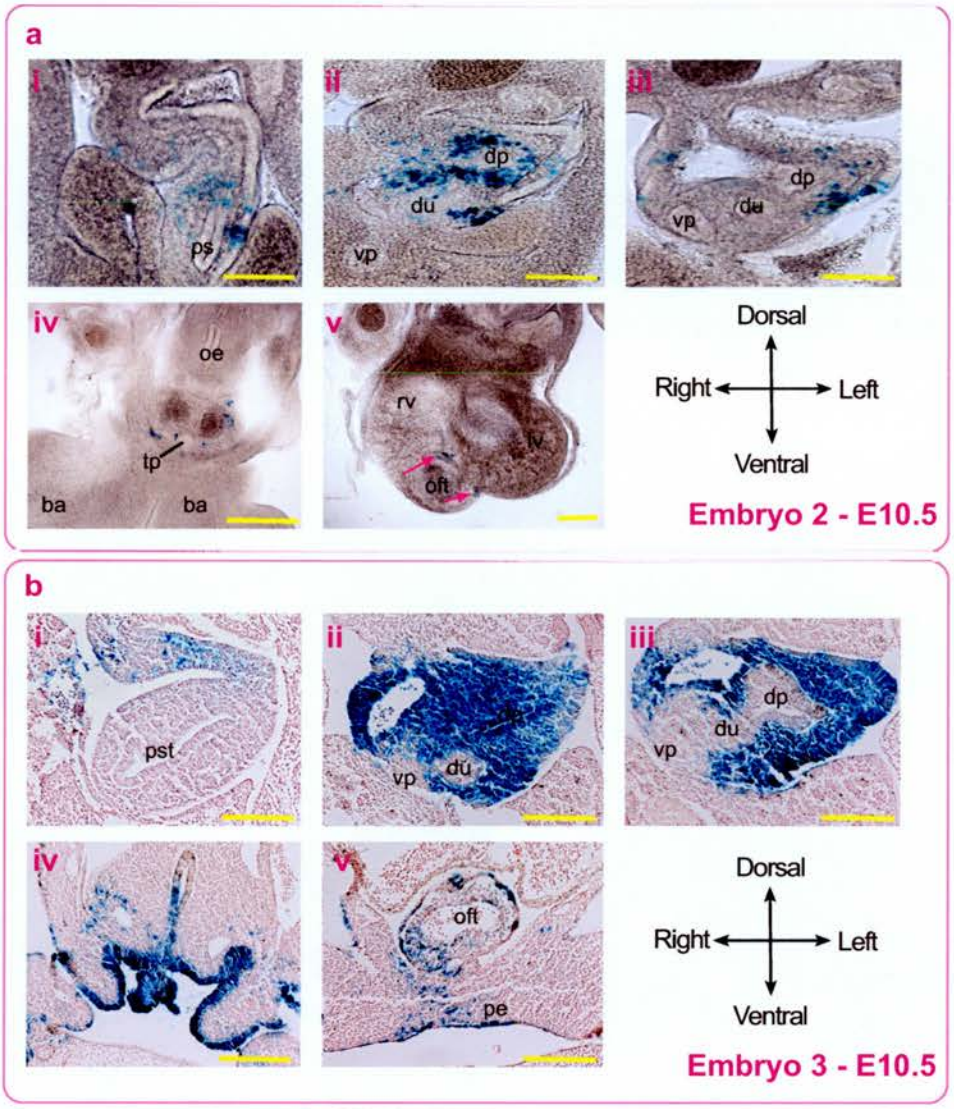

***Figure 2.7* X-gal detection of *NGRS-LacZ* expression in transient transgenic embryos**

a and **b i-iii**: progressive sections through the SMP at E10.5.
a) iv: expression around the thyroid primordium. **v**: cardiac outflow tract expression (**pink arrow**).
b) iv: pharyngeal endoderm expression. **v**: cardiac outflow tract expression.
All images were taken at 10x magnification except **a) v** which is at 5x. **Embryo 2**: 100μm agarose vibratome sections. **Embryo 3**: 9μm paraffin wax microtome sections. **Yellow scale bars** represent 150μm.

c: X-gal staining in the E12.5 heart is minimal and is localised to the outflow tract (arrows). *NGRS-LacZ* is also expressed in the thyroid primordium (*). 9μm wax section counterstained with Nuclear Fast Red.
ps: pyloric sphincter; **vp**: ventral panreatic bud; **du**: duodenum; **dp**: dorsal pancreatic bud; **oe**: oesophagus; **tp**: thyroid primordium; **ba**: branchial arch; **rv**: right ventricle; **lv**: left ventricle; **oft**: outflow tract; **pst**: posterior stomach; **pe**: pharyngeal endoderm.

expression was also noted in the pharyngeal endoderm (**Figure 2.7b-iv**) and cardiac outflow tract, contiguous with the pharyngeal endoderm expression (**Figure 2.7b-v**).

Cardiac expression was minimal and comparable to that reported for a similar enhancer region (Reecy et al., 1999). Hearts from the two E12.5 transient transgenic embryos generated previously were sectioned to further examine cardiac expression. Expression was minimal at E12.5, with only a few X-gal stained cells in the outflow tract and main body of the heart (basal right ventricle) (**Figure 2.7c**). Expression was less than that reported for a -1 to -3300bp region by Searcy and colleagues (Searcy et al., 1998) - who also traced expression back to the E7.5 cardiac crescent - and more akin to that reported in studies in which the *NGRS* region is incapable of driving cardiac expression at E7.5, and confers only sparse expression in the E9.5 and E10.5 heart (Reecy et al., 1999; Tanaka et al., 1999c).

The minimal cardiac expression at E10.5 and E12.5, along with the presence of X-gal stained cells in the SMP and underlying putative splenic mesenchyme at E10.5, suggested that the *NGRS* was of further interest. Stable transgenic lines were therefore generated to facilitate a thorough examination of the developmental expression pattern conferred by the *NGRS*.

2.3.5 Generation and analysis of stable transgenic NGRS-LacZ lines

2.3.5.1 Generation of stable transgenic lines

Microinjection sessions were performed as described and the mice generated were genotyped using combined *LacZ/Myo* PCR. The results of these sessions and of subsequent breeding are shown in **Table 2.2** and genotyping results are shown in **Figure 2.8**.

Session	Number of progeny	Number transgenic	Transmission	X-gal staining	Line established
1	15	0	-	-	-
2	35	0	-	-	-
3	29	2 m	x CD1: yes	Yes	-
			x F1: yes	Yes	**"Line 4"**
			x CD1: no (0/23; 2 plugs)	No (0/23; 2 plugs)	-
			x F1: no (0/19; 2 litters)	-	-
		2 f	x F1: yes	Yes	**"Line 21"**
			x F1: no (0/23; 3 litters)	-	-

***Table 2.2* – Results of *NGRS-LacZ* microinjection sessions to generate stable transgenic lines**

Transgenic mice were identified by duplicate PCR for *LacZ*. Transmission was tested by crossing founder males with CD1 females and genotyping E12.5 embryos, or mating founder females with [CBA x C57BL/6] F1 males and genotyping the offspring. X-gal staining was performed on E12.5 embryos from matings between founder males and CD1 females, or from matings between sons of founder females with CD1 females.
m: male, **f**: female, **F1**: [CBA x C57BL/6] F1

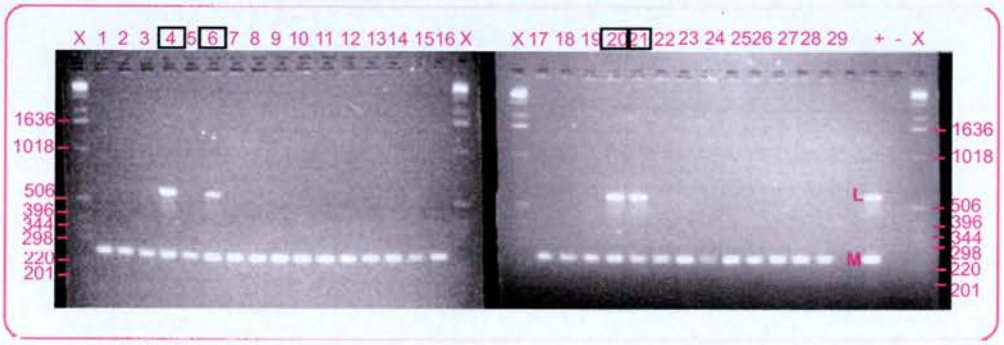

***Figure 2.8 LacZ/Myo* genotyping gel for *NGRS-LacZ* microinjection progeny**

2% agarose gel of combined *LacZ/Myo* PCR on earclip DNA from 29 microinjection progeny (5µl of 25µl PCR in each lane). Mice numbers 4, 6, 20, and 21 were positive for *LacZ*. The penultimate sample lane contains a PCR on *LacZ*+ earclip DNA from an unrelated *LacZ*-expressing line. The final sample lane is a PCR on water. The *LacZ* band (**L**) is approximately 600bp; the *Myo* band (**M**) is approximately 250bp and acts as an internal control for DNA integrity. **X** = 1Kb ladder (278ng/lane; Invitrogen).

2.3.5.2 NGRS-LacZ expression in non-gut tissues

NGRS-driven *LacZ* expression was examined by X-gal staining of at least one litter at half to one day intervals between E8.5 and E18.5. Details of the numbers of transgenic embryos in each litter are provided in **Appendix Table 2 (Line 4)** and **Table 3 (Line 21)**. Stained embryos from each stage are shown in **Figure 2.9 (Line 4)** and **2.10 (Line 21)**. **Figure 2.11 (Line 4)** and **2.12 (Line 21)** contain sections of stained embryos. **Figures 2.13 (Line 4)** and **2.14 (Line 21)** show staining in dissected guts and will be discussed in the next section.

At the earliest stage examined (E8.5) staining was restricted to the pharyngeal endoderm in most embryos. Staining extended into the presumptive outflow tract region in two embryos from Line 4 (not shown), though this was hard to examine given the translucency of the heart tube and the intense underlying pharyngeal staining. Similarly, the Line 21 embryo featured in **Figure 2.10a** appears to have cardiac expression but does not – this is merely the underlying strong pharyngeal expression. Pharyngeal expression was strong and extended towards the neural tube. Sectioning of embryos from Line 4 confirmed the presence of stained cells in the pharyngeal endoderm and outflow tract, and revealed expression in the endoderm of the foregut diverticulum (**Figure 2.11a**).

The pharyngeal endoderm expression was recapitulated at E9.0 and E9.5. Cardiac expression was lower in Line 21 than Line 4, and could not be seen in whole embryos (**Figure 2.10b**). X-gal stained cells were, however, observed in sectioned outflow tracts from both lines (**Figure 2.11a,b; 2.12a**). In addition to greater cardiac expression, Line 4 also displayed increased ectopic *LacZ* expression. Ectopic sites included the face, neural tube, and the nerves between the branchial arches and heart by E10.5; ectopic expression was minimal in Line 21. Outflow tract expression persisted in both lines at E10.5-13.5. Expression could also be observed in the thyroid primordium. Ectopic expression in Line 4 persisted, particularly around the snout, and by E13.5 was also found in the whisker follicles and limbs (**Figure 2.9g**).

The expression pattern conferred by *NGRS* is very similar to that found in mice in which *LacZ* has been knocked into the *Hox11* gene, generating expression in the presumptive pharynx, cardiac outflow tract, and spleen (Dear et al., 1995).

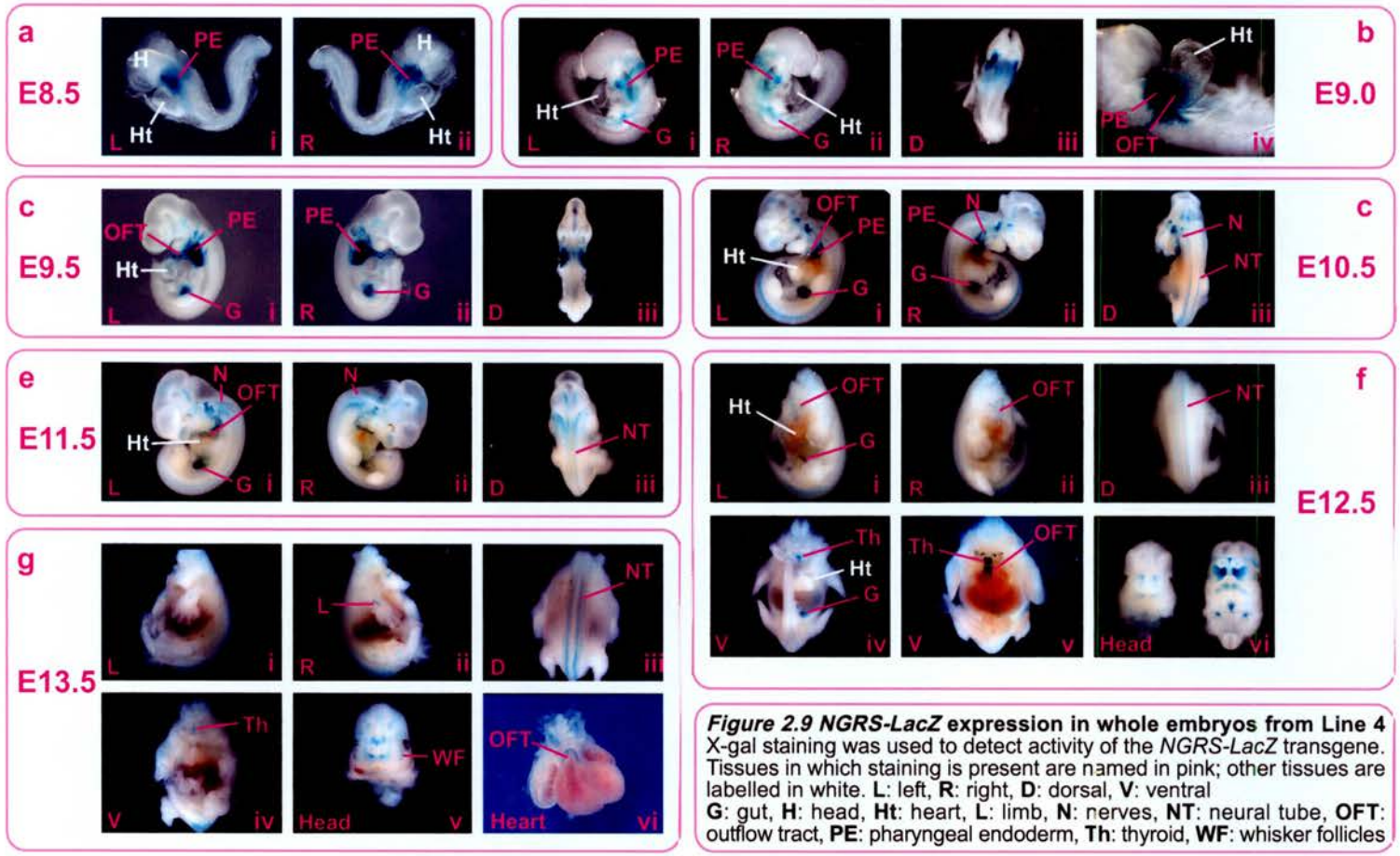

***Figure 2.9 NGRS-LacZ* expression in whole embryos from Line 4**
X-gal staining was used to detect activity of the *NGRS-LacZ* transgene. Tissues in which staining is present are named in pink; other tissues are labelled in white. **L**: left, **R**: right, **D**: dorsal, **V**: ventral
G: gut, **H**: head, **Ht**: heart, **L**: limb, **N**: nerves, **NT**: neural tube, **OFT**: outflow tract, **PE**: pharyngeal endoderm, **Th**: thyroid, **WF**: whisker follicles

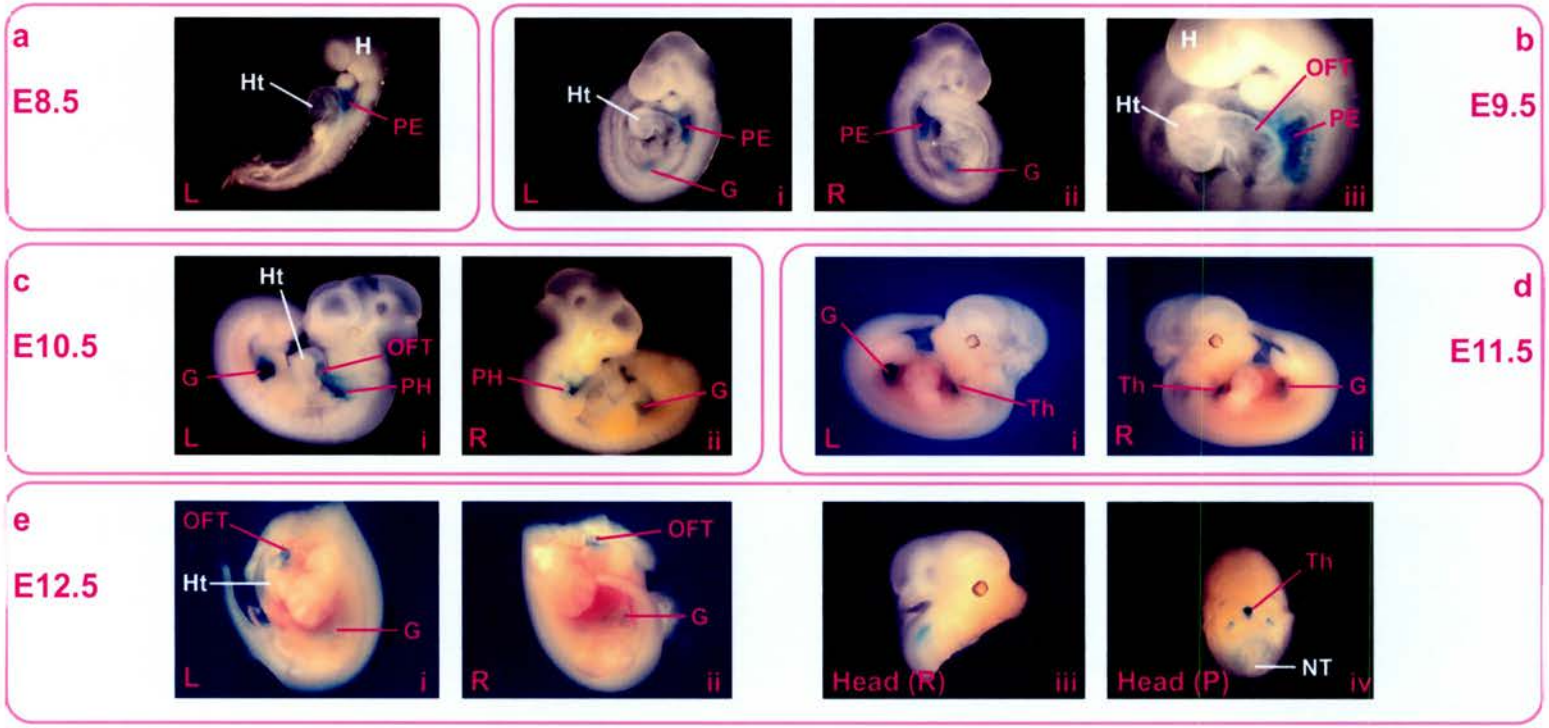

***Figure 2.10 NGRS-LacZ* expression in whole embryos from Line 21**

X-gal staining was used to detect activity of the *NGRS-LacZ* transgene at E8.5, 9.5, 10.5, 11.5, & 12.5. Tissues in which staining is present are named in pink; other tissues are labelled in white. The main regions of expression were the pharyngeal endoderm, gut, thyroid, and cardiac outflow tract. Ectopic expression was minimal.
L: left, **R**: right, **P**: posterior
G: gut, **H**: head, **Ht**: heart, **NT**: neural tube, **OFT**: outflow tract, **PE**: pharyngeal endoderm, **Th**: thyroid.

2.3.5.3 NGRS-LacZ expression in the gut

Sections through guts X-gal stained for *NGRS-LacZ* expression are provided in **Figure 2.11 (Line 4)** and **Figure 2.12 (Line 21)**. Staining in isolated guts is presented in **Figure 2.13 (Line 4)** and **Figure 2.14 (Line 21)**. An analysis of the differential staining intensities of the E13.5 pyloric sphincter and spleen following various stain times is shown in **Figure 2.15**.

2.3.5.3.1 E8.5-10.5

The first indication of gut expression was in the endoderm of the foregut diverticulum at E8.5 in Line 4 (**Figure 2.11a iii-iv**). Bilateral gut expression became evident at E9.0 in Line 4, and was pronounced by E9.5 in both lines. Sections through the SMP region of transgenic embryos at this stage show that the *NGRS* drives expression in the SMP on both the left and right sides (**Figure 2.11b iv-vii, Figure 2.12a iii-iv**), echoing the endogenous *Nkx2-5* and *Bapx1* expression patterns. The SMP expression continues into the flanking horns of thickened coelomic epithelium (**Figure 2.11b iv**). The nascent mesenchyme, which lies between the SMP and endodermal gut tube, is also marked. No expression is found in the endoderm.

Whole mount X-gal staining of E10.5 guts revealed strong expression in the posterior stomach, extending into the presumptive pyloric sphincter region (**Figure 2.13a, Figure 2.14a**). Expression was absent from the anterior stomach, but ectopic liver expression was noted in Line 4 (**Figure 2.13a**). This is specific to Line 4, as it had not been noted in transient transgenics or embryos from Line 21; nor is *Nkx2-5* expressed in the liver.

Whilst the *NGRS* expression pattern matches that of endogenous *Nkx2-5* in the SMP at E9.5, differences exist between these patterns by E10.5. *Nkx2-5* expression is localised to two domains – ventral and dorsal – in the E10.5 SMP and underlying mesenchyme; *NGRS-LacZ*, however, is detected throughout this region, including in the tip of the SMP where *Bapx1* is expressed (**Figure 2.11c, Figure 2.12b i-iv**). However, it may be of significance that in the first two of the four serial sections presented in **Figure 2.12b**, two domains of high transgene expression can be

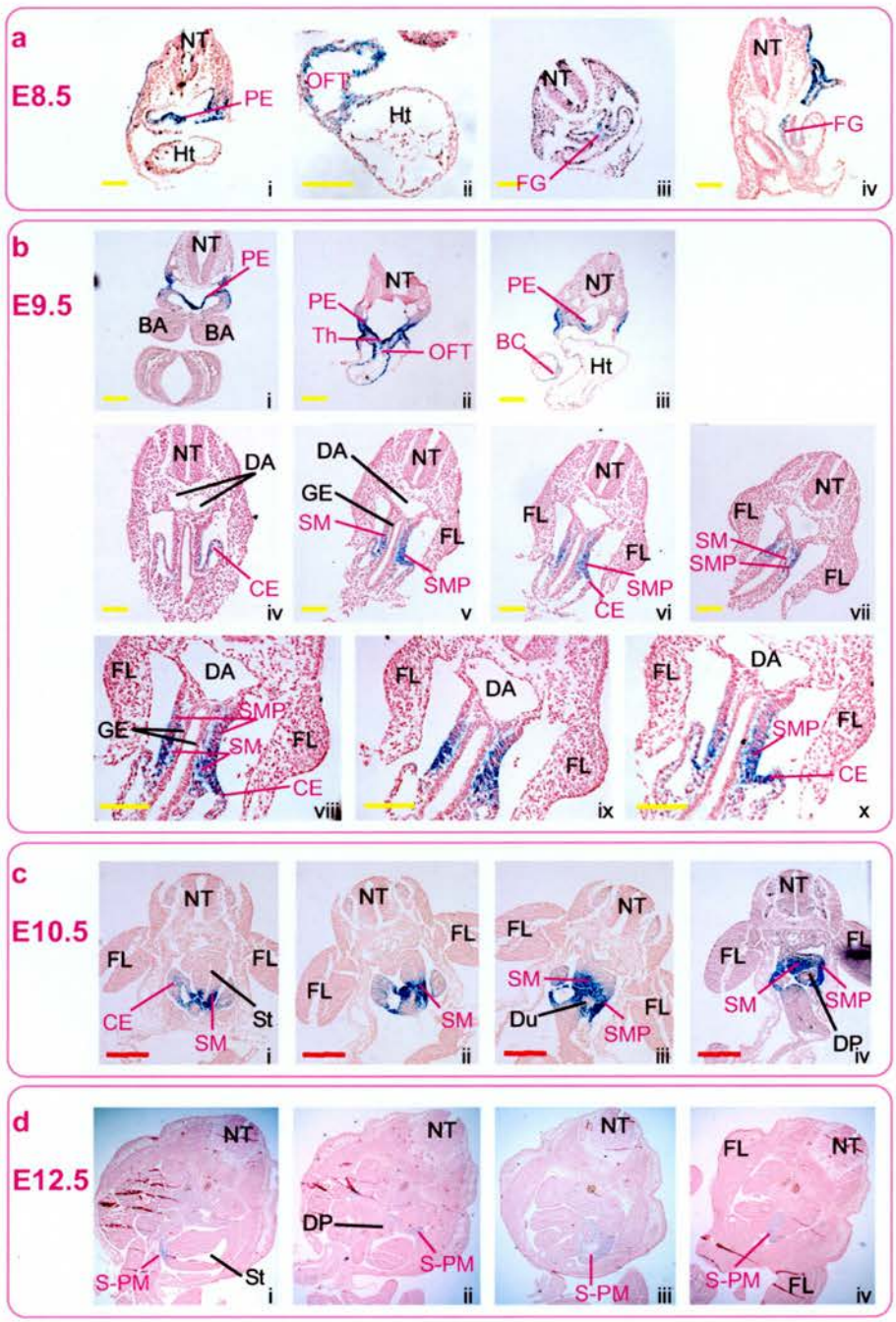

Figure 2.11 **X-gal staining of *NGRS-LacZ* activity in embryos from Line 4**
Embryos were stained wholemount with X-gal and sectioned on a microtome. Positive tissues are labeled in **pink**, negative tissues in **black**. Images proceed in an anterior-posterior (cranial-caudal) direction across the page. Sections are counterstained with Nuclear Fast Red. **a**) 8μm sections, **i, iii, iv**: 5x magnification; **ii**: 10x magnification; **b**) 9μm , **i-vii**: 5x magnification; **viii-x**: 10 x magnification; **c**) 9μm sections, 5x magnification; **d**) 10μm sections, 2.5x magnification. Yellow scale bars: 100μm. Red scale bars: 400μm.

BA: branchial arch, **BC**: bulbus cordis, **CE**: coelomic epithelium, **DA**: dorsal aorta, **DP**: dorsal pancreas (endoderm), **Du**: duodenum, **FG**: foregut, **FL**: forelimb, **GE**: gut endoderm, **Ht**: heart, **NT**: neural tube, **OFT**: outflow tract, **PE**: pharyngeal endoderm, **SM**: splanchnic mesenchyme, **SMP**: Splanchnic Mesothelial Plate **S-PM**: spleno-pancreatic mesenchyme, **St**: stomach, **Th**: thyroid primordium.

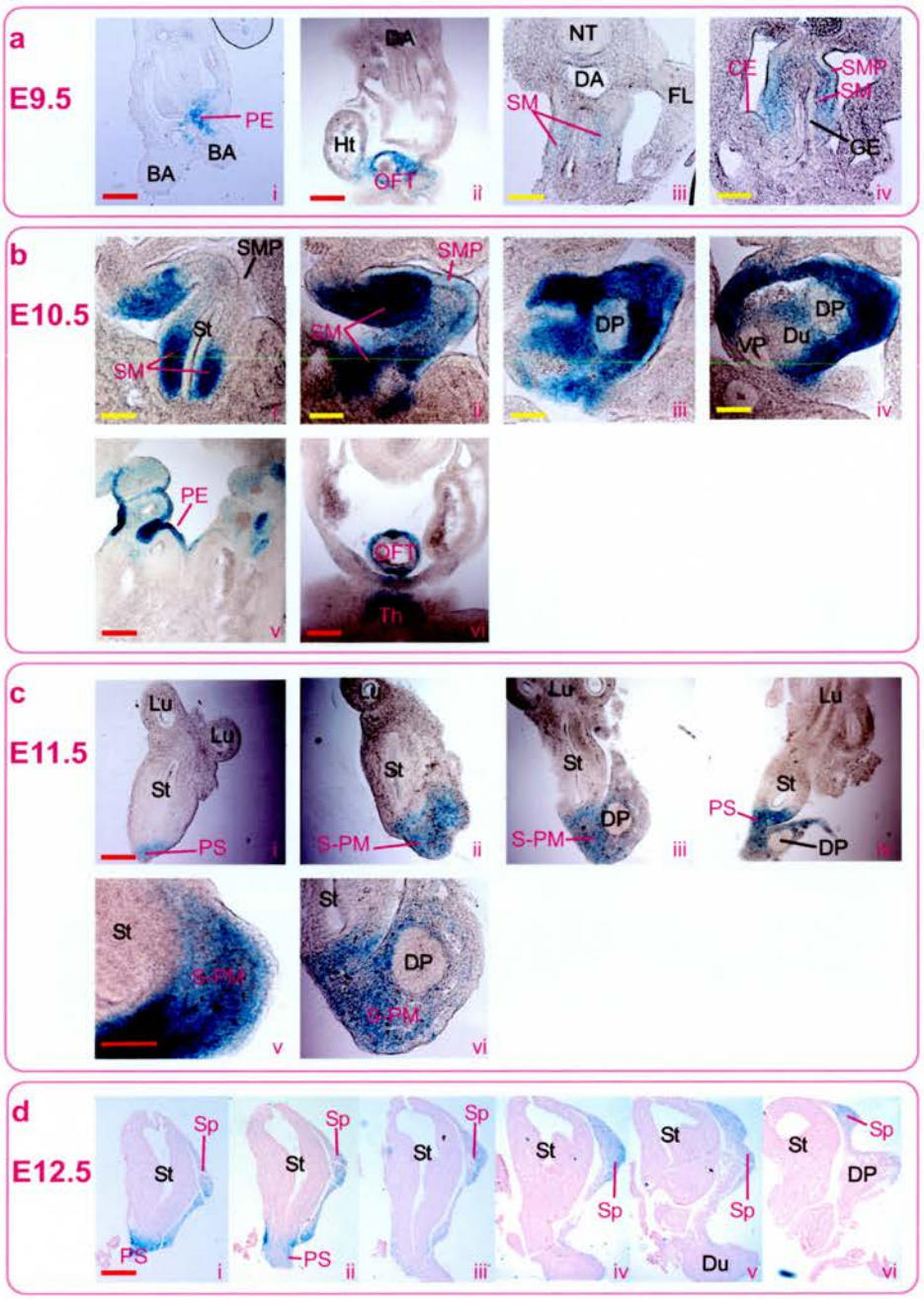

Figure 2.12 **X-gal staining of *NGRS-LacZ* activity in embryos from Line 21**
Embryos were stained wholemount with X-gal; embryos (**a,b**) or guts (**c,d**) were then sectioned on a vibratome (**a-c**) or microtome (**d**). Positive tissues are labeled in **pink**, negative tissues in **black**. Embryo images proceed in an anterior-posterior (cranial-caudal) direction across the page; gut images are presented in a ventral-dorsal series.
a) 50μm sections - **i, ii**: 5x magnification, **iii, iv**: 10x; **b**) 100μm sections - **i-iv**: 10x; **v-vi**: 5x; **c**) 30μm sections- **i-iv**: 5x, **v-vi**: 10x; **d**) 7μm sections - 5x; counterstained with Nuclear Fast Red Yellow scale bars: 100μm. Red scale bars: 200μm.
BA: branchial arch, **CE**: coelomic epithelium, **DA**: dorsal aorta, **DP**: dorsal pancreas (endoderm), **Du**: duodenum, **FL**: forelimb, **GE**: gut endoderm, **Ht**: heart, **Lu**: lung buds, **NT**: neural tube, **OFT**: outflow tract, **PE**: pharyngeal endoderm, **PS**: pyloric sphincter, **SM**: splanchnic mesenchyme, **SMP**: Splanchnic Mesothelial Plate, **Sp**: spleen, **S-PM**: spleno-pancreatic mesenchyme, **St**: stomach, **Th**: thyroid primordium.

seen; these correspond well with the two domains of endogenous *Nkx2-5* expression. *NGRS-LacZ* expression is specific to the SMP and underlying mesenchyme, and is not present in the gut endoderm. Contiguous expression extends into the horns of the coelomic epithelium (**Figure 2.11c i**), as seen at E9.5. Expression commences at the ventral aspect of the posterior stomach and spreads across the SMP at increasingly posterior levels down the gut until the whole SMP can be marked with X-gal. This was at first interpreted as an experimental artefact (sectioning angle), but has since been observed in most sectioned E10.5 (and E9.5) embryos from both lines. As such it is probably a real effect – i.e. the most anterior limit of *NGRS* expression is on the ventral face of the stomach.

2.3.5.3.2 E11.5-13.5

The left-sided nature of *NGRS-LacZ* gut expression was apparent in most whole embryos at E10.5, but was particularly noticeable by E11.5 (**Figure 2.9e, Figure 2.10d**). X-gal staining of guts from this stage revealed that a single gut expression domain still exists, but that this now noticeably corresponds to the pyloric sphincter and splenic mesenchyme (**Figure 2.13b, Figure 2.14b**). Given the continuity of this domain, it seems likely that the splenic mesenchyme expression is not *de novo* but is instead related to that seen in the E10.5 – and possibly the E9.5 – mesenchyme underlying the SMP. Expression is more refined in guts from Line 21 as, although the pyloric sphincter and splenic mesenchyme expression domains are still contiguous, far less of the posterior stomach mesenchyme is marked by transgene expression. Sections through E11.5 guts demonstrate the continuity of the staining in the spleno-pancreatic mesenchyme with that in the mesenchyme of the distal stomach (**Figure 2.12c**). The non-expressing pancreatic endoderm can also be seen embedded in the stained spleno-pancreatic mesenchyme. The lower two images in **Figure 2.12c** show the presence of an SMP-like ridge structure at the periphery of the spleno-pancreatic mesenchyme.

The entire spleen is marked by *NGRS-LacZ* expression by E12.5, and this remains contiguous with expression in the pancreatic mesenchyme and pyloric sphincter (**Figure 2.13c, Figure 2.14c**). The spleen appears to be connected to the

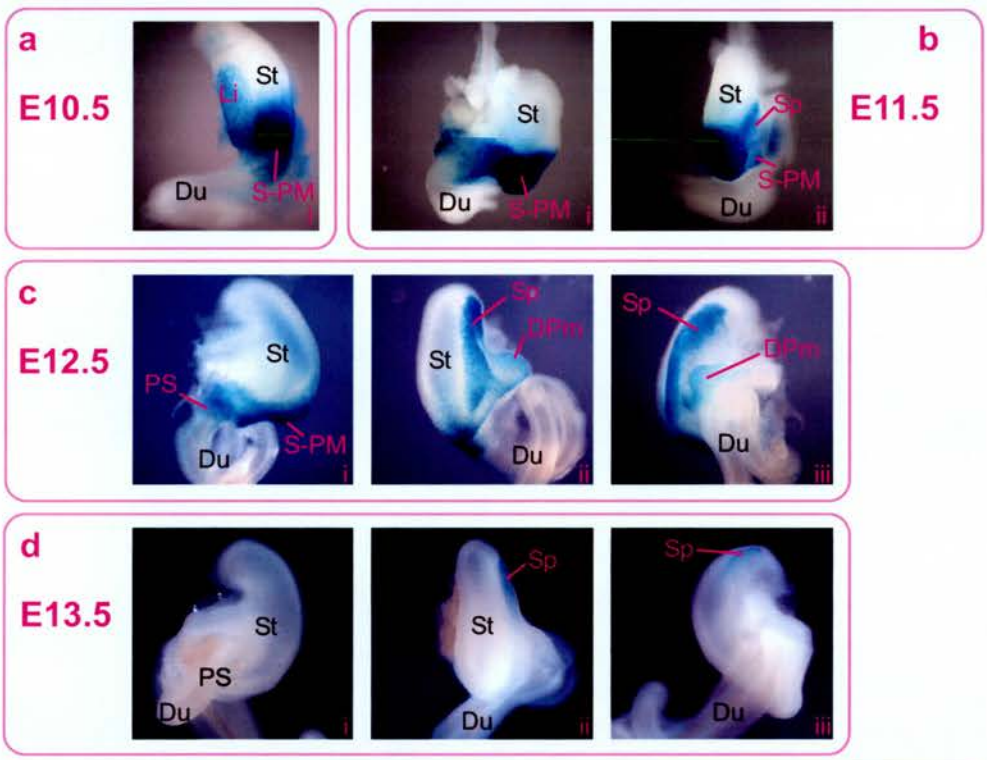

Figure 2.13 **X-gal staining of *NGRS-LacZ* activity in guts from Line 4**

a) E10.5, **b**) E11.5, **c**) E12.5, **d**) E13.5
Positive tissues are labeled in **pink**, negative tissues in **black**. Guts are not shown to scale
Gut faces: **i** - ventral, **ii** - greater curvature, **iii** - dorsal
DPm: dorsal pancreatic mesenchyme, **Du**: duodenum, **Li**: liver bud, **PS**: pyloric sphincter, **Sp**: spleen, **S-PM**: spleno-pancreatic mesenchyme, **St**: stomach

Figure 2.14 **X-gal staining of *NGRS-LacZ* activity in guts from Line 21**

a) E10.5, **b**) E11.5, **c**) E12.5, **d**) E13.5, **e**) E14.5, **f**) E15.5, **g**) E16.5, **h**) E17.5, **i**) E18.5.
The spleen is connected to the stained dorsal pancreatic mesenchyme by a "stalk" of positive cells at E12.5 (**pink arrow** in **c**). At E13.5 the stained spleen is distinct from the stomach; a visible gap exists between the two tissues (**yellow box** in **d-iii**). Two lines of stained cells begin to arise from either side of the pyloric sphincter, up the lesser curvature of the stomach from E14.5 (**blue arrows** in **e, f, g, h, i**). These structures are well-defined by E16.5 (**g-iii**), terminating in non-stained duct-like structures. The identity of the marked tissue is unknown. The *NGRS* appears to no longer be active in the spleen by E17.5 (**h**), but expression is still detected at E18.5 (**i-ii**: weakly stained spleen, **i-iii**: strongly stained spleen) indicating that this is an experimental artefact.
Positive tissues are labeled in **pink**; negative tissues are labeled in **black**. **c-iii, d-iii, g-iii** are at high magnification. Guts are not shown to scale.
V: ventral, **D**: dorsal, **GC**: greater curvature, **LC**: lesser curvature; **DP**: dorsal pancreas, **DPm**: dorsal pancreatic mesenchyme, **Du**: duodenum, **Lu**: lung buds, **PS**: pyloric sphincter, **St**: stomach, **S-PM**: spleno-pancreatic mesenchyme

pancreatic mesenchyme by a "stalk" of stained cells (**Figure 2.14c-iii – pink arrow**). This connection is visible until E14.5. Sections through the E12.5 stomach illustrate this spleno-pancreatic mesenchyme expression and the connection it shares with the mesenchyme of the posterior stomach/pyloric sphincter (**Figure 2.12d**). Though the anterior tip of the spleen appears to be contiguous with the mesenchyme surrounding the stomach, *NGRS* drives expression only in the splenic component. No expression is present in the gut endoderm.

The E13.5 gut expression pattern in Line 21 embryos is much the same as that established by E12.5, albeit with more intense staining (**Figure 2.14d**). The pyloric sphincter and spleen expression domains are still continuous at this stage, and are linked by a layer of *NGRS-LacZ*-expressing mesenchyme which is distinct from the stomach itself (**Figure 2.14d-iii – yellow box**). The effect of staining time on the final expression pattern was studied at E13.5 and this is summarised in **Figure 2.15**. This provided valuable data on the relative expression levels within the gut. The pyloric sphincter is heavily stained after only 30 minutes exposure to X-gal, suggesting that very high levels of β-gal exist in this tissue. Staining of the spleen was not detectable until 2-4 hours, and was initially localised to just a handful of cells. The number of marked cells increased slightly by 8 hours, when a few blue cells could now also be seen overlying the pancreas. Uniform, low-level staining was present throughout the spleen after 10 hours X-gal exposure, and had increased by 12 hours. The pyloric sphincter and spleen expression domains were still separate at this point. Guts were stained for approximately 14 hours during the studies presented in this chapter; it would thus appear that staining in the region between these two domains becomes detectable between 12 and 14 hours of staining. By 24 hours spleen staining was intense and some marked cells were noticeable along the greater curvature of the stomach, extending from the pyloric expression domain.

Expression is no longer detectable in the pyloric sphincter and has been lost from all but the anterior portion of the spleen by E13.5 in embryos from Line 4 (**Figure 2.13d**). Endogenous *Nkx2-5* expression persists in the former tissue until at least E14.5, and in the latter until adulthood (Lints et al., 1993b). The loss of *NGRS-LacZ* expression was specific to Line 4, as expression continues throughout gut development in Line 21. The reduced ectopic and cardiac expression, and prolonged

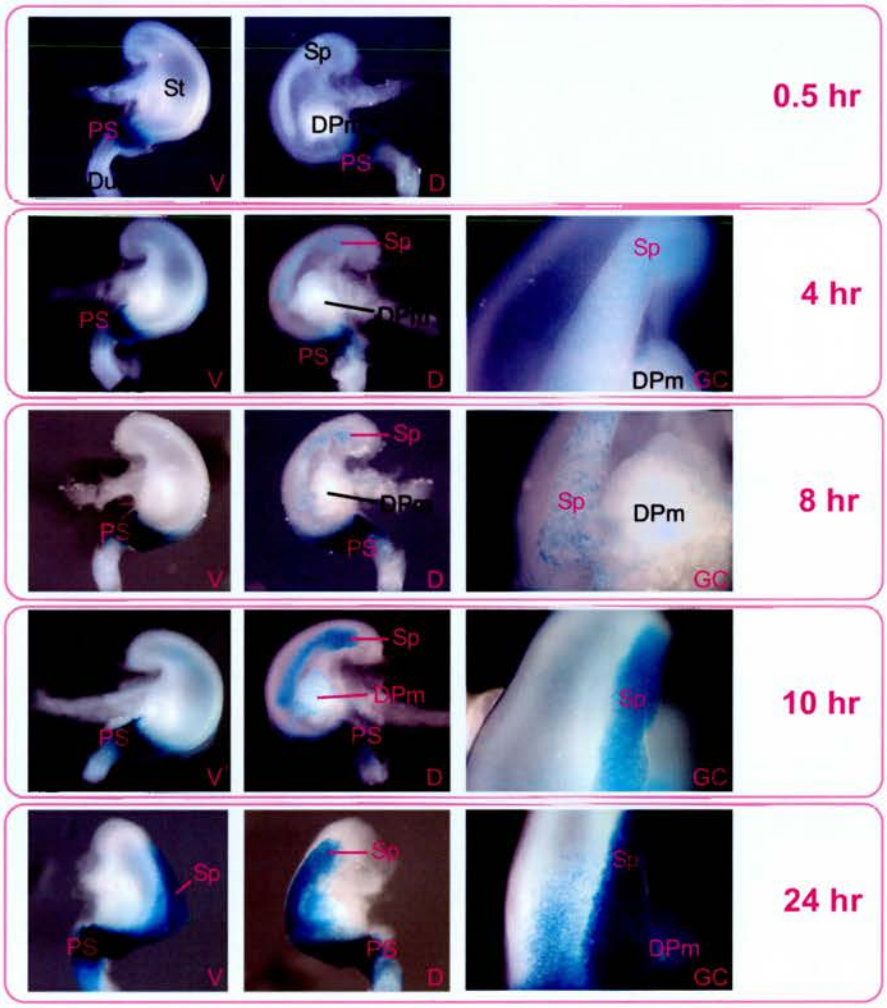

Figure 2.15 **The effect of X-gal staining time on detection of *NGRS-LacZ* activity in guts from Line 21**

The pyloric sphincter expression domain stains strongly after only half an hour, demonstrating the high expression of *NGRS-LacZ* in this tissue. The spleen takes approximately 10 hours to become stained, reflecting lower activity of the transgene. Positive tissues are labeled in **pink**, negative tissues in **black**. Gut faces: **D** - dorsal, **V** - ventral, **GC** – greater curvature.
DPm: dorsal pancreatic mesenchyme, **Du**: duodenum, **PS**: pyloric sphincter, **Sp**: spleen, **St**: stomach

and greater gut expression, therefore makes Line 21 a preferable source of data on the *NGRS* and, as such, only embryos from this line are used in the gut culture experiments described in **Chapter 4**.

2.3.5.3.3 E14.5-18.5

E14.5 *NGRS-LacZ* expression is similar to that at E13.5, though at a morphological level the spleen is now further from the pyloric sphincter (**Figure 2.14e**). By E15.5 the splenic and sphincter expression domains have become distinct, the pancreatic mesenchyme expression is lost, and the spleen stains less intensely for β–gal activity – though this varied between embryos (**Figure 2.14f**). It is also at this stage that two "horns" of stained tissue become particularly noticeable. These projections extend in an anterior direction from either side of the pyloric sphincter. A higher magnification image of these structures at E16.5 is provided in **Figure 2.14g-iii**, showing that they terminate in unstained duct-like tissue. The identity of these "horns" is unclear, though they could be related to the bile ducts. The other sites of E16.5 gut staining are the spleen and pyloric sphincter, with no expression present in the intervening pancreatic mesenchyme (**Figure 2.14g-ii**). Pyloric sphincter expression was also seen at E17.5 and E18.5 (**Figure 2.14h, i**). Splenic expression varied at these late stages, such that it was present in some guts and not in others, even within litters. When the spleen did stain, not all cells were marked, suggesting that only the mesenchymal-derived component of the spleen expresses *NGRS-LacZ*.

2.3.5.3.4 Summary of expression data

In summary, *NGRS* is a good marker of the SMP (E9.5-10.5), spleno-pancreatic mesenchyme (E11.5-12.5), developing spleen (E12.5 onwards), and pyloric sphincter (E11.5 onwards). The minimal ectopic and cardiac expression conferred by this element in Line 21, and its consistent transmission and expression, indicated that this stable transgenic reporter line would be of great use for marking and tracing development of the above tissues.

2.4 *NGRS* is not dependent on *Bapx1*

The results presented so far in this chapter, along with existing data, show the following: 1) that *Nkx2-5* and *Bapx1* share an expression domain in the SMP at E9.5, 2) that *Nkx2-5* expression is lost in the *Bapx1*$^{-/-}$ mutant gut, 3) that a highly conserved *Nkx2-5* upstream regulation region (*NGRS*) drives expression in the gut, and that this overlaps *Bapx1* expression, and 4) that a conserved high affinity Bapx1 binding site – along with other general Nkx binding sites – is present in the *NGRS*. The next question to ask is whether Bapx1 regulation of *Nkx2-5* is achieved through the *NGRS*.

To address this question, expression of the *NGRS* was examined on the *Bapx1*$^{-/-}$ background. Mice from both stable *NGRS-LacZ* lines were crossed with *Bapx1*$^{+/-}$ (phenotypically normal) mice. *Bapx1*$^{+/-}$ offspring carrying the *NGRS* transgene were genotyped for the *Neomycin* insertion which disrupts *Bapx1* and for *LacZ*. Double heterozygotes were then crossed with *Bapx1*$^{+/-}$ mice; one-eighth of the resulting embryos would be expected to carry *NGRS-LacZ* and have the *Bapx1*$^{-/-}$ genotype. X-gal staining was performed at E9.5, 10.5, 11.5, and 12.5 for both *NGRS-LacZ* lines, and also at E16.5 and E18.5 for Line 21. Embryos were genotyped for *LacZ* and also by a second *Bapx1*-based PCR, which can differentiate between the three possible genotypes ("*bap*" primers in **Chapter 7**). Details of numbers of embryos and genotypes are provided in **Appendix Tables 4 & 5** for Line 4 and Line 21, respectively. As can be seen from the figures in these tables, there was some difficulty in obtaining *LacZ/Bapx1*$^{-/-}$ embryos, particularly from Line 4.

X-gal staining patterns were compared with those of wild type and *Bapx1*$^{+/-}$ littermates. On the Line 4 *NGRS-LacZ* background, *LacZ/Bapx1*$^{-/-}$ embryos were successfully produced for three stages: E9.5, E10.5, and E12.5 (**Appendix Table 4**). Images of these embryos are provided in **Figure 2.16**. On the Line 21 background, *LacZ/Bapx1*$^{-/-}$ embryos were obtained at E9.5, E10.5, E11.5, and E12.5 (**Appendix Table 5**). These are shown in **Figure 2.17**. At all stages, in both lines, *LacZ* expression persisted despite the absence of *Bapx1* expression. However, the pattern of expression is obviously not identical between the wild type/*Bapx1*$^{+/-}$ and *Bapx1*$^{-/-}$ mutant guts as the latter are morphologically abnormal. Indeed, the pyloric sphincter

domain appears to be reduced in the Line 4 gut shown in **Figure 2.16d**; however, the twisted and abnormal nature of the mutant guts in this region impeded assignment of staining to specific structures, and staining varied between embryos. Expression was also found in Line 4 in the disorganised tissue that lies in place of the spleen (**asterisk** in **Figure 2.16d**). This expression was absent from Line 21, with staining instead being limited to the region around the pancreatic mesenchyme. It should, however, be noted that Line 21 was crossed onto a *Bapx1* line with a more severe spleen phenotype; the line with which Line 4 was crossed retains some disorganised splenic tissue.

Perhaps most crucially, *NGRS-LacZ* expression was retained in the SMP of *Bapx1*$^{-/-}$ embryos at E9.5 (**Figure 2.17a**). This is the point at which *Nkx2-5* and *Bapx1* expression overlaps and therefore at which dependence of *Nkx2-5* on *Bapx1* would be most expected.

The outcome of this experiment indicates that there may be other *Nkx2-5* gut enhancers through which Bapx1 exerts its control. As the ECRs presented in **Section 2.3.3** can be related to published cardiac elements, it seems unlikely that such an enhancer might reside in the region investigated, unless it is poorly conserved or murine-specific. Alternatively, a Bapx1-dependent gut enhancer may exist further afield. How far afield is uncertain, as genomic regulatory regions can be located far away from the gene they regulate; for example, the ZRS element can regulate *Shh* expression from 1Mb away (Lettice et al., 2003).

2.4.1 Optical projection tomography (OPT) analysis of NGRS-LacZ expression

Although *NGRS-LacZ* expression was maintained on the *Bapx1*$^{-/-}$ background, exactly how this expression related to that in the wild type gut was unclear. The *Bapx1*$^{-/-}$ gut has a twisted appearance, making imaging by standard microscopy difficult. X-gal stained guts from wild type, *Bapx1*$^{+/-}$, and *Bapx1*$^{-/-}$ *NGRS-LacZ*-positive E12.5 embryos (Line 21) were therefore examined using optical projection tomography (OPT). OPT allows three-dimensional visualisation of

Figure 2.16 NGRS-LacZ* activity in Line 4 in the absence of *Bapx1

Line 4 embryos on **wildtype**, ***Bapx1+/-***, and ***Bapx1-/-*** backgrounds were analysed for *NGRS-LacZ* expression by X-gal staining. The resulting staining patterns demonstrated that the *NGRS* is not dependent on *Bapx1* for its activity.
NGRS-LacZ gut expression is marked by a **pink arrow** in **a-c**.
L: left; **R**: right; **DPm**: dorsal pancreatic mesenchyme;**PS**: pyloric sphincter; **Sp**: spleen

Figure 2.17 NGRS-LacZ* activity in Line 21 in the absence of *Bapx1
Line 21 embryos on **wildtype**, ***Bapx1+/-***, and ***Bapx1-/-*** backgrounds were analysed for *NGRS-LacZ* expression by X-gal staining (heterozygote data not shown). The resulting staining patterns demonstrated that the *NGRS* is not dependent on *Bapx1* for its activity.
NGRS-LacZ gut expression is marked by a **pink arrow** in **a-b**. The sections in (**a**) are 7μm wax sections of X-gal stained tissue and are counterstained with Nuclear Fast Red. Yellow scale bars: 100μm. **L**: left; **R**: right; **GC**: greater curvature.
DA: dorsal aorta**; DPm**: dorsal pancreatic mesenchyme; **FL**: forelimb; **PS**: pyloric sphincter; SMP: Splanchnic Mesothelial Plate; **Sp**: spleen; **S-PM**: spleno-pancreatic mesenchyme

anatomy and gene expression (Sharpe et al., 2002). The guts shown in **Figure 2.17** were used to allow comparison of OPT and standard microscopy data.

Virtual sections through the stained guts are presented in **Figure 2.18**. The *NGRS* is clearly active in the pyloric sphincter and spleen of normal (wild type and *Bapx1*$^{+/-}$) guts, and continuity can be observed between these domains (e.g. **Figure 2.18b ii**). *NGRS-LacZ* is also strongly expressed in the abnormal pyloric sphincter region of the *Bapx1*$^{-/-}$ guts, flanking the site where constriction would normally occur (**Figure 2.18 biii ,ciii**). Expression is absent, however, from the tissue which occupies the region where the spleen normally lies (**Figure 2.18 biii, diii**). This tissue contains cysts (**arrowed in Figure 2.18d iii**) – as previously described by Asayesh and colleagues (Asayesh et al., 2006) – and is similar in appearance to the sparse splenic scaffold described by Akazawa *et al.* (Akazawa et al., 2000).

The images contained in **Figure 2.18** are two-dimensional representations of the OPT data. The three-dimensional movies of *NGRS-LacZ* expression can be found on the **CD included with this thesis**. In addition to facilitating examination of *NGRS* activity, the OPT analysis also allowed visualisation of components of the *Bapx1*$^{-/-}$ gut phenotype in a way not possible with standard microscopy or sectioning: for example, the folding of the duodenum back against the stomach (asterixed in **Figure 2.18 aiii, ciii**), the loss of the pyloric sphincter constriction, the cysts in the abnormal splenic region, and the widened duodenum (Watson et al., 2007). Further OPT analysis of *NGRS-LacZ* expression in wild type and *Bapx1*$^{-/-}$ guts from E10.5 onwards ought to be most informative, and a time-series is thus planned.

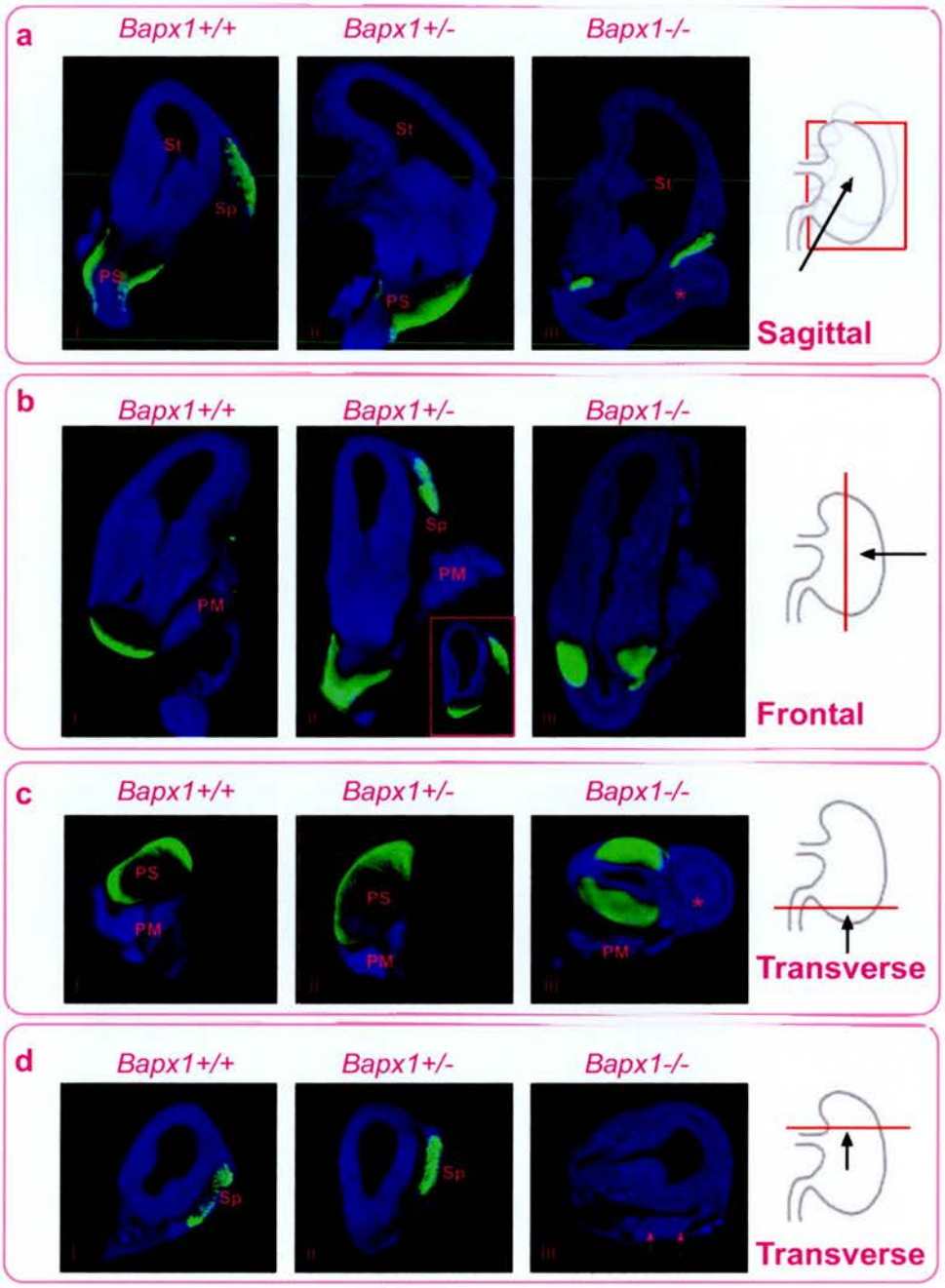

Figure 2.18 **Virtual sections from OPT reconstructions of *NGRS-LacZ* expression in wildtype and *Bapx1* mutant guts at E12.5**

X-gal staining for *NGRS-LacZ* expression is shown in green against blue gut tissue. **a**: Sagittal, **b**: frontal, **c, d**: transverse virtual sectioning planes. Drawings of guts illustrate the sectioning planes (red). The direction from which sections are viewed is denoted by a black arrow. The guts in **a** are "sectioned" at a comparable pyloric sphincter level. The boxed insert in the *Bapx1+/-* image in **b** shows the contiguous nature of the spleen and pyloric sphincter *NGRS-LacZ* expression domains.
St: stomach; **PS**: pyloric sphincter; **Sp**: spleen; **PM**: pancreatic mesenchyme; *: mutant duodenum, folded back onto stomach; **pink arrows**: cysts

2.5 The *NGRS* can be used to mark abnormal spleen development in the *Rwhs* mutant

The *NGRS* is a good marker of the wild type developing spleen. Mutants with defects in spleen development are of obvious interest when trying to understand this process, and so it was of interest to know whether *NGRS-LacZ* expression could also be used to mark abnormal spleen development. Expression has already been shown to persist in the *Bapx1*$^{-/-}$ asplenic mutant. Expression of *NGRS-LacZ* was therefore examined in an unrelated spleen defective mutant: the *Retinal white spots (Rwhs)* mutant.

The *Rwhs* mutation resides on chromosome 11 and was identified in a dominant screen for ENU-induced eye phenotypes (Thaung et al., 2002). *Rwhs* homozygotes die at birth due to breathing difficulties, and have small lungs, congenital diaphragmatic hernia, and gut hypoplasia (spleen, pancreas, stomach, and duodenum) (Dr Alan Hart, personal communication). An interesting case of polysplenia, in the form of a bifurcating spleen, was also observed by Dr Rob Watson in one embryo. I therefore decided to investigate this phenotype further, using the *NGRS-LacZ* reporter as a marker for spleen development.

The *Rwhs* mutation and *NGRS-LacZ* (Line 21) were bred onto the same line. Crosses were then set up between *Rwhs* heterozygotes and *NGRS-LacZ/Rwhs* heterozygotes. Due to time restraints and false pregnancies, only one litter of embryos was analysed during the course of my studies. Of the eight embryos, six carried the *NGRS-LacZ* transgene, and one of these was homozygous for the *Rwhs* mutation. The *Rwhs* genotype is identified by sequencing of the affected region and detection of a T-to-C mutation therein. Details are provided in **Chapter 7**.

X-gal staining of wild type, *Rwhs* heterozygous, and *Rwhs* homozygous E12.5 guts is shown in **Figure 2.19**. Comparison of the stained *Rwhs* homozygous mutant with an unstained (*LacZ*-negative) homozygous mutant littermate highlights the need to specifically mark the affected spleen tissue, in order to assess the phenotype (**Figure 2.19b**). X-gal staining of *NGRS-LacZ* expression showed how the spleen does indeed bifurcate at its posterior base, producing a second, shorter spleen along the greater curvature of the stomach (outlined in **yellow** in **Figure 2.19**).

Sections through the affected region show that, in addition to the normally marked spleen, a second column of blue cells is present along the greater curvature, and that stained cells from this second "spleen" region actually extend relatively far up to the anterior of the stomach (**Figure 2.19c**). An additional element of the phenotype revealed by sectioning was the presence of a mass of unstained mesenchyme between the dorsal pancreatic and splenic mesenchymes (**red** outline in **Figure 2.19c**). This has not been observed in wild type gut sections.

The initial analysis presented in this section confirmed the *Rwhs* bifurcating spleen phenotype, which is of particular interest given the existence of polysplenia in humans. The *NGRS* was also demonstrated to be capable of marking both wild type and abnormal spleen development. The mechanism for development of the bifurcating spleen phenotype is unknown, as is the gene underlying the *Rwhs* mutation. The fact that cells extend up from the "ectopic spleen" towards the anterior stomach suggests that the mutant tissue attempts to recapitulate normal aspects of spleen development, perhaps including migration. Conversely, the mal-positioning of the second "spleen" could also be the result of initial defects in migration of splenic precursor cells. The *NGRS* provides a way to analyse this mutant further.

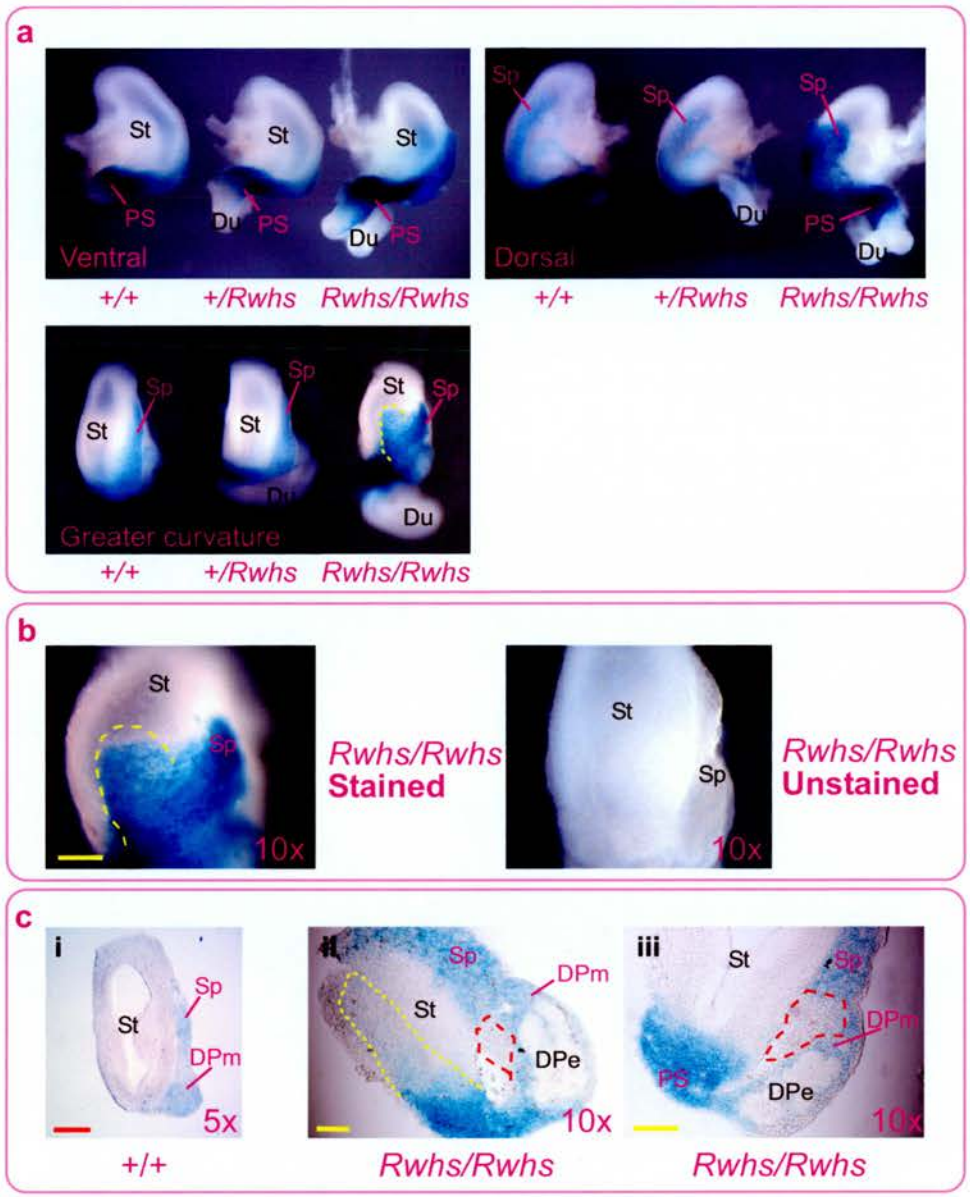

Figure 2.19 **An analysis of the *Rwhs* mutant using *NGRS-LacZ* as a marker of spleen development**

a) X-gal staining for *NGRS-LacZ* expression in E12.5 guts from wildtype (+/+), *+/Rwhs*, and *Rwhs/Rwhs* embryos on the *NGRS-LacZ* background. A bifurcating spleen can be seen on the greater curvature of the *Rwhs/Rwhs* stomach (outlined in **yellow**). **b**) Comparison between visualisation of the bifurcating spleen phenotype on stained and unstained (non-transgenic) guts. *NGRS-LacZ* aids visualisation greatly. **c**) 30μm vibratome sections of +/+ and *Rwhs/Rwhs* guts X-gal stained for *NGRS-LacZ* expression. The anterior extent of the putative ectopic spleen (outlined in **yellow**) is revealed to be greater when viewed in sections than that observed in the wholemount gut. The section in **ii** is from near the surface of the greater curvature of the stomach. A mass of unstained mesenchyme (outlined in **red**) is present between the dorsal pancreatic and splenic mesenchymes. Yellow scale bars: 100μm. Red scale bars: 200μm. **Du**: duodenum, **DPe**: dorsal pancreatic endoderm, **DPm**: dorsal pancreatic mesenchyme, **PS**: pyloric sphincter, **Sp**: spleen, **St**: stomach.

2.6 Discussion

In this chapter I have shown that the pyloric sphincter and spleen marker *Nkx2-5* is expressed bilaterally in the SMP and nascent underlying mesenchyme at E9.5-9.75 - an earlier stage than previously reported. *Nkx2-5* expression overlaps significantly with that of the upstream gene *Bapx1* at this stage. By E10.5 *Nkx2-5* expression is localised to a ventral and a dorsal domain in the SMP. The dorsal domain corresponds to the putative splenic mesenchyme, which expresses a range of splenic markers including *Hox11* and *Capsulin* (Hecksher-Sorensen et al., 2004). Much progress has been recently made on dissecting the genetic regulation of spleen development (e.g. Brendolan et al., 2005), but the role of *Nkx2-5* is far from clear owing to the lack of a gut-specific knockout. The main questions to address are: what is the position of *Nkx2-5* in the spleen development network, and is loss of *Nkx2-5* responsible for the defective spleen and pyloric sphincter development observed in *Bapx1*$^{-/-}$ mice? One model to investigate is that in which Bapx1 regulates *Nkx2-5*, which in turn regulates *Hox11*. *Hox11* expression overlaps that of *Nkx2-5* in the SMP at E10.5 (Hecksher-Sorensen et al., 2004), and is lost in the *Bapx1*$^{-/-}$ gut (Lettice et al., 1999b).

An interesting aspect of the early *Nkx2-5* expression pattern is that transcripts are detected bilaterally in the SMP at E9.5. *Bapx1* is expressed in the same manner; thus there is now evidence that two spleen development markers are expressed bilaterally at E9.5. This bilaterality echoes the situation in *Xenopus*, in which *Nkx2-5*-expressing splenic precursors are initially located on both sides of the embryo, the left-side of which preferentially undergo spleen development (Patterson et al., 2000). The bilateral existence of cells with the potential to undergo differentiation into splenic tissue – and the potential deregulation of this - could provide a mechanism for the early establishment of polysplenia. The *Rwhs* mutant reported in this chapter also has a polysplenic phenotype; it is, however, anticipated that this was caused by a slightly later aberration in the spleen development program, as general gut asymmetry was unaffected.

Bilateral expression in the E9.5 SMP was also observed for *NGRS-LacZ*. The *NGRS* was cloned based on published reports of sequences lying between -1.6 and -3.5kb upstream of *Nkx2-5* which confer gut expression. AR2 (thyroid, pharyngeal endoderm, gut, outflow tract, right ventricle) and IR2 (inhibitory on cardiac expression) elements have been proposed to exist in this region, with an AR7 element encompassing them (Schwartz and Olson, 1999). Most of the published data on *Nkx2-5* regulation supports this model. An exception is that in one study the complete 3.3kb of DNA upstream of *Nkx2-5* was found to confer both gut and major heart expression despite including the IR2 (Searcy et al., 1998). Four other studies have contradicted this finding and instead support the model that inclusion of the IR2 minimises cardiac expression (Lien et al., 1999; Reecy et al., 1999; Tanaka et al., 1999c; Lien et al., 2002). The data presented in this chapter further supports this model.

A number of conserved transcription factor binding sites previously reported in the AR2 were confirmed during the *in silico* analysis: 6 GATA , 4 Smad, 1 HNF-3, and 1 Nkx2-5 site (Sparrow et al., 2000; Lien et al., 2002). Two of these GATA sites are required for spleen expression (Searcy et al., 1998), whilst the HNF-3 site is not (Lien et al., 2002). The *Nkx2-5* site has also been deemed to not be required for gut expression at E11.5 (Lien et al., 2002); the data presented to support this conclusion appears, however, to indicate that gut expression is somewhat reduced when this site is mutated. Novel transcription factor binding sites were also identified during the *in silico* analysis, including four predicted Bapx1 binding sites.

The *NGRS* has been demonstrated to be a good specific marker of spleen (and pyloric sphincter) development, both in wild type and mutant embryos (including the novel spleen mutant *Rwhs*). The putative splenic mesenchyme is marked by *NGRS-LacZ* expression at E10.5-11.5, and the spleen primordium expresses this transgene throughout development. As mentioned previously, the activity of the *NGRS* throughout the SMP at E9.5 may provide information on the earliest origins of the spleen.

NGRS activity is not dependent on *Bapx1* during gut morphogenesis. A positive aspect to this lack of dependence is that it provides the potential for *NGRS* to

drive transgene expression on the *Bapx1*$^{-/-}$ background. This could be exploited in experiments to rescue the *Bapx1*$^{-/-}$ phenotype. The different stages and aspects of the mutant phenotype could be examined by artificially expressing each of the downstream genes known to be lost on the *Bapx1*$^{-/-}$ background. Another potential use for this Bapx1-independent gut enhancer is to mark pyloric sphincter and perhaps splenic precursors and examine what happens to them during development of the *Bapx1*$^{-/-}$ phenotype. The fact that *LacZ* expression was still present in the mutant guts suggests that these two tissues are not lost in *Bapx1*$^{-/-}$ mutants, but instead undergo abnormal development and become disorganised. It is certainly known that spleen cells persist in these mutants (Akazawa et al., 2000). What is now of interest is to examine the subtleties of *NGRS*-driven expression on the *Bapx1*$^{-/-}$ background, especially with respect to the ectopic cysts recently noted in these mutants (Asayesh et al., 2006).

The independence of the *NGRS* from Bapx1 regulation may also be evidenced by its expression pattern in wild type guts. Whereas *Nkx2-5* is expressed in two distinct domains of the SMP at E10.5, the *NGRS* drives expression throughout. The additional *NGRS* expression is in the tip of the SMP and the underlying mesenchyme. *Bapx1* is also normally expressed in these tissues in a manner largely exclusive to that of *Nkx2-5*. It is therefore possible that Bapx1 has a two-fold role in *Nkx2-5* regulation, and can also inhibit endogenous *Nkx2-5* expression, modulating the pattern conferred by the *NGRS*. Further evidence for this idea may be derived from the expression patterns later in development: *NGRS* expression in the spleen and pyloric sphincter is contiguous, whereas *Nkx2-5* expression in these tissues is separate; the gap in *Nkx2-5* expression corresponds to the posterior stomach region where *NGRS* expression overlaps *Bapx1*. Inhibition of *Nkx2-5* by Bapx1 could be mediated by *Fgf10* (which is downstream of *Bapx1* and expressed in an appropriate part of the SMP (Hecksher-Sorensen et al., 2004)), as *Nkx2-5* expression appears to be extended into the mesenchyme underlying the tip of the SMP at E10.5 in *Fgf10*$^{-/-}$ embryos (data not shown). The proposed inhibition of *Nkx2-5* by Bapx1 is not irreconcilable with the loss of *Nkx2-5* expression in the *Bapx1*$^{-/-}$ gut, as expression of these genes overlaps in the SMP at E9.5 and so Bapx1 may be required for initial *Nkx2-5* activation at this stage.

The *NGRS* was used to drive *LacZ* in the studies presented here, but a variety of other transgenes could be placed under its regulation. Depending on the choice of reporter gene, *NGRS* could be exploited in lineage tracing or genetic manipulation experiments, both *in vivo* and in culture. These possibilities are explored in **Chapters 3 & 4**.

CHAPTER 3

Lineage tracing using the *NGRS*

...or: "Science is a wonderful thing if one does not have to earn one's living at it"
– Albert Einstein

3.1 Introduction

3.1.1 The need for lineage tracing

The *Nkx2-5 gut regulatory sequence (NGRS)* discussed in the previous chapter provides a way of tagging cells, by driving reporter gene expression in the developing spleen and pyloric sphincter. Both these tissues are of clinical importance and yet their origins are poorly understood. Some insight into these origins may be drawn from the *NGRS-LacZ* expression data presented in **Chapter 2**. In addition to marking the distinct spleen and pyloric sphincter structures from ~E12.0 and E11.5 respectively, the *NGRS* also confers *LacZ* expression in earlier tissues: the splenic mesenchyme at E10.5 and E11.5, the putative pyloric sphincter region at E10.5, and throughout the SMP and nascent underlying mesenchyme at E9.5. Given these expression patterns - and data from *Xenopus* suggesting that splenic precursors initially reside on both sides of the embryo (Patterson et al., 2000) – I hypothesise the following: that the *NGRS* marks presumptive splenic mesenchyme underlying the SMP on both sides of the gut from E9.5, that this expression becomes restricted at E10.5 to a dorsal region of left-side gut mesenchyme, and that this patch of cells will contribute entirely to the spleen. Lineage tracing is necessary to address these hypotheses.

3.1.2 Inducible Cre systems

An appropriate way to perform lineage tracing during gut development would be to use a tissue-specific marker that upon temporal induction becomes permanently activated. In this way, cells could be marked at a specific time point and any observed staining would be attributable to cells that were expressing the marker at this stage only. An adaptation of the *LacZ* reporter system that would facilitate this goal is activation by a tamoxifen-inducible Cre recombinase, expression of which is driven by a tissue-specific enhancer. A number of versions of tamoxifen-inducible Cre exist (CreER^{TM}, CreERT, CreERT2), each of which is a fusion protein containing the P1 phage recombinase Cre and a mutant oestrogen receptor (ER) ligand-binding domain (LBD) (Danielian et al., 1998; Metzger et al., 1995; Feil et

al., 1997). These fusion proteins are functionally inactive, as they are sequestered in the cytoplasm due to interaction between the LBD and cellular heat shock proteins (Scherrer et al., 1993). However, translocation to the nucleus can take place when the synthetic oestrogen tamoxifen (or its metabolite 4-hydroxytamoxifen [OHT][19]) is administered and this interaction is disrupted. The engineered mutations in the LBD render it unable to interact with endogenous oestradiol (Feil et al., 1996; Feil et al., 1997).

Once in the nucleus, the Cre portion of the fusion protein can utilise its recombinase activity and recombine genomic DNA at artificially inserted 34bp *LoxP* recognition sites (see (Schipani, 2002) for an introduction to the *Cre-LoxP* system) (Feil et al., 1996). Lineage tracing can therefore be achieved using a Cre-inducible reporter line, such as *R26R* (inducible *LacZ*) (Soriano, 1999). This system is summarised in **Figure 3.1**.

The percentage of cells expressing an inducible reporter gene can be controlled by altering the dosage and number of applications of tamoxifen. This drug is usually administered by maternal intraperitoneal injection. Non-specific toxicological effects occurred at high doses with earlier versions of tamoxifen-inducible Cre; this issue was addressed with the creation of the more sensitive CreERT2 line (Feil et al., 1997; Indra et al., 1999). Once the genomic *R26R* locus is cleaved this change is faithfully transmitted to the daughter cells, thus allowing the lineage of a recombined cell to be traced. Most studies report low to undetectable recombination in the absence of tamoxifen. Suboptimal doses can be employed to limit marking to only a few cells in a population (Fischer et al., 2006a).

Recombination by CreERT is induced within 6 hours of a single (3mg) intraperitoneal tamoxifen injection, but cannot be detected at 3 hours (Hayashi and McMahon, 2002). The level of β-gal activity, and the proportion of cells exhibiting activity, increases dramatically between 6 and 12 hours post-injection. At the other end of the scale, the duration of tamoxifen activity is a factor which needs to be taken into account in order to perform a successful lineage tracing exercise. A single 3mg tamoxifen injection administered at E8.5 will exert its main activity within 24 hours, as shown by the major nuclear accumulation of Cre-ERT during this period; by 48

[19] Metabolism occurs in the maternal liver, thus this metabolite must be used directly when being applied to cells in a culture system

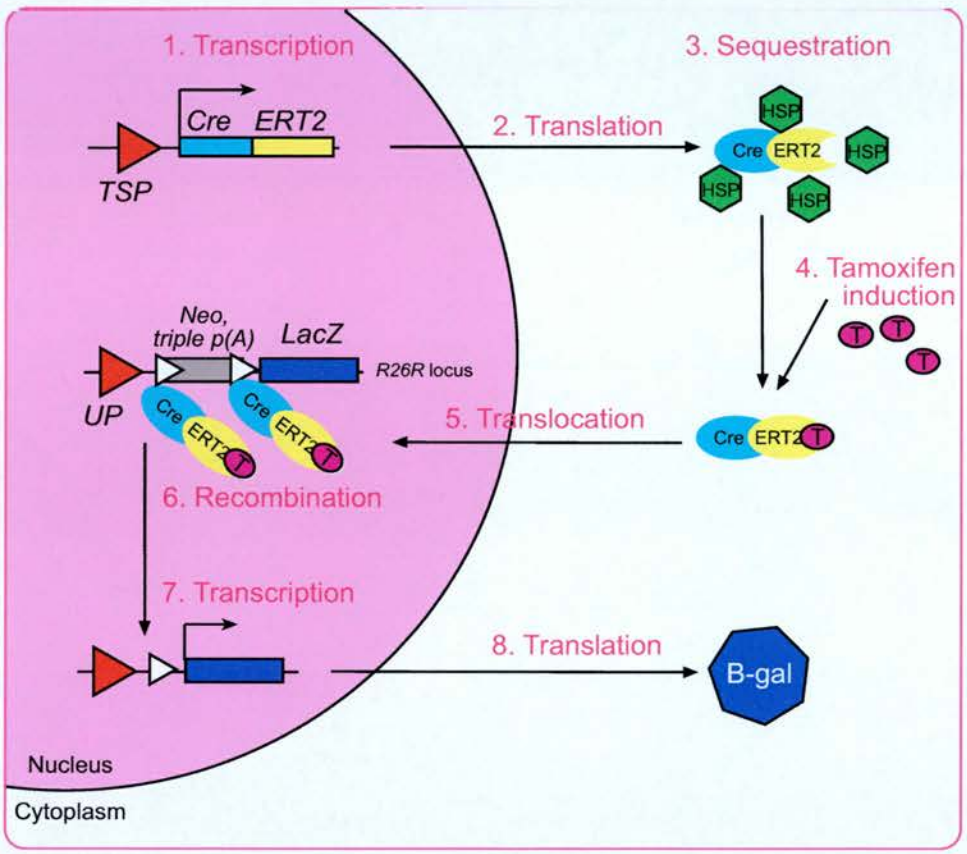

Figure 3.1 **Schematic showing how tamoxifen induces Cre recombinase-mediated activation of reporter gene expression**

1. A transgene encoding a Cre-ERT2 fusion protein, under the control of a tissue-specific promoter (TSP), is transcribed. **2.** The *Cre-ERT2* transcript is exported from the nucleus and translated into a fusion protein. **3**. Cre-ERT2 proteins are sequestered in the cytoplasm with heat shock proteins (HSP), preventing Cre activity. **4.** Exogenous OHT (the metabolite of tamoxifen) (T) binds to the ERT2 ligand binding domain and disrupts the interaction with HSP. **5.** Cre-ERT2 can now translocate to the nucleus. **6.** In this example, Cre-mediated recombination occurs at the *R26R* locus, which contains a ubiquitous promoter (UP), a transcriptional termination STOP cassette (Neo, triple p(A)), and *LacZ*. **7.** Recombination of the Lox sites (white triangles) flanking the STOP cassette permits *LacZ* expression. **8.** The *LacZ* transcript is translated to produce β-gal protein, which can be detected using X-gal staining.

hours, the amount of CreERT in the nucleus is dramatically reduced, but some recombination does still occur during the 24-48 hour period (Hayashi and McMahon, 2002).

The combined use of tamoxifen-inducible Cre with the Cre-inducible R26R reporter has been employed in a number of excellent lineage tracing studies, most notably in the developing limb (Kimmel et al., 2000; Guo et al., 2003; Ahn and Joyner, 2004). Adult tissues and cells in culture can also be marked in this way (Hayashi and McMahon, 2002). In addition to lineage studies, a second, greater body of literature exists on initial studies into the utility of novel tissue-specific *CreERT/ERT2* lines as opposed to full lineage studies. Tissues studied in this way include: limb ectoderm (Indra et al., 2005), epidermal keratinocytes (Indra et al., 2000; Indra et al., 2005), heart (Sohal et al., 2001), liver (Tannour-Louet et al., 2002), pancreatic islets (Zhang et al., 2005), and melanocytes (Yajima et al., 2006).

3.1.3 Experimental plan

The *NGRS* was demonstrated in **Chapter 2** to be a suitable marker of spleen development. No published lineage tracing study has addressed the development of this tissue. We decided to use *NGRS* to drive *CreERT2* on the *R26R* background, in order to mark and trace the descendents of the SMP and splenic mesenchyme in a temporally inducible manner. A second motive for creating an *NGRS-CreERT2* line was to direct a gut-specific *Nkx2-5* knockout. The full *Nkx2-5* knockout is not informative about gut development, as homozygous null mice die before the onset of spleen development (Lyons et al., 1995). Nor can information be derived from chimaeric mutants, as embryonic lethal cardiac defects occur with as little as 20% contribution of knockout cells (Tanaka et al., 1999a). However, inducible gut-specific loss of *Nkx2-5* could be achieved if mice carrying the *NGRS-CreERT2* gene were crossed to homozygous "Floxed" *Nkx2-5* mice – a line already in existence (Pashmforoush et al., 2004).

3.2 NGRS-CreERT2

A cloning strategy was designed to place the *NGRS* and heterologous *β–globin* promoter (used in the *NGRS*-LacZ construct) upstream of *CreERT2* (tamoxifen-inducible Cre), and express this transgene on the *R26R* (Cre-inducible *LacZ*) background. It was envisaged that a number of important questions could be answered about early gut and spleen development using this system, based on the *NGRS* expression patterns in **Chapter 2**. Firstly, by inducing *LacZ* expression in the bilateral SMP at the stage at which no mesenchyme lies between the SMP and the gut endoderm (E9.25-9.5, therefore administering tamoxifen at ~E8.5), the possible derivation of this future mesenchyme from the SMP could be investigated. This would obviously require careful timing of matings and injections, and the analysis of many litters for the data to be valid. More generally, this experiment would allow lineage tracing of the ~E9.5 SMP, with particular attention paid to the contribution of its descendents to the spleen. A similar analysis could be performed by marking the SMP and underlying mesenchyme at E10.0 and E10.5, again with particular emphasis on development of the spleen (and pyloric sphincter).

3.2.1 Cloning of NGRS-CreERT2

An *NGRS-CreERT2* construct was successfully generated, using the strategy depicted in **Figure 3.2**. A detailed written description of the cloning process is provided in the **Appendix**. An earlier cloning strategy was abandoned due to problems in cloning the large *intron-CreERT2-poly(A)* fragment. This was eventually circumvented by sub-cloning through the *pZErO-1* vector, which confers lethality on host bacterial cells unless a cloned fragment disrupts the gene responsible (*ccdB*), thus allowing direct selection of rare cloning events. The rationale behind inclusion of a rabbit *β-globin* intron is that introns increase transgene expression, albeit for not entirely clear reasons (though probably due to the link between splicing and transcription) (Choi et al., 1991; Clark et al., 1993). Similarly, a polyadenylation signal was also included, 3' to *CreERT2*, to direct proper processing of the mRNA.

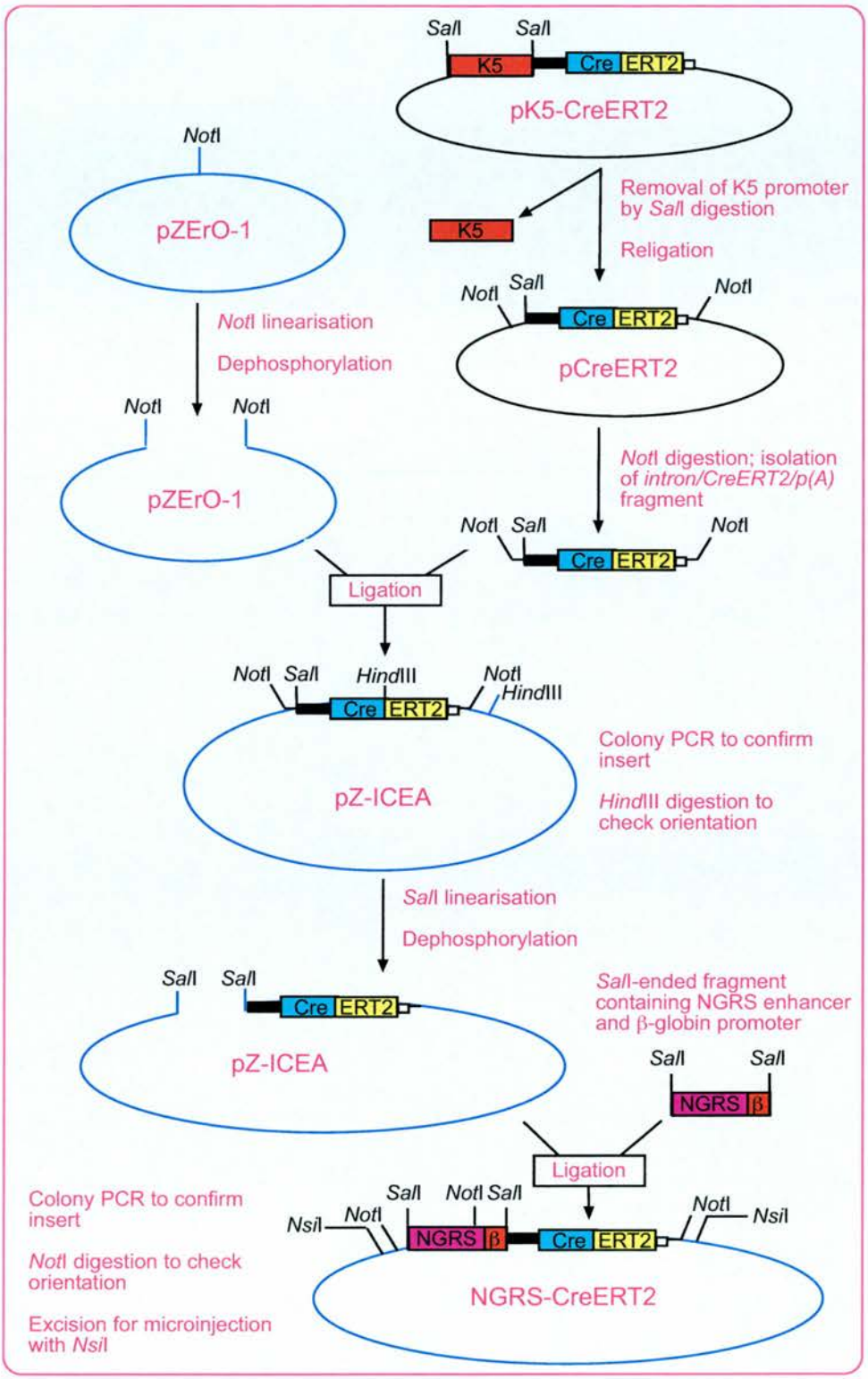

Figure 3.2 **Schematic of *NGRS-CreERT2* cloning strategy**
Details are provided in the main text (**Section 3.2.1**) and in the **Appendix. Black box: rabbit β-globin intron; white box: SV40 poly (A)**

3.2.2 Generation of NGRS-CreERT2 lines

The construct was prepared for pronuclear microinjection and injected in seven sessions. Progeny were genotyped at weaning by PCR for a ~0.25kb *Cre* product ("*ShCre*" primers – detailed in **Chapter 7**). Positive mice were then genotyped in a second confirmatory PCR, to detect a ~1.7kb product spanning the 3' of the *NGRS* through to midway through *Cre* ("*EPCreJn*" primers). The integrity of each DNA sample was confirmed by PCR for a region of the *Myogenin* gene.

The results of genotyping for the *NGRS-CreERT2* transgene - and of subsequent matings - are shown in **Table 3.1**. Of 242 mice generated by pronuclear microinjection, 6 were transgenic (~2.5%). This is unusually low given that a transgene integration frequency of ~28% is expected when microinjecting linear DNA at a concentration of 2ng/μl, as was the case in these sessions (Brinster et al., 1985). DNA preparation and microinjections were performed according to standard protocols, so this is likely to be a construct-specific effect. Genotyping was performed on mice at weaning, so it cannot be known whether more embryos originally carried the transgene, but died *in utero*. Embryonic lethality directly related to the injected DNA could be one explanation for the low frequency of transgenic mice.

Session	Number of progeny	Number transgenic	Lines
1	45	1 m (**Founder 1**)	x F1 – no line established
2	54	1 m (**Founder 2**)	x F1 – "**Line 2**" x *R26R* – line established
3	29	0	-
4	23	0	-
5	35	1 f (**Founder 3**) 1 m (**Founder 4**)	x *R26R* – "**Line 3**" No line established
6	31	1 f (**Founder 5**)	x *R26R* – "**Line 5**"
7	25	1 m (**Founder 6**)	No line established

***Table 3.1* – Results of *NGRS-CreERT2* microinjection sessions and matings**
Lines were established by breeding onto the [CBA x C57BL/6] F1 and/or *R26R* backgrounds. Genotyping was performed using both described *Cre* primers sets and also primers for the *R26R* locus, where appropriate. **Founder 1** failed to produce offspring. Transmission was tested from **Founders 4 & 6** in embryos, and no lines were established.
m: male, **f**: female

3.2.3 NGRS-CreERT2 expression analysis

Tamoxifen is required for translocation of the *NGRS-CreERT2* protein product into the nucleus; expression of the transgene does not require induction. *NGRS-CreERT2* expression was therefore examined in embryos derived from timed matings of the six founder mice or, more commonly, their offspring with CD1 partners. Two methods were employed to examine expression. Firstly, reverse-transcription PCR (RT-PCR) was performed on E12.5 embryos and guts. Secondly, *in situ* hybridisation was performed on both whole mount embryos and isolated guts using a *Cre* probe. These methods were preferable to crossing onto the *R26R* background and attempting to induce *LacZ* expression by maternal tamoxifen injections, as the use of tamoxifen can be a complex process, requiring optimisation of dosage and preparation. A lack of recombination (reporter expression) could be due to problems at a number of stages. Thus expression was chosen as the initial criteria for analysing the embryos rather than detection of site-specific

recombination. If expression was detected then tamoxifen induction would be performed, along with genomic PCR to confirm recombination.

3.2.3.1 RT-PCR

Expression of the *NGRS-CreERT2* transgene was analysed by RT-PCR on E12.5 gut tissue. Males from the F1 generation of each of the three stable lines (**Lines 2, 3,** and **5**[20]), and **Founders 4** and **6** were mated with CD1 females to generate at least one litter of transgenic embryos per founder/line for use in RT-PCR analysis. Embryos were genotyped using both *Cre* primer sets previously described. RNA was then prepared from all *Cre*-positive guts and typically two negative littermates' guts, and random-primed cDNA was synthesised. *Hprt* (*Hypoxanthine guanine phosphoribosyltransferase*) RT-PCR was performed as a control. The primers for *Cre* RT-PCR flank the rabbit *β-globin* intron; there is thus a difference in the size of the product amplified from cDNA and genomic DNA. The expressed form is ~0.3kb long, the genomic form ~0.88kb.

Cre RT-PCR analyses were performed on E12.5 guts for each founder/line at different times during my PhD studies, as microinjection sessions were undertaken throughout. Once all five founders/lines had been tested, genotyping and RT-PCR (*Hprt, Cre*) were repeated in single summary experiments, the results of which are shown in **Figure 3.3**. An adult mouse carrying another *CreERT2* transgene was obtained (K5CE, created by Duncan Whittaker) and RNA extracted from its depilated back-skin (a site of transgene expression) to act as a positive control in this final RT-PCR. The *Cre* RT-PCR primers were complementary to sequences in this transgene.

Cre RT-PCR produced only an unspliced ~0.88kb product from all of the transgenic gut cDNA samples, with no product being amplified from the non-transgenic samples or the water control (**Figure 3.3c**). The original RNA samples were therefore DNase-treated to remove genomic DNA, and thus to investigate the possibility that low level expression was occurring but was being masked by amplification of the more abundant genomic transgene sequences. Fresh cDNA was

[20] Lines 3 and 5 were established on the R26R background but the mice selected for these matings carried only the *NGRS-CreERT2* transgene, and not the *R26R* transgene.

then synthesised and re-analysed by *Hprt* RT-PCR (**Figure 3.3f**). A spliced *Hprt* band was detected in all samples, confirming that good quality cDNA was present. *Cre* RT-PCR, however, failed to detect *Cre* transcripts from any founder/line, demonstrating that *NGRS-CreERT2* is not expressed in the transgenic mice (**Figure 3.3e**).

A minor complication was that the "positive" control cDNA from the K5CE mouse produced only an unspliced band - even after DNase treatment. This band was not present in the –RT (reverse transcriptase) reaction, and thus appeared to be a genuine RT-PCR product (rather than a product of amplification of contaminating genomic DNA). Sequencing confirmed the product to be the *Cre* region to which the primers were targeted. This indicates that, at least in the tissue analysed, an unspliced *Cre* transcript was expressed in the K5CE mouse. The line in question has been problematic for the group using it, producing erratic low-level Cre-mediated recombination. Aberrant splicing could be responsible for this effect. Splicing of the *β-globin* intron is expected to occur in *CreERT2* constructs (Daniel Metzger, personal communication).

3.2.3.2 In situ hybridisation

In situ hybridisation for the *Cre* transcript was performed on E10.5 and E12.5 whole mount embryos and on E12.5 guts. Two ~660bp probes (one to be transcribed from the T7 promoter, one from SP6) complementary to *Cre* were designed and transcribed from a PCR product amplified using the two sets of primers listed in **Chapter 7** ("*CreISH*"). The reverse primer of each of these sets contains at its 5' terminus the recognition sequence for either T7 or SP6 polymerase. No *Cre* expression was observed in any tissue (data not shown). The Cre probe was also used on E11.5 control tissue from the *ZRS-Cre* line[21], and found to detect expression in the limb (data not shown). No expression was detected in age-matched CD1 control tissue. A *Hand2* probe was also used as a positive experimental control.

[21] A line expressing *Cre* under the control of the *ZRS (ZPA [Zone of polarising activity] regulatory sequence)*, created by Dr Laura Lettice. The *ZRS* is an upstream enhancer for *Shh* and confers expression in the developing limb. Embryos from *ZRS-Cre* x CD1 matings were genotyped using the "ShCre" PCR primers and program listed in **Chapter 7**.

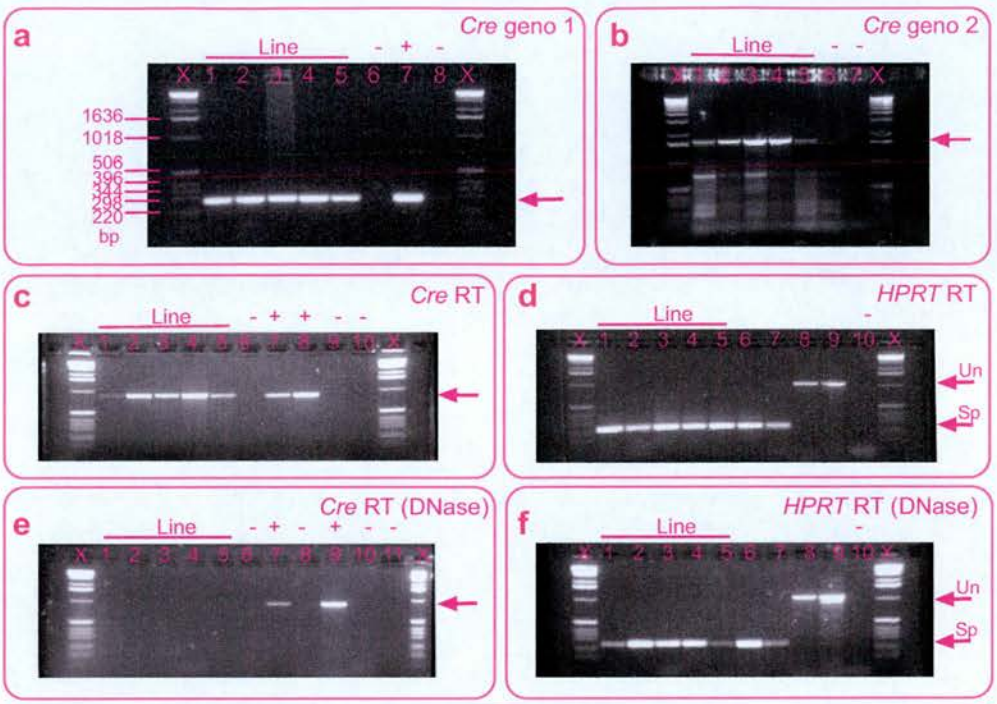

Figure 3.3 **Genotyping and RT-PCR analysis of** *NGRS-CreERT2* **mice**

a. *ShCre* genotyping PCR
Lanes: **1-5** - transgenic founder/line yolk-sac DNA (Line 2, Line 3, Founder 4, Line 5, Founder 6); **6** - non-transgenic yolk-sac DNA; **7** - transgenic ear-clip DNA from *K5CE*; **8** - dH_20

b: *EPCreJn* genotyping PCR
Lanes: **1-5** - transgenic founder/line yolk-sac DNA (Line 2, Line 3, Founder 4, Line 5, Founder 6); **6** - non-transgenic yolk-sac DNA; **7** - dH_20

c: *Cre* RT-PCR on cDNA prepared from non-DNase treated RNA
Lanes: **1-5** - transgenic founder/line cDNA (Line 2, Line 3, Founder 4, Line 5, Founder 6); 6 - non-transgenic cDNA; 7 - transgenic cDNA from *K5CE*; 8 - transgenic genomic DNA; 9 - non-transgenic genomic DNA; 10 - dH_20

d: *HPRT* RT-PCR on cDNA prepared from non-DNase treated RNA
Lanes: as per (**c**). **Un: Unspliced, Sp: spliced.**

e: *Cre* RT-PCR on cDNA prepared from DNase-treated RNA
Lanes: **1-5** - transgenic founder/line cDNA (Line 2, Line 3, Founder 4, Line 5, Founder 6); **6** - non-transgenic cDNA; 7 - transgenic cDNA from *K5CE* (+RT); **8** – transgenic cDNA from *K5CE* (-RT); **9** - transgenic genomic DNA; **10** - non-transgenic genomic DNA; **11** - dH_20

f: *HPRT* RT-PCR on cDNA prepared from DNase-treated RNA
Lanes: as per (**e**)

a-b: All lanes contain 5μl of a 20μl PCR reaction.
c-f: All lanes contain 5μl of a 25μl RT-PCR reaction performed on 2μl cDNA (from 20μl total cDNA, reverse transcribed from approximately 0.9μg RNA).
All gels: Ladder lanes (**X**) contain 6μl of 55.6ng/μl1kb ladder. All gels are 2% agarose/TAE and were run at 100V for 1 hour

3.2.4 NGRS-CreERT2 discussion

The reasons for the lack of *NGRS-CreERT2* expression are unknown. In addition to the absence of detectable expression, very few transgenic mice were actually produced (6/242; ~2.5%). Anecdotal accounts exist of difficulty in generating transgenic mice containing *CreERT2* transgenes by microinjection, though no concrete reason for this supposed effect has been proposed. A fundamental issue with delivery of DNA into the genome by microinjection is that copy number cannot be controlled and so large numbers of tandemly repeated inserts may be introduced. This could obviously be an issue when dealing with a gene such as *CreERT2* which produces a fusion protein which is sequestered along with essential cellular components in the cytoplasm. It might therefore be that only transgenic embryos with a low copy number, and low or no expression, survived. Alternatively, copy number may have just generally been too low for expression, independently of any effect on survival. Transgenes may have also inserted into the genome at locations which prevented their expression. Such issues are inherent to the method of creating transgenic animals through microinjection of DNA.

It should of course also be noted that many published accounts do exist of transgenic mice successfully generated following microinjection of *CreERT2* transgenes. The problem may therefore be specific to the *NGRS*. Expression of this enhancer was not studied before E8.5, though major early cardiac expression was not expected based on the agreement of my *NGRS-LacZ* expression data with similar published accounts of this region. There could, however, be earlier expression in other tissues. The cytoplasmic accumulation of the CreERT2 protein during early development could thus pose problems. It may therefore be that the few transgenic embryos that do survive to term are those which do not express the transgene.

This strategy was abandoned and a new direction pursued. This is described in the next section.

3.3 NGRS-LoxSTOPLox-LacZ

A second strategy for marking splenic precursors was designed following the failure to establish a line expressing *NGRS-CreERT2*. In this new approach, the *NGRS* and *β-globin* promoter are placed upstream of a *LoxSTOPLox* (excisable transcriptional termination sequence) cassette and *LacZ*, to create the *NGRS-LoxSTOPLox-LacZ* transgene. Mice carrying this transgene would be crossed with those ubiquitously expressing *CreERT2*, and the *LoxSTOPLox* sequence recombined in all cells following tamoxifen induction, leaving a functional *NGRS-LacZ* transgene. This genomic change would be transmitted to all descendents of the induced cell; *LacZ* would only be expressed, however, in cells in which the *NGRS* is active. A benefit of this strategy is that it circumvents the need to clone *CreERT2* – a cloning step which posed a number of problems during the previous approach – as a ubiquitous *CreERT2* line was available.

This method has the potential to address some of the questions outlined previously as cells can be marked at a specified time; it also, however, has a major limitation in that continued activity of the *NGRS* is required for *LacZ* expression. In the first (*NGRS-CreERT2*) strategy, Cre-mediated recombination permanently marked cells and their descendents at one specific time-point, thus permitting lineage tracing. Lineage tracing is not possible in the second (*NGRS-LoxSTOPLox-LacZ*) system as the descendents will no longer be tagged if *NGRS* activity ceases or if cells move out of the region of *NGRS* activity (as *LacZ* is no longer driven by the *NGRS*). Conversely, if an unrelated cell moves into the domain of *NGRS* activity, it may commence *LacZ* expression (as the *LoxSTOPLox* sequence is already recombined in all cells). The *NGRS-LoxSTOPLox-LacZ* strategy does however offer the opportunity to perform a form of "clonal analysis", in which the behavioural history of a cell can be visualised by examining the pattern of marked cells (its ancestors) (Petit et al., 2005). The proportion of cells marked can be controlled by altering tamoxifen dosage, thus allowing analysis of individual or small groups of cells. The behaviour of cells in which the *NGRS* is active could be followed in this way.

Information on early spleen development could be gained by performing this type of analysis at day intervals from E9.5-11.5, and examining the behaviour of

marked cells from each stage. Findings would need to be confirmed in other ways, for example by lineage tracing, but nonetheless could be insightful. The strategy of using a ubiquitously expressed tamoxifen-inducible Cre with a tissue-specific *LoxSTOPLox* has been used in published studies, including that of Hayashi & McMahon, who traced cells in the E8.5 embryo (Hayashi and McMahon, 2002).

3.3.1 Cloning of NGRS-LoxSTOPLox-LacZ

The *NGRS-LoxSTOPLox-LacZ* cloning strategy is shown in **Figure 3.4**, and a detailed written account is provided in the **Appendix**.

3.3.2 Generation of NGRS-LoxSTOPLox-LacZ lines

The *NGRS-LoxSTOPLox-LacZ* construct was microinjected in two sessions. The number of pups genotyped was small, due to low numbers of healthy microinjected oocytes being generated and the death of one of the recipient mothers prior to weaning resulting in the death of her offspring. Of the 58 pups genotyped by duplicate PCR for *LacZ/Myo*, two were *LacZ*-positive (one male, one female). These two founders were bred with [CBA x C57BL/6] F1 partners in order to establish stable lines.

3.3.3 NGRS-LoxSTOPLox-LacZ analyses

The *NGRS-LoxSTOPLox-LacZ* mice were to ultimately be crossed with a line expressing tamoxifen-inducible *CreERT2* under the control of a ubiquitous promoter. However, as a proof of principle, males from both lines were first mated with females expressing a standard (non-inducible) ubiquitous *Cre*, to test a) whether *NGRS-LoxSTOPLox-LacZ* could be transmitted to embryos, and b) whether this transgene could be recombined by Cre. The ubiquitous *Cre* line (*gl-Cre*) was kindly

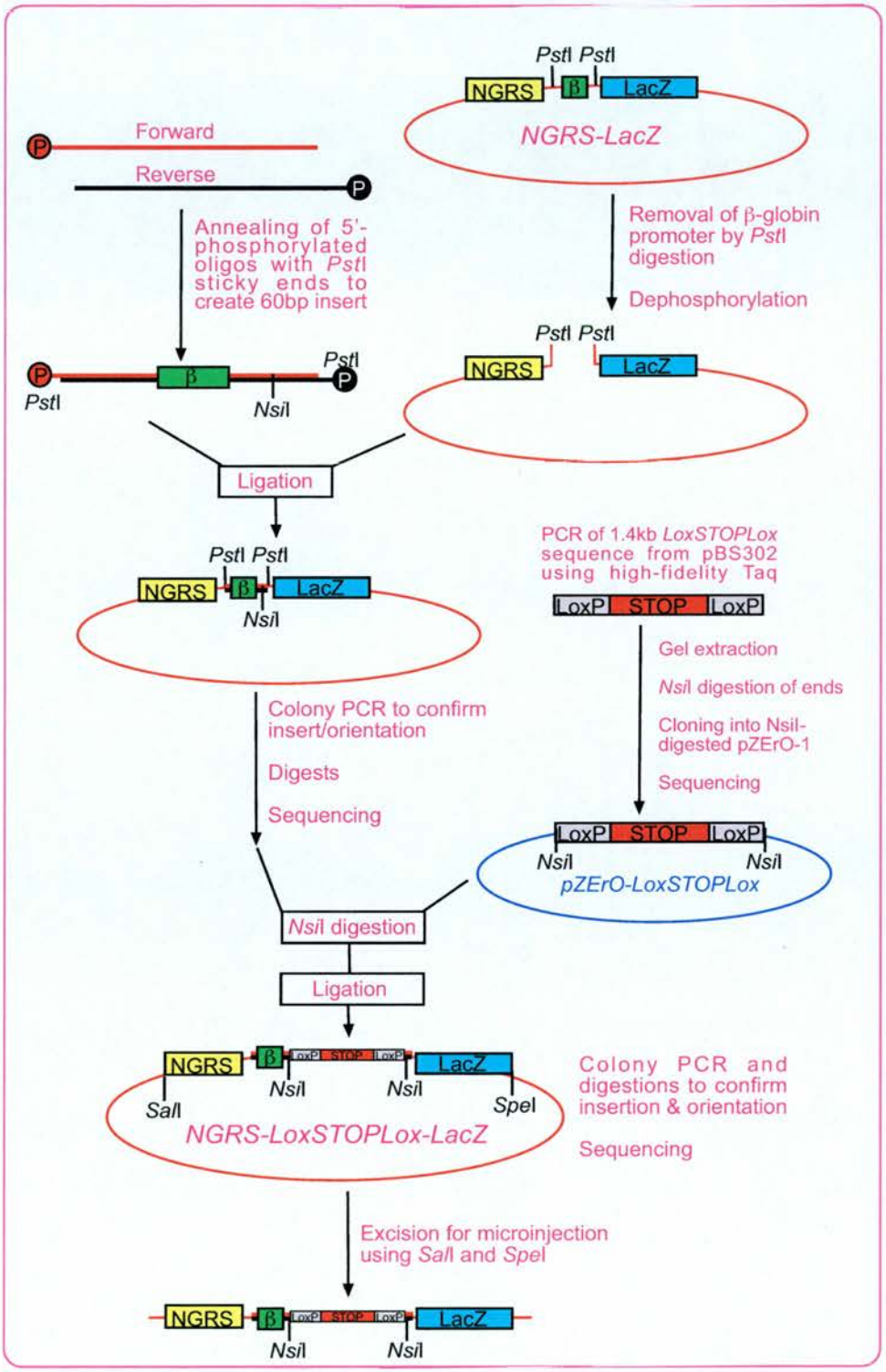

Figure 3.4 **Schematic of *NGRS-LoxSTOPLox-LacZ* cloning strategy** Details are provided in the main text (**Section 3.3**) and in the **Appendix.**

provided by Drs Dirk-Jan Kleinjan and Peter Hohenstein[22]. To confirm that any observed *LacZ* activity was indeed the result of Cre-mediated excision of the *STOP* signal, the *NGRS-LoxSTOPLox-LacZ* males were also mated with CD1 (*Cre*-negative) females. Two litters of embryos were examined on the *Cre* background, and two on the CD1 background, for each founder.

Embryos were recovered and analysed for *LacZ* expression by X-gal staining. DNA was prepared from yolk-sacs and used for genotyping of sequences from the *NGRS-LoxSTOPLox-LacZ* transgene. *Cre* genotyping was not performed as maternal *Cre* is expressed in all oocytes (regardless of whether the zygotic genome carries the transgene) and is known to faithfully instigate recombination, regardless of the source of the Cre (Dirk-Jan Kleinjan, personal communication).

The genotyping procedure is explained in **Figure 3.5a**. Genotyping was performed in at least duplicate for portions of the *LacZ* (PCR 1) and *STOP* (PCR 2) sequences. A positive result from the latter PCR indicated that the embryo was transgenic but that recombination (excision of the *STOP* sequence) had not occurred. The lack of a *STOP* PCR product was indicative of one of two things: 1) that the embryo was not carrying the transgene, or 2) that recombination had successfully occurred (*STOP* excised). Thus a third PCR assay was performed in duplicate on *LacZ*-positive embryos: for recombination (PCR 3). A ~230bp product was only amplified if recombination had taken place; if the *LoxSTOPLox* sequence was still intact then a ~1.6kb product was generated. The result of this final PCR often had to be interpreted on the basis of the presence or absence of the small (recombined) band as the large band could not usually be amplified from yolk sac DNA. The result of these genotyping PCRs are provided for both lines in **Table 6** in the **Appendix**, and are summarised in **Sections 3.3.3.1** and **3.3.3.2**.

[22] *gl-Cre* is expressed from the ubiquitous CAGGS promoter (*β-actin* promoter with upstream CMV enhancer) in all cells, including the germline.

3.3.3.1 Male founder

3.3.3.1.1 Male founder: Analysis

Two E12.5 litters on the *gl-Cre* background (9 and 11 embryos; 20 total) and two E12.5 litters on the CD1 background (10 and 19 embryos; 29 total) were analysed. Two embryos on the *gl-Cre* background (1 from each litter) exhibited X-gal staining in a pattern typical of *NGRS-LacZ* expression: strong staining could be seen in the thyroid primordium and gut region, with sparse expression in the outflow tract (**Figure 3.5b i**). Mild ectopic expression was also present in the limbs. The guts were dissected out and expression was found to be localised to the pyloric sphincter, spleen, and dorsal pancreatic mesenchyme (**Figure 3.5b ii,iii**). Gut expression was low in one of the embryos; the other gut had strong sphincter staining, though expression in the spleen and dorsal mesenchyme was still weaker than that typically conferred by the *NGRS* in *NGRS-LacZ* embryos.

9/20 (including the two X-gal stained) embryos from the *gl-Cre* matings were *LacZ*-positive; none of these carried the *STOP* sequence, suggesting that recombination had occurred in all nine embryos. However, only two exhibited LacZ expression. The recombination PCR subsequently revealed that only the two stained embryos had undergone recombination (i.e. small band in PCR 3); no recombination was detectable in the seven non-stained embryos. This produced a dichotomy as these embryos were shown in triplicate *LacZ* PCRs to be transgenic and yet the *STOP* and recombination PCR results taken together suggested that these embryos had never carried the *STOP* sequence[23]. It is unlikely that the *STOP* and recombination PCRs both failed, as they were performed up to three times for each embryo and only small products needed to be amplified. It therefore seemed possible that two transgenes might be being transmitted: the *NGRS-LoxSTOPLox-LacZ* and a *LacZ* fragment.

[23] The recombination PCR is not often directly informative for the presence of a non-recombined *LoxSTOPLox* sequence as the ~1.6kb product can only rarely be amplified from yolk sac DNA; absence of this large band is not therefore indicative of absence of the *LoxSTOPLox* cassette from the genome. Thus only the presence or absence of the recombined (small) band is informative, when interpreted with respect to the *STOP* PCR results.

The confusion surrounding this line deepened upon analysis of the two litters from CD1 mothers. Whilst no X-gal staining was observed in the first litter of ten embryos (as expected), 4/19 embryos from the second litter exhibited major staining in the gut (**Figure 3.5b**). *NGRS*-typic expression was also present in the thyroid and outflow tract, with strong ectopic expression again noted in the limbs. Staining in these embryos was stronger than in those on the *gl-Cre* background, though splenic expression was still lower than in *NGRS-LacZ* embryos and was not contiguous with the sphincter expression domain.

Genotyping of the embryos from CD1 mothers revealed that 4/10 in the first litter (none of which stained) were *LacZ*-positive. Three of these transgenic embryos also carried a non-recombined *LoxSTOPLox* sequence, as expected (i.e. *STOP*-positive). A *STOP* sequence could not however be amplified from the fourth embryo's DNA; this was not due to recombination of the sequence out of the genome and so once again it appeared that the *NGRS-LoxSTOPLox-LacZ* transgene and a separate *LacZ* fragment might be segregating independently.

In the second litter on a CD1 background 11/19 were *LacZ*-positive, and four of these displayed X-gal staining. This was totally unexpected as the CD1 line does not carry *Cre* and as such recombination should not occur. And indeed recombination had not occurred: 8/11 of the *LacZ*-positive (including the four stained) embryos were PCR-positive for the intact *STOP* sequence. The remaining three *LacZ*-positive (non-stained) embryos did not carry a *STOP* sequence; once again this was a genuine absence as opposed to a result of recombination (i.e. no small band in recombination PCR, suggesting the presence of only a *LacZ* fragment).

3.3.3.1.2 Male founder: Interpretation

The male founder was of no immediate use for further experiments as gut-specific X-gal staining occurred even in the absence of *Cre* on the CD1 background. The reasons for this anomaly were unclear and the genotyping results confusing. I propose the following explanation, which is summarised in **Figure 3.5c**: at least two transgenes are propagated from the male founder. The first is the intact *NGRS-LoxSTOPLox-LacZ* transgene, recombination of which results in *LacZ* expression.

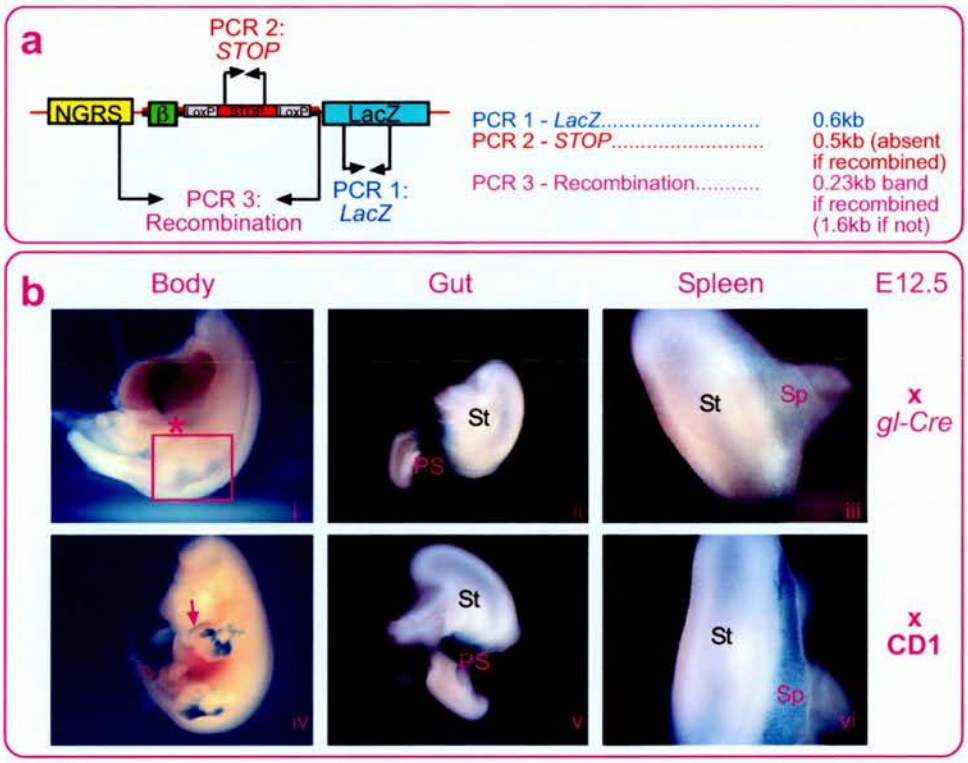

c

Transgene DNA present	Status	PCR results	x *gl-Cre* 1	x *gl-Cre* 2	x CD1 1	x CD1 2
	NTG	*LacZ-* *STOP-* Recombination not tested	3	8	6	8
NGRS β lox2 lox2 LacZ	TG, not recombined	*LacZ+* *STOP+* Large recombination band (not always amplifiable)	0	0	3	8 (4)
NGRS β LacZ	TG, recombined	*LacZ+* *STOP-* Small recombination band	1 (1)	1 (1)	0	0
LacZ	TG, fragment	*LacZ+* *STOP-* No band in recombination PCR	5	2	1	3
			9	11	10	19

= leaky expression from intact transgene?
= a 3rd variant of the transgene? Defective STOP...?

Figure 3.5 **Analysis of *NGRS-LoxSTOPLox-LacZ* embryos**
a) Genotyping primers. Embryos were genotyped in the first instance for part of the ***LacZ*** **(PCR 1)** and ***STOP*** **(PCR 2)** sequences. *LacZ*-positive embryos were then subjected to a PCR assay for **recombination (PCR 3)** which produces differentially sized bands dependent on whether recombination has occurred. The results of the genotyping are presented in **Table 6 of the Appendix**.
b) X-gal staining of *LacZ* activity in offspring from the male founder: **i-iii** - embryos carrying a recombined transgene, from *gl-Cre* mothers; **iv-vi** - embryos with a non-recombined transgene, from CD1 mothers. Staining was present in embryos on both backgrounds in (**i, iv**) the outflow tract (**arrow**), gut (**asterisk**), and ectopically in the limbs (**boxed** in **i** for clarity), and upon dissection was found to be in the pyloric sphincter (**ii,v**) and spleen (**iii, vi**).
c) Possible explanation for the observed genotyping and staining results in embryos from the male founder. This is a companion to the discussion in **Section 3.3.3.1.2**. The numbers in the table show the number of embryos with each possible genotype; the numbers in brackets denote how many exhibited X-gal staining. **NTG**: Non-transgenic, **PS**: pyloric sphincter, **Sp**: spleen, **St**: stomach, **TG**: transgenic.

The second transgene is a fragment containing *LacZ* (or at least the portion examined by PCR), which was not expressed/functional in any of the embryos examined.

The finding that four of the eight embryos on the CD1 background carrying an intact *NGRS-LoxSTOPLox-LacZ* transgene (*LacZ*-positive, *STOP*-positive) could still express *LacZ* may be explained by one of two possibilities:

1) *NGRS-LoxSTOPLox-LacZ* is "leaky" and some read-through of the *LoxSTOPLox* sequence occurs in ~half of the embryos (0/3 CD1 litter one, 4/8 CD1 litter two). The "leakiness" would go unnoticed on the *gl-Cre* background, as recombination would occur regardless.

2) A third insertion event occurred, of a defective version of the *NGRS-LoxSTOPLox-LacZ* transgene. Small deletions within the *STOP* sequence would not be detectable as a size change in the *STOP* PCR product. Such deletions could permit read-through/inactivation of the *STOP* sequence, thus allowing *LacZ*-expression in the four stained *LacZ+;STOP+* embryos on the CD1 background. The DNA used for microinjection was re-sequenced and confirmed to match that of the *LoxSTOPLox* cassette (in pBS302) from which it was amplified, suggesting that there is no sequence-based reason for inefficient transcriptional termination. However, the proposed alteration(s) of *NGRS-LoxSTOPLox-LacZ* could have occurred following microinjection (perhaps in the germline) or may have been present already in the injected DNA at a lower copy number than the correct transgene. If the latter occurred and the altered transgene were to integrate in multiple copies (as is the nature of microinjected DNA) then this could also explain the more intense staining noted in these four mice than on the *gl-Cre* background. A tandem array of "correct" transgenes in this latter group might undergo Cre-mediated recombination of all sequences between the first and last *LoxP* sequences in the array, thus leaving only one functional copy; a tandem array of defective transgenes which do not require Cre for their activity would, on the other hand, possess many constitutively-active functional copies. It is also conceivable that the "correct" transgene in one or both of the stained *gl-Cre*

embryos was in fact the proposed third defective transgene, recombination of which occurred.

The ideas above are purely speculative, and the likelihood of them occurring is unknown. Regardless of the explanation, the line was of no further use.

3.3.3.2 Female founder

The X-gal staining and genotyping results from the female line were decidedly easier to interpret. Two male offspring were mated with a *gl-Cre* and CD1 female each. A total of 6/14 embryos from the *gl-Cre* mothers were transgenic (*LacZ*-positive), and all carried a recombined *STOP* sequence (*STOP*-negative; small band in recombination PCR). None had only a *LacZ* fragment.

On the CD1 background, 26/30 embryos were transgenic (*LacZ* and *STOP* positive) and none had undergone recombination, as expected. Again, *LacZ* and *STOP* genotyping status correlated, demonstrating that the anomalies in the offspring of the male founder were line-specific.

Despite the promising genotyping results none of the embryos displayed X-gal staining. It is therefore assumed that the recombined *NGRS-LoxSTOPLox-LacZ* was not expressed, possibly due to positional effects (silencing). This line was therefore terminated.

3.3.4 NGRS-LoxSTOPLox-LacZ discussion

An *NGRS-LoxSTOPLox-LacZ*-based "clonal analysis" system was not established. Often a relatively large number of microinjection sessions must be performed before a line is successfully generated, but this was not an option for this construct due to time restraints. It is this need for multiple sessions and the problems outlined over the last few pages (potential fragmentation of DNA, copy number,

positional effects) that highlight the limitations of microinjecting fertilised oocytes as a method for generating transgenic mice. Though time did not permit it in this instance, the option of introducing constructs into ES (embryonic stem) cells and deriving transgenic mice from these should be given great consideration when designing transgenic strategies. The ES cell approach allows isolation of cells containing expressed single-copy transgenes, and permits "knocking-in" of transgenes into a specified genomic locus.

Some mice from the male founder-derived *NGRS-LoxSTOPLox-LacZ* line are still available and so the lab is now considering the possibility of breeding them to try and transmit only the apparently "correct" transgene.

3.4 Discussion

Many of the questions surrounding SMP and early spleen development will only be answered through lineage tracing studies. Given the large number of non-transgenic and non-expressing mice generated during the *NGRS-CreERT2* investigations, it is unlikely that this particular approach will be revisited by our lab. There are of course other routes that can be explored, both utilising the *NGRS* and otherwise. Upstream regulatory regions of other important spleen development genes, particularly *Hox11*, may provide a way to direct a spleen lineage tracing exercise.

A knock-in of standard (non-inducible) *Cre* into the endogenous *Nkx2-5* locus exists (Moses et al., 2001; Stanley et al., 2002). Although not inducible, when used in conjunction with the ubiquitously expressed *R26R* reporter this would allow tagging of the descendents of a splenic precursor to be marked even if expression from the *Nkx2-5* locus stopped (as permanent recombination of the *R26R* locus occurred in the ancestral cell). Of course, *LacZ* expression in the *Nkx2-5-Cre;R26R* line is obviously present in more tissues than that conferred by the *NGRS* (Moses et al., 2001), and so this could confuse matters somewhat. However, such an approach has been successfully used to map the fate of the cardiac neural crest (using *Cre* under the control of the *Wnt1* promoter and enhancer (Jiang et al., 2000)), the apical

ectodermal ridge of the limb (with *Cre* knocked into the *En1* locus (Kimmel et al., 2000)), pancreatic epithelium (*nestin* controlled *Cre* (Esni et al., 2004)), and the serosal mesothelium (using *Cre* inserted into a *Wt1* YAC (Wilm et al., 2005)). Knocking *Cre* into an endogenous locus also overcomes the problem of position effects – i.e. microinjected *Cre* DNA inserting in the genome at a position where it comes under the regulation of local elements. Efforts to knock *CreERT2* into the endogenous *Bapx1* locus were made during my PhD studies; this is discussed later in this section.

3.4.1 Alternative uses for the NGRS

Spleen-specific expression of GFP would be an ideal way to follow splenic cells. In addition to the *LoxSTOPLox-LacZ* vector used in many lineage studies, *LoxSTOPLox-GFP* also exists (Esni et al., 2004), and this could be used in conjunction with an *NGRS*-driven inducible Cre line. The major advantage of GFP detection is that it is immediate and can be performed on live tissue (unlike X-gal staining). GFP is thus ideally suited to live imaging of reporter gene expression in organ culture. An analysis of spleen development in an organ culture system has not yet been reported, but data provided in the following chapter suggests that this is a worthwhile avenue to explore.

A further way to perform lineage tracing is by specific cell ablation. The loss of cells in the tissue of interest following ablation of precursor cells is an indicator of lineage (though of course these absent cells may not be direct progenitors but simply require some interaction with the actual ablated cells). Complete loss of *Nkx2-5* expression would not be the way to achieve this, due to the early lethal effect (Lyons et al., 1995; Ivanova et al., 2005)[24]. The *NGRS* could therefore be put to use to drive

[24] Indeed, *Nkx2-5-Cre* has been used to drive diphtheria toxin subunit A expression, thus resulting in specific ablation of *Nkx2-5*-expressing cells and a phenotype similar to the full knockout (lethal cardiac defects by ~E9.0) (Ivanova et al., 2005). A diphtheria toxin receptor is not required on the cell surface in this strategy, as the A subunit is manufactured within and acts inside of the cell to inactivate elongation factor 2. This leads to failure of protein synthesis and thus causes apoptosis (Ivanova et al., 2005).

ablation. One method to achieve this is by expressing the diphtheria toxin receptor on the surface of cells in the tissue of interest and using maternal diphtheria toxin injections to induce cell-autonomous ablation in the embryo (Saito et al., 2001). This has been successfully used to dissect the islet cell lineage during pancreatic development (Herrera et al., 1994).

3.4.2 Towards a gut-specific Nkx2-5 knockout

It was mentioned at the start of this chapter that an *NGRS-CreERT2* line would provide a way to direct a gut-specific *Nkx2-5* knockout by crossing onto the existing "floxed" *Nkx2-5* strain. This "floxed" allele contains two *LoxP* sites which flank the second (homeodomain-containing) exon of *Nkx2-5* (Pashmforoush et al., 2004). Mice carrying this floxed allele have been crossed with those expressing a ventricle-specific *Cre*, thus generating a ventricle-specific *Nkx2-5* knockout (Pashmforoush et al., 2004). No gut mesenchyme-specific *Cre* lines exist and so this is where the *NGRS-CreERT2* line would have come into use. Though this line was not established, generating a gut-specific knockout of *Nkx2-5* should still remain a major focus of work on early gut and spleen development. Using a gut-specific *Cre* line in conjunction with the floxed-*Nkx2-5* mouse seems the most logical approach, and the use of a *CreERT2* line would provide greater control. The *NGRS* could be used to direct such a knockout, though awareness must be maintained that using a regulatory element of the gene being knocked out could carry autoregulatory issues. Indeed, autoregulation of *Nkx2-5* in the embryonic gut has been proposed (Tanaka et al., 1999c).

An alternative approach is to knock *CreERT2* into another gene expressed in regions of the gut comparable to those in which *Nkx2-5* is expressed. To this end, I made constructs to allow cloning of *CreERT2* into the *Bapx1* locus (replacing the *Bapx1* exon 1 coding sequence by homologous recombination), to be followed by recombination of this DNA into the endogenous *Bapx1* locus; this was not, however, completed. Nonetheless, this may be a method to investigate further as it circumvents the issue of copy number because the transgene is homologously recombined into the

genome in ES cells. *Bapx1* heterozygotes have normal gut development, so the knock-in should not cause any complications. It should of course be noted that any use of the *CreERT2* system to produce a knockout could have a drawback in that the knockout may not be 100% complete, for example if the pattern of recombined cells is mosaic. However, dosage could be first optimised on the *R26R* background to avoid this problem. Crossing of the *Bapx1-CreERT2* line onto the *R26R* background would also permit lineage tracing of *Bapx1*-expressing gut cells.

CHAPTER 4

Examining spleen development in an *in vitro* gut culture system

...Or: "Science may be described as the art of systematic oversimplification" – Karl Popper

4.1 Introduction: Examining development in organ culture

4.1.1 The need for organ culture systems

The laboratory mouse *Mus musculus* provides an excellent system in which to study the fundamental processes of mammalian development. Another well-favoured model is the zebrafish (*Danio rerio*); one of the main reasons for its popularity is that the embryo is transparent and so cells can be tagged and followed during development (Beis and Stainier, 2006). And herein lays a fundamental disadvantage of using the mouse: developmental processes cannot be viewed as they happen because mice develop within the uterus. All that can be achieved is to take a "snapshot" at the stage at which the embryo was obtained - of what a tissue looked like, of what genes it was expressing - and to try and relate this to comparable data from earlier and later stages. Whilst such an approach can be informative there are many questions which cannot be answered in this manner. Development is by definition comprised of dynamic processes involving morphological change, proliferation, apoptosis, and cell movement; the nuances of these processes cannot be fully appreciated by looking at a time-course of staged embryos.

Progress has been made in recent years on imaging mouse development *in utero*, by means of ultrasound (Turnbull et al., 1995) and magnetic resonance microscopy (Hogers et al., 2000; Smith, 2001). External structures such as the heart and neural tube have been examined by these methods (Turnbull et al., 1995). However, *in utero* imaging is unlikely to become a reality for studying gut development in detail. The emphasis must therefore fall on live imaging of explanted organs and tissues. Embryonic mouse tissues which have been successfully cultured as explants include the lung, limb, and ureteric buds, and even the whole embryo (McAteer et al., 1983; Friedman, 1987; Srinivas et al., 1999; Moore-Scott et al., 2003). Studies have focussed both on observing normal morphogenesis and on manipulating development. A recent example of this latter type of study is the use of siRNA-mediated repression of gene expression in embryonic kidney culture (Davies et al., 2004).

4.1.2 Foregut organ culture

Foregut organ culture is still a relatively unexplored technique, but one extremely worthy of attention:

"Techniques to better study gut development are direly needed. If explant culture of the entire gut as an organ early in development could be realized, then experimental embryologic and molecular techniques could be combined, vastly improving the ability to study specific factors and their role in gut patterning. These areas should be the focal points of research during the next decade."

- (Roberts, 2000)

The majority of published gut explant studies have been concerned with the intestine (Nishijima et al., 1990; Kapur et al., 1992; Young et al., 1996; Quaroni, 1985; Altmann and Quaroni, 1990; Hearn et al., 1999; Duh et al., 2000); there is a relative dearth of information on the optimal ways to culture foregut (stomach) tissue. Segments of embryonic intestine are tubular and initially uniform making them ideal candidates for explant culture. However, the tissue of interest in this chapter – the spleen – develops in close association with, and must therefore be cultured in contact with, the stomach, which is not such a uniformly shaped piece of tissue. Nonetheless, stomachs can be cultured: for example, Aubin and colleagues cultured E12.5 stomachs for 72 hours in 1:2 Matrigel:BGJb medium[25] to study the effects of FGF10-soaked heparin beads on gene expression (Aubin et al., 2002). Spleen-only cultures have also been performed: E13.0 spleens were reported to grow for four days on Nucleopore membranes in complete medium[26] (Bertrand et al., 2006). However, explant morphology was not important in this latter study, as the method of assessment was flow cytometry of cell suspensions obtained from the cultures. The spleens were also in isolation from other gut tissues and thus this system is not of any use when hoping to understand how normal spleen morphogenesis progresses. Analysis of early spleen morphogenesis in culture therefore remains unexplored territory.

[25] Containing 0.2mg/ml ascorbic acid and 0.1% heat-inactivated foetal bovine serum.
[26] OptiMEM, 10% foetal calf serum (FCS), 1% Pen/Strep.

4.1.3 Experimental rationale

Development of the murine spleen is a rapid process and hence an ideal candidate for investigation in organ culture. At E11.5 the spleen is visible only as a bulge of mesenchyme on the dorsal face of the posterior stomach, and yet by E12.5 the spleen is present along the length of the dorsal stomach as a distinct elongated structure. An interesting feature of both these early spleen structures is the existence of connections with the underlying stomach. A posterior connection links the splenic mesenchyme with that surrounding the dorsal pancreatic bud, whilst an anterior connection exists between the tip of the spleen and the stomach (**Figure 4.1**). The nature of the cells constituting these connections is unknown, though from my own observations they appear to be mesenchymal. The cells lying between these connections – comprising the main body of the spleen - do not maintain a physical connection with the underlying stomach; the mechanism for this separation is unclear.

The anterior connection adopts an increasingly anterior position along the stomach between ~E11.5-12.5, in conjunction with the leading edge of the spleen; the anterior connection may therefore play a role in the expansion of the spleen towards the anterior stomach. The mechanism for how this rapid expansion occurs is unknown. **Migration** of the spleen primordium along the dorsal face of the stomach (presumably with concomitant proliferation) is one attractive model, with many aspects to investigate: what are the splenic cells migrating towards; by what mechanism do they move along the stomach; is there cellular or tissue migration? The anterior spleen connection could feasibly direct this migration towards the anterior stomach, particularly if the leading edge is undergoing rapid proliferation. An alternative view is that the splenic precursors **arise from the stomach** itself, in a posterior-anterior wave along the length of the future spleen. Again, there are many avenues to investigate with this model: what properties specify these cells as being splenic precursors; can they be identified at an earlier stage; is the cue to commence splenic development conferred by a signal which is propagated in a posterior-anterior wave; if so, what is the nature of this signal? A role for the anterior connection could again be envisaged in this model, if it represents the anterior limit of a splenic

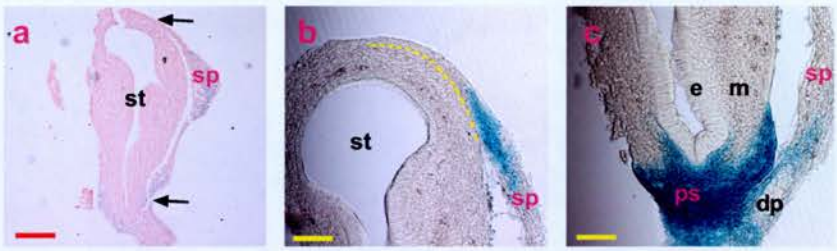

***Figure 4.1*: The connections of the E12.5 spleen**

a: Section through an E12.5 gut showing the connections (**black arrows**) the spleen mesenchyme makes with the underlying gut tissue. Blue cells are X-gal stained for *NGRS-LacZ* activity. 7μm paraffin wax microtome section, counterstained with Nuclear Fast Red to aid visualisation. 5x magnification.
b: The anterior spleen connection appears to be continuous with the outer layer of stomach mesenchyme/mesothelium. The boundary of this apparent continuum is marked by a **dashed yellow line**. *NGRS-LacZ* expression is denoted by X-gal staining. 30μm agarose vibratome section. 10x magnification.
c: The posterior spleen connection is continuous with the mesenchyme surrounding the dorsal pancreatic bud (**dp**). *NGRS-LacZ* expression can also be seen in the mesenchyme of the primitive pyloric sphincter. 30μm agarose vibratome section. 10x magnification.
Yellow scale bars: 100μm. Red scale bars: 200μm.
e: endoderm, **m**: mesenchyme, **ps**: pyloric sphincter, **sp**: spleen, **st**: stomach.

development wave, and is the point at which cells are contributed to the spleen from the underlying stomach.

Explant culture may provide the ideal environment in which to investigate these models. The chief stage of interest is E11.0-11.5. At this stage, however, the spleen primordium is largely indistinguishable from the stomach and associated pancreatic mesenchyme. A splenic marker is therefore required to identify splenic precursor cells and successfully track them. Hence the second use of the *Nkx2-5* gut enhancer element (*NGRS*) reported in this thesis is as a splenic marker in explant culture.

4.2 Initial aims of gut culture experiments

The first line of investigation was to assess whether E11.5 foreguts could a) survive in a culture system, and b) undergo growth and development to such an extent that experimental findings could be related to normal development. E11.5 whole gut (Natarajan et al., 1999) and E12.5 stomach (Aubin et al., 2002) cultures have been reported in the literature, but an account of culturing E11.5 stomachs has not been published.

A spleen marker was required, as the spleen is not easily distinguished from the underlying stomach at E11.5. The ideal marker would be one that is expressed from the earliest stages of spleen morphogenesis, does not interfere with normal development, and specifically marks splenic cells. The *NGRS-LacZ* transgene discussed in **Chapter 2** fulfils at least the first two of these criteria, and is likely to be satisfactory for the third. *NGRS-LacZ* expression is detected in the elongated spleen structure from E12.5, and is found in the region of condensed dorsal mesenchyme known to express splenic markers at both E10.5 and E11.5. These transgene-marked tissues are the earliest reported primordia of the spleen, and thus *NGRS-LacZ* satisfies the first criterion. The morphology of *NGRS-LacZ*-expressing guts is identical to that in non-transgenic littermates, and adult mice carrying *NGRS-LacZ* grow and reproduce normally; thus the second criterion is also fulfilled. The final criterion – that the marker should be specific to splenic precursors - cannot however be totally met by this enhancer. The non-gut expression sites (outflow tract, pharyngeal endoderm, and thyroid primordium) are experimentally irrelevant as the guts are to be cultured as explants, but the major pyloric sphincter expression could complicate matters. The splenic and pyloric expression domains are linked at E11.5, and arise from an earlier single domain. It may not therefore be possible to ascribe a *LacZ*-positive cell seen in the E11.5 gut to the future spleen or pyloric sphincter. Although this would obviously complicate lineage tracing analyses, *NGRS-LacZ* was deemed sufficient for the purpose of merely visualising the spleen in order to examine its development in a way not previously possible.

4.3 Optimising the gut culture system

A number of factors are important when creating an environment in which an explant can survive and, hopefully, grow. Firstly, the culture media must be suitable and not contain exogenous growth factors. Secondly, the culture conditions must be optimised (temperature, CO_2 concentration) and, finally, the surface on which the explant is grown must be appropriate. The initial studies into the ideal dissection and growth conditions discussed in this section were performed by Dr Marit Boot, adapting published culture methods. Explants in these optimisation studies were grown on both reduced growth-factor Matrigel (BD Biosciences) and on filter-discs (Millicell-CM culture plate inserts, Millipore). Both techniques supported explant survival and growth; details are provided in **Chapter 7 (Materials & Methods)**.

During the optimisation experiments it became apparent that landmarks were required to correctly orientate the gut; the lungs, oesophagus, stomach, and a short length of proximal duodenum were therefore isolated *en bloc* from E11.5 embryos. The lungs also provided an internal control for assessing explant health as lung buds develop well in culture, undergoing branching morphogenesis (Bellusci et al., 1997). Explants with these additional tissues did not display any behaviour to suggest that the inclusion was detrimental. Embryos varied slightly in age depending on the time of night at which they were conceived, the time of day at which they were dissected, and both inter- and intra-litter differences. Only the second of these variables could be controlled and so litters were taken at the same time each morning, with any deviation noted.

The conclusions reached were that E11.5 guts from CD1 embryos can survive for periods of 24 and 48 hours, when cultured on either filter-discs or Matrigel[27]. Guts cultured in Matrigel retained a slightly more three-dimensional shape. The extent of growth and development was variable, but encouraging. An E11.5 gut was not as developed as an E12.5 gut after 24 hours in culture, and did not resemble an E13.5 gut after 48 hours. Retardation of cultured explants and embryos was expected (Copp and Cockroft, 1990). The extent of growth and development was, however, adequate for the planned experiments. Overall increases in growth were achieved,

[27] And for 72 hours on Matrigel; filter-discs were not assessed at 72 hours

and the anterior stomach grew out normally such that the oesophagus began to adopt a position on the inner curvature rather than at the anterior limit of the stomach. These findings were recapitulated in the explants shown throughout this chapter and so images from these optimisation studies are not presented.

4.4 *NGRS* expression in culture

Expression of the *NGRS-LacZ* transgene was assessed by X-gal staining of E11.5 guts grown on both filter-discs and Matrigel. In addition to examining whether expression could be detected following a period in culture, another key issue was the extent to which this expression resembled that in non-cultured guts. The experiments presented in this chapter were performed in collaboration with Dr Marit Boot.

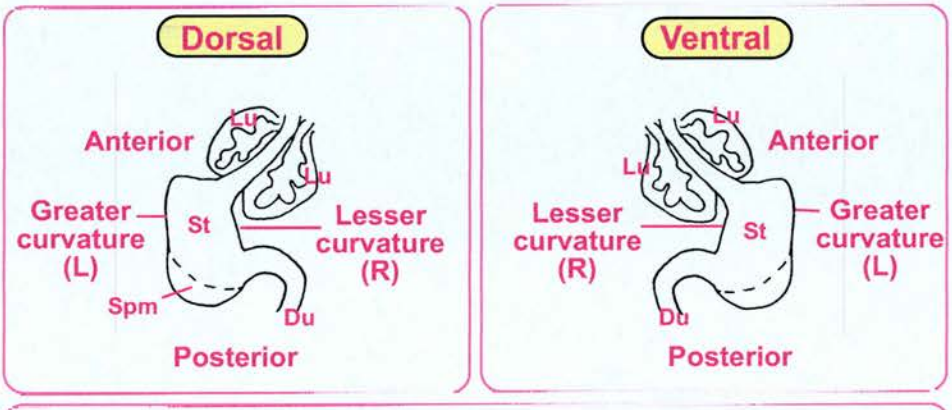

***Figure 4.2*: Terminology used in this chapter**

Gut explants are described as being cultured "dorsal" side upwards (i.e.: lying on their ventral face) or "ventral" side upwards (i.e.: lying on their dorsal face); the former is depicted in the first box, the latter in the second. The spleen develops on the dorsal face during normal development.
Lu: lung buds, **St**: stomach, **Spm**: spleno-pancreatic mesenchyme, **Du**: duodenum, **L**: left, **R**: right

4.4.1 Culturing on filter-discs

NGRS-LacZ expression was examined in E11.5 guts from an *NGRS-LacZ* with CD1 mating; nine guts were recovered and cultured on filter-discs using the method described in **Chapter 7**. Non-cultured controls were not retained in this initial investigation. Half of the group was cultured dorsal ('spleen') side-up, and the remainder ventral side-up. Illustrations of the faces of the gut and the terminology used in this chapter are provided in **Figure 4.2**. Guts were photographed at t0 (time = 0 hours) and then cultured for 24 hours at which point photographs were again taken (t24). The guts were then fixed, washed, and X-gal stained as described. Following overnight staining, three of the nine guts were positive for *LacZ* expression (**Figure 4.3**).

The *NGRS* drove *LacZ* expression in the appropriate domain in the cultured guts: encompassing the pyloric sphincter and the spleno-pancreatic mesenchyme. The side on which the gut was cultured (dorsal or ventral face) affected neither growth nor transgene expression. The stained guts grew beyond their initial ~E11.5 size and displayed characteristics typical of later development: the anterior stomach grew such that the oesophagus was displaced from the anterior tip of the stomach, the lung buds developed well, and the pancreatic buds (outlined in red in **Figure 4.3**) grew, pushing the tip of the overlying mesenchyme to a more anterior point along the greater curvature of the stomach. However, overall E12.5 morphology was not achieved and normal E12.5 spleen development (a column of mesenchyme along the length of the stomach) was not observed. *LacZ*-positive cells were instead observed in a smaller spleen-like domain (outlined in yellow in **Figure 4.3**) that extended from the spleno-pancreatic mesenchyme towards the anterior stomach in all three stained guts. These putative splenic expression domains were specific to the dorsal face of the stomach, as in normal spleen development.

The *LacZ*-marked splenic growth was promising but perhaps not sufficient for studies into spleen development. The next step was thus to examine transgene expression after a longer culture period (48 hours). This was tested on Matrigel - as guts retained better morphology on this surface – and is presented in the next section.

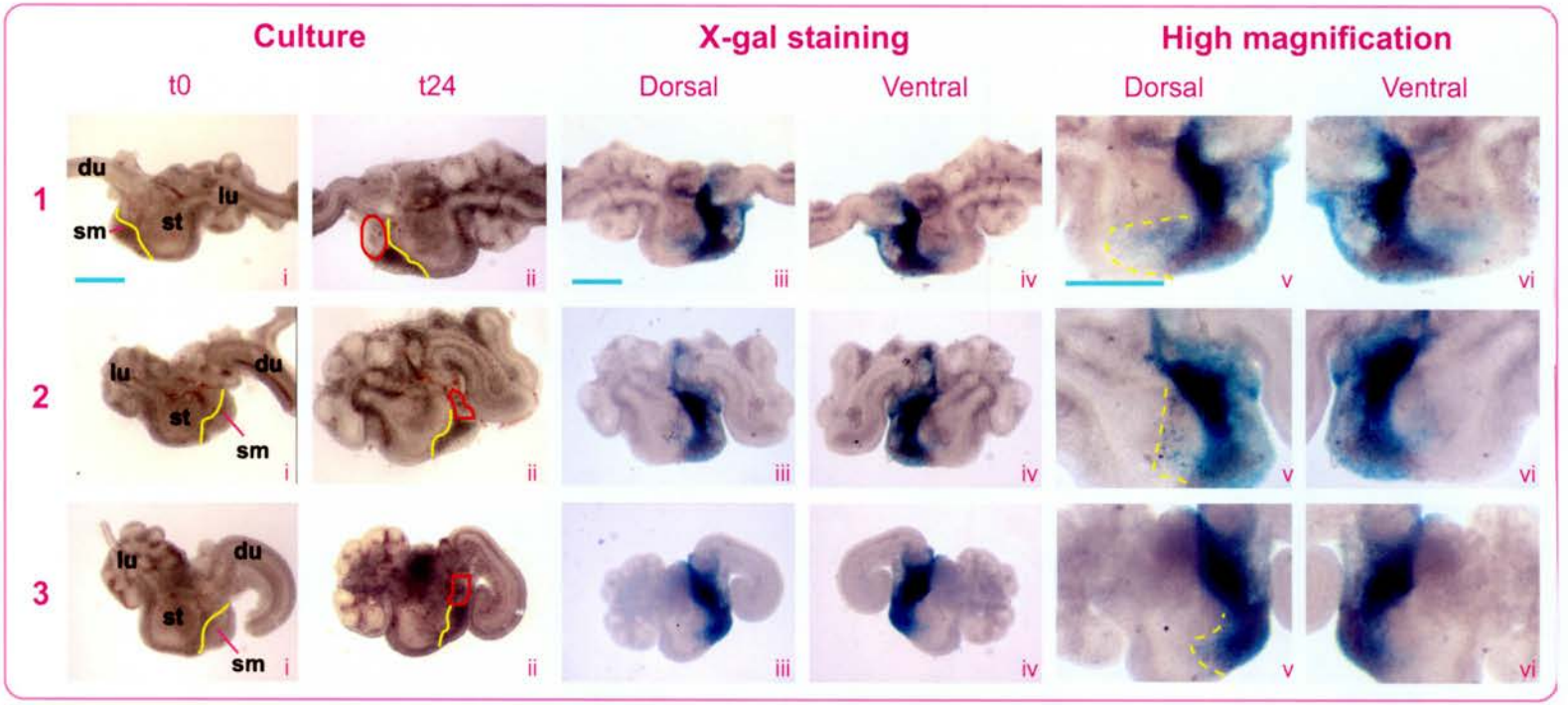

Figure 4.3 **X-gal staining of** *NGRS-LacZ* **activity in E11.5 gut explant cultures grown on filter-discs**
Images are shown for each of the three *NGRS-LacZ*-positive guts (**1-3**). The first column shows the explants at t0; the second column is after 24 hours in culture; the third and fourth columns show X-gal staining at 5x magnification; the fifth and sixth columns show staining at 10x magnification. **The blue scale bars in 1 i, iii, v represent 500μm and are relevant for all gut culture images in this chapter.** Explant **1** was cultured on its dorsal face (ventral side up), and explants **2** & **3** were cultured on their ventral sides (dorsal side up). The putative splenic mesenchyme (darker tissue) is outlined on the unstained guts in **yellow**, and the dorsal pancreatic bud in **red**. The putative splenic staining (outlined in **yellow**) is specific to the dorsal face, as in normal development, though it can also be seen from the ventral side due to the transparency of the guts. **lu**: lung buds, **st**: stomach, **du**: duodenum, **sm**: putative splenic mesenchyme.

4.4.2 Culturing on Matrigel

Fourteen E11.5 guts were obtained from an *NGRS-LacZ* with CD1 mating, and cultured for 48 hours on Matrigel. Photographs were taken at t0, t24 and t48; the guts were then fixed and stained overnight.

Five of the 14 guts showed *LacZ* expression, demonstrating that culture on Matrigel is compatible with correct transgene expression and X-gal staining. Spleen development was marked specifically on the dorsal side of the stomach by *NGRS-LacZ* expression, but again did not extend all the way up to the anterior stomach as would be expected by E12.5. Three representative explants are shown in **Figure 4.4**. Patterns similar to those shown were observed for all intact gut explants cultured for 48 hours in subsequent experiments.

4.4.3 Recommendations following initial experiments

It is difficult to ascertain whether the spleen development seen in culture is particularly retarded or if this delay is proportional to that of the rest of the gut. The extent of development observed in the studies outlined above was not advanced enough to indicate that this system would allow E11.5-12.5 spleen development to be fully recapitulated. Despite this, the planned splenic mesenchyme manipulation experiments were still attempted. Serendipitously, these experiments produced some interesting findings, and these are discussed in the subsequent sections.

During the initial experiments it became apparent that non-cultured controls would be needed from each litter to monitor how the X-gal staining pattern at the end of the culture period relates to that at t0. Thus in an attempt to control for the differences in developmental stage between litters, a number of guts from each were immediately fixed and stained to provide a record of transgene expression at t0 for each experiment, unless otherwise stated. This obviously cannot control for differences between embryos within a litter.

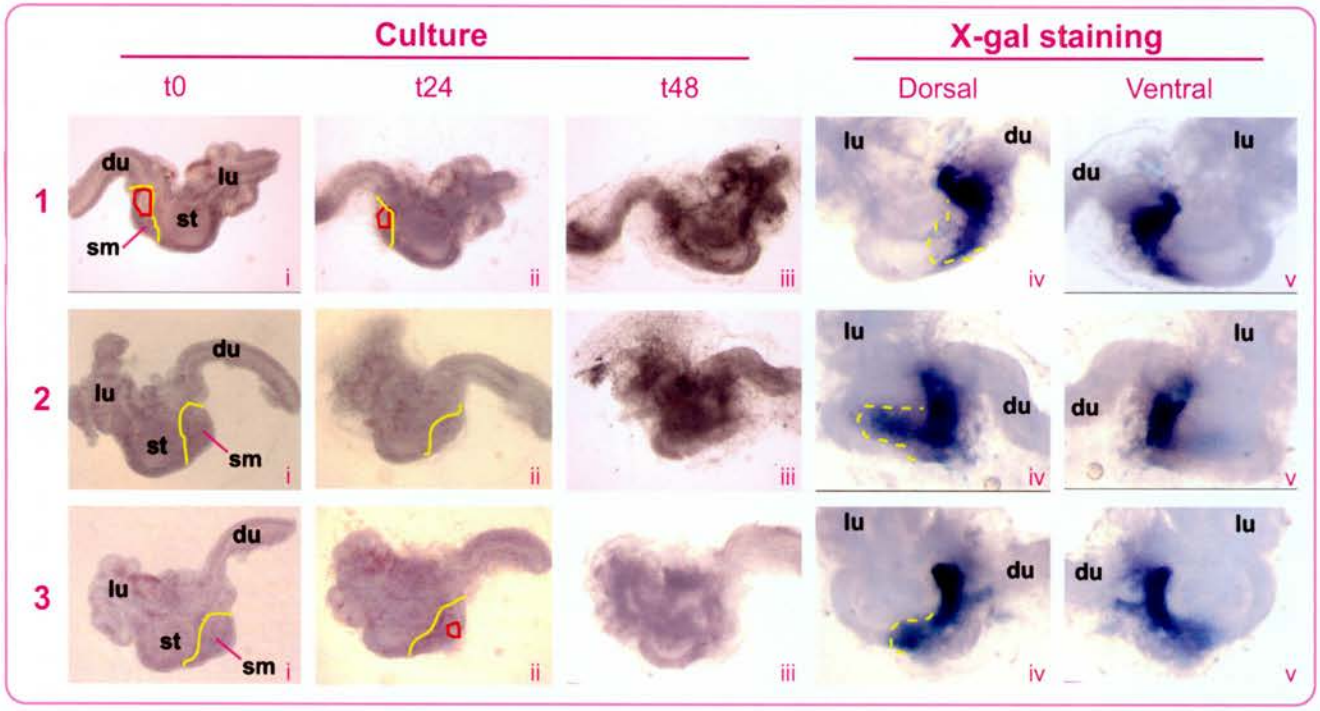

Figure 4.4 **X-gal staining of** *NGRS-LacZ* **expression in E11.5 gut explant cultures grown on Matrigel**

Images are shown for three of the stained guts (**1-3**). The first column shows the explants at t0; the second column is at t24; the third column shows explants at the end of the 48 hour culture period. The fourth and fifth columns show X-gal staining at 8x magnification. **Explant 1** was cultured on its dorsal face (ventral side up); **explants 2 & 3** were cultured on their ventral sides (dorsal upwards). The putative splenic mesenchyme (darker tissue) is outlined on the unstained guts in **yellow** and the dorsal pancreatic bud in **red**. The putative spleen staining was specific to the dorsal face and is outlined in **yellow. lu**: lung buds, **st**: stomach, **du**: duodenum, **sm**: putative splenic mesenchyme.

4.5 Migration versus stomach derivation

No published work has addressed the question of how the patch of splenic mesenchyme associated with the posterior stomach at E11.5 relates to the elongated structure lying along the length of the stomach at E12.5. Two distinct models (discussed previously in **Section 4.1.3**) can be invoked for how this transition might occur:

1) The "**migration**" hypothesis: the splenic primordium proliferates and "**migrates**" (as cells or a tissue) up the dorsal face of the stomach towards its anterior limit, possibly with some role played by the anterior connection of the spleen to the stomach.
2) The "**stomach derivation**" hypothesis: spleen cells are **derived from the stomach**, with their contribution occurring in a posterior to anterior wave, such that the anterior limit of the spleen is located further towards the anterior tip of the stomach as time progresses between E11.5 and E12.5.

Distinction between these models is not possible from a time-course of staged guts between E11.5 and E12.5, as their manifestations would look identical. Manipulations, tailored to disrupt the outlined mechanisms, are therefore necessary to distinguish between the two.

4.5.1 Physical obstruction experiments

The first manipulation to be attempted was to place a physical barrier between the anterior limit of the E11.5 splenic mesenchyme and the underlying stomach, with the aim being to obstruct the migration proposed in the first model. Although spleen development in culture is slow, it was hoped that some insight might be gained since the detection of any blue cells anterior to the barrier would lend credence to the second model (derivation from the stomach).

Aluminium foil was chosen as the blocking material as it is malleable, yet strong, and can be cut to a small size. It is also opaque, thus aiding visualisation. Ten guts from an *NGRS-LacZ* with CD1 mating were cultured on Matrigel for 48 hours; six had a foil barrier inserted. Three manipulated guts and five guts in total were positive for *LacZ* expression following X-gal staining. Overall growth and health was good, and transgene expression was as expected.

The foil was positioned in the intended location – between the anterior limit of the putative splenic mesenchyme and the underlying stomach - in two of the three stained manipulated guts. X-gal staining was normal around the pyloric sphincter region, and continued up to the foil (**Figure 4.5**). No stained cells were observed beyond the foil, whereas they had been observed beyond this point in non-manipulated guts; this provides evidence against the second model (stomach derivation). The first model (migration) may be supported by the fact that staining extended right up to, but stopped abruptly at, the foil (e.g. **Figure 4.5 2vi**).

The above conclusions are tentative as it is impossible to know for each individual explant how much of the mesenchyme posterior to the foil insert was initially *LacZ* positive at t0. Additionally, development in explant culture is inherently variable, and only two explants were examined. Recombination experiments to further investigate the migratory potential of the splenic mesenchyme are therefore reported in the next section.

A criticism of the experimental technique employed is that the effect exerted by the physical obstruction cannot be distinguished from the effects of cutting the explant in order to insert this obstruction. The effects of cutting alone are, however, investigated later in this chapter. A further criticism could be that if a posterior-to-anterior signalling wave exists (as in the second model) then this would also be disrupted by the barrier. The aforementioned recombination experiments were designed to attempt to overcome these experimental limitations.

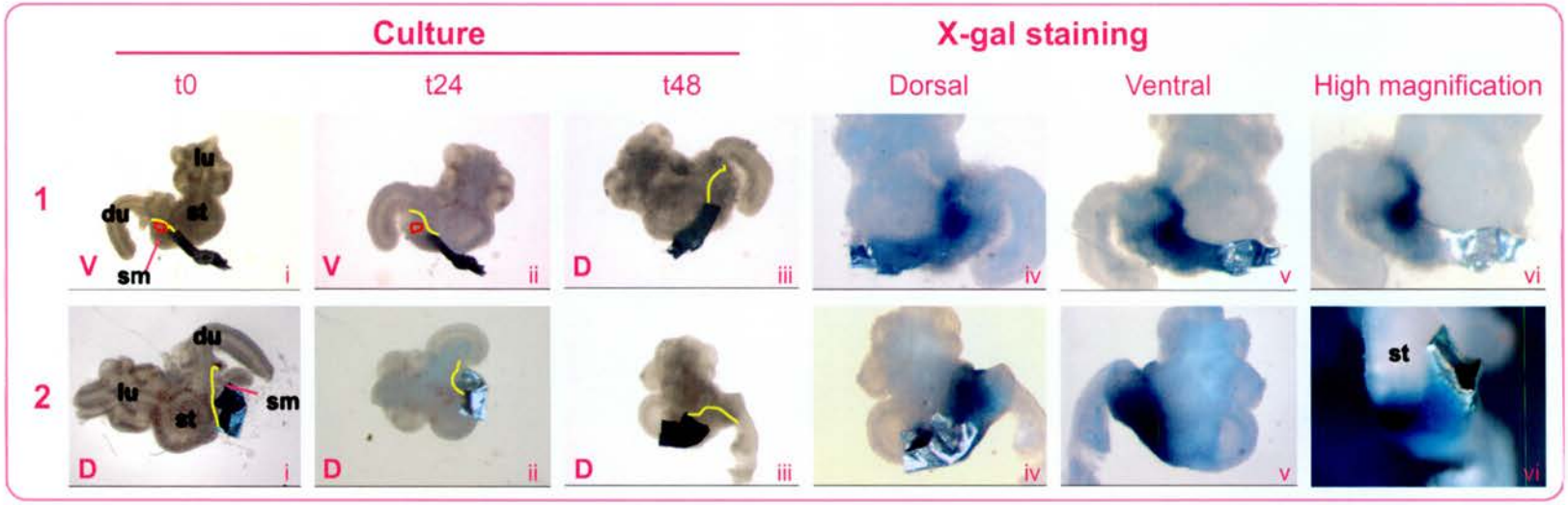

Figure 4.5 **E11.5 gut explant cultures on Matrigel - physical obstruction experiments**

Images are shown for two of the three *NGRS-LacZ*-positive guts which had a foil barrier inserted (**1,2**). The first column shows the explants at t0; the second column is at t24; the third column shows the explants at t48. The fourth and fifth columns show X-gal staining at 8x magnification. The final column shows staining at 10x magnification. The high magnification for **explant 2** is taken from above the greater curvature and shows the beginnings of a spleen structure which ends abruptly at the foil block. No stained cells were observed beyond the foil barriers. The putative splenic mesenchyme (darker tissue) is outlined on the unstained guts in **yellow**, and the dorsal pancreatic bud is in **red** on the t24 unstained guts. **lu**: lung buds, **st**: stomach, **du**: duodenum, **sm**: putative splenic mesenchyme.

4.5.2 Recombination experiments

4.5.2.1 Posterior stomach recombinations

The posterior halves of *NGRS-LacZ* stomachs were recombined with the anterior portions of stage-matched CD1 guts to test the migration hypothesis. The premise of this experiment was that if the splenic mesenchyme (attached to the posterior *NGRS-LacZ* gut portion) does indeed harbour migratory potential then cells may move in an anterior direction onto the adjacent CD1 stomach. The recombination of a transgenic with a non-transgenic gut provided the opportunity to examine the origin of any splenic tissue observed. The abilities of isolated anterior and posterior stomach halves to survive in a 48 hour culture were confirmed in a separate experiment (**Section 4.7.2**).

E11.5 litters were taken simultaneously from a) CD1 with CD1 and b) CD1 with *NGRS-LacZ* matings, and the embryos matched by developmental stage. Seven guts were dissected out from each litter and cut in half; suitably staged posterior *NGRS-LacZ* and anterior CD1 gut halves were then recombined by forcing them into close proximity (illustrated in **Figure 4.6a**). The reciprocal recombination was also performed for each gut pair (CD1 posterior with transgenic anterior); any stained cells found on the anterior *NGRS-LacZ* stomach portion would support the notion of derivation of the spleen from the stomach. There were thus 14 recombination experiments performed in total. Three additional *NGRS-LacZ* guts and one CD1 gut were kept intact as cultured controls for health, growth, and staining. All explants were cultured on Matrigel for 48 hours.

X-gal staining was observed in all three intact *NGRS-LacZ* control explants, and in four of the seven gut pairs, two of which are shown in **Figure 4.6b**. Whilst the expected staining pattern was observed in the pyloric sphincter and spleno-pancreatic mesenchyme, no evidence was found for migration of marked splenic precursors onto the CD1 anterior stomach. However, nor was support found for the stomach derivation hypothesis as no stained "spleen" cells were found in the anterior *NGRS-LacZ* gut portions (data not shown).

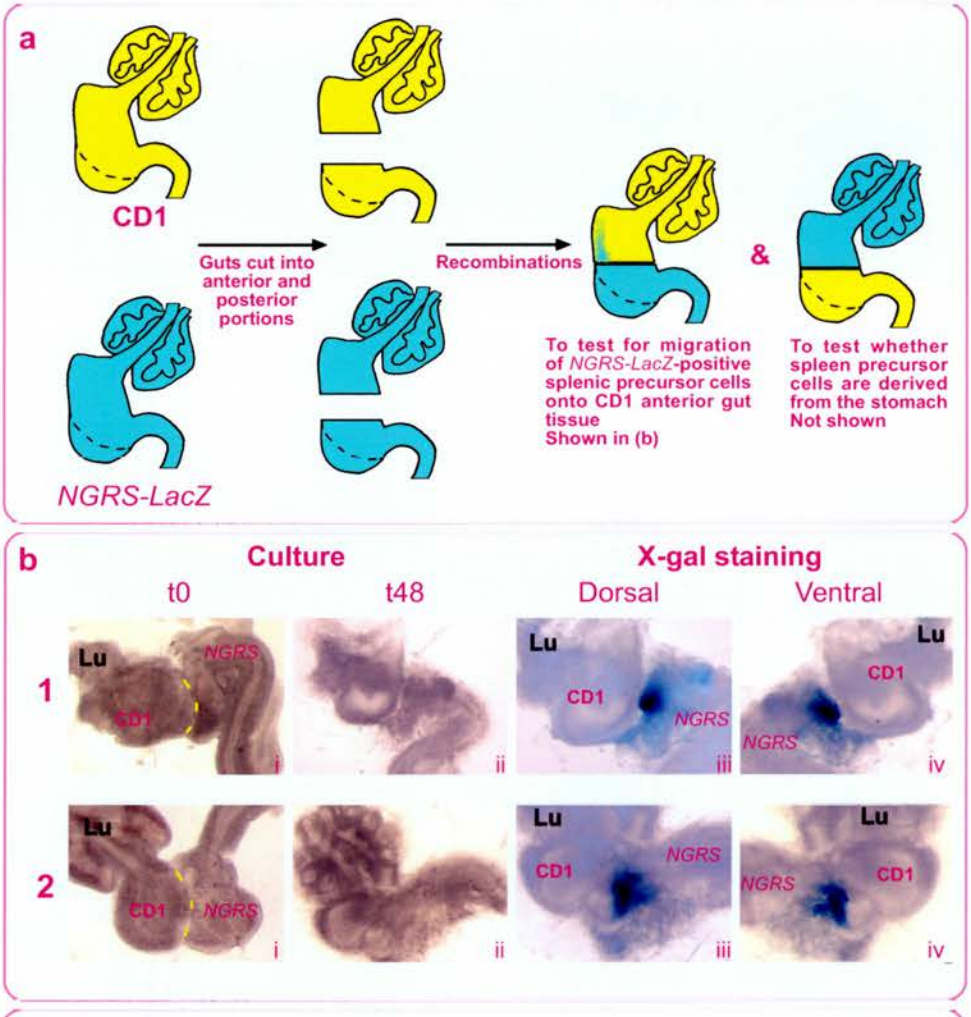

***Figure 4.6* Recombinations between CD1 and *NGRS-LacZ* guts to investigate migration of splenic precursors**

Stage-matched E11.5 guts from CD1 or *NGRS-LacZ* with CD1 matings were recombined as illustrated in (**a**).
a) CD1 guts are shown in yellow, *NGRS-LacZ* guts in blue. Recombinations of transgenic posterior gut portions with CD1 anterior gut portions were performed to investigate whether splenic precursors (marked by *NGRS-LacZ* expression) would migrate towards the anterior stomach from the splenic mesenchyme. The reciprocal recombination (CD1 posterior gut with transgenic anterior gut) was also performed for each gut pair, to test whether spleen precursors are derived from the stomach, but is not presented in the examples shown in (**b**).
b)Two examples of recombinations. Explants were stained with X-gal after 48 hours in culture. Migration of transgenic splenic precursors onto the CD1 anterior gut tissue was not observed.
Culture images were taken at 5x magnification, stained images at 8x. **Lu**: lung buds

4.5.2.2 Spleno-pancreatic mesenchyme recombinations

A refinement of the previous experiment was performed in a separate set of cultures: isolated *NGRS-LacZ* spleno-pancreatic mesenchyme was used instead of a larger posterior gut portion. The endogenous mesenchyme was removed from the CD1 guts, and the *NGRS-LacZ* mesenchyme used to replace this (illustrated in **Figure 4.7a**). The premise of this experiment was as before: if splenic precursor cells in the splenic mesenchyme have migratory potential, then they may move onto the CD1 gut. Once again, lack of spleen development on the mesenchyme-less *NGRS-LacZ* guts would provide evidence against stomach derivation.

Matings were set up as before, and an equal number (seven) of E11.5 CD1 and *NGRS-LacZ* guts were prepared for culturing. The two gut components (transgenic spleno-pancreatic mesenchyme and CD1 gut with the analogous mesenchyme removed) were recombined and cultured on Matrigel for 48 hours. The mesenchyme-less transgenic guts and the CD1 mesenchyme were retained and cultured separately.

Both the recombined CD1 stomach + *NGRS-LacZ* mesenchyme and the mesenchyme-less *NGRS-LacZ* stomachs grew well and appeared healthy throughout the culture process. Conversely, the isolated CD1 mesenchymes – which were not in contact with stomach tissue - either did not appear to undergo any growth (2/7) or, more commonly, deteriorated markedly during culture (5/7).

Three of the seven recombinations exhibited *LacZ* expression; two examples are provided in **Figure 4.7b**. In the first, the recombination was stained in the donor transgenic mesenchyme, but no cells from this tissue had migrated onto the recipient CD1 gut (**Figure 4.7b 1 iii-iv**). Staining of the mesenchyme-less *NGRS-LacZ* gut showed expression was retained in the pyloric sphincter but that all of the spleno-pancreatic mesenchyme had been successfully removed (**Figure 4.7b 1 vii-viii**). No spleen formation was detected, again suggesting that contribution from the splenic mesenchyme is required and that derivation of *NGRS-LacZ*-expressing splenic cells from the stomach does not occur.

In the second recombination shown (**Figure 4.7b 2**) some stained tissue appeared to extend from the *NGRS-LacZ* mesenchyme onto both the CD1 stomach

and duodenum (asterisked on **Figure 4.7b 2 iv**). This may have been due to one of two things: firstly, the transgenic mesenchymal cells may have indeed migrated onto the CD1 stomach or, alternatively, this effect may be due to non-migratory effects such as the initial positioning or non-specific growth of the *NGRS-LacZ* tissue. The presence of stained cells on the CD1 gut is more noticeable on the ventral face – as opposed to the dorsal side where spleen development normally occurs - supporting the notion of random growth. The potential for directed migration of splenic precursors thus does not appear to have been demonstrated.

Not all of the spleno-pancreatic mesenchyme was successfully removed from the *NGRS-LacZ* gut in the second recombination shown (**Figure 4.7b 2 v-viii**). A small piece of the anterior splenic mesenchyme can still be seen attached to the stomach at t0 (arrowed), and by t48 this had apparently contributed to a structure reminiscent of the anterior tip of the spleen – a phenomenon revisited in **Section 4.7**. As residual mesenchyme could be seen at t0, this is not viewed as support for the stomach derivation hypothesis.

In the final recombination (not shown), transgene activity was detected in the pyloric sphincter region of the *NGRS-LacZ* gut and yet not in the removed recombined mesenchyme. This may be explicable by the small amount of mesenchyme transplanted, and its subsequent poor heath and growth.

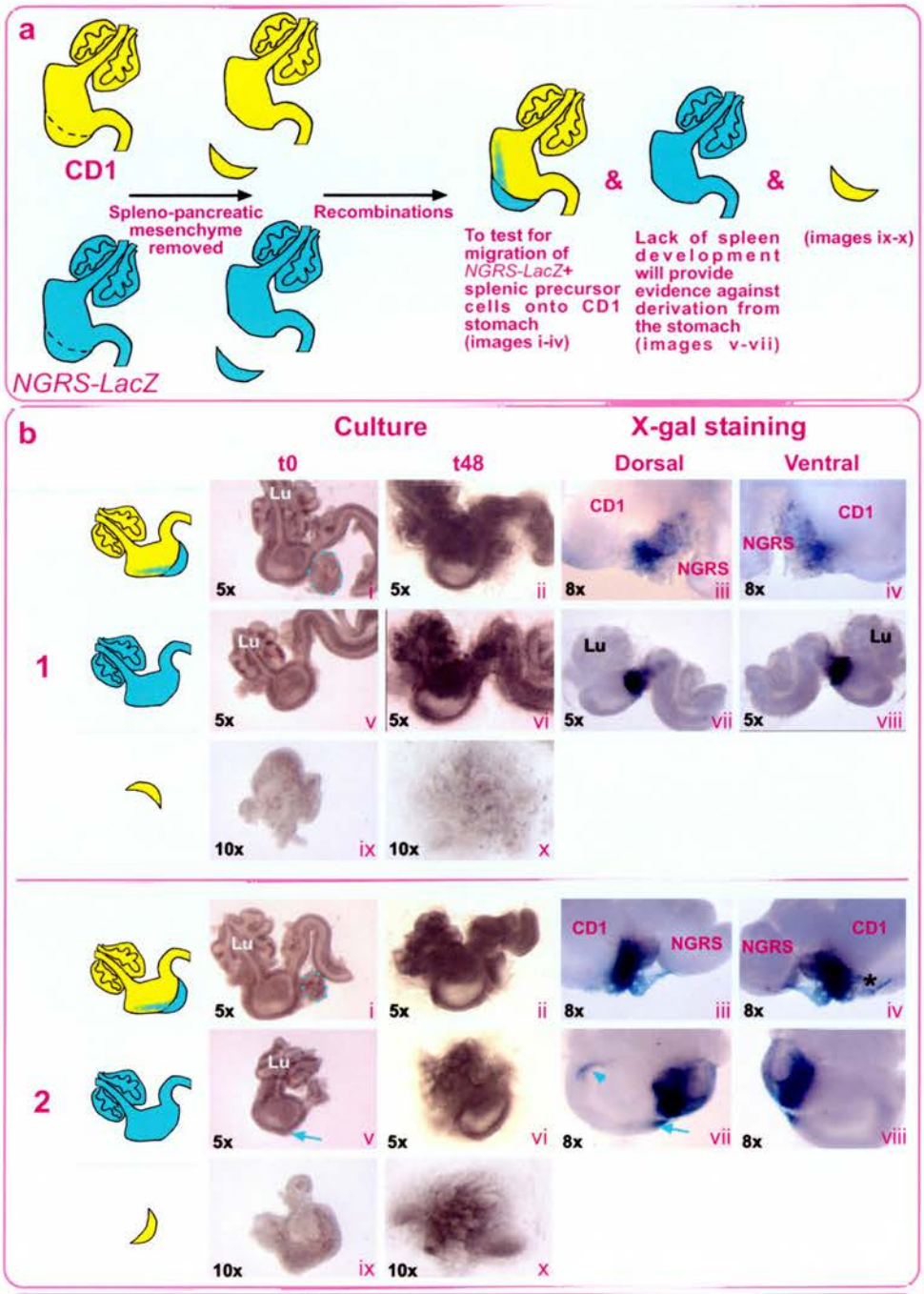

Figure 4.7 **Spleno-pancreatic mesenchyme recombinations to examine migration of transgenic splenic precursor cells**
a. Schematic of experimental strategy. CD1 guts are in yellow, *NGRS-LacZ* guts in blue. **b**. Two examples of recombinations. The transplanted transgenic (*NGRS-LacZ*) mesenchyme is outlined with a dotted blue line. The stained cells observed on the CD1 gut tissue in **recombination 2** (discussed in the main text) are marked with a **black asterisk**. The splenic mesenchyme left attached to the *NGRS-LacZ* gut (again, discussed in the text) is marked by a **blue arrow**, and the resulting spleen development by a **blue arrowhead**. Magnifications at which images were obtained are in the bottom left of each image. **Lu**: lung buds

4.6 An inhibitory signal from the posterior stomach?

4.6.1 Preliminary evidence from physical obstruction experiments

The foil barrier was only correctly positioned in two of the three *LacZ*-positive manipulated guts discussed in **Section 4.5.1**. The foil was inserted in too posterior a position in the third explant, such that X-gal stained cells were found anterior to the foil at t48. This explant was thus of no use in addressing the models outlined in **Section 4.5**. It did, however, provide an interesting result: spleen development - or at the very least the presence of transgene-expressing cells – extended up to a far more anterior level of the stomach and was greatly increased compared to that in non-damaged explants (marked in red in **Figure 4.8 iv, vi**). The outline of the "spleen" structure also seemed to extend slightly beyond that marked by *LacZ* expression. In addition to the spleen-like expression, a crescent of transgene-expressing cells was also present anterior to the foil.

One possible explanation for the apparently advanced spleen development was that the gut had been disrupted such that the anterior-most splenic mesenchyme remained in contact with the stomach whilst being freed from connections with more posterior gut tissue (posterior to the barrier). This raises the possibility of an inhibitory signal or physical anchoring from/by the posterior stomach which "holds back" spleen development, providing tight control during normal development. Additional culture experiments were thus performed to investigate this serendipitous finding; these studies are presented in the next section.

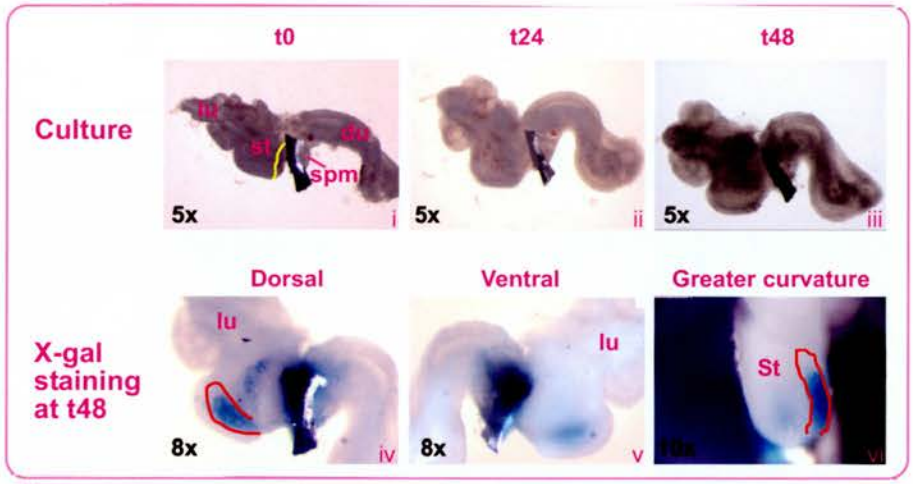

Figure 4.8 **Separation of the anterior and posterior spleno-pancreatic mesenchyme appears to cause advanced spleen development**

The spleno-pancreatic mesenchyme is outlined in **yellow**. Some mesenchyme remained anterior to the foil and appeared to contribute to an X-gal stained spleen structure by t48 (outlined in **red**); this "splenic" tissue was far more developmentally advanced than those in intact explants. The final image is taken from above the greater curvature. Magnifications at which images were obtained are at the bottom left of each image.
lu: lung buds, **st**: stomach, **spm**: spleno-pancreatic mesenchyme, **du**: duodenum

4.7 Investigating an inhibitory effect of the posterior spleno-pancreatic mesenchyme on spleen development

The potential inhibitory role of the posterior spleno-pancreatic mesenchyme was investigated by attempting to separate the anterior (putative splenic) mesenchyme from this negative influence. Separation was achieved by two methods: 1) by making **incisions** (**Sections 4.7.1**) and 2) by **dividing** (bisecting) (**Section 4.7.2**) guts in the spleno-pancreatic mesenchyme. The manipulations were performed across three separate culture experiments; the explants grew well on all occasions and were X-gal stained after 48 hours in culture on Matrigel.

4.7.1 Releasing inhibition: incisions

An incision was made in the spleno-pancreatic mesenchyme of eight guts, three of which stained. No tissue was removed in this process, and so the only factor under investigation was the loss of physical contact between the two gut regions. Spleen development was observed in all three stained explants; stained cells extended as a column out from the spleno-pancreatic mesenchyme *NGRS-LacZ* domain towards the anterior stomach. Images of two of the stained guts are shown in **Figure 4.9**. The third gut generally stained poorly, though spleen development was still marked (data not shown).

The extent of spleen development in **explant 1** was greater than that seen in any intact explant (n=13) examined during the course of the studies in this chapter, and was more akin to that seen *in utero*. Spleen development in **explant 2** was also more pronounced than in intact guts. The observed spleen development was not explicable by developmental stage, as the two depicted guts were no more advanced at t0 than in other experiments. These findings may therefore support the notion of an inhibitory effect of the posterior spleno-pancreatic mesenchyme from which the

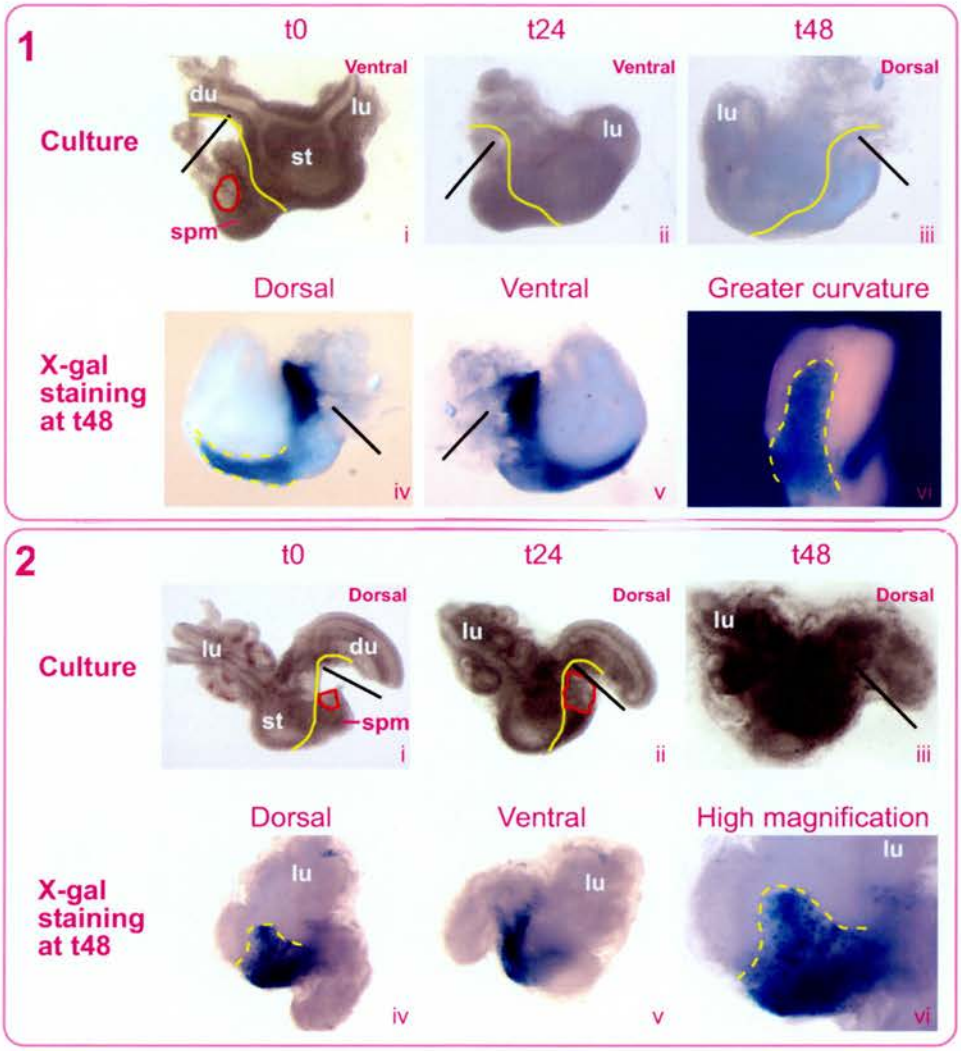

Figure 4.9 **Releasing inhibition: Incisions**

Disruption of the E11.5 spleno-pancreatic mesenchyme with an incision (**black line**) results in dramatic spleen development after 48 hours in culture. The boundary of the spleno-pancreatic mesenchyme with the stomach in the unstained explants is indicated by a **solid yellow line**; the pancreatic bud is outlined in **red**. The putative spleen tissue is outlined with a **dotted yellow line** in the stained images. The images in (**1**) are at 8x magnification, bar **vi** which was obtained at 10x. The images in (**2**) were taken at 5x, with the exception of **vi** which is at 10x.
lu: lung buds, **st**: stomach, **spm**: spleno-pancreatic mesenchyme, **du**: duodenum

splenic mesenchyme can be freed by physical manipulation. However, the numbers analysed are low and so can only be treated as preliminary data.

4.7.2 Releasing inhibition: division

Nine gut explants were completely divided into two portions. Variations were made on the level of the cut so that information could be extrapolated on where a spleen "anchor" signal might reside and also on how much spleno-pancreatic mesenchyme is required for spleen development. The bisection levels are indicated on the gut illustrations included in **Figure 4.10**. Both portions of the severed guts were retained and cultured in separate wells. All tissue remained healthy, and was cultured for 48 hours.

Six of the nine explants stained with X-gal; staining patterns for all six are presented in **Figure 4.10**. One explant (**explant 1**) exhibited spleen development akin to that seen in the incised **explant 2** described in the previous. However, a novel staining pattern was found in four of the other guts (with **explant 2** in **Figure 4.10** providing a pattern intermediate between the two). In these four guts (**explants 3, 4, 5, 6**), a faint trail of stained cells could be seen leading from the main patch of mesenchymal staining; at the end of this trail – at the anterior of the stomach – was a patch of stained cells in a position and shape reminiscent of the anterior of the E12.5 spleen (yellow asterisks in **Figure 4.10 3iii, 4ix/x, 5xi/xii, 6**). The remainder of each of these explants was certainly not representative of an E12.5 gut, and thus it would appear that precocious spleen development may have occurred as a consequence of removing the posterior tissues (duodenum, pancreatic buds, and associated posterior spleno-pancreatic mesenchyme). This lends credence to the idea of a posterior stomach/mesenchyme inhibitory effect.

It is difficult to draw conclusions on what influence the anterior-posterior level of bisection has on spleen development from the limited number of guts examined. A general trend seemed to be that removal of only the most posterior part of the spleno-pancreatic mesenchyme is required for the novel pattern of advanced "spleen" development. However, this is tentative.

As a note in proof, it should be stated that a stained "precocious spleen leading edge" was also observed in two other guts following removal of the most posterior spleno-pancreatic mesenchyme. These are not presented, as the posterior halves were used in unrelated experiments. "Precocious" development was also observed in one of the recombinant experiments described in **Section 4.5.2**, in which some splenic mesenchyme was left attached to the anterior transgenic gut portion (e.g. blue arrowhead in **Figure 4.7b 2vii**). This type of development was not, however, seen when all of the splenic mesenchyme was successfully removed (e.g. **Figure 4.7b 1vii**), indicating that the blue cells seen on the anterior stomach are derived from the spleno-pancreatic mesenchyme and not the stomach.

4.7.3 Releasing inhibition: conclusions

The data presented in this section is derived from a limited number of explants as a consequence of the time required for each experiment and the unpredictability of which guts will be transgenic and/or grow well. Nonetheless, the initial findings support the existence of a posterior spleno-pancreatic mesenchymal "anchor" effect. The novel pattern of advanced anterior "spleen" development reported in this section has not been observed in any intact guts (n=13). The supposition is thus that the posterior spleno-pancreatic mesenchyme exerts a negative, restraining effect on spleen development – an effect presumably necessary for regulated growth during normal development. Physical separation from this "anchor" effect may allow precocious "spleen" development in culture.

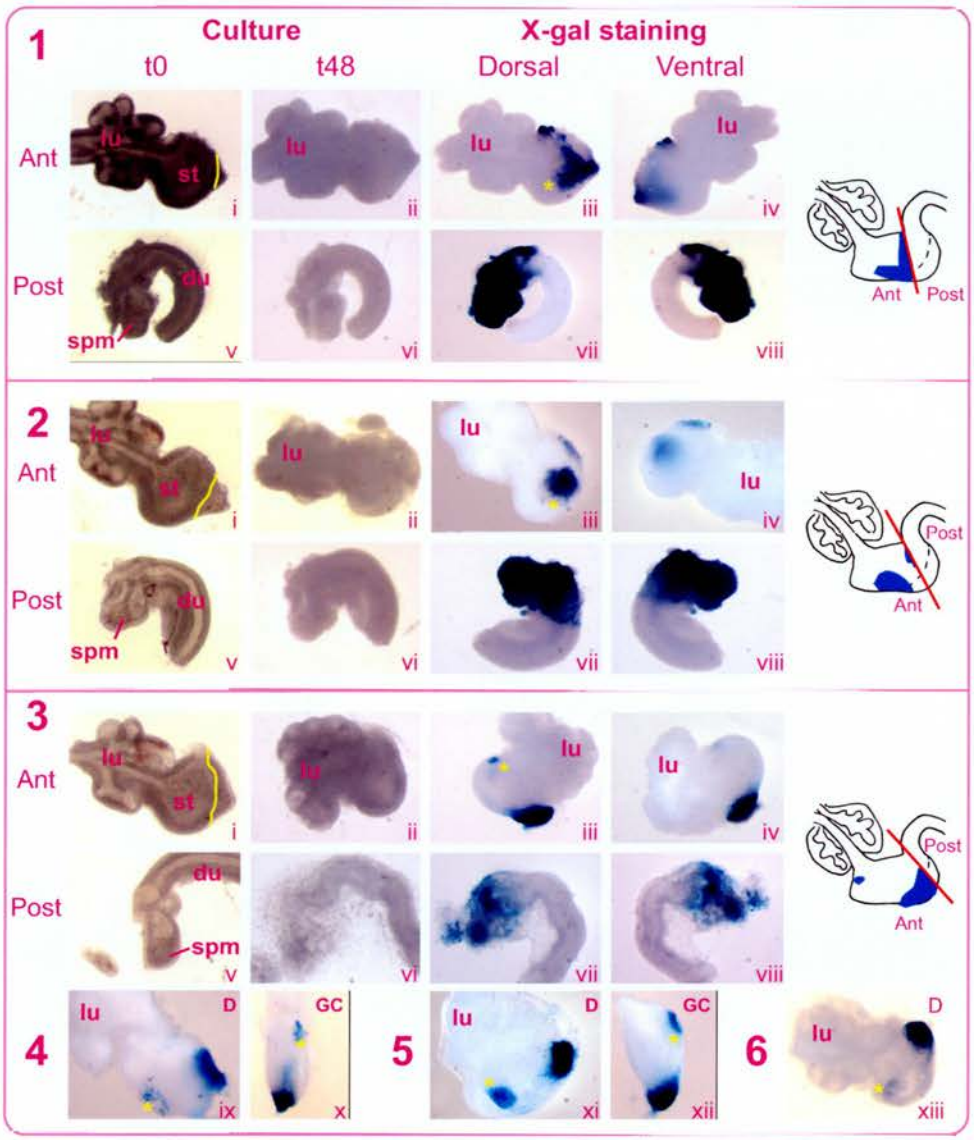

Figure 4.10 **Releasing inhibition: Division**

E11.5 *NGRS-LacZ* gut explants were cut at a number of levels (**1, 2, 3/4/5/6**) within the spleno-pancreatic mesenchyme in an attempt to release the splenic mesenchyme from the proposed inhibitory effect of the more posterior tissue. The resulting "spleen" development was greater than that in intact guts, supporting such an effect.
The third division level produced a novel staining pattern: an apparently precocious "spleen" leading edge (anterior tip). Four explants are presented for the third division level (**explants 3, 4, 5, 6**). Only stained images are shown for **explants 4, 5, & 6**. The views of the greater curvature for **4 & 5** (images **x, xii**) emphasise the absence of staining from the main body of the spleen; only the leading edge (anterior tip) of the spleen is stained. The **red lines** on the gut illustrations indicate where explants were bisected. The observed X-gal staining patterns are marked in **blue** on the illustrations. The boundary of the spleno-pancreatic mesenchyme with the stomach is indicated by a **solid yellow line** in the t0 images. The putative spleen tissue is indicated by a **yellow asterisk** on the stained explants.
D: dorsal, **GC**: greater curvature; **lu**: lung buds, **st**: stomach, **spm**: spleno-pancreatic mesenchyme, **du**: duodenum

4.8 Investigating the existence of a chemoattractant in the anterior stomach

Between E11.5 and E12.5 of *in utero* mouse development, the spleen undergoes a transition from a clump of mesenchyme at the dorsal posterior aspect of the stomach, to an elongated column of tissue extending up to the anterior stomach. Spleen development in culture does not progress as dramatically, but certainly begins this transition. The progress of spleen development towards the anterior stomach in culture is apparently accelerated by separation of the splenic mesenchyme from the more posterior mesenchyme or gut tissues.

Migration seems the most likely mechanism for elongation of the spleen towards the anterior stomach. This raises the question of how spleen precursors 'know' where they should go. The existence of a chemoattractant at the anterior tip of the stomach is an attractive idea to investigate. The anterior limit (leading edge) of the spleen becomes situated towards the anterior of the dorsal face of the stomach by E12.5 of normal development. Despite the apparently precocious nature of the spleen development observed in the manipulated gut explants in **Section 4.7.2** - and, by definition, the artificial nature of these manipulations - the leading edge of the spleen was always located in the correct position. This implies that the information required to correctly position the spleen is contained either in the anterior stomach or in the splenic leading edge itself. The latter is unlikely, as external cues would be necessary. Most logically the information would take the form of a signal to which the splenic cells can "home" to – a chemoattractant. Cells at the leading edge of a tissue can become polarised in the direction of chemoattractants and commence movement up a chemoattractant gradient – chemotaxis (reviewed in (Firtel and Chung, 2000)). The role of chemoattractants in development has been well documented, for example that of FGF10 in lung morphogenesis, as shown in explant culture studies (Park et al., 1998b). FGF10 also acts in the gut as a chemoattractant for cecal epithelium, as shown in cecal explant cultures (Zhang et al., 2006). Explant culture could therefore provide an ideal system in which to investigate spleen chemotaxis; experiments were thus undertaken and are reported in this section.

The existence of a chemoattractant signal in the E11.5 anterior stomach was investigated by co-culturing intact CD1 guts alongside stage-matched *NGRS-LacZ* gut tissue: either a) guts with the anterior stomach removed (**Section 4.8.1**), or b) the spleno-pancreatic mesenchyme alone (**Section 4.8.2**). The rationale was that if splenic precursors do migrate towards an anterior stomach chemoattractant signal then, in the absence of an endogenous anterior stomach, *NGRS-LacZ*-expressing splenic cells may migrate towards and perhaps onto the CD1 anterior gut.

One litter each of E11.5 CD1 and *NGRS-LacZ* embryos were removed from uteri simultaneously. Embryos were stage-matched, and the guts dissected out. An equal number (eight) of CD1 and transgenic guts were recovered. Four of the *NGRS-LacZ* guts were divided such that they were devoid of an anterior stomach region; the final four guts were separated into the spleno-pancreatic mesenchyme alone and the remainder of the explant. All gut tissues were retained and cultured to confirm that the spleen cannot form without contribution from the spleno-pancreatic mesenchyme, and thus provide further evidence against derivation of the spleen from the stomach.

4.8.1 Co-culture of CD1 guts with NGRS-LacZ posterior gut portions

One of the four co-cultures displayed *LacZ* expression, with staining present in the *NGRS-LacZ* posterior gut portion but not in the removed anterior gut portion or on the CD1 gut (**Figure 4.11a**). The existence of a spleen chemoattractant in the anterior stomach was thus not supported, as no stained cells were detected on the CD1 gut. However, the lack of staining in the removed anterior *NGRS-LacZ* gut portion (data not shown) confirmed that *NGRS*-marked splenic precursors are not endogenous to this region at E11.5, once again disputing the stomach derivation hypothesis. The staining in the posterior *NGRS-LacZ* gut portion was not, however, as expected; whilst normal pyloric sphincter expression was present, the spleno-pancreatic mesenchyme was devoid of staining. The reason for this loss is unknown,

though a similar effect was noted in an isolated *NGRS-LacZ* spleno-pancreatic mesenchyme in the recombination experiments reported in **Section 4.5.2.2**.

4.8.2 Co-culture of CD1 guts with NGRS-LacZ *spleno-pancreatic mesenchyme*

Three of the four *NGRS-LacZ* mesenchyme + CD1 gut co-cultures stained with X-gal; all are presented in **Figure 4.11b**. These studies were performed on filter-discs. The mesenchyme-less *NGRS-LacZ* guts exhibited pyloric sphincter staining (data nor shown) but no spleen development; this again provides evidence against derivation of the spleen from the stomach mesenchyme. The removed *NGRS-LacZ* spleno-pancreatic mesenchymes stained, but cells from these transplanted mesenchymes failed to colonise the CD1 guts, arguing against migration towards an anterior stomach chemoattractant. Of course, the expectation that cells would move onto foreign tissue may have been overly ambitious. Indeed, the two observations outlined below may provide some evidence for movement towards an anterior stomach chemoattractant.

Firstly, whilst cells did not move from the transplanted mesenchyme onto the CD1 guts, the mesenchyme as a whole appeared to move in the direction of the anterior gut (in all three stained and one non-stained co-cultures) as it had a more anterior limit with respect to the CD1 gut by t48 (denoted by black dashed lines in **Figure 4.11b**). It may therefore be that an anterior chemoattractant signal does indeed exist and that this has been demonstrated by the apparent movement of the mesenchymal explants specifically in this direction (movement towards a more posterior point is not observed, and there is no major growth to account for the change in anterior limit). The splenic mesenchyme may therefore move as a tissue rather than as lone cells – a recognised trend in migrational morphogenesis (Lecaudey and Gilmour, 2006). It may also be of course that the mesenchymes simply adhered to the CD1 guts and were pulled along with their growth. Additionally, growth of the pancreatic bud within the *NGRS-LacZ* mesenchymal explant may be responsible for some displacement.

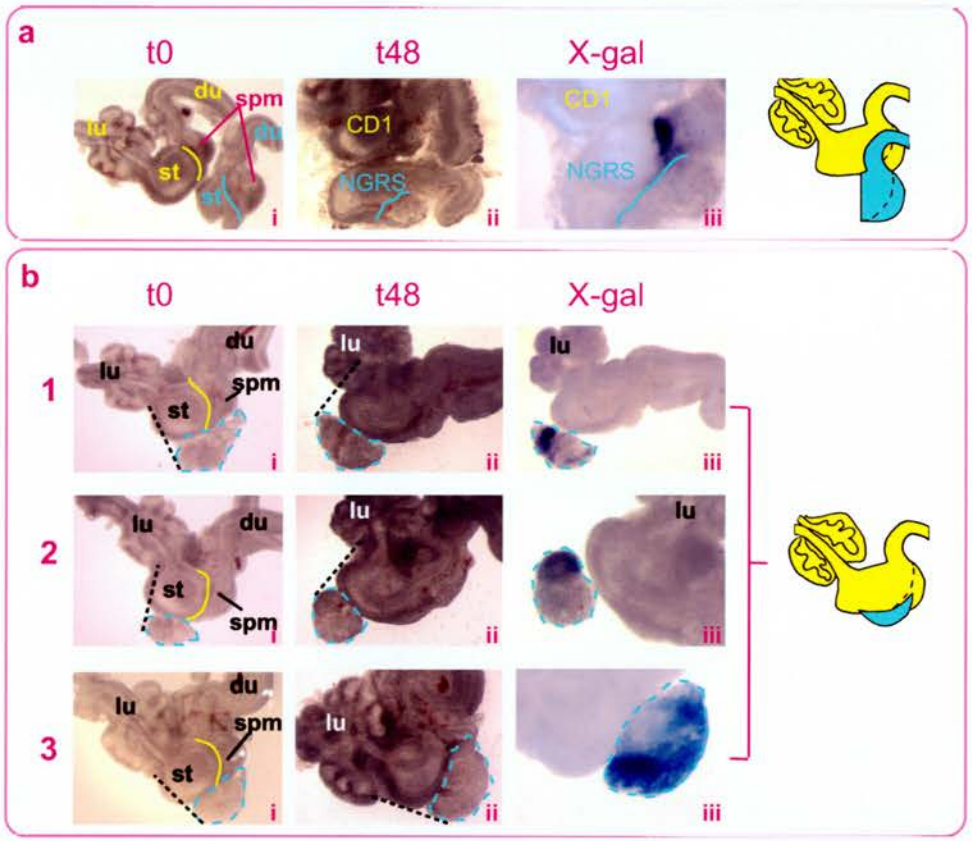

Figure 4.11 **Investigating a chemoattractant at the anterior of the stomach**

CD1 gut explants were co-cultured with *NGRS-LacZ* **a**) posterior gut portions or **b**) spleno-pancreatic mesenchyme (as illustrated) to investigate whether marked splenic precursors would migrate towards and onto the CD1 stomach, in the absence of endogenous anterior stomach signals. This was not demonstrated, though the anterior limit of the transgenic mesenchymes in (**b**) appeared to become located more anteriorly (with respect to the CD1 stomach) by t48 - as denoted by the **black dashed lines**. Note that the positioning of the explants is disrupted during X-gal staining and hence the relative positions differ between the non-stained and stained t48 images.
The boundary of the spleno-pancreatic mesenchyme with the stomach is indicated by a **yellow line** for the CD1 guts, and a **solid blue line** for the *NGRS-LacZ* guts. The isolated *NGRS-LacZ* mesenchymes are outlined by a **dashed blue line**. All images were taken at 5x magnification, bar (**a**) **iii** (10x), (**b**) **2-iii** (8x), **3-iii** (10x).
lu: lung buds, **st**: stomach, **spm**: spleno-pancreatic mesenchyme, **du**: duodenum.

A final observation was that the cells in which the *NGRS* is active are localised to the anterior of the transplanted mesenchymes by t48. Whilst the absence of staining at the posterior end could be due to overgrowth of the pancreatic endoderm (which does not express the transgene), the majority of the transplanted tissue would be expected to stain in the endogenous situation. It is therefore possible that the *NGRS*-marked splenic precursors have migrated towards the anterior end, perhaps in response to a chemoattractant in the CD1 anterior stomach. The *NGRS-LacZ*-marked cells could therefore be responsible for the apparent anterior extension of the mesenchymes, constituting a migratory "leading edge". Leading edges are found at the forefront of migratory groups of cells, and are thought to contain the cells which are competent to respond to extrinsic cues such as chemoattractants (Lecaudey and Gilmour, 2006). These leader cells can then instruct the cells following them to act accordingly. The application of this concept to spleen development is, however, only casual, as the experimental numbers are too low to draw conclusions.

4.9 Discussion

4.9.1 Appraisal of gut culture system

The main concern with explant cultures is whether the observed effects are real - reflecting normal development or genuine responses to manipulation – or are simply artefacts of the experimental procedure. Conditions must therefore be kept constant between studies in order to allow accurate comparison and analysis of results. Experimental artefacts may be a result of suboptimal conditions (oxygen concentration, temperature, serum, and media) or of mechanical damage to the explants. This latter problem is even more common when culturing early gut explants as opposed to, for example, the externally placed limb buds. Careful gut dissection is time-consuming and must be balanced against the need for rapid entry of tissue into culture. The numbers of experimental and control explants in - and thus the statistical

significance of - gut culture studies may therefore be less than in other systems, again such as the limb. Nonetheless, the findings presented in this chapter demonstrate that culture of E11.5 mouse guts provides a good system in which to study and manipulate spleen development.

Cultures were performed on filter-disc or Matrigel supports; an issue with both methods is that after 48 hours the explants are flat and retain little three-dimensional morphology (though Matrigel reduced this effect slightly). A potential solution to this problem could be free-floating cultures. However, free-floating cultures may not offer any advantage for spleen development studies, as growth has been most noticeable in the intestines in published accounts[28], with little growth observed in the stomach region. Such cultures are also obviously not of any use when performing recombination experiments.

In conclusion, the experimental system used was suitable for the objectives and should permit future investigations into spleen development. A major aim now is to adapt this system for live imaging, as splenogenesis is a rapid and dynamic process.

4.9.2 Mechanisms of spleen morphogenesis: migration

Directed cell movement is central to many morphogenetic processes (Lecaudey and Gilmour, 2006). The studies presented here support the notion of posterior-anterior "migration" of splenic precursors from the spleno-pancreatic mesenchyme versus derivation in a posterior-anterior wave from the stomach. No spleen development was observed in stained explants totally devoid of spleno-pancreatic mesenchyme (n=10 across all experiments), nor did it occur anterior to a barrier placed between the stained spleno-pancreatic mesenchyme and stomach (n=2).

It should be noted at this point that expression of the *NGRS-LacZ* transgene in the spleno-pancreatic mesenchyme has been regarded as being synonymous with

[28]E11.5 guts (oesophagus to large intestine) (Natarajan et al., 1999)
E10.5 whole guts (Pitera et al., 2001)

splenic identity in these studies. There is thus a danger that observations have been made not of spleen cells *per se*, but rather of *NGRS* activation. It could therefore be argued that specified mesenchymal splenic precursors might already exist along the AP axis of the stomach, and that subsequently a posterior-anterior wave of *NGRS-LacZ* activity occurs. However, this does not seem likely given the observed correlation of *NGRS-LacZ* expression and spleen development from E10.5 onwards (summarised in **Chapter 2**), and general histological observations of stained guts between E11.5-12.5. Subsequent to these studies being performed, clonal analysis of randomly tagged cells lead to the observation that the mesenchymal cells of the spleen are not derived from the underlying stomach mesenchyme (Dr Marit Boot, unpublished data). Migration is thus assumed, though it would be certainly worthwhile – if not absolutely necessary - to repeat the experiments presented in this chapter using a second spleen marker (*Hox11* for example).

4.9.3 Three mechanism hypotheses

Three potential mechanisms for the regulated control of spleen development can be proposed following analysis of the results presented. It is predicted that these mechanisms would not be mutually exclusive and, indeed, would have a combinatorial effect to allow tight regulation. They are as follows:

1) **Migratory potential resides in the leading edge (anterior tip) of the spleen**
2) A restraining **"anchor" effect from the posterior spleno-pancreatic mesenchyme** acts on the anterior splenic mesenchyme
3) A **chemoattractant exists at the anterior of the stomach** and so the spleen migrates or develops in this direction

Each of these points is discussed in the following sections.

4.9.3.1 The leading edge of the spleen has migratory potential

The evidence outlined points to the spleno-pancreatic mesenchyme as the source of splenic precursor cells and implies some role for migration; it is unclear, however, whether the spleen is entirely constituted of cells migrating out from the mesenchyme or whether other mechanisms (such as proliferation) are also involved in elongation of the spleen towards the anterior stomach. One possibility is that the ability to migrate resides in the leading edge (anterior tip) of the spleen, which may also undergo proliferation. The concept of a leading edge is well-founded in developmental biology, and has been implicated in a range of developmental processes (Lecaudey and Gilmour, 2006). In a generalised model, cells form a cohesive organised group, the leading edge of which elongates in the direction of migration; at the rear of this migratory group lays the trailing edge, which displays a lack of adhesion. Only cells in the leading edge are thought to be responsive to extrinsic cues (such as chemoattractants); the leading cells may then instruct the lagging cells in how to act.

Applying the above concept to spleen morphogenesis, the leader cells would be located in the anterior limit of the splenic mesenchyme and would forge forward, colonising a path towards the anterior limit of the stomach. The anterior connection of the spleen primordium with the stomach shown in **Figure 4.1** may play a role in this. The spleen cells posterior to this leading edge would be instructed to follow, and would also need to sever their physical connection with the stomach to create the gap normally found between the stomach and majority of the spleen. Proliferation may also occur concomitantly with migration, given the relatively larger size of the E12.5 spleen versus the E11.5 splenic mesenchyme. Whether the leading edge would contain the youngest cells, with the older cells forming the main body of the spleen, or whether instead the oldest cells would form this edge and proliferate to populate the lagging bulk of the spleen is unclear. An important future direction is thus to examine the dynamics of cell proliferation and death during this period of spleen development, by using markers for these processes in culture. Clonal analysis could also be a valuable tool.

The presence of a patch of *NGRS-LacZ*-marked "splenic" tissue at the anterior tip of the stomach, without concomitant spleen formation posterior to this, in the manipulated guts is certainly reminiscent of the above description of a migratory leading edge. This patch of expression was in some cases separated from the main splenic mesenchyme, and in other cases was connected by a faint trail of blue cells. In non-cultured guts, however, the spleen is marked throughout by expression of the *NGRS-LacZ* transgene, regardless of how far up the stomach spleen development has progressed. One possible explanation for the lack of staining between the "leading edge" and spleno-pancreatic mesenchyme in the cultured guts is that splenic precursors destined to populate the mid-section were left in the posterior part of the gut following cutting/division of the explant. This would imply that the splenic mesenchyme already possesses positional identity at E11.5, with cells destined to adopt a specific AP position along the spleen. The alternative – though not necessarily mutually exclusive – explanation is that the potential to migrate up to the anterior stomach is the property of only a subgroup of splenic precursors, which reside in the leading edge. This is certainly a recognised phenomenon: the ability to migrate is located in the tip of *Dictyostelium* slugs (migrating bodies of cells), and separation of the tip from the main slug body results in continued migration of the tip and an immobilised collection of body cells (Dormann and Weijer, 2001). A pattern very similar to this was observed in the studies presented.

During normal spleen development the leading edge cells might also proliferate to fill the void posterior to them; coupled migration and proliferation would ensure that the leading edge moves in a controlled manner such that the region posterior to it is always populated. Release of these migratory cells from the inhibitory influence of the posterior mesenchyme may therefore not only permit too rapid a migration towards the anterior stomach, but also decouple migration from proliferation to populate the main body of the spleen. This inhibitory influence is discussed in the next section.

A final point to note is that the putative splenic mesenchyme was demonstrated to form a structure reminiscent of the anterior limit of the E12.5 spleen at an earlier stage in culture than in normal development. The gut explants were taken at E11.5 and cultured for 48 hours, during which time they did not adopt the

physical characteristics of an E12.5 gut. This may therefore suggest that the ability to form a spleen is an innate property of the splenic mesenchyme from at least E11.5. One past hypothesis on spleen development was that a general dorsal pancreatic mesenchyme exists up until ~E13.0 and it is only at this stage that commitment to a splenic fate occurs in a subset of *Hox11*-expressing cells, in response to a second spleen development signal (Kanzler and Dear, 2001)[29]. Whilst the authors of that study largely dismissed the possibility of late commitment to a splenic fate, the data presented here further rejects the theory.

4.9.3.2 Posterior anchoring by the spleno-pancreatic mesenchyme

A restraining "anchor" effect appears to be exerted by the posterior spleno-pancreatic mesenchyme on the more anterior, migratory portion of this tissue. The existence of an inhibitory effect is suggested by the observations that removal or disconnection of the posterior-most mesenchyme permits apparently accelerated development of an anterior "spleen leading edge" structure. The "anchor" may therefore be required during normal development to ensure tight control of the posterior-anterior progression of spleen development. It is perhaps of significance then that the spleen and pancreatic tissues fail to correctly separate in the asplenic *Bapx1*$^{-/-}$ mutant. The splenic mesenchyme remains in prolonged contact with the pancreatic mesenchyme and subsequently fails to develop into a spleen (Asayesh et al., 2006).

The nature of the "anchor" is unknown, but a couple of possibilities exist:

1) ***Signalling*** from the posterior mesenchyme (via an unknown pathway) may prevent precocious spleen development during normal morphogenesis. Accelerated "spleen leading edge" development only occurred following

[29] This was one possible explanation for the findings that *Hox11*$^{-/-}$ embryos initiate spleen development and that this does not arrest until ~E13.0, implying *Hox11* is not required for initial spleen development (Kanzler and Dear, 2001). ~E13.0 is also the stage at which *Hox11*$^{-/-}$ cells fail to aggregate with and thus become excluded from chimaeric spleens, most probably due to lack of some cell adhesion molecule (Kanzler and Dear, 2001). It was thus postulated that *Hox11*$^{-/-}$ mesenchymal cells might not be competent to respond to a second signal and hence fail to aggregate with wild type splenic cells.

complete removal of posterior spleno-pancreatic mesenchyme tissue and was not observed in guts which were simply cut. This could imply that a signal is responsible for the inhibition and that this can still act across the cut surface.

2) The inhibition could alternatively be due to ***physical*** retention of the splenic mesenchyme by the more posterior mesenchyme. An incision might not release the splenic mesenchyme from such retention as fully as bisection, again fitting the trend outlined above. A physical anchor could act very simply, physically preventing the spleen from advancing up the stomach at too rapid a rate. It could also act in a more elegant way, as mechanical stress has been shown to activate gene expression during *Drosophila* foregut development (Farge, 2003; Scott and Stainier, 2003) and mechanical forces are known to be central to tissue migration (Lecaudey and Gilmour, 2006). The stress exerted on splenic precursor cells by being physically "restrained" might therefore regulate gene expression such that spleen development progresses in a controlled manner. Mechanical induction of gene expression in the *Drosophila* embryo can be mediated through β-catenin, which also plays roles in cell adhesion (Scott and Stainier, 2003). This is particularly interesting given my findings that the β-catenin (canonical) Wnt signalling pathway is active in the developing spleen (presented in **Chapter 5**).

4.9.3.3 A chemoattractant at the anterior of the stomach

The existence of a chemoattractant in the anterior stomach, to which spleen cells "migrate" was postulated as this would be an obvious explanation for how the spleen leading edge always arrives at the same location, both during normal development and when "precocious" development occurs in manipulated explants. The assays used to investigate such a signal – migration of *NGRS-LacZ*-marked spleen cells onto CD1 guts – did not provide evidence for this idea. This is not to say that a chemoattractant does not exist, however, as the concept that cells might migrate across a junction and colonise a gut from a different genetic strain to reach a foreign chemoattractant may be overly optimistic. Cells also move more commonly

as large units or tissues rather than as individuals (Lecaudey and Gilmour, 2006). A variation on these studies is now being performed in the lab, in which only the anterior stomach region from a CD1 gut will be placed alongside the lesser curvature of a posterior *NGRS-LacZ* gut portion. If a chemoattractant signal does exist, then it is hoped that cells from the *NGRS-LacZ* spleno-pancreatic mesenchyme will alter their migration path from along the greater curvature, and instead traverse the stomach to reach the foreign signal at the lesser curvature. Migration across the host stomach seems more likely than moving onto a foreign tissue.

Migration of gut cells is certainly known to be possible in culture. Fu and colleagues added GDNF (Glial cell Derived Neurotrophic Factor) to their culture medium, inducing marked (*LacZ*-positive) enteric neural crest cells to migrate through the intestine and out onto a Millipore filter, from where they were collected and counted by flow cytometry (Fu et al., 2004). This demonstrates the potential to use a suitable pro-migratory factor to induce migration in culture, and that cells can indeed migrate out of explanted gut tissue onto an artificial substratum.

The nature of the proposed chemoattractant is unknown. Chemoattractants can take the form of signalling pathway components which induce changes in the cytoskeleton of cells at the leading edge, thus facilitating alteration of cell polarity and subsequent chemotaxis (Chung et al., 2001). However, the chemoattractant itself is not the only component of the migration tool box which lends itself to further investigation. Factors involved in other aspects of migration could be focused upon. For example, cells must alter their adhesion to their neighbours to allow passage through the tissue, and this conversely includes increasing adhesion to other cells involved in the movement, most commonly using cadherins (Grapin-Botton and Melton, 2000). Migrating cells must also be able to degrade the surrounding extracellular matrix by secreting suitable enzymes, such as metalloproteinases (Grapin-Botton and Melton, 2000). Appropriate cell movement is dependent upon orientation signals and, although these mainly take the form of chemoattractants, endogenous electric fields are also known to elicit directional cell migration (galvanotaxis) (Mycielska and Djamgoz, 2004). Changes in cell polarity and number, and cell-cell contacts are also likely to play roles in migration (Hogan, 1999; Young

et al., 2004). There are thus many further paths of investigation which can be followed in pursuit of the migrating spleen.

4.10 Future work

The use of a culture system in these studies allowed spleen development to be monitored over a 24 or 48 hour time period – a feat not possible *in utero*. A number of interesting observations were made which now need to be confirmed – or otherwise – by increasing the numbers of explants analysed.

A major restriction on these studies was that whilst gross development could be observed, specific visualisation of spleen development required fixing and X-gal staining of the tissue. The next step is thus to adapt the culture system such that live imaging can be realised. A fluorescent protein such as green fluorescent protein (GFP) is an excellent candidate for tagging spleen precursors in explant culture; for an introduction to the use of fluorescent proteins in live imaging see Hadjantonakis et al., 2003 (Hadjantonakis et al., 2003). Tagged cells producing GFP can be visualised whenever required during the culture period, by excitation of GFP with a suitable light source. Thus the movement of marked cells can be visualised without the need to disturb manipulated or recombined guts. GFP has already been successfully used to visualise and measure the speed of neural crest-derived cell migration during hindgut development in explant culture (Young et al., 2004). GFP might also therefore provide the opportunity to examine the migration versus stomach derivation hypotheses outlined in **Section 4.5**. Likewise, movement towards an anterior stomach chemoattractant, and the precocious development of spleen tissue upon removal of a posterior inhibitory signal, could be further investigated using *GFP* in place of *LacZ*.

An obvious strategy would be to use the *NGRS* to drive gut-specific *GFP* expression. As an alternative, there already exists a knock-in of the *GFP* gene into the *Nkx2-5* locus (exon 1) which recapitulates the full *Nkx2-5* expression pattern (Biben et al., 2000). The conferred *GFP* expression pattern is therefore not gut-specific, but in a gut explant culture system this would be irrelevant. A disadvantage of this approach is that mild heart defects occur in a low percentage of the *GFP-*

expressing heterozygotes, variable by genetic background (Biben et al., 2000). *Nkx2-5-GFP BAC* mice also exist, in which *IRES-hrGFP* replaces the first exon and intron of *Nkx2-5* in a BAC containing the *Nkx2-5* coding sequence and all the reported regulatory elements (Chi et al., 2003). The endogenous *Nkx2-5* expression pattern is again marked by GFP, albeit with an absence of tongue expression. Pyloric sphincter and spleen GFP activity is strong in embryos from this line, probably due to insertion of multiple copies of the BAC. More importantly, these two gut expression domains remain separate at E13.5, unlike in the *NGRS-LacZ* mice, which would be an advantage when investigating spleen morphogenesis.

Other spleen development markers, such as *Hox11* and *Wt1*, could also be exploited to drive GFP-based studies. Indeed, a mouse line carrying a knock-in of *GFP* into the *Wt1* locus has been obtained and is to be used in our lab in studies to follow up the findings presented in this chapter. A final strategy would be to use inducible *GFP* expression, to facilitate lineage tracing in culture.

CHAPTER 5

An analysis of Wnt signalling in spleen development

...Or: "Science never solves a problem without creating ten more"

– George Bernard Shaw

5.1 Background to research

A major aspect of the *Bapx1* (*Nkx3-2*)$^{-/-}$ phenotype is the overgrowth of the posterior stomach, with concomitant loss of the pyloric sphincter constriction (Akazawa et al., 2000; Watson et al., 2007). This overgrowth is specific to the region of the stomach which normally expresses *Bapx1*. It is thus tempting to speculate that *Bapx1* loss may permit expression or upregulation of growth factors which would normally not be active in the posterior stomach, leading to disorganised overgrowth. Certainly, Nkx3-2 is known to act as a transcriptional repressor in chick, and transcriptional repression is a general feature of Drosophila *NK* genes (Murtaugh et al., 2001; Smith and Jaynes, 1996). Furthermore, conversion of chick Nkx3-2 into a transcriptional activator produces ectopic *Bmp4* and *Wnt5a* expression in the gizzard (posterior stomach) (Nielsen et al., 2001)[30].

A collaborator – Dr Jacob Hecksher-Sørensen (Hagedorn Research Institute, Denmark) – compared the expression of a number of growth factors between wild type and *Bapx1*$^{-/-}$ posterior stomachs at E11.0 (when the expanded stomach phenotype is first observed). RNA was extracted from two regions: 1) the spleno-pancreatic mesenchyme and 2) the posterior stomach (mesenchyme plus underlying endoderm). Following cDNA synthesis, multiplex RT-PCR was performed for a range of genes. Multiplex RT-PCR uses multiple primer pairs within a single reaction to allow amplification of multiple specific sequences from a sample. The products of this multiplex PCR were analysed by gel electrophoresis and are shown in **Figure 5.1.**

The validity of this technique was demonstrated by the inclusion of primers specific to known Bapx1 targets, thus confirming known expression changes in the *Bapx1*$^{-/-}$ gut: loss of *Hox11* expression from the spleno-pancreatic mesenchyme, loss of *Bapx1* expression from both the spleno-pancreatic mesenchyme and posterior stomach tissues, and loss or downregulation of *Nkx2-5* from both regions. Three factors were novelly shown to be upregulated in the mutant posterior stomach (mesenchyme or endoderm): *Bmp6*, *Wnt3*, and *Wnt8a*. This final results chapter describes my initial investigation into the potential roles of *Wnt3* and *Wnt8a* in the

[30] Though it also produces a thinner stomach muscle layer

Bapx1$^{-/-}$ phenotype, and the subsequent work on Wnt signalling in the developing spleen that evolved from this.

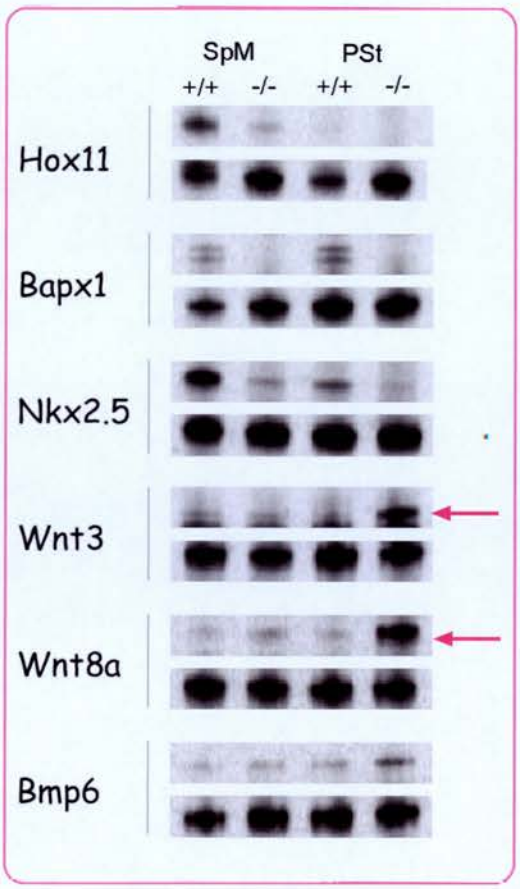

***Figure 5.1* Multiplex RT-PCR for changes in gene expression in the *Bapx1*$^{-/-}$ gut**

Expression of a number of growth factors was compared between wildtype (**+/+**) and *Bapx1*$^{-/-}$ (**-/-**) posterior stomachs at E11.0 by Dr Jacob Hecksher-Sørensen. Two tissues were analysed: spleno-pancreatic mesenchyme (**SpM**), and posterior stomach (**PSt**) (mesenchyme plus underlying endoderm). Shown here is a selection of the results. *Hox11*, *Bapx1* and *Nkx2.5* expression changed as expected (decreased *Hox11* expression in the SpM, loss of *Bapx1* expression in both the SpM and PSt, downregulation of *Nkx2.5* in both tissues), thus providing controls.
Three factors were novelly shown to be upregulated in the mutant posterior stomach (mesenchyme or endoderm): *Bmp6*, *Wnt3*, and *Wnt8a*.

5.2 Wnt signalling

Wnt signalling is one of the major components of the developmental tool box and as such its functions are well-studied. Wnt family members play fundamental roles in an array of key processes across a range of tissues, including cell proliferation, differentiation, migration (adhesion), and polarity. *Wnt* genes are highly conserved between vertebrate species, and encode secreted glycoproteins which signal to neighbouring cells. The murine *Wnt* gene family contains 19 members (Miller, 2002).

Binding of secreted Wnt factors to transmembrane Frizzled (Fzd) receptors activates a signalling cascade, resulting in transcriptional activation of target genes. The events occurring between receptor binding and transcription are best understood for the canonical β-catenin pathway (see (Huelsken and Behrens, 2002) and (Miller, 2002) for a detailed review). Receptor binding triggers a series of interactions involving Dsh and GSK3, amongst others, culminating in stabilisation and nuclear translocation of β-catenin. The subsequent association of β-catenin with TCF/LEF transcription factors leads to activation of target genes.

The concept of a single Wnt signalling "pathway" has in recent years become something of a misnomer as signalling can proceed through at least two non-canonical pathways: the Wnt/Ca^{2+} and the Wnt/JNK[31] pathways (Kuhl et al., 2000; Huelsken and Behrens, 2002; Pandur et al., 2002). The latter pathway exerts its effects on the cytoskeleton as opposed to gene transcription, facilitating cell polarisation within epithelial sheets.

5.2.1 Wnt signalling in the developing gut

Several components of the Wnt signalling pathways are expressed during murine gut development. These expression patterns are summarised in **Table 5.1**. Examples also exist of functional Wnt signalling in the developing gut. A major role of this signalling may be to regulate EM interactions in order to specify regional

[31] Comparable to the planar cell polarity path in *Drosophila*

identity within the foregut. For example, *Wnt1* is not expressed in the pancreas until E15.0, but transgenic misexpression of *Wnt1* from the earliest stages of pancreatic development (under the control of the promoter of the foregut/pancreatic epithelium gene *Pdx1*) causes a transition from a duodenal to stomach phenotype (Heller et al., 2002). The posterior boundary of gastric markers is shifted and the stomach is extended posteriorly: the proximal duodenum is widened and the pyloric sphincter constriction is lost. Pancreatic and spleen development are also aberrant, to the extent that these structures are often absent. This is most interesting as these phenotypes echo those seen in *Bapx1*$^{-/-}$ mice (Akazawa et al., 2000; Watson et al., 2007). There is thus a precedent for misexpression of *Wnt* genes in the spleno-pancreatic region causing inappropriate growth of the posterior stomach. Overexpression of *Wnt5a* in the *Pdx1*-driven assay does not appear to alter tissue identity, but instead causes a reduction in the size of the stomach, spleen, and pancreas (Heller et al., 2002). The pancreatic tissue is also observed to invade the spleen in some cases.

A further example of Wnt signalling directing EM interaction and thus gut patterning is that of mesenchymal Barx1, which regulates specification of the stomach epithelium through inhibition of canonical Wnt signalling in this latter tissue. *Barx1* is expressed in the stomach mesenchyme at E9.5-16.5, and loss of this expression produces a shrunken stomach with disorganisation and infolding of the epithelial lining, resulting in failure of lumen formation (Tissier-Seta et al., 1995; Kim et al., 2005a). The endogenously expressed *Sfrp1* and *Sfrp2* Wnt inhibitor genes are down-regulated in the mutant mesenchyme. The secreted products of these genes are normally responsible for the negative regulation of Wnt signalling in the epithelium, and this inhibition is required for correct epithelial differentiation, following initial activation of the canonical pathway. Similarly, Foxf1- and Foxf2-mediated inhibition of Wnt signalling is necessary for correct intestinal development (Ormestad et al., 2006). Loss of this inhibition results in excessive proliferation and a lack of normal apoptosis, resulting in a range of gut defects. Again, these are examples of inappropriate activation of Wnt signalling leading to defective gut development.

Though no link has yet been shown between Wnt signalling and *Bapx1*, Wnt signalling in *Drosophila* plays a vital role in bap-mediated development of the

midgut (Azpiazu et al., 1996a). Interplay between Hedgehog and Wingless creates differences in *bap* expression within the dorsal mesoderm parasegments: Hedgehog promotes *bap* expression in the anterior part, whilst Wingless suppresses expression in the posterior.

Gene	Stage	Tissue	Reference
Wnt1	E15.0	Pancreatic mesenchyme	(Heller et al., 2002)
Wnt2b (Wnt13)	E8.5	Foregut diverticulum	(Zakin et al., 1998)
	E12.0-17.0	Pancreas	(Heller et al., 2002)
	E12.5	Caecal epithelium	(Burns et al., 2004)
Wnt4	E12.5	Pyloric sphincter, intestinal epithelium, oesophagus (weak)	(Lickert et al., 2001)
Wnt5a	E11.0	Pancreatic epithelium and mesenchyme	(Heller et al., 2002)
	E11.5	Anterior stomach	(Smith et al., 2000a)
	E12.5	Anterior stomach, intestinal mesenchyme	(Lickert et al., 2001)
	E14.5	Tip of anterior stomach	(Lickert et al., 2001)
Wnt5b	E16.5	Oesophageal epithelium	(Lickert et al., 2001)
	E12.0-17.0	Pancreas	(Heller et al., 2002)
Wnt6	E16.5	Oesophageal epithelium	(Lickert et al., 2001)
Wnt7b	E11.0	Pancreatic mesenchyme	(Heller et al., 2002)
Wnt11	E14.5	Stomach mesenchyme, oesophageal and colon epithelium	(Lickert et al., 2001)
	E12.0-17.0	Pancreas	(Heller et al., 2002)
Fzd1	E12.0-17.0	Pancreas	(Heller et al., 2002)
Fzd2	E11.0	Pancreatic epithelium and mesenchyme	(Heller et al., 2002)
Fzd3	E11.0	Pancreatic mesenchyme	(Heller et al., 2002)
Fzd4	E12.0-17.0	Pancreas	(Heller et al., 2002)
Fzd5	E12.0-17.0	Pancreas	(Heller et al., 2002)
Fzd6	E12.0-17.0	Pancreas	(Heller et al., 2002)
Fzd7	E17.5	Pancreas (endocrine cells)	(Heller et al., 2002)

Fzd8	E12.0-17.0	Pancreas	(Heller et al., 2002)
Fzd9	E12.0-17.0	Pancreas	(Heller et al., 2002)
Sfrp1[32]	E11.0	Pancreatic mesenchyme	(Heller et al., 2002)
Sfrp2	E17.5	Pancreas (endocrine cells)	(Heller et al., 2002)
Sfrp3	E17.5	Pancreas (endocrine cells)	(Heller et al., 2002)
Sfrp4	E12.0-17.0	Pancreas	(Heller et al., 2002)

***Table 5.1* – Expression of Wnt signalling component genes during mouse development**

5.2.2 Wnt3 and Wnt8a

Wnt3 and *Wnt8a* are proposed to be upregulated in the absence of *Bapx1* (**Figure 5.1**). *Wnt3* is expressed in the posterior epiblast and mesoderm layers at E6.5, in the diencephalon and spinal cord at E9.5, in the E10.5 nasal ectoderm, E11.0 head, E11.5-12.5 whole embryo, and in the thalamus at E14.5 (Perea-Gomez et al., 2001; Parr et al., 1993; Lan et al., 2006; Juriloff et al., 2005; Roelink et al., 1990; Warren and Price, 1997). Loss of *Wnt3* results in embryonic lethality by E10.5, due to an essential role in AP axis formation (Liu et al., 1999). *Wnt8a* is expressed at E9.5-10.5 in the developing head and brain, and in the eye from E9.5-18.5 (Ang et al., 2004).

Given that *Wnt3* may be upregulated in the absence of Bapx1, and that *Nkx2-5* is downstream of Bapx1, it may be of interest that a conserved high-affinity Nkx2-5 binding site (5'-TCAAGTG-3') lies upstream of the *Wnt3* gene (Katoh, 2005). *Nkx* genes are predicted to encode transcriptional repressors (Smith and Jaynes, 1996; Harvey, 1996; Jagla et al., 2001) and so *Nkx2-5* loss might be predicted to allow target gene expression.

[32] Secreted frizzled-related protein (Sfrp)

5.3 Investigations into potential upregulation of Wnt signalling in the *Bapx1*$^{-/-}$ posterior stomach

5.3.1 Examination of Wnt3 and Wnt8a expression by in situ hybridisation

DIG-labelled RNA probes for *Wnt3* and *Wnt8a* were designed and synthesised as described in **Chapter 7**. *In situ* hybridisation was performed on ~E11.25 and E12.5 wild type and *Bapx1*$^{-/-}$ guts, and on appropriate control tissues. A probe known to work well was included as an experimental control (*Hand2* on E10.5 embryos).

Whilst appropriate staining was seen in the control tissues (E10.5 heads; data not shown) for both probes, no signal was detected in the guts on either genetic background (**Figure 5.2**). This finding confirms the multiplex RT-PCR data that these *Wnt* genes are not expressed in the wild type posterior stomach, but does not support their expression on the *Bapx1* null background. Very low level expression, detectable by RT-PCR, may however fail to be detected by *in situ* hybridisation.

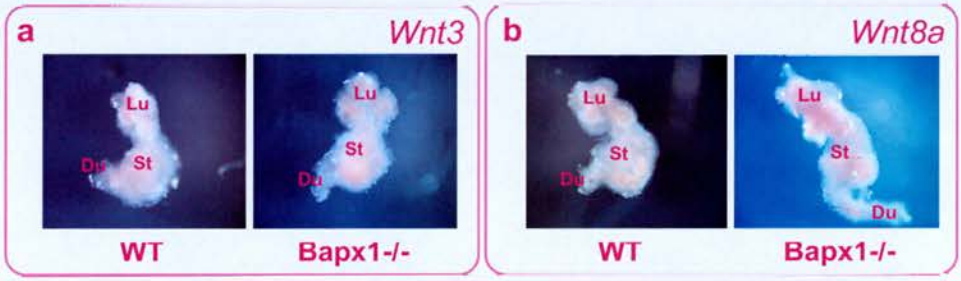

***Figure 5.2 In situ* hybridisation analysis of *Wnt3* and *Wnt8a* gene expression**

Expression of *Wnt3* and *Wnt8a* was investigated in wildtype and *Bapx1*$^{-/-}$ guts at ~E11.25 by *in situ* hybridisation, using DIG-labelled RNA probes. No expression was detected in the guts on either genetic background.
Lu: lung buds, **St**: stomach, **Du**: duodenum

5.3.2 Analysis of canonical Wnt signalling in the gut using the BAT-gal reporter line

The expression patterns of most *Wnt* genes have been well studied. However, Wnt factors act non-cell autonomously and so it is also imperative to know in which cells signalling has been initiated in response to these factors. Activation of the canonical β-catenin pathway can be used to infer the presence and activity of Wnt factors in a tissue, and so a number of reporter strains have been engineered to visualise this. One such model is the *BAT-gal* mouse in which *LacZ* is downstream of seven TCF/LEF binding sites and the *siamois* minimal promoter (Maretto et al., 2003). β-catenin, stabilised and translocated to the nucleus in response to Wnt signalling, activates expression of this transgene. *BAT-gal* expression marks sites of known Wnt activity, and has also been used to detect novel regions of signalling (Maretto et al., 2003).

The *BAT-gal* line was used to examine canonical Wnt signalling in the gut. Mice from this line were mated with *Bapx1*$^{+/-}$ mice and the offspring genotyped at weaning for *LacZ/Myo* and *Neo* (knocked into the *Bapx1* locus). Compound heterozygotes were crossed with *Bapx1*$^{+/-}$ mice to allow examination of the *BAT-gal* expression pattern on the *Bapx1* homozygous null background. Embryos from plug-checked matings were taken at ~E10.5, 11.25, 12.5, 14.5, 17.5, and 18.5, and stained with X-gal. Genotyping for *LacZ/Myo* and *Bapx1* was performed on yolk sac DNA. No differences in morphology or staining were observed between wild type and heterozygous mutants, as expected, and so only the wild type and homozygous knockout staining patterns are discussed.

The earliest stage examined was E10.5. Embryos were stained intact, thus providing numerous control tissues. X-gal can penetrate through to the gut at this stage, as shown by the studies in **Chapter 2**. Activity of the canonical Wnt pathway was apparent in the lung buds[33] of wild type and *Bapx1*$^{-/-}$ mice at E10.5 but was not significant in the gut tube of either (**Figure 5.3a**). Some stained cells were located along the left-side of the wild type gut, with fewer cells on the right. A more bilateral distribution was noted in the mutant gut shown in **Figure 5.3a**. However, there was

[33] *Wnt2b* (*Wnt13*) is expressed in the lung buds from E9.5 (Zakin et al., 1998)

not an appreciable overall difference between the number and distribution of stained cells between these genotypes, particularly given the variation between guts of the same genotype. In no instance though were cells clustered in the posterior stomach.

By ~E11.25 (the stage most relevant to the multiplex RT-PCR findings), *BAT-gal* expression is evident in the oesophagus[34] - and perhaps the most anterior limit of the stomach - and lungs of embryos of both genotypes (**Figure 5.3b**). No staining was observed in the mutant posterior stomachs. The multiplex RT-PCR data is thus not supported by this assay. There were, however, some stained cells present in the spleno-pancreatic mesenchyme of both genotypes (discussed further in **Section 5.4**).

LacZ expression was also absent from both the wild type and *Bapx1*$^{-/-}$ posterior stomach at later stages (E12.5, 14.5, 17.5, 18.5). These older guts were dissected out from the embryo prior to staining, and lungs (E12.5, 14.5) or heads (E17.5, 18.5) retained as control tissues in which canonical Wnt signalling is known to be active. The E12.5, E14.5, and E18.5 staining patterns are shown in **Figures 5.3 c, d, & e** respectively. Whilst no posterior stomach staining was observed, the canonical Wnt signalling pathway was found to be active in several other regions of the gut. Staining was found in the oesophagus at E12.5 and E14.5, and in the anterior stomach from E12.5, in both wild type and mutant guts. These staining patterns support the validity of this assay, as *Wnt4* and *Wnt11* are expressed in the E12.5 oesophagus, whilst *Wnt4*, *Wnt5b*, and *Wnt6* have been detected in the E14.5 and E16.5 oesophagus (Lickert et al., 2001). The anterior stomach domain of X-gal staining matches that of *Wnt5a* expression at E12.5 and E14.5 (Lickert et al., 2001).

Whilst no difference was observed in *BAT-gal* expression between the wild type and mutant posterior stomachs, there was one tissue which did display differential staining: the wild type spleen appears to be a novel site of canonical Wnt signalling, and this is disrupted in the asplenic *Bapx1*$^{-/-}$ gut. Wnt signalling has not previously been reported in the developing spleen, and so these findings are discussed in more detail in **Section 5.4**.

[34] Oesophageal expression of *Wnt4* and *Wnt11* is known to occur at E12.5 (Lickert et al., 2001).

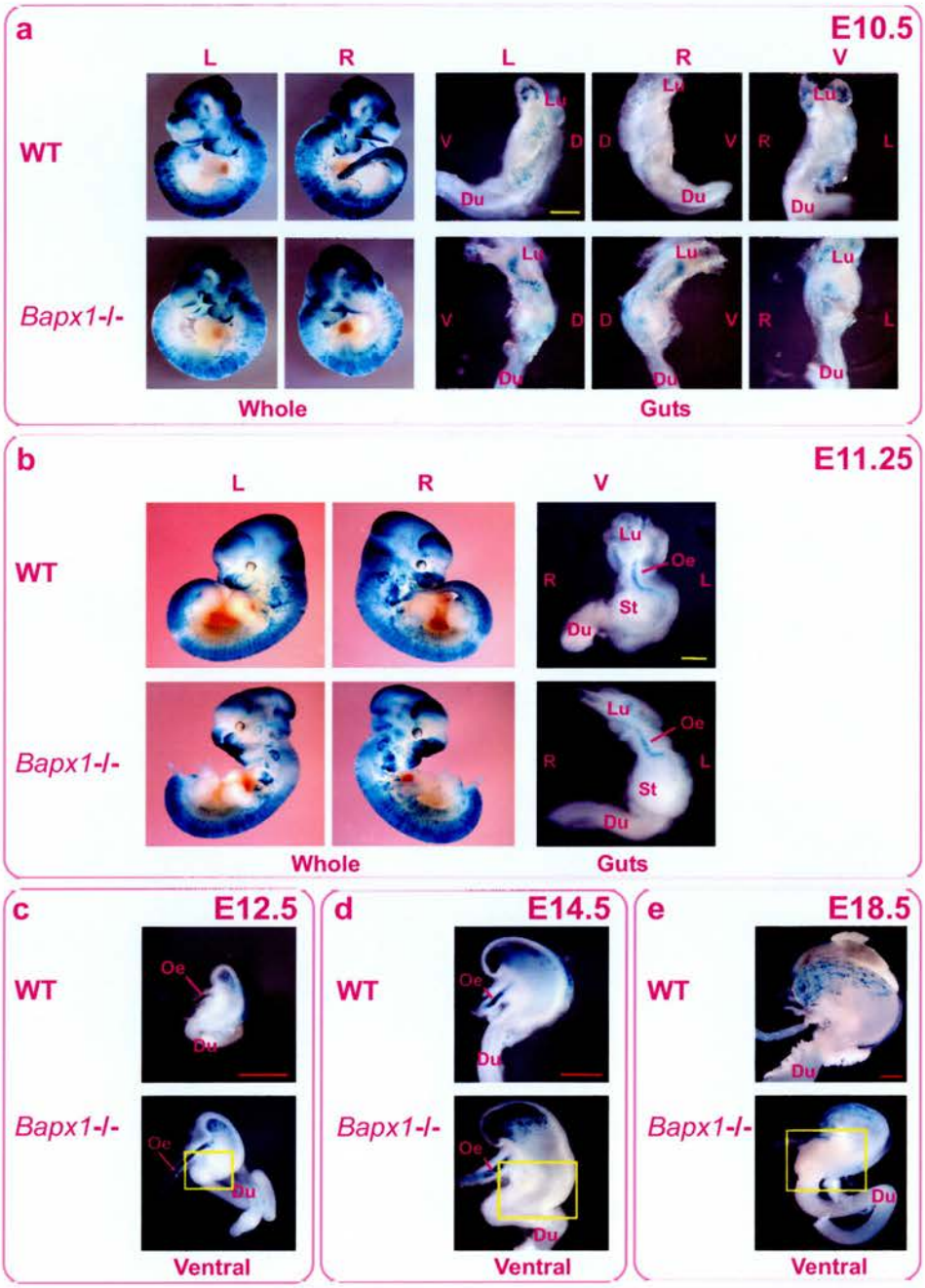

Figure 5.3 **Canonical Wnt signalling in wildtype and *Bapx1*$^{-/-}$ embryos and guts**

Activity of the canonical (β-catenin) Wnt signalling pathway was visualised by X-gal staining of embryos and guts carrying the *BAT-gal* transgene at **a**) E10.5, **b**) ~E11.25, **c)** E12.5, **d**) E14.5, and **e**) E18.5. Posterior stomach activity was not detected on the wildtype or the *Bapx1*$^{-/-}$ background. The expanded posterior stomach is indicated by a **yellow box** in the mutant guts. **Yellow scale bars** represent 200μm, **red scale bars** respresent 500μm. **L**: left, **R**: right, **D**: dorsal, **V**: ventral, **Lu**: lung buds, **Oe**: oesophagus, **St**: stomach, **Du**: duodenum

5.3.3 Upregulation of Wnt signalling in the *Bapx1*$^{-/-}$ posterior stomach is not supported

Neither the *in situ* hybridisation nor the *BAT-gal* reporter assays supported the findings from multiplex RT-PCR that *Wnt3* and *Wnt8a* are upregulated in the *Bapx1*$^{-/-}$ posterior stomach. There are, however, a few caveats to this conclusion. Firstly, low level gene expression may be detectable by RT-PCR, but fail to be recognised by *in situ* hybridisation. The gut is a particularly troublesome tissue in which to perform *in situ* hybridisation, and often presents high background staining as well as trapping in the lumen, making signal recognition difficult. However, it should be noted that staining of control tissues (E10.5 heads) indicated that the probes could successfully detect both genes.

Known sites of Wnt activity were identified using the *BAT-gal* reporter assay and so this appears to be a reliable method for detecting Wnt signalling. *BAT-gal* expression was not seen in the mutant posterior stomach, again contradicting the multiplex RT-PCR results. It should, however, be borne in mind that some instances of Wnt signalling are not detected with this system. Firstly, *BAT-gal* activity is not found in the intestinal crypt cells – a known site of Tcf4-mediated Wnt signalling (Maretto et al., 2003). There is thus the possibility that activity below a certain threshold is not detected, or that some activity is not registered for other unknown reasons. Secondly, this reporter recognises only the canonical β-catenin pathway and so there may be regions of Wnt activity which will not be detected. Wnt3 can act through the canonical pathway during limb development, as well as during primitive streak and mesoderm formation (Barrow et al., 2003; Morkel et al., 2003), but it may not utilise this pathway in all of the tissues in which it is secreted. In addition, even if *Wnt3* and *Wnt8a* are upregulated, downstream signalling may not necessarily be activated, as inhibitors could also be present.

In conclusion, the assertion that *Wnt3* and *Wnt8a* are upregulated as a result of *Bapx1* loss in the developing posterior stomach is not supported by the data presented here. Contamination of the RNA used in the original multiplex RT-PCR - or of the PCR itself – is one potential explanation for the original data. This potential contamination would probably not be from the rest of the stomach as *BAT-gal*

staining did not reveal significant canonical Wnt activity in the ~E11.25 gut. There are, however, many other sites of Wnt activity in the relatively compact space of the E11.0 embryo and so tissue contamination is certainly a possibility.

5.4 Analysis of canonical Wnt signalling in the developing spleen

Wnt signalling is not known to play a role in spleen development. However, as discussed earlier, misexpression of *Wnt1* or *Wnt5a* in the foregut/pancreatic epithelium disrupts mesenchymal spleen development, suggesting that the absence of certain Wnt factors is essential for correct patterning of the spleno-pancreatic region (Heller et al., 2002). A search for Wnt genes expressed in the spleen at the Mouse Genome Informatics (MGI) gene expression database[35] identified seven *Wnt* genes as being expressed in the spleen. These genes are, however, only detected in the spleens of postnatal weeks 6-8 (*Wnt1, 3, 5a, 11*) or adult (*Wnt9b, 10a, 10b*) mice, and not during development. The report here of canonical Wnt signalling in the embryonic spleen is therefore extremely interesting.

5.4.1 BAT-gal expression in the spleen

Sparse *BAT-gal* expression was first detected in wild type spleno-pancreatic mesenchyme at E11.5 (**Figure 5.4a**); very few stained cells were present in the *Bapx1*$^{-/-}$ mutant mesenchyme. By E12.5, X-gal stained cells were present throughout the wild type spleen (**Figure 5.4b**), and also in the mesenchyme overlying the pancreatic buds. Staining was absent from the rest of the posterior stomach region, suggesting specificity for the spleno-pancreatic mesenchyme. The proportion of

[35] As at 13.9.06

spleen cells stained by X-gal varied between embryos within a litter. Whether this variance reflects different levels of activity at the different stages of development found within a litter, or is simply an artefact of the transgene expression and/or staining protocol is unclear. It is perhaps timely at this juncture to remember that the *BAT-gal* reporter does not reflect *Wnt* gene expression *per se*, but instead non-cell autonomous responses to such expression. It is perhaps therefore to be expected that variation will be found when factors such as developmental stage, *Wnt* expression levels, Wnt secretion levels, and differential responses are considered. Expression was, however, consistently low in *Bapx1*$^{-/-}$ mutant guts, with the majority of stained cells localised over the dorsal pancreatic bud. Distinct spleen staining was not observed, as would be expected given the asplenic phenotype.

The E12.5 spleno-pancreatic expression pattern was recapitulated at E14.5, again with intra-litter variance in staining (**Figure 5.4c**). A greater proportion of splenic cells were stained at E14.5 compared to 48 hours earlier, whilst pancreatic mesenchyme staining was far less. Some pancreatic mesenchyme staining was also observed on the *Bapx1*$^{-/-}$ background, but no splenic expression was present.

Embryos were also assessed for β-gal activity at E17.5 and E18.5 (**Figure5.4d**). A small proportion of the wild type spleen cells were positive at these stages, though some spleens were totally devoid of staining. This may suggest that Wnt signalling functions during earlier spleen development, but may also be an experimental artefact as the late embryonic spleen is packed with blood cells and often stains poorly with X-gal. No splenic expression was noted in the mutant guts, whilst some stained cells were still present in the pancreatic mesenchyme (though not in the wild type guts).

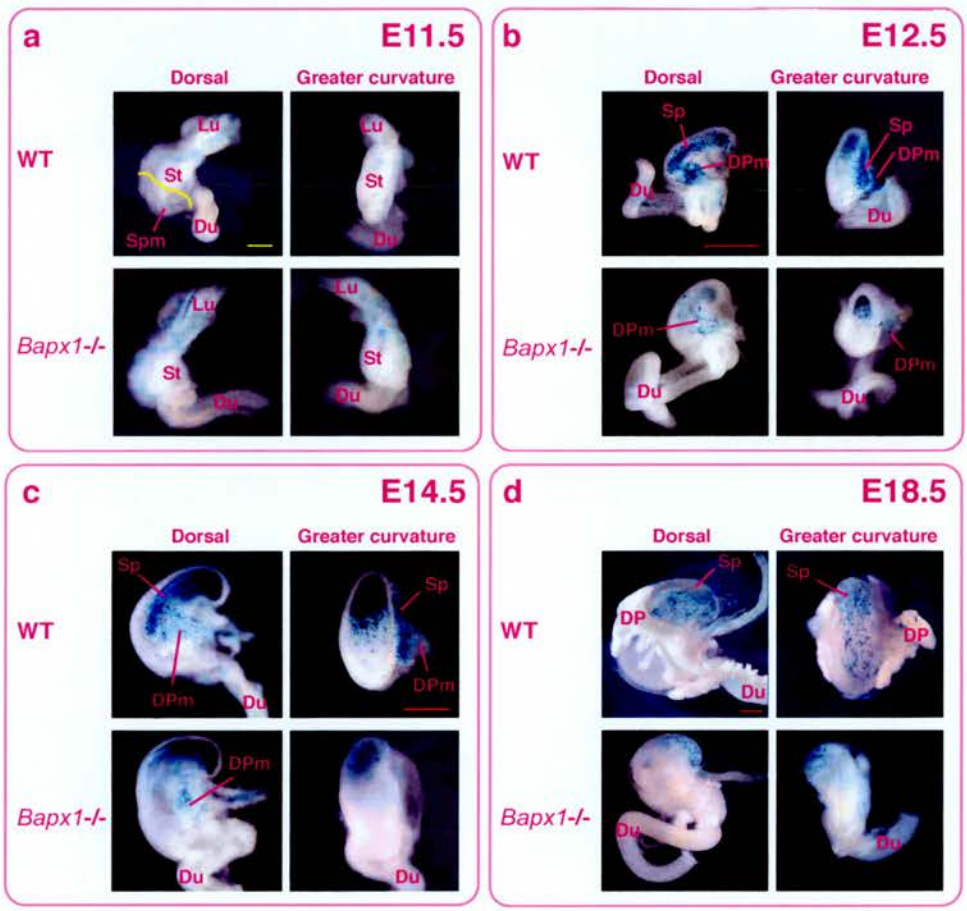

Figure 5.4 **X-gal staining for *BAT-gal* activity reveals that the canonical Wnt signalling pathway is active in the developing spleen of *BAT-gal* mice**

a) At E11.5 stained cells are present in the spleno-pancreatic mesenchyme (outlined in **yellow**) of wildtype guts, with few cells noted in the *Bapx1*$^{-/-}$ posterior stomach. **b**) By E12.5 staining is present throughout the wildtype spleen, extending into the mesenchyme overlying the pancreatic buds. Few stained cells are present in the asplenic *Bapx1*$^{-/-}$ mutant; these are located in the pancreatic mesenchyme. **c**) Stained cells are located throughout the wildtype spleen at E14.5. **d**) The proportion of stained cells in the spleen is diminished by E18.5.

Yellow scale bars represent 200μm, **red scale bars** represent 500μm.**Lu**: lung buds, **St**: stomach, **DPm**: dorsal pancreatic mesenchyme, **DP**: dorsal pancreas, **Du**: duodenum, **Sp**: spleen, **Spm**: spleno-pancreatic mesenchyme

In summary, the major onset of Wnt signalling through the canonical pathway in the spleen was at E12.5, though some activity was also detected in the E11.5 spleno-pancreatic mesenchyme. Signalling then persisted until at least E14.5, but had been largely attenuated by E17.5. Thus the main period of Wnt activity in the spleen appears to be between E12.5 and E14.5 – a key period of splenic growth and differentiation. This activity is lost in the asplenic *Bapx1*$^{-/-}$ mutant, though stained cells were detected in the pancreatic mesenchyme.

Many Wnt factors act through the canonical pathway and so there are numerous candidates for which family member(s) are involved in spleen development. Thus degenerate RT-PCR approachs to identify the splenic Wnt(s) (**Section 5.5**), and the Fzd receptor(s) through which signalling is achieved (**Section 5.6**), are described in the following sections.

5.5 Screen for expression of Wnt genes in the E14.5 spleen

A number of the murine *Wnt* genes were first identified by RT-PCR using degenerate primers described by Gavin et al., 1990 (Gavin et al., 1990). These primers are specific to two highly conserved amino acid sequences first identified in Wnt1 and Wnt2. *Wnt4, Wnt5a, Wnt6*, and *Wnt7a* were originally isolated using this approach (Gavin et al., 1990). These primers have since been used in a number of studies to examine the array of *Wnt* genes expressed in a specific tissue (Ricken et al., 2002; Dabdoub et al., 2003), including the developing gut (Lickert et al., 2001).

Two stages of spleen development – E12.5 and E14.5 – were of interest, based on the *BAT-gal* expression pattern. It was felt, however, that only one stage should be investigated - at least initially - given the large number of bacterial colonies from which DNA would need to be prepared and sequenced. An analysis of *Wnt* gene expression at E12.5 would be very interesting as this thesis is primarily concerned with spleen establishment and early development, as opposed to its

ongoing development and differentiation. However, *BAT-gal* expression was stronger at E14.5 and the spleen is also larger at this stage, thus providing a larger amount of RNA. This larger size also facilitates easier separation of the spleen from the stomach, decreasing the chances of contamination from stomach tissue. The E14.5 spleen was thus considered more amenable to an initial screen of *Wnt* gene expression.

A control tissue was also required, to check the validity of the screen. *BAT-gal* analysis of the E14.5 embryo revealed heavy staining in the head, and a perusal of the literature confirmed that many *Wnt* genes are expressed here. Detection of *Wnt* genes known to be expressed in the head thus provided a positive control.

The screen was carried out largely as described in the original report (Gavin et al., 1990), albeit without restriction digestion of RT-PCR products. Blunt-ended products were instead ligated into pGEM-T Easy. An agarose gel of the RT-PCR products is shown in **Figure 5.5**.

***Figure 5.5* RT-PCR using degenerate primers for *Wnt* genes**

Degenerate RT-PCR was performed on DNase-treated cDNA prepared from E14.5 spleens (**S1**: RNA extracted using an RNeasy kit [QIAgen]; **S2**: RNA extracted using TRIZOL [Invitrogen]) and heads (**H**), and also on a water control (**-**). cDNA was synthesised from 1μg DNase-treated RNA in a 20μl standard first strand cDNA synthesis reaction; 5μl of this was used in a 50μl RT-PCR. Primers were as described in Gavin *et al.* (1990), and amplified a mixture of approximately 0.4kb products. 5μl of a 50μl PCR was electrophoresed on a 2% agarose/TAE gel.
X: 1kb ladder (333ng/lane; Invitrogen)

5.5.1 Control tissue (head) results

RNA was extracted from three E14.5 heads using TRIZOL and was DNase-treated prior to cDNA synthesis. RT-PCR for *Hprt* was performed to check that genomic DNA was no longer present[36] (data not shown). The cDNA was then used as a template for RT-PCR using the *Wnt* degenerate primers described above, resulting in a mixture of ~0.4kb products (**Figure 5.5**) which were cloned as described. DNA was prepared and sequenced (M13 forward and reverse primers) from 96 clones. Sequences were assembled into contigs using the Sequencher program (Gene Codes); contigs were then analysed using the nucleotide-nucleotide BLASTn program (against the mouse genome) to find which genes they shared sequence identity with. Individual sequences, not in contigs, were also analysed in this way. A strict cut-off point for establishing homology was not required as each contig or sequence showed homology to only one *Wnt* gene, with high identity across the ~400bp.

The results of the head control screen are shown in **Table 5.2** and **Figure 5.6**. Four *Wnt* genes were found to be expressed in the head at E14.5: *Wnt2, Wnt2b (13), Wnt4,* and *Wnt7a. Wnt2b* is expressed in the telencephalon at E14.5, *Wnt4* in the E14.0 salivary gland, and *Wnt7a* in the E14.5 eye – thus supporting the validity of this assay (Grove et al., 1998; Hoffman et al., 2002; Ang et al., 2004). The facts that these genes were detected in different proportions, and that not more of the 19 murine *Wnt* genes were identified, suggest that this method is a reliable way to detect the genuine spectrum of gene expression in a tissue. Whilst this screening technique is not quantitative *per se*, the relative frequencies may be informative.

[36] RT-PCR of genomic DNA and cDNA for *Hprt* produces differentially sized bands as the primers flank an intron (details in **Chapter 7**)

Gene	*Wnt2*	*Wnt2b*	*Wnt4*	*Wnt7a*	Other	Fail	Total
F	38	30	14	10	2	2	96
R	37	30	15	10	2	2	96
Total	75	60	29	20	4	4	192

***Table 5.2* – Results of *Wnt* degenerate RT-PCR screen on E14.5 head cDNA**
The figures in the table show the number of sequences sharing high sequence identity with each *Wnt* gene. There were unequal numbers of forward and reverse sequences generated, as some sequencing reactions failed, and so the forward and reverse sequences were analysed separately. ("**F**", "**R**"). "**Other**" includes vector and other genomic sequences. "**Fail**" describes sequences which were of insufficient quality and/or length to produce a hit.

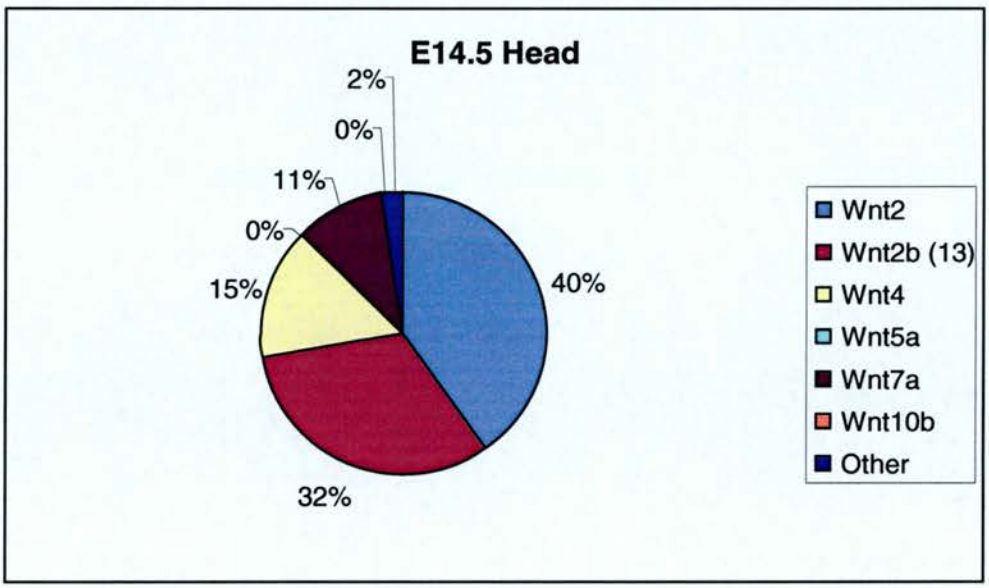

***Figure 5.6* – Results of *Wnt* degenerate RT-PCR screen on E14.5 head cDNA**
Graphical depiction of results presented in **Table 5.2** (total sequences). Failed sequences have been removed.

5.5.2 Spleen results

Guts were dissected out from E14.5 CD1 embryos and cuts made such that the main middle section of the spleen was taken for RNA extraction, whilst the terminal connections with the stomach were left behind. Two tubes containing 18 spleens each were frozen in liquid nitrogen. RNA was subsequently extracted from each of these by one of two methods: using 1) an RNeasy kit (QIAgen), or 2) TRIZOL (Invitrogen) (see **Chapter 7** for details). The two methods were tested so that the procedure could be optimised for future use; both produced good quality RNA at a similar concentration. Each RNA sample was DNase-treated prior to cDNA preparation and the absence of genomic DNA confirmed by RT-PCR for *Hprt* (data not shown). RT-PCR, cloning of products, and sequence analysis were then performed as in **Section 5.5.1**. 96 colonies were sequenced from each preparation, using forward and reverse M13 primers (192 sequencing reactions per preparation).

The results of the spleen screens are shown in **Table 5.3** & **Figure 5.7** (RNeasy RNA preparation) and **Table 5.4** & **Figure 5.8** (TRIZOL RNA preparation). Six *Wnt* genes were found to be expressed in the screen of RNA prepared using RNeasy: *Wnt2, Wnt2b* (*Wnt13*), *Wnt4, Wnt5a, Wnt7a*, and *Wnt10b*. *Wnt2* and *Wnt2b* were the most represented genes (27 and 23% of sequences, respectively). Five of these genes were also detected in the screen on TRIZOL-prepared RNA: *Wnt2, Wnt4, Wnt5a, Wnt7a*, and *Wnt10b*. *Wnt2b* was not detected. The most frequently detected gene was *Wnt7a*, which corresponded to 61% of the sequences. *Wnt4* was the least frequent (2%).

Gene	*Wnt2*	*Wnt2b*	*Wnt4*	*Wnt5a*	*Wnt7a*	*Wnt10b*	Other	Fail	Total
F	25	21	11	10	8	4	12	5	96
R	23	21	12	10	9	4	12	5	96
Total	48	42	23	20	17	8	24	10	192

***Table 5.3* – Results of *Wnt* degenerate RT-PCR screen on E14.5 spleen cDNA, synthesised from RNA extracted using an RNeasy kit**
The figures in the table show the number of sequences sharing high sequence identity with each *Wnt* gene. There were unequal numbers of forward and reverse sequences generated, as some sequencing reactions failed, and so the forward and reverse sequences were analysed separately. ("**F**", "**R**"). "**Other**" includes vector and other genomic sequences. "**Fail**" describes sequences which were of insufficient quality and/or length to produce a hit.

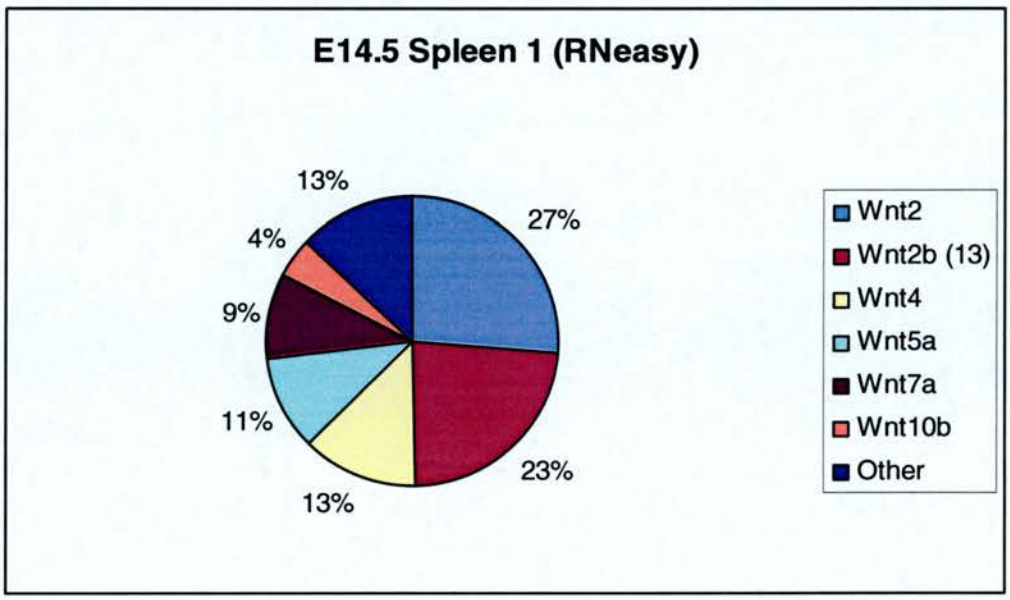

***Figure 5.7* – Results of *Wnt* degenerate RT-PCR screen on E14.5 spleen cDNA, synthesised from RNA extracted using an RNeasy kit**
Graphical depiction of results presented in **Table 5.3** (total sequences). Failed sequences have been removed.

Gene	*Wnt2*	*Wnt4*	*Wnt5a*	*Wnt7a*	*Wnt10b*	Other	Fail	Total
F	9	3	2	51	11	9	11	96
R	7	0	10	55	11	4	9	96
Total	16	3	12	106	22	13	20	192

***Table 5.4* – Results of *Wnt* degenerate RT-PCR screen on E14.5 spleen cDNA, synthesised from RNA extracted using TRIZOL**
The figures in the table show the number of sequences sharing high sequence identity with each *Wnt* gene. There were unequal numbers of forward and reverse sequences generated, as some sequencing reactions failed, and so the forward and reverse sequences were analysed separately. ("**F**", "**R**"). "**Other**" includes vector and other genomic sequences. "**Fail**" describes sequences which were of insufficient quality and/or length to produce a hit.

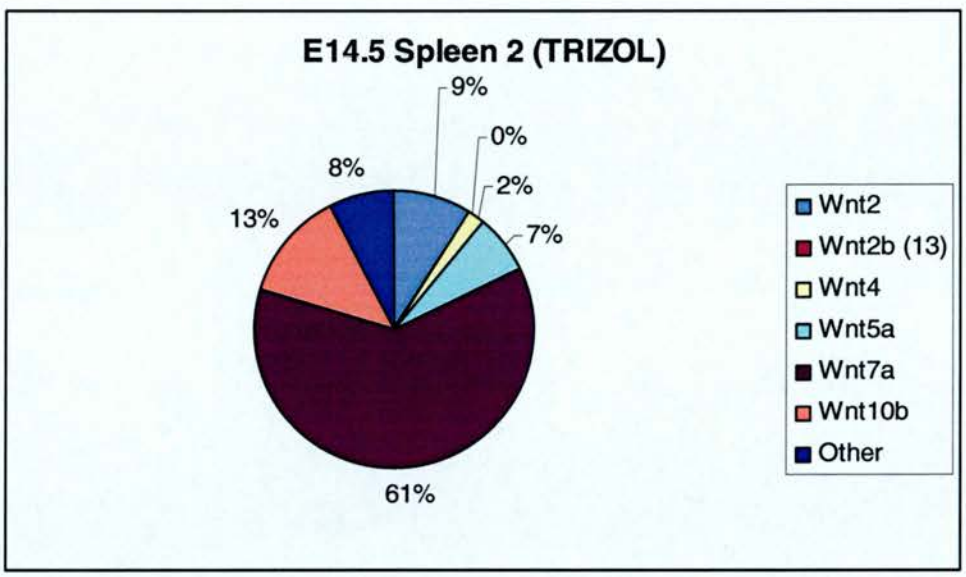

***Figure 5.8* – Results of *Wnt* degenerate RT-PCR screen on E14.5 spleen cDNA, synthesised from RNA extracted using TRIZOL**
Graphical depiction of results presented in **Table 5.4** (total sequences). Failed sequences have been removed.

A major peculiarity was that whilst *Wnt2b* was detected in cDNA synthesised from RNA prepared using the RNeasy kit, it was not found in that prepared with TRIZOL, using spleens from the same litter. The reason for this discrepancy is not clear as both methods produce total RNA preparations. However, one published report showed that RT-PCR failed to amplify two targets - including *β-actin* - from

cDNA prepared from TRIZOL-extracted RNA, whereas these RT-PCRs worked well with five other extraction methods (Deng et al., 2005). The TRIZOL-prepared transcripts only became amenable to RT-PCR once diluted down. This may relate to the findings in other comparative studies that TRIZOL produces a higher yield (Xiang et al., 2001; Lamarcq et al., 2002). Which method produces the higher purity appears to vary between studies/samples (Xiang et al., 2001; Lamarcq et al., 2002).

The RNeasy method is based on selective binding by a silica gel-based membrane; it is inefficient at recovery of RNA transcripts less than 200nt long, resulting in a 15-20% loss of total RNA by this method (Xiang et al., 2001)(RNeasy Mini Handbook, QIAgen). TRIZOL is based on the acid guanidinium thiocyanate-phenol-chloroform technique. One major difference is that the RNeasy kit columns contain DNase and so RNA prepared by this method is subjected to two DNase treatments in total; TRIZOL-prepared RNA is treated only once. It may be that the *Wnt2b* transcript is preferentially retained or lost when using one of the RNA extraction methods, or that this transcript becomes more or less amenable to PCR with one of the methods. This could be due to differing conditions such as salt concentration, which may affect the specificity of the degenerate primers. Indeed, varying the salt concentration in future assays might produce a different set of results.

The relative frequencies of the other *Wnt* genes also varied between the preparations. Most notably, *Wnt7a* was detected in 61% of the successful sequencing reactions from the TRIZOL clones, but in only 9% of those from the RNeasy set. This could be taken as an indication that the results of the screens are random. However, this is not the case, as one would therefore expect the numbers of sequences matching each *Wnt* gene to be roughly equal. Also, at least 13 more murine *Wnt* genes exist and yet were not detected, despite the degenerate primers having the ability to amplify other *Wnt* genes, including *Wnt1* and *Wnt6* (Gavin et al., 1990), *Wnt5b* and *Wnt11* (Lickert et al., 2001), and *Wnt7b* and *Wnt8* (Dabdoub et al., 2003)[37]. In the first of these cited studies, *Wnt2* was the most frequent hit (46%),

[37] It was not possible to ascertain whether the primers would identify all known *Wnt* genes as BLAST analysis is not possible using such degenerate sequences. The forward primer contains five degenerate bases (two possibilities each) which translates to 32 possible primer sequences. Similarly, the reverse primer contains four variable bases.

whilst over 70% of sequences corresponded to *Wnt4* in the second study, and more than 50% related to *Wnt7a* in the third. Tissue-specific differences in the array of expressed *Wnt* genes can therefore be detected using theses primers.

On a technical note, these screens performed favourably compared to published studies using the same primers. For example, in the original study, 80 colonies were screened, of which only 28 contained an insert (25 pertained to *Wnt* genes) (Gavin et al., 1990). Additionally, published studies have not tended to include an independent screen on a control tissue to confirm known gene expression, as performed with head cDNA here.

A final pie chart is provided in **Figure 5.9** that summarises the combined results of the two spleen screens.

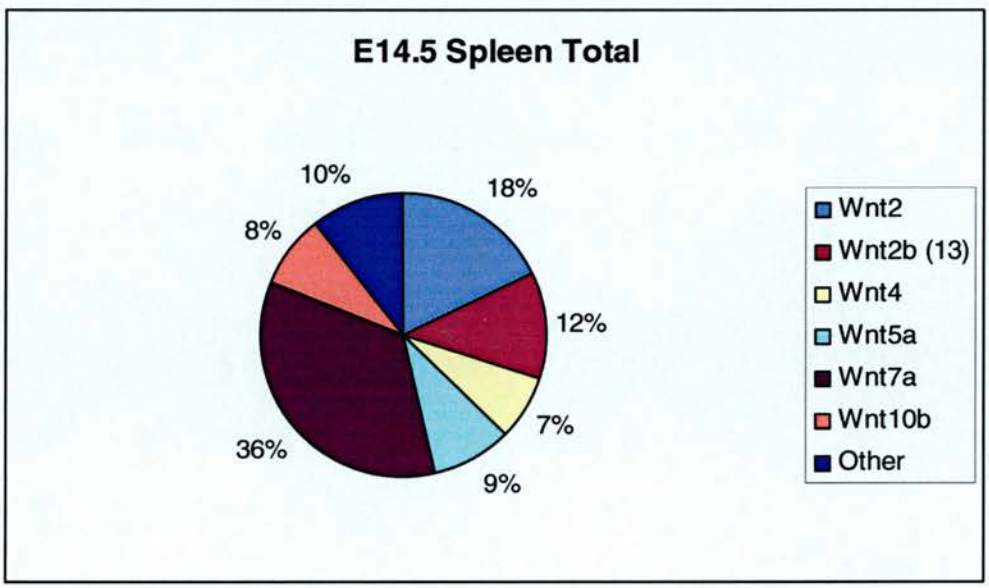

***Figure 5.9* – Combined results of *Wnt* degenerate RT-PCR screen on both E14.5 spleen cDNA preparations**
Failed sequences have been removed.

5.5.3 Confirmation of candidate Wnt genes

Two methods were chosen to confirm expression of the candidate *Wnt*s. Firstly, RT-PCR was repeated, but this time using primers specific to each individual *Wnt*. Secondly, *in situ* hybridisation was performed.

5.5.3.1 RT-PCR

RT-PCR primer pairs were designed for each of the candidate spleen *Wnt* genes (*Wnt2, 2b, 4, 5a, 7a,* and *10b*). These primers were based on those available in the literature, and are detailed in **Table 7.4**. All of the primers flanked introns, thus allowing contaminating genomic DNA products to be distinguished from those amplified from cDNA. In fact, the targeted *Wnt* introns are so large that a genomic product would be too big to amplify. Each RT-PCR was performed on the E14.5 spleen (RNeasy preparation) cDNA, in addition to the following controls: cDNA from a tissue known to express the gene of interest, genomic DNA, and sterile water. The E14.5 head cDNA was also tested for *Wnt2*, *Wnt4*, and *Wnt7a* expression (there was insufficient cDNA to test for *Wnt2b*). The positive cDNA controls were as follows: E10.5 whole embryo (*Wnt2, Wnt5a, Wnt7a*), E10.5 head (*Wnt2b/13*), E13.5 body (*Wnt4*), and E13.5 head (*Wnt10b*).

The RT-PCR results can be seen in **Figure 5.10**. Splenic expression of *Wnt2, Wnt2b, Wnt4*, and *Wnt5a* was confirmed, as was expression of *Wnt2*, *Wnt4*, and *Wnt7a* in the head. Faint bands were also observed for *Wnt7a* and *Wnt10b* in the spleen, but were not strong enough to be taken as evidence for expression. *Wnt7a* and *Wnt10b* were also the least represented genes in the degenerate RT-PCR screen on this cDNA. It should be noted, however, that *Wnt7a* was the most highly expressed gene in the cDNA synthesised from the TRIZOL RNA preparation, highlighting the major effect that cDNA preparation method can have on screens such as those reported here. There is thus a necessity for *in situ* confirmation of results from such screens.

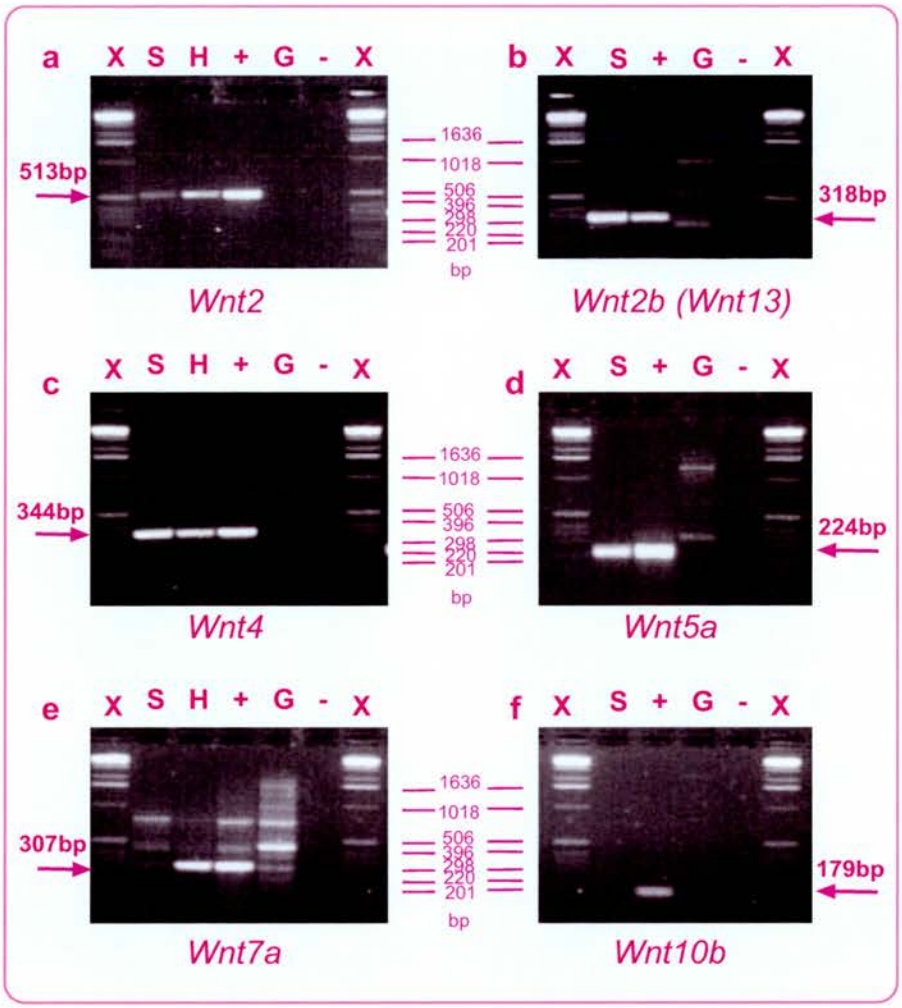

Figure 5.10 **Individual RT-PCR for each candidate *Wnt* gene potentially expressed in the E14.5 spleen**

a) *Wnt2* - 513bp, **b)** *Wnt2b (Wnt13)* - 318bp, **c)** *Wnt4* - 344bp, **d)** *Wnt5a* - 224bp, **e)** *Wnt7a* - 307bp, **f)** *Wnt10b* - 179bp (expected genomic band of 2.1kb can be faintly seen in the genomic DNA lane). RT-PCR products were analysed on 2% agarose/TAE gels.
RT-PCR templates: S: spleen cDNA, **H**: head cDNA, **+**: positive control cDNA, **G**: genomic DNA, **-**: water. **X**: 1kb ladder (333ng/lane; Invitrogen)

5.5.3.2 In situ hybridisation

In situ hybridisation probes for *Wnt2* and *Wnt10b* were designed and synthesised from PCR products containing a 3' T7 promoter site, as described in **Chapter 7**. *Wnt2b (Wnt13), Wnt4, Wnt5a,* and *Wnt7a* probes were transcribed from plasmids. E14.5 CD1 guts were analysed, along with suitable control tissues: E9.5 embryos (*Wnt2*), E11.5 embryos (*Wnt10b*), E12.5 embryos (*Wnt2b, Wnt5a, Wnt7a*), and E12.5 guts (*Wnt4, Wnt5a*). Expression was noted in control tissues for *Wnt2b* (E12.5 retina), *Wnt5a* (E12.5 head/nasal/brain, forelimbs), and *Wnt7a* (E12.5 head/brain) (data not shown). However, no splenic expression was identified using any of the probes (data not shown).

5.5.4 Wnt genes are expressed in the developing spleen

Embryonic spleen expression has not been previously demonstrated for any *Wnt* gene. In this degenerate RT-PCR screen, *Wnt2, 2b (13), 4, 5a, 7a,* and *10b* were found to be expressed in the spleen at E14.5 by degenerate RT-PCR. Splenic expression of the first four of these genes was confirmed by individual RT-PCR.

Wnt2 is expressed in the heart and surrounding tissues from E8.5 to E10.5 (Monkley et al., 1996), and in the lung at E11.5-15.5 (Bellusci et al., 1996), but has not been studied in the spleen. *Wnt2b (Wnt13)* is expressed in a variety of tissues between E5.5 and E8.5, including the foregut diverticulum (Kemp et al., 2005; Zakin et al., 1998), and is also expressed in the lung and brain at E9.5 (Zakin et al., 1998). Again, it is not known to be expressed in the spleen. Nor has *Wnt4* expression previously been found in the spleen, though a number of expression domains exist in the E12.5-14.5 embryonic gut (Lickert et al., 2001). *Wnt5a* is expressed in the anterior stomach as well as in more posterior regions of the gut tract at E12.5-14.5 – a pattern also observed for chick *Wnt5a* (Lickert et al., 2001; Theodosiou and Tabin, 2003). Expression is also present in the developing limb and spinal cord (Parr et al., 1993), and in the E14.0 liver (Austin et al., 1997), but has not been detected in the

spleen. *Wnt7a* is expressed in the head, brain, limb, and eye from E9.5 (Parr et al., 1993; Ang et al., 2004), but once again no spleen expression has been noted. *Wnt10b* is expressed in the mandible from E11.5 and in developing molars from E13.5 (Dassule and McMahon, 1998), and also in the yolk sac at E11.0 and liver at E14.0 (Austin et al., 1997). Interestingly, *Wnt10b* is expressed in the adult spleen (Wang and Shackleford, 1996).

The obvious next step is to confirm expression of these genes in the E14.5 spleen, by *in situ* hybridisation or other analyses such as immunohistochemistry. Expression should also be investigated in the E12.5 spleen and E11.5 splenic mesenchyme. Similarly, it will be worthwhile to repeat the degenerate RT-PCR screen on cDNA prepared from these earlier tissues. The method of RNA extraction used had a profound effect on the outcome of the spleen expression screens, and so this should be taken into account when performing further studies. The published screens using these primers have only used one RNA preparation method and so caution may need to be exercised when evaluating and comparing the outcomes of such studies.

Most of the findings were confirmed by individual RT-PCRs on the same spleen cDNA as which the screen was performed, but not by *in situ* hybridisation; this could therefore be interpreted as evidence of contamination of the spleen RNA sample with RNA from nearby tissues. Certainly, *Wnt10b* is expressed in the E14.0 liver, and *Wnt4* and *Wnt5* in the E14.5 gut (Austin et al., 1997; Lickert et al., 2001). However, this is unlikely to be the correct interpretation for a number of reasons. Firstly, the spleens from which RNA was extracted were detached extremely carefully from the underlying stomach and attached gut tissues. Secondly, *in situ* hybridisation often fails to detect low-level expression.

5.6 Screen for expression of Frizzled genes in the E14.5 spleen

A similar screen to that performed for the *Wnt* genes was carried out to identify which, if any, *Fzd (Frizzled)* genes are expressed in the E14.5 spleen. The Fzd receptors encoded by these genes are an essential part of the canonical signalling response to *Wnt* gene activity.

The screen was carried out on the same E14.5 head and spleen (RNeasy preparation) cDNA samples as in the *Wnt* screen, using two published sets of *Fzd* degenerate primers (Daudet et al., 2002; Ricken et al., 2002). These primer sets were originally used to detect expression of rat *Fzd* genes and so it was uncertain how well they would perform in a screen on mouse cDNA; hence the decision was made to perform a screen with each set. An initial BLAST analysis revealed that these primers are indeed complementary to *Fzd* sequences in the mouse genome. The products of RT-PCR using these primers are expected to be 180-270bp (**"Daudet"**) (Daudet et al., 2002) and 210-340bp (**"Ricken"**) (Ricken et al., 2002).

Following initial PCR confirmation that both pairs could amplify appropriately sized products, they were used to perform a screen on spleen and head cDNA. Agarose gels of the RT-PCR products are shown in **Figure 5.11**. The method employed was the same as that used for the *Wnt* primers in **Section 5.5**, albeit with two deviations. Firstly, sequencing was only performed using the M13 forward primer, as the inserts were not large and thus there was no need to sequence in both directions. This would certainly be more efficient given the time needed to analyse all of the sequences. This also meant that results (number of *Fzd*-homologous sequences) could be directly related to the number of clones matching each gene, as in other published studies. Secondly, sequences were analysed by BLASTn analysis individually, as opposed to within contigs. The reason for this is that upon initial assembly of sequence contigs it became obvious that there was far greater homology between members of the *Fzd* family than those of the *Wnt* family - at least in the regions amplified in these studies - and so some sequences became grouped into inappropriate contigs. This high degree of similarity also meant that one sequence often showed homology to more than one *Fzd* gene during the individual BLAST

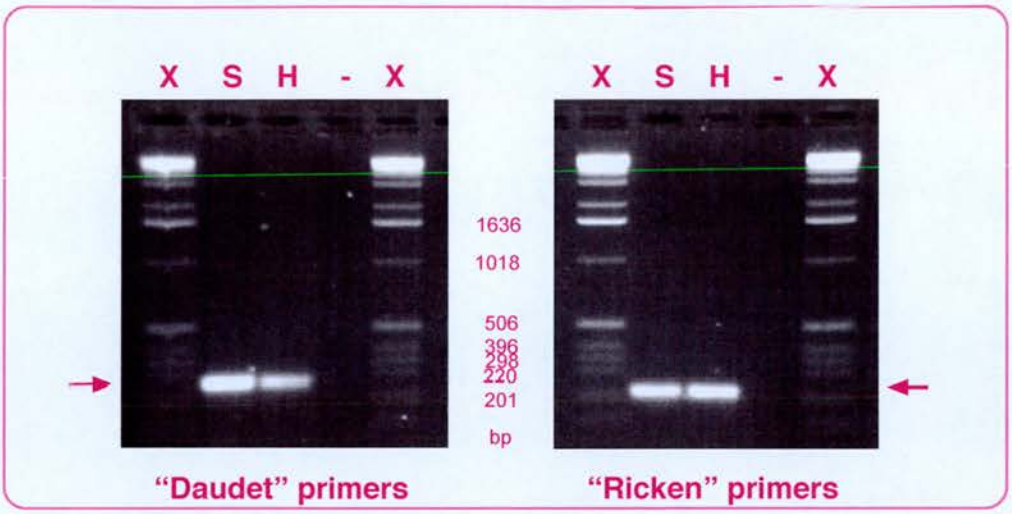

Figure 5.11 **RT-PCR using degenerate primers for *Frz* genes**

Degenerate RT-PCR was performed on DNase-treated cDNA prepared from E14.5 spleens (**S**) and heads (**H**), and also on a water control (**-**). cDNA was synthesised from 1μg DNase-treated RNA in a 20μl standard first strand cDNA synthesis reaction; 3μl of this was used in a 50μl RT-PCR. The primer sets used were those described in Daudet *et al.* (2002) (**"Daudet")** and Ricken *et al.* (2002) (**"Ricken"**), both of which amplified mixes of approximately 0.2-0.3kb products (arrowed). 5μl of each 50μl PCR were electrophoresed on a 2% agarose/TAE gel.
X: 1kb ladder (333ng/lane; Invitrogen)

analyses. However, one hit always exhibited far greater identity (typically 98-100%) over a larger distance (~200bp), and so this was considered the true match.

5.6.1 Control tissue (head) results

An RT-PCR screen was performed on E14.5 CD1 head cDNA using both degenerate *Fzd* primer sets. As the head screen was merely a control, only the products generated using the "Daudet" primers were subsequently cloned and sequenced. The results of the BLASTn analysis of these sequences are shown in **Table 5.5** and **Figure 5.12**. A large proportion (72%) of the sequences were of insufficient quality to produce a match with known genes, due to substandard

sequencing reactions. Of the 27 colonies that did produce hits, approximately half contained an insert homologous to *Fzd2/10/10a*[38].

Gene	*Fzd1*	*Fzd2/ 10 /10a*	*Fzd4*	*Fzd5*	*Fzd6*	*Fzd7*	*Fzd9*	Other	Fail	Total
Number of sequences	2	14	2	1	1	1	2	4	69	96

***Table 5.5*– Results of *Fzd* degenerate RT-PCR screen on E14.5 head cDNA, using the "Daudet" primer set**
The figures in the table show the number of sequences sharing high sequence identity with each *Fzd* gene. **"Other"** includes vector and other genomic sequences. **"Fail"** describes sequences which were of insufficient quality and/or length to produce a hit.

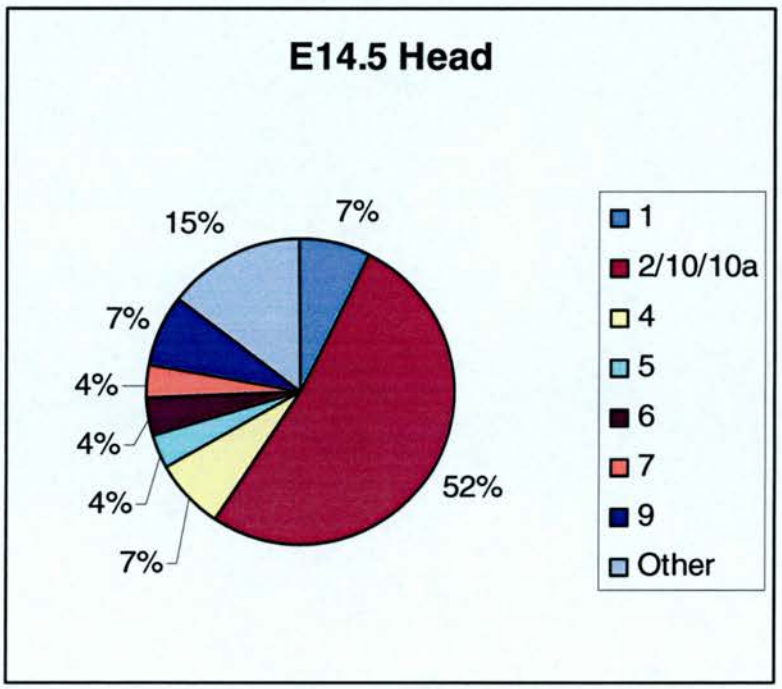

***Figure 5.12* – Results of *Fzd* degenerate RT-PCR screen on E14.5 head cDNA, using the "Daudet" primer set**
Graphical depiction of results presented in **Table 5.5**. Failed sequences have been removed.

[38] *Fzd2*, *Fzd10*, and *Fzd10a* are synonyms for the same gene

Fzd genes known to be expressed in the head at E14.5 include: *Fzd1* (eye), *Fzd2* (eye), *Fzd4* (head), *Fzd5* (eye, brain), *Fzd6* (salivary gland), *Fzd7* (head), *Fzd8* (brain), and *Fzd9* (brain, eye) (MGI gene expression database at 1.12.06). All of these genes - with the exception of *Fzd8* – were detected in this study confirming the validity of this technique. No additional *Fzd* genes (e.g. *Fzd3*) were picked up, again supporting the specificity of this assay.

5.6.2 Spleen results

A degenerate screen for *Fzd* gene expression was performed on E14.5 spleen cDNA (prepared from RNeasy-extracted RNA) using both the "Daudet" and "Ricken" primer sets. Sequences were analysed from 96 clones for each set. The results of both screens are shown in **Table 5.6** and **Figure 5.13**.

RT-PCR analysis with the "Daudet" primers identified the five *Fzd* genes detected in the "Ricken" screen (*Fzd1, Fzd2/10/10a, Fzd4, Fzd5,* and *Fzd7*), and also *Fzd6*. The most frequently detected gene was *Fzd2/10/10a*, which was found in 27% of clones. The next most abundant sequences were *Fzd1* and *Fzd4*, each constituting 17% of the total sequences. *Fzd5* was similarly frequent, whilst *Fzd6* and *Fzd7* were rare. The *Fzd9* gene detected in the E14.5 head cDNA was not detected, demonstrating the specificity of the assay.

Gene	*Fzd1*	*Fzd2/ 10/10a*	*Fzd4*	*Fzd5*	*Fzd6*	*Fzd7*	Other	Fail	Total
"Daudet"	16	24	16	12	1	2	21	5	97*
"Ricken"	6	4	8	9	0	1	0	68	96

***Table 5.6* – Results of *Fzd* degenerate RT-PCR screen on E14.5 spleen cDNA, using the "Daudet" and "Ricken" primer sets**
The figures in the table show the number of sequences sharing high sequence identity with each *Fzd* gene. **"Other"** includes vector and other genomic sequences. **"Fail"** describes sequences which were of insufficient quality and/or length to produce a hit.
* The total number of sequences from the "Daudet" screen is 97, from 96 clones. This is because one clone contained two inserts (*Fzd2/10/10a* and *Fzd5*).

The pie charts in **Figure 5.13** demonstrate the overall similarity between the two data sets, supporting the validity of this approach and authenticity of the results obtained.

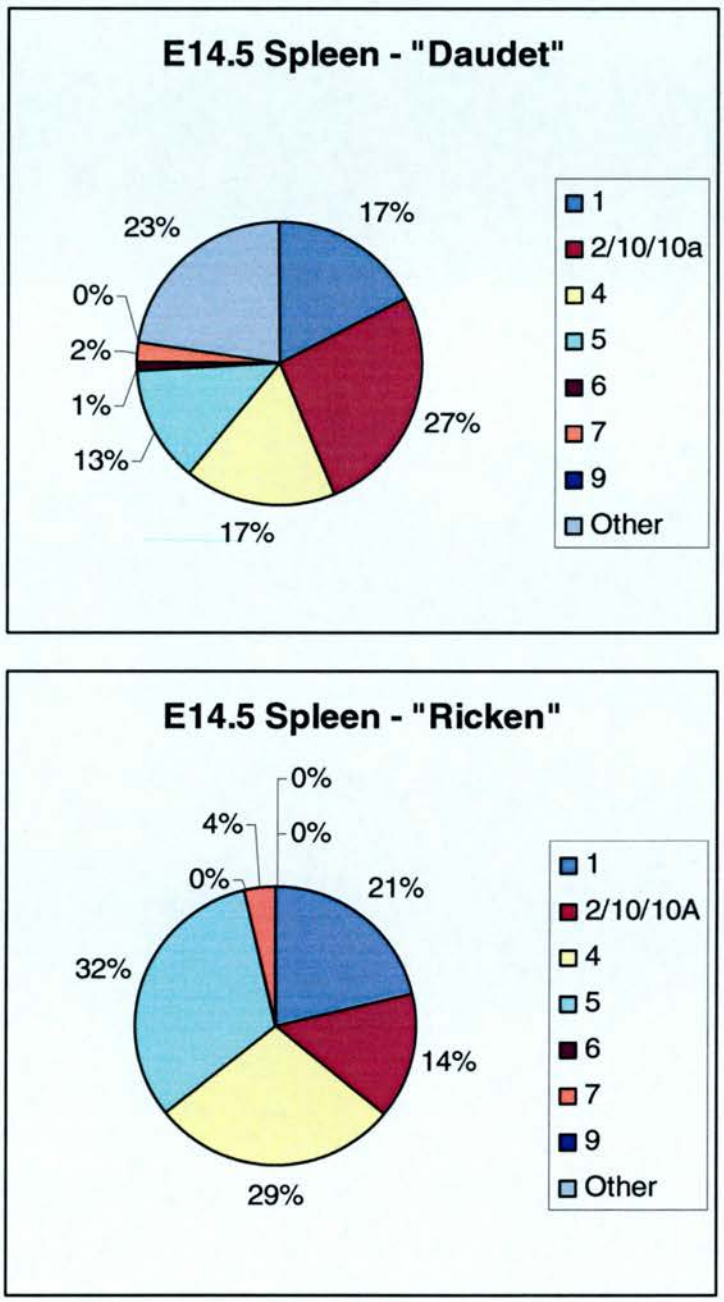

***Figure 5.13* – Results of *Fzd* degenerate RT-PCR screen on E14.5 spleen cDNA, using the "Daudet" and "Ricken" primer sets**
Graphical depiction of results presented in **Table 5.6**. Failed sequences have been removed.

5.6.3 Fzd genes are expressed in the developing spleen

A number of *Fzd* genes are known to be expressed in the postnatal and adult spleen: *Fzd1, Fzd3, Fzd6, Fzd7, Fzd8,* and *Fzd10* (MGI gene expression database at 1.12.06) (Austin et al., 1997). Members of the *Fzd* gene family have not however been implicated in embryonic spleen development. The degenerate RT-PCR screen reported here showed that *Fzd1, Fzd2/10/10a, Fzd4, Fzd5, Fzd6,* and *Fzd7* are expressed in the E14.5 spleen. These genes were detected at different frequencies to one another, suggesting that the results are not random and instead reflect genuine expression. In addition, the results from the two primer sets were similar, supporting their authenticity.

This screen was intended as a preliminary accompaniment to the *Wnt* screen and thus the results have not been confirmed. Nonetheless, the detection of the same set of *Fzd* genes by the two primer sets is both significant and promising. Though *Fzd3, 5,* and 7 are expressed in the E14.0 liver (Austin et al., 1997), care was taken to ensure no liver tissue contaminated the spleen samples, and so these results are considered to be reliable. The next step is thus to confirm the findings and extend the analysis to earlier spleen development.

5.7 Discussion

The original findings which initiated the work described in this chapter – that *Wnt3* and *Wnt8a* are upregulated in the *Bapx1*$^{-/-}$ posterior stomach – were not supported. They did however lead to some unexpected results, as is the nature of scientific serendipity. Canonical Wnt signalling was shown to be active in the splenic mesenchyme at ~E11.25 and in the developing spleen at E12.5 and E14.5. Staining was also found in the left/dorsal region of the E10.5 posterior stomach (**Figure 5.3a**). This may relate to the presumptive splenic mesenchyme marked by *Nkx2-5*, *NGRS-LacZ*, and other splenic markers at E10.5.

Wnt signalling was active during the period of initial establishment of splenic progenitor cells and their apparent migration towards the anterior tip of the stomach. Likely roles for the signalling would therefore be in proliferation, differentiation, or maintenance of splenic cells. Immunohistochemical analysis of the cell types in which the canonical pathway is active would be extremely useful to address these possibilities. As the major period of Wnt activity in the spleen was between E12.5 and E14.5, there is a possibility that this is localised to haematopoietic cells, which begin to populate the spleen at around this time. However, it is more probable that signalling is active in cells of mesenchymal origin, given the following facts: *BAT-gal* is expressed in the ~E11.25 splenic mesenchyme, *BAT-gal* is expressed in the E12.5-14.5 pancreatic mesenchyme (which is contiguous with that of the spleen), and staining was absent from the liver (the embryonic organ from which spleen-colonising haematopoietic cells arise).

In addition to the spleen, the anterior stomach also displayed *BAT-gal* expression. This is of particular interest as an anterior stomach chemoattractant for spleen development was proposed in **Chapter 4**. The *Wnt5a* expression pattern closely matches that of the X-gal staining observed in the anterior stomach (Lickert et al., 2001), and so the potential expression of this gene in the spleen, and the potential role of *Wnt5a* as a spleen chemoattractant, are of future interest.

Expression analysis revealed which specific components of the Wnt signalling network are expressed in the E14.5 spleen. *Wnt2, Wnt2b (Wnt13), Wnt4, Wnt5a, Wnt7a, Wnt10b, Fzd1, Fzd2/10/10a, Fzd4, Fzd5, Fzd6,* and *Fzd7* were detected at varying frequencies, the most abundant transcripts being *Wnt2, Wnt2b, Wnt7a, Fzd2/10/10a, Fzd4*, and *Fzd5*. None of these genes have been previously implicated in spleen development. Expression now needs to be confirmed using *in situ* methods.

Wnt signalling is of critical importance to both development and adult life, and has therefore been well studied in murine cells, tissues, and embryos. There is accordingly a large pool of resources available for studying and manipulating the Wnt signalling pathways. It will therefore be very exciting to follow up these results and unmask a potential role for Wnt signalling in mammalian spleen development.

The first step towards this goal will be repeating both the *Wnt* and *Fzd* degenerate RT-PCR screens at E12.5 and earlier (E11.0-11.5), when the transition between splenic mesenchyme and the distinct elongated spleen structure occurs. This transition presumably involves a range of developmental processes, such as proliferation, differentiation, migration, and controlled cell death – processes in which Wnt signalling may play essential roles.

CHAPTER 6

Discussion

"We shall not cease from exploration
And the end of all our exploring
Will be to arrive where we started
And know the place for the first time"
- T.S. Eliot (Four Quartets)

6.1 Summary of work

The initial aim underlying the work presented in this thesis was to characterise a putative spleen regulatory region upstream of *Nkx2-5*. The isolation of the *Nkx2-5* gut regulatory sequence (*NGRS*), and investigations into the expression pattern conferred by it, were reported in **Chapter 2**. The potential uses for the *NGRS* as a genetic tool were explored in **Chapter 3**, and its use as a marker of spleen development in explant culture was reported in **Chapter 4**. Finally, the initial experiments in **Chapter 5** were prompted by preliminary data on *Bapx1*, a gene upstream of *Nkx2-5*. A potential novel role for Wnt signalling in early spleen development was revealed as a consequence.

The implications of the results presented are considered in this chapter.

6.2 The origin of the spleen

The spleen is a vertebrate-specific organ that performs both immunological and haematopoietic functions. Loss of the spleen can have fatal consequences and its abnormal placement within the body can be an indicator of life-threatening cardiac defects related to aberrant development of left-right asymmetry. Yet, despite this obvious clinical importance, the early development of the spleen is poorly understood. A number of studies have attempted to address this problem in recent years (Roberts et al., 1994; Dear et al., 1995; Patterson et al., 2000; Kanzler and Dear, 2001; Hecksher-Sorensen et al., 2004; Brendolan et al., 2005; Asayesh et al., 2006) but there still remains a number of important questions to be answered.

The first major question is that of where the splenic precursors are derived from. At E10.5 a patch of mesenchyme underlying the SMP, lying dorsal to the junction of the stomach and duodenum, expresses a number of genes known to mark the spleen later in development (*Hox11, Capsulin, Wt1, Nkx2-5*) (Hecksher-Sorensen et al., 2004). These same genes are expressed in the condensed mesenchyme which lies dorsal to the posterior stomach at E11.5 and is considered the classical splenic primordium (Thiel and Downey, 1921). It thus seems logical to assume that the

aforementioned E10.5 dorsal mesenchyme is indeed the earliest known splenic tissue, particularly given its abnormal development in the asplenic *Bapx1 (Nkx3-2)*$^{-/-}$ mutant (Hecksher-Sorensen et al., 2004).

But is the E10.5 dorsal mesenchyme the absolute origin of the splenic precursor cells? This tissue is located on the left-side of the embryo, yet evidence from *Xenopus* suggests that splenic precursors (marked by *Nkx2-5* expression) originate bilaterally and that the left-side preferentially develops into the spleen (Patterson et al., 2000). Aberrant development of such an initially bilateral system might provide a model to explain how asplenia and polysplenia occur. It is thus of great interest that both *Nkx2-5* and an upstream regulatory region of this gene (the *NGRS*) were found to be expressed bilaterally in the SMP (and underlying mesenchyme) at E9.5, as presented in **Chapter 2**. Given this expression pattern, *Nkx2-5* could potentially be the earliest marker of the spleen in mouse, as well as in *Xenopus*. This cannot, unfortunately, be assessed in mouse embryos lacking *Nkx2-5* expression, as such loss proves lethal before recognisable spleen development initiates (Lints et al., 1993b). There is thus a need to develop suitable tools to facilitate dissection of the role of *Nkx2-5* in early spleen development.

The *NGRS* was shown in **Chapter 2** to be an excellent marker of spleen development when used to drive *LacZ* expression. The element drives expression in the E9.5-E10.5 SMP and underlying mesenchyme, and in the spleno-pancreatic mesenchyme at E11.5. Expression is then present in the developing spleen until the end of gestation. The *NGRS* might therefore be suitable to direct gut-specific loss of *Nkx2-5* expression. The *NGRS* also marks the developing pyloric sphincter – another tissue of clinical importance with poorly understood development, due to a paucity of mutants and early markers.

In addition to providing a good marker of normal spleen development, the *NGRS* also has the potential to mark aberrant spleen morphogenesis, as shown by the analysis of the *Rwhs* mutant. The data in **Chapter 2** provides the first report of the spleen defects in this mutant, and further characterisation ought to prove most interesting, potentially providing a mouse model of polysplenia. Given the relative normality of the rest of the spleno-pancreatic region, it is expected that the underlying mutation causes the polysplenia phenotype at a later stage than that

proposed to occur in response to the disruption of initial splenic bilaterality discussed above.

6.3 The relationship between *Bapx1* and *Nkx2-5*

Nkx2-5 is not expressed in *Bapx1*$^{-/-}$ guts (Watson et al., 2007), suggesting that Bapx1 may regulate *Nkx2-5*. A point of expressional overlap between these two genes had not, however, been previously detected. I found that *Nkx2-5* is expressed throughout the bilateral SMP at E9.5, as is *Bapx1*, thus providing a potential interaction point. The phenotypic effects of *Bapx1* loss become noticeable in the 24 hours that follow (Watson et al., 2007), though loss of *Nkx2-5* expression at E9.5 was not successfully investigated.

Expression of the *NGRS* was found to be independent of *Bapx1*. It may therefore be that whilst the *NGRS* can recapitulate the entire *Nkx2-5* gut expression pattern during normal development, a second regulatory sequence mediates the dependence on Bapx1. The fact that the *NGRS* does not require *Bapx1* for its activity may prove useful. Genes downstream of *Bapx1* could be rescued by driving their expression with *NGRS* on the *Bapx1*$^{-/-}$ background. This would facilitate dissection of the genetic cascades downstream of Bapx1.

The *NGRS* expression domain is wider than that of endogenous *Nkx2-5*. Both the regulatory element and the gene are expressed bilaterally in the SMP at E9.5, but *Nkx2-5* expression then becomes refined to two domains, whereas the *NGRS* is active throughout the SMP at E10.5. The *Nkx2-5* pyloric sphincter domain is also more refined than that of *NGRS-LacZ* from E11.5, as the latter is contiguous with the spleen expression domain.

The most interesting facet of the above disparity is that, from E10.5 onwards, the regions in which *NGRS* but not *Nkx2-5* is expressed are those in which *Bapx1* expression is also detected. *Bapx1* is expressed in the tip of the SMP and the underlying mesenchyme at E10.5, whilst *Nkx2-5* is expressed in two domains flanking this expression; the *NGRS* confers expression encompassing all of these domains. Similarly, both *Bapx1* and *NGRS-LacZ* are expressed in the posterior

stomach region just anterior to the pyloric sphincter from E11.5; *Nkx2-5* is not. It may therefore be that the endogenous *Nkx2-5* expression pattern conferred by the *NGRS* (and possibly other elements) is negatively modulated by Bapx1 from E10.5 onwards. As *Nkx2-5* and *Bapx1* expression overlap fully in the SMP at E9.5, it must be assumed that Bapx1 does not exert an inhibitory effect at this stage. Conditional loss of *Bapx1* expression at E10.5 would thus be interesting to investigate.

6.4 Transgenic approaches to using the *NGRS* as a tool

A major motivation behind cloning and characterising the *NGRS* was to use it in lineage tracing exercises, to investigate the origins and development of the spleen in a way not previously reported. Two approaches to realising this goal were reported in **Chapter 3**: the first was a true lineage tracing approach (*NGRS-CreERT2*), the second a clonal strategy in response to the failure of the first approach (*NGRS-LoxSTOPLox-LacZ*). Both methods were designed to utilise the Cre-ERT2 temporally inducible expression system, but successful transgenic lines were not established for either. The possible reasons for the failure of these strategies were discussed in **Chapter 3** and so will not be reiterated here. The important message is that a temporally-inducible, tissue-specific lineage tracing system to investigate early spleen development would be a valuable asset to the field of gut developmental biology - if not an absolute necessity - and thus further efforts should be made to pursue this goal. The *NGRS* could be central to driving these efforts, though a number of other options exist, including the *Hox11* gene or potential spleen regulatory regions affiliated with it.

Given the problems experienced when creating transgenic lines by microinjection (e.g. *NGRS-LoxSTOPLox-LacZ*, plus more general issues of copy number and insertion effects), it may be sensible to target future transgenes directly into the genome. *Bapx1* and *Hox11* are good candidates for a knock-in approach as they are expressed during spleen morphogenesis and heterozygous loss does not produce an abnormal phenotype (Lettice et al., 1999b; Roberts et al., 1994; Dear et

al., 1995). The placing of an inducible *Cre* transgene under the control of the endogenous regulatory elements of either of these genes would provide a valid way to engineer a spleen-specific lineage tracing system.

The origins of the splenic precursor cells could be addressed using an inducible lineage tracing system, as could a number of other key questions. One such question is that of the origin of the more general mesenchyme that populates the region between the SMP and gut endoderm from E9.5-10.5. Later in development, an important question is that of how the spleen makes the transition from a patch of condensed mesenchyme dorsal to the posterior stomach at E11.5 to an elongated spleen structure by E12.5. This question was examined in **Chapter 4** using an alternative culture-based approach, and is discussed in the next section.

6.5 Gut explant culture: a novel way to study spleen morphogenesis

In **Chapter 4**, the *NGRS-LacZ* transgene was employed as a marker of spleen development in gut explant cultures. The explant culture system provided the opportunity to observe spleen morphogenesis and produced a number of insights into how the spleen undergoes the transition from condensed mesenchyme at ~E11.5 to an elongated structure at ~E12.5. The most unexpected of these findings was that, whilst spleen development was poor in normal cultures, if the posterior region of the E11.5 spleno-pancreatic mesenchyme was damaged then accelerated splenic growth apparently occurred. This inappropriate growth manifested as an apparent splenic leading edge (anterior tip) – more appropriate to the spleen structure seen from E12.5 onwards - at the anterior of the stomach. Such precocious development was only observed following disruption or removal of the posterior spleno-pancreatic mesenchyme, suggesting that this tissue may normally exert an inhibitory or "anchor" effect on spleen development. Once unleashed from this inhibition, accelerated spleen development can occur. This phenomenon shows striking parallels

with that of the leading edge migration that occurs upon separation of the tip (leading edge) from the main body of *Dictyostelium* slugs (Dormann and Weijer, 2001).

Preliminary evidence from the culture experiments also suggested that the spleen originates from the spleno-pancreatic mesenchyme located dorsal to the posterior stomach at E11.5, as opposed to being derived in a posterior-anterior wave from the underlying stomach mesenchyme. Development from the spleno-pancreatic mesenchyme has certainly seemed the most likely mechanism, given that this tissue - and later the spleen - expresses spleen markers such as *Hox11, Wt1, Nkx2-5*, and the *NGRS-LacZ* transgene. Physical obstruction of the spleen using aluminium foil barriers demonstrated that spleen development does not occur if *NGRS*-expressing cells exist only posterior to this barrier. Similarly, *NGRS-LacZ* stomachs with their spleno-pancreatic mesenchyme removed did not undergo spleen morphogenesis.

The mechanism by which splenic precursor cells from the spleno-pancreatic mesenchyme might colonise the future spleen region between E11.5 and E12.5 of normal development is unknown, though roles for proliferation and migration seem likely. Migration of *NGRS-LacZ*-expressing splenic precursor cells towards a chemoattractant at the anterior of the stomach was also investigated, though the existence of such a signal could not be confirmed. This may become possible in the future with further honing of the gut culture and/or explant recombination techniques. Similarly, the use of a fluorescent tag for spleen development may aid in these studies. Indeed, a mouse line expressing a *Wt1-GFP* transgene has been obtained for these experiments, the results of which should provide some exciting insights in the near future.

6.6 Wnt signalling in spleen development

The expression pattern of *Wnt5a* closely matches that of where the proposed spleen chemoattractant would be secreted. *Wnt5a* is expressed in the anterior stomach at E12.5 in mouse, and in a comparable region in chick and *Xenopus* (Lickert et al., 2001; Theodosiou and Tabin, 2003; Smith et al., 2000a). A number of

other Wnt genes are also expressed in the developing gut, but thus far none have been detected in the embryonic spleen. However, I have found that the canonical Wnt signalling pathway is active in the splenic mesenchyme at E11.5 and in the spleen itself at E12.5-14.5. More specifically, expression analyses revealed that *Wnt2, Wnt2b (Wnt13), Wnt4, Wnt5a, Wnt7a, Wnt10b, Fzd1, Fzd2/10/10a, Fzd4, Fzd5, Fzd6,* and *Fzd7* are expressed in the spleen at E14.5. Wnt signalling is a key component of the developmental tool box and has been shown to be active in most embryonic tissues. It is perhaps not surprising then that so many genes encoding components of the Wnt signalling network should be expressed during spleen morphogenesis. These findings therefore merit further investigation, particularly at the earliest stages of spleen development.

A recent development in the Wnt signalling field lends credence to the discovery that canonical Wnt signalling is active in the embryonic spleen. Mariyama and colleagues developed GFP-based reporter lines for the canonical pathway and found it to be active in the spleen of adult mice (Moriyama et al., 2007). The application of such a reporter to the study of Wnt signalling during embryonic spleen development could provide a further way to investigate the role of this pathway in splenogenesis. Again, gut explant culture may provide the ideal system in which to perform such a study.

6.7 Final thoughts

The work presented in this thesis has provided two types of information. Firstly, it has provided a number of facts or insights into development of the murine spleen. These include: the establishment of the point of expressional overlap between *Nkx2-5* and *Bapx1*; the findings that a conserved upstream regulatory region (the *NGRS*) can direct the gut component of the *Nkx2-5* expression pattern and that this is Bapx1-independent; the reporting of a novel spleen mutant (the *Rwhs* mutant); evidence that the spleen is derived from the spleno-pancreatic mesenchyme and does not receive contribution from the underlying stomach mesenchyme; the discovery of an inhibitory effect on spleen development exerted by the posterior spleno-pancreatic

mesenchyme; the finding that the canonical Wnt signalling pathway is active during spleen development, and the detection of a number of *Wnt* and *Fzd* genes in the developing spleen. Secondly, it has established tools and systems for investigating spleen development further. These include the *NGRS-LacZ* gut reporter line, the *NGRS-LacZ* line on the *Bapx1*$^{-/-}$ background, the *Rwhs* novel spleen mutant, and the gut explant culture system.

CHAPTER 7

Materials & Methods

"It ain't what you do it's the way that you do it
It ain't what you do it's the time that you do it
It ain't what you do it's the place that you do it
And that's what gets results"
- Bananarama (It Ain't What You Do)

7.1 Manipulation of nucleic acids

7.1.1 General molecular biology reagents

Unless otherwise stated, reactions were performed in autoclaved DNase-free, RNase-free 0.5 or 1.5ml microcentrifuge tubes (Eppendorf). Chemicals were analytical grade and were supplied by Sigma, Roche, Fisher, Invitrogen, and BDH, unless otherwise stated. Restriction enzymes were obtained from Roche and New England BioLabs (NEB). The following general solutions were prepared by MRC Human Genetics Unit (HGU) Core Scientific Services, then autoclaved and stored at room temperature:

Tris.HCl

Tris base (tris[hydroxymethyl]aminomethane) was dissolved in sterile water and HCl used to adjust pH as required.

EDTA

EDTA (ethyldiaminetetra-acetic acid di-sodium salt) was dissolved in sterile water. Solid NaOH was added to bring the solution to pH8.0.

TE buffer

10mM Tris.HCl (pH7.5), 1mM EDTA.

TAE buffer, 50X stock

Tris base	242g
Glacial acetic acid	57.1ml
0.5M EDTA	100ml

To a final volume of 1 litre with distilled water

Stock was diluted to 1X with distilled or MilliQ water for use in agarose gel electrophoresis

PBS (phosphate buffered saline)

NaCl	8g
KCl	0.2g
Na_2HPO_4	1.44g

KH_2PO_4 0.24g

Disssolved in 800ml distilled water, pH adjusted to 7.4, then brought to a final volume of 1 litre with distilled water

20X Saline Sodium Citrate (SSC)

NaCl 175.3g

Sodium citrate 88.2g

Disssolved in 800ml distilled water, pH adjusted to 7.0, then brought to a final volume of 1 litre with distilled water

7.1.1.1 DEPC-treatment of solutions

Sterile water (dH_2O), PBS and SSC were DEPC-treated in a fumehood by the addition of 1µl/ml DEPC (diethylpyrocarbonate) (Sigma). Solutions were mixed overnight then autoclaved to hydrolyse (inactivate) the DEPC.

7.1.2 Restriction enzyme digestion

Digestion of DNA was achieved using a suitable restriction enzyme - as determined by the restriction sites available - and the appropriate 10x buffer for that enzyme. Typically, between 0.1µg and 5µg DNA was digested in a volume of 20-200µl. Enzyme was used at a concentration of 1-10U/µg DNA, depending on the duration of the digests (1U cuts 1µg in 1hr at 37°C, and a 10-fold excess of enzyme was typically used). The final reaction volume was reached by adding dH_2O. Digestions were incubated at the appropriate temperature for the enzyme, as recommended in the manufacturer's instructions.

Digestion with multiple enzymes in a single reaction was possible when buffers and incubation temperatures were compatible. If incubation temperatures were incompatible, then digestion was first performed with one enzyme, then the second enzyme added and the incubation temperature adjusted appropriately. Digests were performed sequentially in cases where enzymes required different buffers. The first enzyme and associated buffer salts were removed by phenol-chloroform extraction and ethanol precipitation, prior to digestion of DNA with the second enzyme.

7.1.3 Electrophoresis

7.1.3.1 Standard gel electrophoresis of DNA samples

DNA fragments were separated by size using agarose gel electrophoresis. Standard (High Pure, BioGene) or low melting point (LMP) (Invitrogen) agarose was dissolved in 1X TAE by heating in a microwave. Different amounts of agarose in 1X TAE were used to make 0.7-4% (weight/volume) gels as required; larger DNA fragments (>1kb) were analysed on a ≤1% gel, with smaller pieces (<1kb) being run out on ≥2% gels. Molten agarose was cooled and ethidium bromide (BDH, 10mg/ml) added to a final concentration of 50µg/100ml. Agarose was then poured into a suitable tray and a plastic comb used to create the required number of sample wells.

DNA was mixed with loading buffer (see **7.1.3.3**) and loaded onto the set gel in an electrophoresis tank containing 1X TAE. DNA size markers were run alongside to estimate the size and amount of DNA in samples. The most commonly used size marker was the 1kb DNA ladder (Invitrogen); 100bp ladder was also used as required (NEB). Gels were typically run at between 60-120V, depending on the separation required.

Electrophoresed DNA was visualised under UV illumination and photographed on a BioDocit (UVP) imaging system.

7.1.3.2 Standard gel electrophoresis of RNA samples

RNA samples were analysed by electrophoresis as per DNA samples, with the following exceptions: tanks, combs, and gel trays were cleaned overnight by soaking in 0.02M NaOH, prepared with DEPC water. These were rinsed with DEPC water prior to use. RNA gels were run at 160V for 10 minutes.

7.1.3.3 Agarose gel loading buffer

Loading buffer was prepared as a 6X stock and stored at room temperature.

	Amount	Final concentration
Ficoll (Sigma)	5g	10%
Orange G (Sigma)	0.15g	0.3%

To a final volume of 50ml with TE, pH8.0.

7.1.4 Determining the concentration of DNA and RNA samples

Nucleic acid concentrations were determined by agarose gel electrophoresis and/or spectroscopy (DNA absorbance).

By electrophoresis:

A number of different volumes of the DNA sample were run alongside various volumes of a standard DNA size marker of known concentration, and an estimate of the DNA concentration made by visual comparison between these.

By ultraviolet (UV) spectroscopy:

DNA and RNA samples were diluted 1:100 with dH_2O or DEPC-dH_2O respectively, and the spectrophotometer (GeneQuant Pro) was set to recognise this dilution. The spectrophotometer was calibrated using a water only sample. ≥70µl of the nucleic acid sample was placed in a clean cuvette and the absorbance at 260nm (A_{260}) was measured. The concentration of the sample was given by the machine in ng/µl, calculated on the following basis:

1 A_{260} unit of dsDNA = 50µg/ml H_2O
1 A_{260} unit of ssRNA = 40µg/ml H_2O

The concentration of the original sample in µg/ml is calculated as follows:
A_{260} value x dilution factor x 50µg/ml for DNA; 40µg/ml for RNA.

Concentrations provided by spectrophotometery were occasionally confirmed by running a volume of sample predicted to contain a certain amount of DNA against the same amount of standard marker DNA on an agarose gel.

7.1.5 Nucleic acid purification

Purification of DNA from reaction mixtures was performed by gel extraction, following electrophoresis, and/or phenol-chloroform extraction.

By gel extraction:

PCR products or restriction-digested DNA fragments were electrophoresed on LMP agarose gels, then visualised on a UV light-box and excised from the gel using a clean scalpel blade. DNA was extracted from the gel using a gel extraction kit (QIAGEN), according to the manufacturer's instructions. All optional steps were included.

Depending on what the DNA was to be subsequently used for, gel extraction was sometimes followed by phenol-chloroform extraction.

By phenol-chloroform extraction:

Sterile distilled water or TE was added to the DNA sample to reach a final volume of 200µl. This was then mixed with 200µl phenol:chloroform:isoamyl alcohol (25:24:1), and briefly vortexed before centrifugation for three minutes at 13,000 revolutions per minute (rpm). The upper aqueous layer was transferred - carefully avoiding protein at the phase interface - to a clean 1.5ml tube and 200µl phenol:chloroform:isoamyl alcohol was again added, before mixing and centrifugation as before. The upper layer was removed to a clean tube and 200µl chloroform added to this, followed by vortexing and centrifugation as before. The resulting final upper layer was transferred to a clean tube and DNA precipitated from this (see **7.1.7**).

RNA was similarly extracted, albeit using DEPC-treated water and reagents reserved for use with RNA only.

7.1.6 Precipitation of nucleic acids

DNA was precipitated by the addition of 2.5 volumes EtOH (ethanol) and 1/10 volume 3M sodium acetate (NaOAc, pH5.2). The precipitation reaction was then placed at –20°C for ≥2 hours, or on dry-ice for 10mins, and centrifuged for 15-30 minutes at 4°C, 13,000rpm. The supernatant was discarded and the pelleted sample washed in 70% EtOH/dH_2O. The supernatant was once again removed and the DNA air dried before re-suspension in an appropriate volume of dH_2O.

RNA precipitation was performed as above, with DEPC-dH_2O being used instead of standard dH_2O in the 70% EtOH and for resuspension.

7.1.7 Ligations

7.1.7.1 Alkaline phosphatase treatment of vector DNA

To prevent self-ligation, the 5' termini of vector DNA were dephosphorylated using calf intestinal phosphatase (CIP) (Roche). Linearised, purified DNA was made up to a final volume of 45µl with sterile dH_2O, then mixed with 5µl 10X CIP buffer and 1µl CIP. The reaction was incubated for 15min at 37°C, then at 56°C for a further 15min. 1µl CIP was then added and the two incubations repeated. 2µl 0.5M EDTA was used to stop the reaction, and the CIP heat-inactivated at 65°C for 20min. The resulting dephosphorylated vector DNA was recovered from the reaction by phenol-chloroform extraction followed by ethanol precipitation.

7.1.7.2 Ligation

When performing a new ligation a number of vector:insert molar ratios were tried, most commonly 1:1 and 1:3. A no insert (1:0) control ligation was also always performed. 20-50ng vector was used as standard.

Ligations were performed either for 5-60 min at room temperature (RT), or overnight at 16°C, depending on the ligase used. Rapid ligations were performed in a final volume of 21µl, using the Rapid DNA Ligation Kit (Roche) according to the manufacturer's instructions. Overnight ligations were carried out with standard T4 DNA ligase and ligation buffer (Roche), in a total reaction volume of 10µl. Following overnight ligation, the ligase was inactivated by heating the reaction mixture to 65°C for 20 minutes.

7.1.8 Annealing of oligos

5µg of each (forward and reverse) oligo were annealed in a screw-cap 1.5ml Eppendorf tube at 100°C for five minutes in a reaction including 5µl standard ligation buffer (salt), made up to 50µl with sterile water. The reaction was left to cool for up to two hours and was then ethanol precipitated. The precipitated annealed oligo was resuspended in 50µl sterile water.

7.2 Microbiology

Aseptic technique was observed for all microbiological procedures (pouring agar plates, picking colonies, setting up cultures, storage of bacterial stocks). Liquid cultures were grown under antibiotic selection at 37°C with vigorous shaking (220rpm). Dry cultures were grown on selective agar plates, inverted and incubated at 37°C overnight.

7.2.1 Growth media for bacterial cultures

Luria-Bertani broth (LB) and Luria-Bertani agar (L-Agar) were prepared by HGU Core Scientific Services staff as follows:

LB

Tryptone	10.0g
Yeast extract	5.0g
NaCl	10.0g
Glucose	1.0g

Made up to 1 litre with dH_2O and then autoclaved

Low salt LB (for use with Zeocin)

Tryptone	10.0g
Yeast extract	5.0g
NaCl	5g

Made up to 950ml with dH_2O, brought to pH 7.5 with NaOH, then made up to 1 litre with dH_2O and autoclaved

L-Agar

To prepare solid media, 15.0g agar was added to 1 litre LB or low salt LB prior to autoclaving.

7.2.1.1 Antibiotic selection

	Stock concentration	Working concentration
Ampicillin (Amp)	100mg/ml in dH_2O	100µg/ml
Zeocin (Zeo)	100mg/ml in dH_2O	50µg/ml

Aliquots were stored at -20°C.

7.2.1.2 X-gal/IPTG indicator plates

X-gal (5-bromo-4-chloro-3-indoly-b-d-galactoside) (Melford) at 50mg/ml in DMF (N,N-dimethylformamide) (BDH) and IPTG (Isopropyl-β-d-thiogalactopyranoside) were added to the surface of plates. 150µl X-gal/IPTG solution (12µl 100mM IPTG, 48µl 50mg/ml X-gal, 90µl SOC) was spread over each L-Agar/antibiotic plate and allowed to adsorb for 30 minutes. Both plate spreading and drying were performed in a hood.

7.2.2 Transforming electrocompetent cells

Following heat inactivation of the ligase and purification (salt removal) of the ligation reaction using a nitro-cellulose filter (Millipore), electrocompetent (OneShot TOP10, Invitrogen) *E.coli* cells were transformed with 10-100ng (1-2ul ligation) plasmid DNA by electroporation. Cells were thawed on ice and 50µl were added to each DNA sample in an ice cold centrifuge tube. Transformation reactions were gently mixed with a pipette tip and then transferred to a pre-chilled 0.1cm electroporation cuvette (EquiBio). Cells were electroporated using a BioRad Gene Pulser using the following settings: 200Ω, 25µF, 1.8kV. Immediately after electroporation 250µl RT L-Broth was added to the cells and mixed with a pipette tip; the cells were then moved to 4ml snap-cap polypropylene tubes and incubated at 37°C for 1hr with shaking at 200rpm. 5µl and 100µl aliquots of transformed cells were then plated on L-Zeo plates and incubated overnight at 37°C.

7.2.3 Transforming DH5α competent cells

Library-efficiency DH5α competent cells were transformed by heat shock, according to the manufacturer's protocol (Invitrogen).

7.2.4 Isolation of DNA

7.2.4.1 Plasmid DNA

Plasmid DNA was prepared using a commercially available kit (QIAGEN): a Miniprep kit for production of small amounts of plasmid DNA, a Maxiprep kit for preparing large amounts. Miniprep cultures were made by inoculating 3ml LB/antibiotic with a single plasmid-containing

colony and growing this overnight at 37°C with shaking. Maxiprep cultures were prepared by inoculating 200ml LB/antibiotic with a starter culture - either 1.5ml of an overnight culture or 2ml of an 8hr culture – and growing this at 37°C overnight in a large conical flask to permit aeration of the bacteria.

The following morning, plasmid DNA was extracted from the cultures using the chosen kit according to the manufacturer's instructions. Miniprep DNA prepared was eluted in 30µl dH_2O, Maxiprep DNA in 250-500µl dH_2O. DNA concentration was determined as described in **Section 7.1.4**. Appropriate restriction digests were performed to check the correct identity of the plasmid DNA, and these analysed by agarose gel electrophoresis.

7.3 Polymerase chain reaction (PCR)

7.3.1 Reagents

dNTPs:

Deoxyribonucleotide triphosphates (dNTPs) were purchased from ABgene as 100mM stocks of each dNTP (dATP, dCTP, dGTP, dTTP), and were stored at -20°C in working stocks of 25mM, prepared by mixing the four dNTPs in a 1:1:1:1 ratio. dNTPs were used in PCRs at a final concentration of 0.2mM.

Oligonucleotide primers:

PCR primers were designed using the Primer3 program (see **Section 7.9**) and/or by manual sequence analysis. The following guidelines were observed as far as possible when designing primers for standard PCRs: a sequence length between 20 and 25 nucleotides long, ~50% G/C content, and limited ability to self-anneal or anneal with the other primer in the PCR. Longer primers were designed when inclusion of an RNA promoter was necessary and for certain cloning procedures. Primers were purchased from MWG, Invitrogen, and Sigma as lyophilised desalted compounds, and from EuroGentec as desalted solutions. Stocks were kept at a concentration of 100µM (in sterile dH_2O) at -20°C; primers were used at a final concentration of 0.5-1µM.

Primer details are provided in **Table 7.1** (general), **Table 7.2** (sequencing), and **Table 7.3** (genotyping).

Additional reagents:

Taq DNA polymerase [5u/µl] (Invitrogen) was used at 0.2µl per 20-25µl reaction. PCR buffer (200mM Tris.HCl (pH 8.4), 500mM KCl) (Invitrogen) was a 10X stock and therefore used at

1:10 in reactions. Mg^{2+} (Invitrogen) was used at a final concentration of 2.5mM unless stated otherwise (range: 1-2.5mM). The reaction was made up to the required volume with sterile dH_2O. PCR amplification using the *Bapx1* primers required the addition of DMSO (dimethyl suphoxide; Sigma) at a final concentration of 10% in order to enhance the efficiency of the PCR (DMSO destabilises base-pairing, thus inhibiting DNA self-complementarity and allowing the strands to be separated at a lower temperature; it is particularly useful for GC-rich templates). Routine PCRs were performed in 0.5ml centrifuge tubes.

Some PCRs required the use of Platinum *Taq* polymerase (Invitrogen), Expand Hi-fidelity *Taq* polymerase (Roche), or KOD Hot Start DNA polymerase (Novagen), in place of standard *Taq* polymerase. These requirements are listed in **Table 7.4**. Platinum *Taq* was used as a direct replacement for standard polymerase in otherwise standard PCRs; Hi-Fidelity and KOD polymerases were used in reactions according to the manufacturers' protocols.

Template/ Primer set	PCR conditions		Primers	
	Anneal (°C)	Product size (bp)	Primer sequence 5' → 3'	
IfOligoIn	57	140 – in 70 – not in	F	GATCGCCATTTCCTGTTTGTC
			R	GGAAGGCTGCGCTCCTCG
LSL **(NsiI ends)**	60	~1400	F	GATCATATGCATCCGGAACCCTTAATATAACTTCG
			R	GATCATATGCATCCTCTTCGAGGGACCTAATAAC
OligoOri	55	399 – if correct orientation	F	ATTGGCGAGAAAGCAAACAG
			R	TAGATGGCTCTGCCCTGACT
LSLOri	55	366– if correct orientation	F	CAGCTCTGCAACGAGGTACA
			R	GCAGGTCGAGGGACCTAATA

***Table 7.1* - PCR primers used in cloning procedures**

Template/ Primer set	PCR conditions		Primers	
	Anneal (°C)	Product size (bp)	Primer sequence 5' → 3'	
Rwhs	56	~600	F	CTTTCCACCCCATTTCCTCT
			R	AGGCTCTGTCAGCCCAGTTA
M13	50	Variable	F	GTAAAACGACGGCCAGT
			R	GGAAACAGCTATGACCATG

***Table 7.2* - PCR primers used for sequencing**

Template/ Primer set	PCR conditions		Primers	
	Anneal (°C)	Product size (~kb)	Primer sequence 5' → 3'	
LacZ	60	0.6	F	GCGACTTCCAGTTCAACATC
			R	GATGAGTTTGGACAAACCAC
Myo	60	0.25	F	TTACGTCCATCGTGGACAGC
			R	TGGGCTGGGTGTTAGTCTTA
Bapx1	58	wt: 0.28 -/-: 1.4kb	F	CCGAACCAGAACAGCCGTGG
			R	CAGCCCCCTTCCTGGAGAAC
Neo	65	0.2	F	CATCGCCTTCTATCGCCTTC
			R	CAGCCCCCTTCCTGGAGAAC
Rwhs	56	0.6	F	CTTTCCACCCCATTTCCTCT
			R	AGGCTCTGTCAGCCCAGTTA
ShCre	57	0.28	F	CAATTTACTGACCGTACAC
			R	CAGATTACGTATATCCTGG
EPCreJn	63	1.7	F	GAGCGCGACTCTGCTCTTCG
			R	GTTACCCCCAGGCTAAGTGCC
R26R	58	0.5	F	GGAGCGGGAGAAATGGATATG
			R	AAAGTCGCTCTGAGTTGTTAT
LoxSTOPLox **genotyping**	55	0.49	F	CCTCTACAAATGTGGTATGG
			R	TCCAACCTATGGAACTGATG
LoxSTOPLox **recombination**	57	Recomb.: 0.23 Not: 1.6	F	GATCGCCATTTCCTGTTTGTC
			R	GGAAGGCTGCGCTCCTCG

Table 7.3 **- Genotyping PCR primers used**

7.3.2 PCR amplification programs and primers

PCR programs are provided in **Table 7.4**. Programs were run on an MJ Research DNA Engine Tetrad.

Program	1 (°C/t)	2 (°C/t)	3 (°C/t)	4 (°C/t)	5 (cycles)	6 (°C/t)	Product (~kb)	Taq used/ [Mg^{2+}]
LacZ/ Myo	94/3m	94/20s	59/30s	72/50s	x 34	72/10m	L 0.6 M 0.25	St
Bap	94/3m	94/15s	58/30s	72/2m	x 34	72/10m	WT: 0.28 -/-: 1.4	Pl 1.25mM Mg^{2+}
Neo	94/3m	94/15s	65/25s	72/25s	x 29	72/10m	0.2	St
Rwhs	94/3m	94/30s	57/30s	72/45s	x 39	72/10m	~0.6	St
ShCre	94/3m	94/1m	57/1m	72/1m	x 29	72/10m	0.25	St
EPCreJn	94/3m	94/1m	61/1m	72/2m	x 34	72/10m	1.7	Pl
Hprt	94/3m	94/45s	58/45s	72/2m	x 29	72/10m	Sp 0.3 Un 1.2	St
CreRT	94/3m	94/45s	56/45s	72/50s	x 34	72/10m	Sp 0.3 Un 0.88	Pl
CreISH	94/2m	94/15s	54/30s	72/45s	x 34	72/10m	0.66	Hi
IfOligoIn	94/3m	94/45s	57/30s	72/25s	x 34	72/10m	In 0.14 Not 0.07	St
LSL	94/2m	94/15s	60/30s	68/90s	x 29	68/10m	1.4	KOD
OligoOri	94/2m	94/30s	55/30s	72/45s	x 29	72/10m	0.4	St
LSLOri, LSL genotyping	94/2m	94/30s	55/30s	72/45s	x 29	72/10m	0.37	St
LSL recombination	94/3m	94/45s	57/30s	72/1m	x 34	72/10m	R 0.23 NR 1.6	St
M13 sequencing	96/2m	96/30s	50/15s	60/4m	x 29	-	Variable	Big Dye
***Wnt* degenerate**	94/2m	94/1m	55/90s	72/1m	x 29	72/10m	0.4	St 1.5mM Mg^{2+}
***Wnt2, Wnt7a* RT**	94/3m	94/30s	56/30s	72/30s	x 34	72/10m	0.3 0.5	Pl 2mM Mg^{2+}
***Wnt2b/13, Wnt4, Wnt5a, Wnt10b* RT**	94/3m	94/30s	60/30s	72/30s	x 34	72/10m	0.32 0.34 0.22 0.18	Pl 2mM Mg^{2+} *Wnt4* 1.5mM *Wnt10b* 1mM
***Wnt3/8a ISH* probe**	94/3m	94/30s	59/30s	72/30s	x 34	72/10m	0.74 0.4	Hi
***Wnt2 ISH* probe**	94/2m	94/30s	55/30s	72/45s	x 34	72/10m	0.47	Pl
***Wnt10b ISH* probe**	94/2m	94/30s	55/30s	72/45s	x 34	72/10m	0.6	Pl
***Fzd* degenerate**	95/5m	95/1m	55/90s	72/90s	x 34	72/10m	0.18-0.34	Pl 1.5mM Mg^{2+}

***Table 7.4* - PCR programs used**

This table includes details of programs used for cloning procedures, genotyping, RT-PCR, making *in situ* probe templates, and for BigDye sequencing reactions.
Steps: (1) Initial denaturation, (2) denaturation, (3) annealing, (4) elongation, (5) repeat stages 2-4 x *n* cycles, (6) final extension. Samples were maintained at 16°C following step (6).
Key: t: time, m: minutes, s: seconds; Sp: spliced, Un: Unspliced; H: Hi-fidelity *Taq* polymerase, St: standard *Taq* polymerase, Pl: Platinum *Taq* polymerase, KOD: Hi-fidelity Hot Start KOD polymerase; R: recombined, NR: non-recombined

7.3.3 Molecular cloning of PCR products

7.3.3.1 Sub-cloning via pGEM-T Easy vector (Promega)

PCR products amplified using standard *Taq* polymerase (without 3'-to-5' exonuclease proofreading activity) – and hence mostly with a single adenine overhang - were ligated directly into the pGEM-T Easy vector (Promega) according to the manufacturer's instructions. 3µl of the ligation was transformed into library-efficiency DH5α competent cells according to the manufacturer's protocol (Invitrogen).

7.3.3.2 Screening for transformants

Selection was performed on X-gal/IPTG/ampicillin L-agar plates. The pGEM-T Easy vector confers ampicillin resistance on host cells, allowing positive selection of vector-containing cells. Clones containing a successful insert:vector ligation were selected for by X-gal/IPTG, as insertion of the PCR product into the pGEM-T Easy vector disrupts the *LacZ* gene; thus transformants were identified as white, as opposed to blue, colonies.

7.4 Sequencing

Plasmid DNA for sequencing was prepared as described in **Section 7.2.4.1** (Miniprep). DNA was sequenced using the dye-labelled terminator BigDye (Applied Biosystems). Reagents were thawed on ice and dyes protected from light as much as possible. Reactions (20µl final volume) were prepared in 0.5ml centrifuge tubes as follows:

200-500ng plasmid DNA in dH_2O	11µl
BigDye reaction mix	8µl
Primer (3.2 pmoles)	1µl

Sequencing primers are provided in **Table 7.2.**

Cycle sequencing was performed in an MJ Research DNA Engine Tetrad using the programs listed in **Table 7.4**. Reactions were then transferred to a fresh 1.5ml centrifuge tube and were ethanol precipitated as described in **Section 7.1.7**. Reactions were left on ice for 15 minutes to precipitate, before centrifuging at 13,000rpm for 30 minutes at 4°C. Pellets were washed with 200µl 70% EtOH. The supernatant was removed following a second centrifugation step and pellets were dried at room temperature for approximately 20 minutes. Samples were submitted to the HGU sequencing service to be run on an ABI machine.

7.5 Animal husbandry

Mice were housed in two facilities: a barrier facility for animals created by transgenic approaches (Transgenic Unit [TGU]), and a semi-barrier facility for all other mice (Biomedical Research Facility [BRF]). All procedures were carried out under Home Office licence where required, and with respect to the "3Rs" (Reduction, Refinement, Replacement). Wild type animals (CD1, CBA, and C57BL/6) were obtained from Charles River Laboratories. For timed matings, embryonic day 0.5 (E0.5) was the morning when a vaginal plug was detected.

7.5.1 Genotyping of breeding mice

Ear clips were taken from breeding animals both as a means of identification and as a source of genomic DNA for genotyping by PCR. Ear clips were collected in sterile 0.5ml tubes, and DNA extracted from each clip by immersion in 50µl of 25mM NaOH, 0.2mM EDTA, followed by incubation at 95°C for 20 minutes. Reactions were neutralised with 50µl of 40mM Tris.HCl, and then briefly vortexed to break up the tissue. Genotyping PCRs were usually performed immediately on samples, although genotyping after storage at 4°C or -20°C was also practiced. 2µl of extracted DNA solution was typically used in a 20µl genotyping PCR assay; primer sequences are provided in **Table 7.3**. The use of filter tips, a dedicated PCR room under positive pressure, and care to avoid cross-contamination of DNA samples reduced the chances of mis-genotyping.

The *Rwhs* mutation was detected by sequencing and identification of the following base change: GGCCAAACGGA**T=>C**

7.5.2 Harvesting of postimplantation embryos

Post-implantation embryos were harvested for use in RNA/cDNA preparation, X-gal staining, *in situ* hybridisation, and gut culture studies. Pregnant mothers were sacrificed by cervical dislocation, the abdominal cavity opened and the uterus removed. Uteri were placed in 50ml falcon tubes containing ice-cold PBS, ice-cold DEPC-PBS (for RNA experiments), or 37°C DMEM culture medium (for gut culture). Embryos were dissected out from the uteri in the above solutions, and the extra-embryonic membranes removed using scissors and forceps. Extra-embryonic membranes (yolk sacs) were retained for genomic DNA extraction if genotyping was required. Embryos were staged according to the Emap "Theiler Staging Criteria for Mouse Embryo Development" chart (http://genex.hgu.mrc.ac.uk/Atlas/theiler2.ppt)

7.5.2.1 Genotyping of embryos

Genotyping of embryos was performed on genomic DNA extracted from extra-embryonic membranes (yolk sacs). Each removed membrane was placed in an individual 1.5ml tube, and digested overnight at 55°C using Proteinase K (Sigma); frozen stocks of 10mg/ml Proteinase K were added to Tail Tip Buffer to a final concentration of 0.1mg/ml, and 0.5ml of this placed in each tube.

Tail Tip Buffer (Proteinase K lysis buffer):

	Final concentration
Tris.HCl pH8.0	100mM
EDTA	50mM
NaCl	100mM
SDS	1%

The following morning, DNA was extracted from the digestions. If the yolk sac had been taken from an E10.5 or younger embryo, then the digest was briefly vortexed and then centrifuged for a few seconds, to recover liquid from the tube cap, and this same tube used for the subsequent steps. Digests of yolk sacs taken from E11.5 or older embryos were vortexed briefly and then centrifuged for 10 minutes at 13,000rpm to pellet debris; the supernatant was removed to a new tube and this used for subsequent steps. 1ml chilled 70% acetone/5% DMF (in 25% dH_2O) was added to each tube, and mixed with the digest solution by inversion. DNA was then pelleted by centrifugation for 10 minutes at 13,000rpm. The supernatant was then carefully decanted and the pelleted DNA washed in 70% ethanol on a rotator for two hours at RT. Tubes were centrifuged for 5 minutes at 13,000rpm, the supernatant discarded, and samples air-dried at RT. DNA was resuspended in 50-200µl TE, pH8.0 depending upon the size of the pellet. Resuspension was aided by incubation at 55°C for 15 minutes.

PCR genotyping assays:

Genotyping PCRs were typically performed on 2µl of the yolk sac DNA, using primers and programs detailed in **Tables 7.2 and 7.4**, and were examined by agarose gel electrophoresis.

7.5.3 Microscopy

Dissections of p ost-implantation embryos were visualised using a Leica Stereo MZFLIII stereo fluorescence microscope (Leica Microsystems, Milton Keynes, UK) fitted with a fibre optic cold light source and illuminated base for incident/transmission illumination. Images were captured with a Photometrics CoolSnap colour CCD camera (Roper Scientific, Tucson, Arizona) controlled by scripts written for IPLab Spectrum (Scanalytics Inc., Fairfax, VA).

7.5.4 Production of transgenic mice

7.5.4.1 Preparation of linearised recombinant DNA for microinjection into fertilised oocytes

Maxiprep plasmid DNA was linearised using the appropriate enzyme(s) to release the transgene for microinjection (50-100µg DNA in a 100µl reaction). Pipette tips used for setting up the digestion were first cleaned with MilliQ water. Digested DNA was electrophoresed on a 1% LMP agarose gel in TAE alongside DNA size markers to check that digestion had worked correctly. The band containing the transgene was then excised from the gel and the agarose digested by treatment with Agarase (Roche) according to the manufacturer's instructions.

The DNA was purified and concentrated using Microcon-30 spin columns (Amicon) according to the manufacturer's instructions. Briefly, DNA was passed through the column and washed three times using 0.1mM EDTA/1mM Tris pH7.4. The DNA was eluted in 10µl 0.1mM EDTA/1mM Tris pH7.4 and the eluate was then diluted 1:10 in microinjection buffer (0.1mM EDTA/10mM Tris pH7.4). The DNA concentration was determined by electrophoresis and spectrophotometery. DNA was stored at -20°C until the day of microinjection, at which point it was diluted in transgenic buffer to a final concentration of 2ng/µl and spun through a Spinex 0.22µm column (Costar) according to the manufacturer's protocol. The final DNA preparation was provided in individual aliquots for microinjection.

Alternatively, the digested DNA was run on a 1% SEAKEM GTG agarose/MilliQ TAE gel, and the transgene recovered from the excised gel slice by electro-elution, using an Elutrap starter kit

(Schleicher & Schuell) according to the manufacturer's instructions. The eluted DNA was then subjected to precipitation with isopropanol (equal volume) and sodium acetate (1/10 volume) at -20°C for two hours. Following centrifugation (as per EtOH precipitation), a 70% EtOH wash and further centrifugation were performed and the pelleted DNA resuspended in microinjection buffer (as above). The concentration of the DNA was determined by electrophoresis and spectrophotometery. When needed the DNA was diluted in microinjection buffer to a final concentration of 2ng/µl and spun through a Spinex 0.22µm column (Costar). Again, DNA was provided in individual aliquots for microinjection.

7.5.4.2 Microinjection of recombinant DNA and oviductal transfers

Microinjections and subsequent oviductal transfers into pseudopregnant females were performed by Brendan Doe, Simon Heaney, Paul Devenney, and Laura Lettice, as described in (MacKenzie et al., 1997). The one-cell embryos used for microinjection were derived from superovulated [CBA x C57BL/6] F1 females.

7.5.5 Identification of transgenic mice

Progeny from recipient female mice were ear clipped at weaning (approximately 21 days of age) to provide genomic DNA for genotyping to identify those in which the transgene DNA had integrated. Genotyping was performed as described in **Section 7.5.2.1**, and was carried out in at least duplicate. Mice carrying the transgene constituted the founders of subsequent lines, and were mated with [CBA x C57BL/6] F1 mice from around 6-8 weeks of age (sexual maturity). Subsequent generations were genotyped to confirm faithful transmission of the transgene. Male founders were also mated with CD1 females to examine transgene expression during embryonic development.

7.5.6 Analysis of transgenic mice

7.5.6.1 Solutions

Detergent wash:

Compound	Per litre	Final concentration
Na_2HPO_4 (Fisher)	9.94g	0.1M, pH7.3
NaH_2PO_4 (BDH)	4.14g	0.1M, pH7.3
$MgCl_2$ (Riedel-de Haen)	0.406g	2mM
Sodium deoxycholate (Sigma)	1g	0.1%
Nonidet P-40 (ICN Biomedicals Inc.)	200µl	0.02%

Bovine Serum Albumin (BSA) (Sigma)	0.5g	0.05%

The solution was made up to 1 litre with dH_2O.

X-gal staining solution:

Compound	Per 250ml	Final concentration
NaCl (BDH) (5M)	3.6ml	0.085%
$K_3Fe(CN)_6$ (Sigma)	410mg	5mM
$K_4Fe(CN)_6$ (Sigma)	525mg	5mM

The solution was made up to 250ml with detergent wash.

Prior to use, 30µl X-gal substrate (50mg/ml in DMF) (Melford) was added per 5ml staining solution to the volume required.

7.5.6.2 X-gal staining protocol

LacZ expression was assayed using X-gal. Embryos were dissected in PBS and fixed in 4% PFA/PBS at RT for the following times:

Whole embryos:

E8.5 – 30 min, E9.5 – 45 min, E10.5 – 1 hr, E11.5 – 1½ hr, E12.5 – 2 hr, E13.5-16.5 – 3 hr

Guts:

E11.5-12.5 – 20 min, E13.5-14.5 – 30 min, E15.5-16.5 – 45 min, E17.5-18.5 – 1hr

Fixed embryos/guts were rinsed in PBS and then washed in detergent wash for 20 minutes, three times, at room temperature. Staining was performed overnight in X-gal staining solution, protected from light, at 37°C. The staining solution was removed the following morning and the samples were rinsed in detergent wash for 20 minutes, three times, at room temperature before being fixed a final time in 4% paraformaldehyde (PFA)/PBS at 4°C overnight. The fix was then removed and the tissues washed, and stored, in PBS.

7.6 Detection of gene expression

7.6.1 RNA in situ *hybridisation*

7.6.1.1 Preparation of templates for in vitro *transcription*

Details of probes used for *in situ* hybridisation can be found in **Table 7.5**. Digoxygenin (DIG) labelled anti-sense RNA probes were transcribed *in vitro* from either cDNA-containing plasmids or PCR products amplified from cDNA.

Plasmids were linearised by digestion with a suitable restriction endonuclease at the 5' end of the cDNA insert, such that transcription progressing from the RNA polymerase promoter 3' to the insert terminated at this cleaved point; this generates an RNA transcript complimentary to the region of the gene being analysed. 20μg Maxiprep plasmid DNA was linearised overnight in a 100μl reaction and then purified by phenol-chloroform extraction followed by ethanol precipitation. From the precipitation stage onwards, RNase-limiting precautions were taken, as described in **Section 7.6.2.1**. 70% EtOH was made with DEPC-dH_2O, and DNA was resuspended in 10-50μl DEPC-dH_2O. DNA concentration was measured by gel electrophoresis and spectrophotometery as described in **Section 7.1.4**, and ~1μg used as the template for *in vitro* transcription.

The alternative type of template used was generated by PCR, using a standard forward primer and a reverse primer incorporating a suitable RNA promoter at its 5' terminus. Primer details and programs are given in **Tables 7.4 and 7.5**. PCR was performed in a 100μl reaction volume, using Hi-Fidelity Taq polymerase (Invitrogen) and a cDNA template. If additional bands were generated in the PCR, the desired product was excised and gel extracted. If no contaminating bands were present, the PCR product was used directly as the template for *in vitro* transcription. DNA concentration was estimated by gel electrophoresis, and 0.05-0.2μg used for *in vitro* transcription.

7.6.1.2 Preparation of labelled riboprobes

Immediately prior to *in vitro* transcription, template DNA was heated to 55°C for two minutes and then chilled on ice. *In vitro* transcription from the appropriate RNA polymerase promoter (SP6, T3, or T7) and concomitant labelling of the transcript with DIG was achieved using the DIG RNA labelling kit from Roche. The manufacturer's instructions were employed, with the following alterations: reaction volumes were scaled up 2x, and only half of the total RNA polymerase was added at the start of the 37°C incubation, with the remainder being added after 1 hour of incubation. After two hours total incubation, residual template DNA was destroyed by the addition of 2μl RNase-free

DNaseI for 15 minutes at 37°C. The reaction was stopped with the addition of 0.8µl 0.5M EDTA (pH8).

7.6.1.3 Purification of labelled riboprobes

Labelled riboprobes were purified using NucTrap Probe Purification columns (Stratagene), according to the manufacturer's instructions. 2µl RNase inhibitor (Roche) was added to the probe which was then aliquotted for storage at -20°C. Purified products were examined by electrophoresis on a 1% agarose gel, using the conditions described in **Section 7.1.3.2**. Precautions were taken throughout both the transcription and purification stages to limit RNA degradation, as described in **Section 7.6.2.1**.

7.6.1.4 Whole mount in situ *hybridisation*

Gene expression in both embryos and embryonic guts was analysed by whole mount *in situ* hybridisation.

7.6.1.4.1 Solutions for whole mount in situ hybridisation

To protect RNA from degradation by RNases, solutions were made using DEPC-dH_2O, DEPC-PBS and DEPC-SSC for all steps prior to, and inclusive of, riboprobe hybridisation. Additionally, the general precautions described in **Section 7.6.2.1** were taken in order to limit RNA degradation.

DEPC-PBT

PBT was made by adding 0.5ml 10% Triton X-100 (Sigma) to 50ml DEPC-PBS (final concentration 0.1%). DEPC-PBT was prepared fresh for each *in situ* hybridisation run.

4% paraformaldehyde (PFA)

4% PFA (Sigma) was freshly prepared on the day it was required, by dissolving PFA in DEPC-PBS (weight/volume) at 65°C. NaOH was added to a concentration of 1.75mM to help get the PFA into solution. The PFA solution was then chilled and kept on ice until needed.

Probe	Template	Size (nt)	Restriction enzyme	RNA polymerase	Source
Wnt2b/13	Plasmid	n/a	EcoRI	SP6	Ragsdale, C
Wnt4	Plasmid	~1200	HindIII	T7	Kispert, A
Wnt5a	Plasmid	~360	EcoRI	SP6	McMahon, A
Wnt7a	Plasmid	~400 n/a	BamHI EcoRI	T7 T7	McMahon, A Ragsdale, C
Hand2	Plasmid	n/a	n/a	n/a	Srivastava, D
Probe	**Template**	**Size (nt)**	**Primer sequence 5' => 3'**	**RNA polymerase**	**Source**
Nkx2-5	PCR product	328	F: ACTTGAACACCGTGCAGAGTCC R: TAATACGACTCACTATAGGGGTGTGGAATCCGTCGAAAGTGC	T7	Hecksher-Sørensen, J. (primers)
Cre	PCR product	663	F: CATTTGGGCCAGCTAAACATG R (T7): TAATACGACTCACTATAGGGCATGATCTCCGGTATTG R (SP6): ATTTAGGTGACATATAGATGCATGATCTCCGGTATTG	T7 SP6	Burn, S
Wnt2	PCR product	472	F: CTCCCTCTGCTCTTGACCTG R: TAATACGACTCACTATAGGGTGTCCTTGGCACTTCCTTTC	T7	Burn, S
Wnt3	PCR product	740	F: ACCTGGAGAAGGCTGGAAGTG R: TAATACGACTCACTATAGGGAACAGTCCATGCTCCTTGCTG	T7	Burn, S
Wnt8a	PCR product	425	F: TGGAGGAGAGGAGAGCAGAG R: TAATACGACTCACTATAGGGAGTAACTGCGCAGGAAAGG	T7	Burn, S
Wnt10b	PCR product	597	F: GAAAACCTGAAGCGGAAGTG R: TAATACGACTCACTATAGGGCTACACCCCCAGAGCTGTTC	T7	Burn, S

Table 7.5 - Probes used for *in situ* hybridisation
The top part of the table contains cloned probe details - the restriction enzyme used to cleave at the 5' end of the insert, and the RNA polymerase required for production of an anti-sense probe. The lower part of the table shows details of probes generated from PCR products primed with a promoter-containing reverse primer. The incorporated promoter sequence is shown in red, and the annealing temperature used in the PCR program indicated for each primer pair. F, forward; R, reverse. Unavailable details are written as "n/a" (not available).

Pre-hybridisation solution (pre-hyb)

Compound	Amount added per 50ml	Final concentration
De-ionised formamide (Sigma)	25ml	50%
20XDEPC-SSC	12.5ml	5X
Blocking powder (Roche)	1g	2%
Triton X-100 (10%) (Sigma)	0.5ml	0.1%
CHAPS (10%) (Sigma)	2.5ml	0.5%
Yeast RNA (50mg/ml) (Sigma)	1ml	1mg/ml
EDTA (0.5M)	0.5ml	5mM
Heparin (10mg/ml) (Sigma)	250µl	50µg/ml

The solution was made up to 50ml with DEPC-dH_2O and gently mixed.

Post-hybridisation solution (post-hyb)

Compound	Amount added per 50ml	Final concentration
De-ionised formamide	25ml	50%
20XSSC	12.5ml	5X
Triton X-100 (10%)	0.5ml	0.1%
CHAPS (10%)	2.5ml	0.5%

The solution was made up to 50ml with dH_2O.

TNT

Compound	Amount added per 50ml	Final concentration
TRIS (1M, pH7.5)	2.5ml	50mM
NaCl (5M)	1.5ml	150mM
Triton X-100 (10%)	0.5ml	0.1%

The solution was made up to 50ml with dH_2O.

Blocking solution

Compound	Amount added per 50ml	Final concentration
Sheep serum*	7.5ml	15%
BSA	1g	2%
TRIS (1M, pH7.5)	2.5ml	50mM
NaCl (5M)	1.5ml	150mM
Triton X-100 (10%)	0.5ml	0.1%

* Heat inactivated at 50°C for 1 hour.

The solution was made up to 50ml with dH_2O and filtered before use using a 0.45µm syringe filter (Millipore).

NMT

Compound	Amount added per 50ml	Final concentration
TRIS (1M, pH9.5)	5ml	0.1M
NaCl (5M)	1ml	0.1M
$MgCl_2$ (1M)	2.5ml	50mM

The solution was made up to 50ml with dH_2O.

NMT-T

NMT-T was made by adding Triton X-100 (10%) to NMT to a final concentration of 0.1%

7.6.1.4.2 Preparation and storage of tissue for *in situ* hybridisation

Embryos were dissected in chilled DEPC-PBS and the extra-embryonic membranes saved for genotyping purposes where necessary. Embryos and guts were fixed immediately after dissection in 4% PFA (in DEPC-PBS) at overnight. The fix was removed the following morning and the tissue washed with chilled DEPC-PBT for three times 10 minutes at 4°C. Unless the tissue was to be used immediately, dehydration through a methanol (MeOH) series was performed. Tissues were washed for 15 minutes in each increasing concentration of MeOH: 25%, 50%, 75% MeOH in DEPC-PBT, followed by storage at -20°C in 85-100% MeOH.

7.6.1.4.3 Procedure for whole mount *in situ* hybridisation

Day 1

Dehydrated tissue was rehydrated through a MeOH series consisting of decreasing concentrations of MeOH in DEPC-PBT - 75%, 50% and 25% - and then washed three times in DEPC-PBT for five minutes each. All washes were carried out at 4°C in 5ml solution, in 50ml tubes, and all solutions were pre-chilled.

Tissues were subjected to mild digestion at RT with 10µg/ml Proteinase K (Roche) in DEPC-PBT. Treatment time varied according to the size of the tissue: E9.5, E10.5, E11.5, and E12.5 whole embryos were treated for 20, 25, 25, and 30 minutes respectively; E11.5, E12.5, and E14.5 guts were treated for 10, 15, and 20 minutes respectively. Tissue was then washed in chilled DEPC-PBT 3 times for 5 minutes each, and re-fixed in 4% PFA (in DEPC-PBT) for 30-45 minutes on ice.

Following re-fixation, tissues were subjected to another three 5 min chilled DEPC-PBT washes and then transferred to 2ml cryotubes. The DEPC-PBT was replaced with RT pre-hyb solution and the samples left for up to 30 minutes at RT to equilibrate (indicated by sinking). The pre-hyb solution was then changed and samples again left to equilibrate. The pre-hyb was then once again replaced and samples incubated in this solution at for 1 hour until the pre-hyb was replaced a final time. This final 65°C incubation lasted 3-4 hours, after which as much as possible was removed prior to addition of the probes.

Samples were incubated overnight at 65°C with pre-hyb containing the appropriate DIG-labelled riboprobe. Probes were thawed on ice and the required amount added to 100µl chilled pre-hyb solution to reach a probe final concentration of 250ng/ml. Precautions were taken to limit RNase activity, as described in **Section 7.6.2.1**. Immediately before introduction of this probe mixture to samples, the probe was denatured by heating to 80°C for 3 minutes in pre-hyb.

A control probe (*Hand2/Hand2*) was always used on an appropriate tissue (E10.5 whole CD1 embryo) to confirm that the *in situ* hybridisation procedure had worked (expression detected in limb buds, heart, and arches).

Day 2

The probe hybridisation solution was removed and replaced with a series of pre-warmed 1ml washes in fresh post-hyb solutions, each for 10 minutes at 65°C: 100% post-hyb, 100% post-hyb again, 75% post-hyb/25% 2XSSC, 50% post-hyb/50% 2XSSC, 25% post-hyb/75% 2XSSC. Tissues were then washed twice in 2XSSC/0.1% CHAPS for 30 minutes at 65°C and twice in 0.2XSSC/0.1% CHAPS, again at 65°C for 30 minutes. Fresh TNT was used to wash the samples at RT, three times for 5 minutes each, prior to blocking. Samples were incubated in fresh blocking solution for at least 4 hours (with 3 changes) at 4°C.

Finally, tissues were incubated in 1ml antibody solution at 4°C overnight with gentle rocking. The antibody solution was prepared by adding anti-DIG-AP fab fragments (Roche) at a 1:2000 dilution to chilled blocking solution.

Day 3

Unbound anti-DIG antibody was removed from samples by washing 5 times in TNT/0.1% BSA (filtered using a 0.45µm syringe filter) for 1 hour each at RT, with gentle rocking. Tissues were then left in a further change of TNT/0.1% BSA at 4°C, either overnight or for up to 2 days, again with gentle rocking.

7.6.1.4.4 Standard detection of riboprobes

Day 4

Prior to staining, tissues were washed 3 times for 30 minutes each in NMT-T at room temperature. Staining solution was prepared by the addition of 3.3µl/ml NBT (100mg/ml in DMF) (Roche) and 3.5µl/ml BCIP (50mg/ml in DMF) (Roche) to NMT-T, and was filtered using a 0.45µm syringe filter. Samples were stained at RT in the dark, in glass vials containing 3-5ml staining solution. Staining progress was examined every 20 minutes until a suitable staining pattern had developed with minimal background. Development time was dependent upon the probe used and expression pattern being examined, but typically occurred within 1 to 3 hours. The staining reaction was terminated by washing the samples 3 times in PBS, for 5 minutes each on ice. Stained tissues were then fixed in 4% PFA (in PBS) overnight at 4°C.

7.6.1.4.5 Fast Red detection of riboprobes

Day 4

In preparation for Fast Red staining, embryos/foreguts were washed 3 times in 0.1M TRIS pH8.2 for 20 minutes each. The staining solution was prepared by the addition of 1 Fast Red tablet (Roche) per 2ml 0.1M TRIS pH8.2, followed by vortexing the solution until the tablet was dissolved. Tissue was stained at 37°C in the dark, monitored and the reaction terminated as described in **Section 7.6.1.2.4**. Fast Red detection permitted both brightfield and fluorescence imaging of the resultant gene expression pattern. Fluorescent signal was visualised by confocal microscopy (**Section 7.7.4**).

7.6.2 Expression analysis via RT-PCR

7.6.2.1 RNA extraction

RNA was extracted from the tissue of interest in order to make template cDNA for use in reverse transcription (RT)-PCR. Extreme care was taken during RNA extraction to avoid contamination with RNases: work surfaces were cleaned with the RNase-inactivating agent RNAZap (Ambion), tubes and filter-tips used were guaranteed RNase-free, solutions were made with DEPC-dH_2O, reagents were kept on ice until required, gloves were worn at all times, and only reagents reserved solely for RNA work were

used. RNA was extracted as quickly as possible after thawing samples in order to minimise the activity of endogenous RNases and thus limit degradation.

Embryos were dissected in ice-cold DEPC-PBS and the tissues of interest transferred to chilled screw-cap eppendorf tubes. Samples were then frozen in liquid nitrogen and stored at -70°C. To isolate total RNA, the tissue was removed to dry ice and RNA extracted by one of two methods: using the RNeasy Micro kit according to the manufacturer's instructions (QIAgen), or with TRIZOL treatment followed by chloroform extraction and isopropanol/ethanol precipitation. To extract total RNA with TRIZOL, the tissue was immediately homogenised in 1ml TRIZOL (Invitrogen) with the aid of a 1ml syringe and needle. 100µl chloroform was then added and the sample vortexed for 15 seconds before being placed on ice for 5 minutes. The sample was then centrifuged for 15 minutes at 13,000rpm, 4°C, and the upper (non-pink) layer transferred to a fresh screw cap eppendorf tube. An equal volume of isopropanol was added, and the sample vortexed for 15 seconds. The sample was then put on ice for 15 minutes, followed by a further centrifugation as before. The resulting supernatant was discarded and the pellet washed in 70% ethanol (made up in DEPC-dH_2O). RNA was re-suspended in 50µl DEPC-dH_2O, and the concentration determined by spectrophotometery.

If RT-PCR was to be performed using intron-spanning primers - hence giving differently sized spliced (expressed) and unspliced (genomic) products – then DNase treatment was not necessary. RNA which was to be used to generate cDNA for use in RT-PCRs which did not differentiate between spliced and unspliced sequences was treated with DNase, to remove contaminating genomic DNA. 1µl DNaseI (RNase-free; Roche) was typically used to treat 3-5µg RNA in a 30µl reaction (3µl 10X transcription buffer [Roche]; to final volume with DEPC-dH_2O) at 37°C for 15 minutes. Following DNA digestion, the DNase was removed by phenol-chloroform extraction and NaOAc/ethanol precipitation to prevent DNase digestion of newly amplified DNA in subsequent RT-PCRs.

7.6.2.2 cDNA synthesis

A First Strand cDNA Synthesis kit (Roche) was used according to the manufacturer's instructions for cDNA synthesis prior to RT-PCR.

7.6.2.3 RT (Reverse Transcription) PCR

RT-PCR primers are detailed in **Table 7.6**, and the programs used are summarised in **Table 7.4**. PCR reactions were performed as described in **Section 7.3**.

Template/ Primer set	PCR conditions		Primers	
	Anneal (°C)	Product size (bp)	Primer sequence 5' → 3'	
Hprt	55	Spliced: 295 Unspliced: ~1200	F	CTGTAGATTTTATCAGACTGAAGA
			R	GTCAAGGGCATATCCAACAACAAA
CreRT	56	Spliced: 304 Unspliced: 876	F	TTTGCAAAAAGCTGGATCG
			R	CGGTTATTCAACTTGCACCA
Wnt degenerate	55	~400	F	GGGGAATTCCARGARTGYAARTGYCAT
			R	AAAATCTAGARCARCACCARTGRAA
Wnt2	55	Spliced: ~500 Unspliced: large	F	CGGCCTTTGTTTACGCCATC
			R	TGAATACAGTAGTCTGGAGAA
Wnt2b (13)	60	Spliced: 318 Unspliced: 4kb	F	TGTACTCTGCGCACCTGCT
			R	TGCACTCACACTGGGTGAC
Wnt4	60	Spliced: 344 Unspliced: 6kb	F	TGTACCTGGCCAAGCTGTCAT
			R	TCCGGTCACAGCCACACTT
Wnt5a	60	Spliced: 224 Unspliced: 4kb	F	TCCTATGAGAGCGCACGCAT
			R	CAGCTTGCCCCGGCTGTTGA
Wnt7a	57	Spliced: 307 Unspliced: 30kb	F	CAAGGCCAGTACCACTGGGA
			R	GGCTCCACGTGGACGGCCTC
Wnt10b	59	Spliced: 179 Unspliced: 2.1kb	F	CGGCTGCCGCACCACAGCGC
			R	CAGCTTGGCTCTAAGCCGGT
Fzd degenerate - Daudet	55	180-270	F	NNNGAATTCTAYCCNGARMGNCCNAT
			R	NNNAAGCTTNGCNGCNARRAACCA
Fzd degenerate - Ricken	55	210-240	F	TAYCCNGARCGNCCNATYAT
			R	AGAGTNAGDATNACCCACCA

Table 7.6 - RT-PCR primers used

7.7 Analysis of gene expression

Gene expression patterns were examined in both whole and sectioned tissues. Sectioning was performed physically using either a microtome or vibratome, or virtually by Optical Projection Tomography (OPT) analysis. Embedding and sectioning procedures for each technique are described below.

7.7.1 Agarose embedding

Fixed tissue was placed in a 50ml falcon tube and brought to 58°C in PBS in preparation for embedding. Tissue was then incubated at 58°C in increasing concentrations of LMP agarose (Invitrogen) in PBS: 1%, 2%, 3%, and 4%. The final (4%) wash was made using high-grade LMP. Each incubation lasted at least 15 minutes to allow the tissue to sink. The molten 4% LMP agarose containing the tissue was poured into a chilled small histological mould or petrel dish. Samples were orientated under a microscope using forceps and monitored at room temperature until the agarose set. In preparation for sectioning, the solid agarose block was trimmed using a surgical blade (Swann Morton) and stuck to the vibratome mount in the desired orientation with super-glue. Embedding and sectioning were performed on the same day for the best results (to prevent pulling away of the gel from the tissue).

7.7.1.1 Vibratome sectioning

Agarose-embedded samples were sectioned at 30-100μm on a vibratome. Sections were carefully transferred out of the vibratome waterbath onto a Superfrost Plus slide (VWR International) with the aid of a fine paintbrush. Excess water was removed from the slide using the tip of an absorbent tissue, and a drop of PBS placed on each section. Sections were then covered with a glass coverslip (VWR International) and the edges sealed with vulcanising solution (Rema Tip Top, Germany). Slides were stored flat at 4°C in the dark.

7.7.2 Wax embedding

Thinner histological sections were permitted by microtome sectioning of wax embedded samples. Prior to wax embedding, tissue was dehydrated in an increasing ethanol series: 30 (x2), 50 (x2), 70 (x2), 85 (x2), 95 (x2), and 100% (x3) EtOH in dH_2O. Each EtOH wash lasted 15 minutes, with the exception of the 100% washes which were of a half hour duration each. Tissue was then washed three times in Histoclear (National Diagnostics), for 20-45 minutes each, depending on tissue size. The final Histoclear wash was performed at 60°C. The tissue was then poured in a small volume of the hot Histoclear into a pre-warmed watchmaker's glass dish or glass bottle, and molten wax added to this to create a 1:1 mixture. After 5 minutes at 60°C the molten Histoclear:wax mix was removed and replaced with liquid paraffin wax. Three 45 minute incubations in wax were performed at 60°C, with the wax being replaced for each wash. Samples were then transferred to fresh molten wax in a pre-warmed plastic mould; transferral was facilitated by heated metal implements or heated pastettes with cut ends, and was performed on a heated surface. The tissue was orientated (using heated forceps or needles) with the aid of a microscope and then allowed to set at room temperature. Blocks were stored at room temperature or 4°C.

7.7.2.1 Microtome sectioning

The room-temperature wax block was trimmed to the desired size and the edges angled with a scalpel-blade to improve the capture of sections and facilitate correct orientation of the sections. Wax-embedded samples were sectioned at 5-10μm, depending on developmental stage, on a microtome according to standard operating procedures. Strings of serial sections were floated out in a 42°C waterbath and transferred to Superfrost Plus slides (VWR International) with the aid of a fine paintbrush. Slides were placed on a 37°C slide dryer for up to an hour and then incubated at 50°C overnight.

To de-wax the sections, the slides were washed three times in Histoclear for 5 minutes each, followed by two 10 minute washes in 100% ethanol and then a rinse in 100% ethanol. Sections were then subjected to a decreasing ethanol wash series: 90, 70, 50, and 30%, in dH_2O, for 5 minutes each. A two minute water wash followed and sections were then counterstained with Nuclear Fast Red (Vector Laboratories) if required, for 0.5-2 minutes. Following counterstaining, the sections were rinsed in running tap water for 10 minutes, and then dehydrated back through the ethanol series (30 seconds each wash this time). Slides were then washed three times for 2 minutes each in 100% ethanol, followed by three 5 minute washes in Histoclear. To mount the slides, Histomount (National Diagnostics) was added to each slide and a coverslip placed gently on top.

7.7.3 Optical projection tomography (OPT) analysis

7.7.3.1 Preparation of tissue

Fixed tissue was embedded in 1% LMP agarose (in sterile dH_2O). The set agarose block was trimmed with a surgical blade and glued to a cylindrical metal mount in the required orientation. The block was then placed in a clean glass scintillation vial and dehydrated at room temperature overnight with methanol. Samples were optically cleared for scanning the next day by replacing the methanol with fresh BABB (1 part Benzyl Alcohol (Sigma) to 2 parts Benzyl Benzoate (Sigma)). Samples were monitored every 15-30 minutes and OPT scanned once the tissue reached the desired transparency.

7.7.3.2 OPT scanning and data analysis

Samples were scanned in a BABB-filled cuvette by transmission OPT on an OPT scanner (BIOPTONICS). Information regarding OPT can be found at http://genex.hgu.mrc.ac.uk/OPT_Microscopy/. Data reconstructions and 3D movies were produced using scripts written by Dr. James Sharpe. GIMP software (a Unix version of Photoshop) was used to capture still images

7.7.4 Microscopy

Tissue sections were analysed on a Zeiss Axioplan II fluorescence microscope (Carl Zeiss Ltd., Welwyn Garden City, UK) equipped with colour additive filters (Andover Corp, Salem, NH) for sequential colour imaging and a Photometrics CoolSnap HQ monochrome CCD camera (Roper Scientific, Tucson, Arizona). Image capture was performed using scripts written for IPLab Spectrum (Scanalytics Inc., Fairfax, VA) which controlled camera capture and filter selection via motorised filter wheels (Ludl Electronic Products Ltd., Hawthorne, NY).

Fast-Red stained tissue was examined by confocal microscopy, using a Zeiss LSM510 confocal system attached to a Zeiss Axiovert 100m microscope. The system was fitted with an Argon laser (488 and 514 lines), and two HeNe lasers (lines at 543nm and 633nm). Images were captured and viewed using Zeiss LSM510 v3.00 software.

7.8 Gut organ culture

7.8.1 Preparation of explant tissue

In preparation for gut cultures, all media was heated to 37°C. Embryos were harvested as described in **Section 7.5.2**. Uteri were removed from sacrificed pregnant mice as quickly as possible and placed in 37°C DMEM (GIBCO) culture medium. Once the embryos had been dissected out from the uteri, and all extra-embryonic membranes removed, they were incubated in DMEM containing 10% foetal calf serum (FCS) (Hyclone) and 1% Pen/Strep (Sigma) at 37°C/5% CO_2; each embryo was removed from incubation only when it was to be dissected. DMEM is a cell-culture medium rich in amino acids, salts, glucose and vitamins. Pen/Strep is a combination of penicillin and dihydrostreptomycin; these antibiotics are active against mainly Gram-positive and Gram-negative bacteria respectively. The gas equilibrium of 5% CO_2 is known to be optimal for culture of embryos with more than 30 somites (>~E10.0/TS16) (Copp and Cockroft, 1990).

Guts were dissected out in warm DMEM/10% FCS/1% Pen/Strep using forceps cleaned in 70% ethanol/dH_2O, and returned to incubation at 37°C/5% CO_2 until all guts were ready for culturing. To aid in maintaining the structure of the guts in culture, and to provide landmarks for orientation, the oesophagus, lungs, and duodenum were left attached. Cutting and division of explants was achieved using tungsten needles.

Guts were cultured at 37°C/5% CO_2 in 24-well plates for 24-48hrs on either filter discs or Matrigel; each technique is described below.

7.8.2 Culture on filter discs

Millicell-CM culture plate inserts (Millipore) were placed in a 24-well plate, on top of DMEM/10% FCS/1% Pen/Strep. A thin layer of agarose (in PBS) was then added to each disc to provide support for gut cultures, and a further 200µl of DMEM/10% FCS/1% Pen/Strep dispensed onto this. Each gut was placed on a filter disc, positioned with forceps using a brightfield microscope, and excess media pipetted off such that the gut suctioned onto the disc but was not left dry.

Time 0hr (t0) photographs were taken once all guts had been prepared for culture using the QCapture imaging system (QImaging). The remaining wells of the culture plate were each filled with~1ml of media, to prevent evaporation from the explant cultures. The plate was then incubated at 37°C/5% CO_2 for the desired culture period.

7.8.3 Culture on Matrigel

The reduced growth factor form of Matrigel (BD Biosciences) was used to avoid potential interference with normal growth by exogenous factors. Matrigel is a commercially available substance which provides a biologically active extracellular matrix on which to submersion culture cells or tissue. It is composed of solubilised basement membrane extracts from Engelbreth-Holm-Swarm (EHS) mouse sarcomas. Matrigel is a solid both in -20°C storage and at 37°C, but can be dispensed as a liquid at 0-4°C. Accordingly, an aliquot of Matrigel was thawed on ice during gut dissections, and kept chilled along with pipette tips and a 24-well plate until needed. The Matrigel was then mixed 1:1 with chilled DMEM/10% FCS/1% Pen/Strep just prior to positioning of the guts within the 24-well plate. The 1:1 ratio was found to be optimal, as growth and survival was poorer at a higher concentration of Matrigel, whilst support and adhesion was lost with too high a concentration of media.

Guts were removed from incubation and transferred in DMEM/10% FCS/1% Pen/Strep to the chilled 24-well plate, then positioned with forceps using a brightfield microscope. Following each orientation, culture media was pipetted off and 20µl of chilled 1:1 Matrigel: DMEM/10% FCS/1% Pen/Strep was dispensed onto the gut.

A preliminary 1hr incubation at 37°C/5% CO_2 was performed to polymerise the Matrigel once all guts had been processed. If the guts were to be manipulated using aluminium foil strips (prepared using a sterile scalpel blade) then this was performed at RT during this time window. Photographs were also taken at t0 during this time using the QCapture imaging system (QImaging). At the end of the 1hr incubation, 200µl DMEM/10% FCS/1% Pen/Strep was added on top of each gut culture, and 1ml of this media also placed in each well of an empty row in the plate to minimise evaporation. The plate was then returned to incubation at 37°C/5% CO_2 for 24-48hrs. When the culture period was 48hrs, guts were checked at 24hrs and 50µl additional DMEM/10% FCS/1% Pen/Strep added if they were drying out.

7.8.4 Analysis of gut cultures

After culturing guts for the required time, they were removed from incubation and photographed using the QCapture system (QImaging). Forceps were then used to excise the guts from the Matrigel and the guts moved to a new 24-well plate to be washed and fixed. CD1 (non-transgenic) guts were washed three times in PBS, and then fixed in 4% PFA/PBS for 15 minutes. Guts derived from *NGRS-LacZ* (transgenic mice) were washed three times in detergent wash, fixed for 15 minutes in 4% PFA/PBS, and then assayed for *LacZ* expression by staining with X-gal overnight (**Section 7.5.6**). Stain solution was removed the following morning and guts were washed three times in PBS, followed by fixation in 4% PFA/PBS for 20 minutes. Both sides of the stained guts were then photographed using QCapture.

7.9 Bioinformatics

The following bioinformatics programs and resources were used:

Name	Web address/ Manufacturere	Function
Ensembl	http://www.ensembl.org	Provides annotated genome information
NCBI	http://www.ncbi.nlm.nih.gov	Molecular biology and genomic information repository
BLAST	http://www.ncbi.nlm.nih.gov/BLAST/	Detects sequence similarities
Primer3	http://biotools.umassmed.edu/bioapps/primer3_www.cgi	Picks primers from a sequence
Evolutionary conserved region (ECR) browser	http://ecrbrowser.dcode.org/	Identification of ECRs by multi-species genome alignment
MGI	http://www.informatics.jax.org/	Mouse Genome Informatics, including expression data
Sequencher	Gene Codes	Sequence analysis/ comparisons; contig assembly

***Table 7.7* - Bioinformatics programs and resources used**

Appendix: Chapter 2

Appendix Table 1 - Nkx2-5 regulatory elements

Study	Region (nt)	Conferred expression
(Reecy et al., 1999) Regions cloned directly in front of *LacZ*, in pBS; fragment micro-injected. All contain endogenous exon1 or 1a promoter	-1 ← -1626	E12.5: None
	-1 ← -3512	E12.5-13.5: I/OFT (portion), PH, TH, **ST, SP**. Ectopic: PCS (sparse); majority of heart is negative
	-1 ← -4059	E12.5: **ST**, TH, PH. Not in RV, AVC, IVS
	-1 ← -4434	E12.5: **ST**, TH, PH. Not in RV, AVC, IVS
	-1 ← -5011	E12.5: **ST**, TH, PH, RV (sparse)
	-1 ← -5870	E12.5: **ST**, TH, PH. Not in RV, AVC, IVS
	-1 ← -8554	E12.5: **ST**, TH, PH. Not in RV, AVC, IVS
	-1 ← -10765	E7.5: RV, LV, AT; E12.5-13.5: AVC, IVS, RVT, OFT, **SP, ST/PY,** TH, PH
	-887 upstream of Exon1a start Met	E12.5-13.5: OFT
	-7238 upstream of Exon1a start Met	E12.5-13.5: AVC, IVS, OFT
Conclusions	-1626 ← -3512	TH, PH, **SP, ST**. Not capable of driving heart expression at E7.5; sparse at E9.5 (PCS, I/OFT)
	-3512 ← -10765	CC and linear heart tube
	-4434 ← -5011	RV: positive element
	-5011 ← -5870	RV: negative element
	-8554 ← -10765	RV: positive element
(Searcy et al., 1998) Regions cloned in front of *LacZ*, in pBS, exon1 promoter; -2776 ← -3299 uses 1) **endogenous** TATA promoter, or 2) **hsp68** promoter	-1 ← -9276	E7.5-8.0: CC (anterior), PH; E12.5: OFT, RV, **SP**, PH.
	-1 ← -3299	E7.5-8.0: CC (anterior), PH, **left LPM;** E10.5: **mesenchyme underlying ST**, PH (NB: gut investigated more than with -2776 ← -3299)**;** E12.5: OFT, RV, **SP**, PH; E14.5: cardiac, **SP**, no ST
	-1 ← ~ -1200	None
	-2776 ← -3299 (chosen on basis of dense coverage of TF binding sites)	1) E7.5: CC; E10.5: OFT, PH, **SP**; E14.5: none 2) E8.5: heart tube; later: OFT, PH, **SP**. Not in E7.5 CC; heart expression weaker overall than with -3.3kb Paired GATA sites at -3018 ← -3035 are required for heart and **SP** expression

	-3300 ← -9270	Negative cardiac element within here, as heart expression with ~-9.3kb construct is less than with ~-3.3kb
	-2776 ← -3299	Sufficient for **SP** expression; but associated cardiac expression
(Lien et al., 1999) Regions cloned into an **hsp68/*LacZ*** reporter construct	-1 ← ~-9980	E11.5: PH, TH, **ST/PY**, **PP**, OFT, RV (SP not examined)
	-1 ← ~-2250	E11.5: None
	~-2250 ← ~-8300	E11.5: **ST/PY**, TH, PH. Not cardiac
	~-8300 ← ~-9980	E11.5: None
	~-2250 ← ~-3300	E11.5: **ST**, TH, PH. Not cardiac
	~-3300 ← ~-9980	E7.5-8.0: CC; E8.5-10.5: Looping heart tube. By E10.5: RV only; E11.5: TH, RV. Not ST, PH.
	~-6450 ← ~-9980	E11.5: TH, RV
	~-7600 ← ~-9980	E11.5: TH, RV
	~-7600 ← ~-9700	E11.5: RV. Not TH
	~-7600 ← ~-9200	E11.5: None
	~-9200 ← ~-9700	E11.5: RV (weaker than with ~-7600 ← ~-9980)
	~-7600 ← ~-9700 Δ -8300 ← -9200	E11.5: RV
	~-7600 ← ~-8300	E11.5: None
	~-7600← ~-9550	E11.5: None
Conclusions	~-2250 ← ~-3300	Sufficient for **ST**, PH, TH (3' element) at E11.5, not heart
	~-7600 ← ~-8300	RV positive element
	~-8300 ← ~-9200	RV negative element
	~-9200 ← ~-9700	RV positive element
	~-9700 ← ~-9980	TH (5' element)
(Tanaka et al., 1999c) Regionc cloned into pBS, upstream of *LacZ*. **Endogenous** promoters were used	-1 ← ~-3300	Transients - E10.5: OFT, basal RV, PH, TH, distal **ST (mesenchymal)** Stable line – E7.5: None; E15.5: **SP**, TH, OFT; Adult: heart is negative
	~+1400 of intron between exon1c & 2 ← *LacZ* ← ~-3300	E10.5: OFT, basal RV, PH, TH, **ST**
	-1 ← ~-4000	E10.5: OFT, RV, PH, TH, **ST**
	-1 ← ~-6000	E10.5: None

	-1 ← ~-14,000	Transients - E10.5: increased heart expression vs. -4 or -6k - nearly entire RV, LV, OFT, plus other cardiac sites. PH, TH. In one of four transient, was weak **ST**. Stable line – E7.5: CC; E8.25: OFT, common ventricle; E9.5: RV, LV, OFT, septum; E15.5: **SP**, scant heart; Adult = some cardiac
	~+6000 of sequence 3' to exon2 ← *LacZ* ← ~-3300	E10.5: Entire RV (even greater than with -14kb), PH, TH, **ST**
Conclusions	-1 ← ~-3300	OFT, base of RV
	~-4000 ← ~-6000	Dominant repressor element
	~-6000 ←~-14,000	CC, RV medial wall & inner trabeculae, LV medial wall, septum
	6kb 3' to exon2	RV lateral wall
	There is **negative** autoregulation in the heart	β-gal staining more than twice as strong in the hearts of *Nkx2-5* homozygous mutants than in heterozygotes. Abundance of *LacZ* transcripts in homozygous hearts ~8-fold that in heterozygotes.
	There is **positive** autoregulation in the gut	No β-gal staining is detectable in stomachs of *Nkx2-5* nulls (heterozygous or homozygous). It may therefore be that Nkx2-5 is required to positively autoregulate itself in the gut.
(Lien et al., 2002)	-52 ← -3288	E11.5: OFT, PH, TH, **ST/PY/SP**. AR2 region contains conserved binding sites: 6 x GATA, 4 x Smad, 1 x Hnf3, 1 x Nkx2-5. Nkx2-5 binding site at -3177←-3181; if mutated, expression is not affected according to the authors. However, **ST** expression appears greatly decreased, suggesting positive autoregulation.
(Liberatore et al., 2002)	Searcy *et al.* -1 ← -3299 with 5' most 48nt deleted	Cluster of three conserved Smad consensus binding sites deleted, leading to delayed *LacZ* expression in heart; no CC or linear heart tube expression, unlike with intact construct. E10.5 gut expression unaffected, though earlier LPM expression is absent.
(Brown, III et al., 2004)	~-5974 ← ~-6211	Identified due to clustered GATA and Smad sites; acts as a cardiac enhancer *in vivo*. E8.5: heart tube; E9.5: looped tube; During chamber specification: ventricular myocytes, AV junction.
(Chi et al., 2005) *Hsp68, LacZ*	-19kb ← -21kb	UH4 - E11.5-12.5: strong tongue; weak somites, body wall muscle
	-15kb ← -18.5kb	UH5 – E9.5: looping heart, **foregut**; E12.5: atria, AVC, IVS, LV, not RV; **E11.5 distal stomach**
	-8.5kb ← -15kb	UH6 – E10.5-12.5: RV, IVS, LV

Appendix Table 1 - *Nkx2-5* regulatory elements

Expression is in transient transgenics, unless otherwise stated. All genomic locations are relative to the translational start point and, where necessary, have been altered from the original base numbering to reflect this. Exons are numbered according to (Schwartz and Olson, 1999). **Abbreviations used:** I/OFT – inflow/outflow tract; PH – pharynx (pharyngeal endoderm); TH – thyroid; **ST – stomach; SP – spleen;** PCS – pericardial sac; RV – right ventricle; AVC – atrial-ventricular canal; IVS – interventricular septum; LV – left ventricle; AT – atrium; RVT – right ventricle trabecula; **PY – pyloric region of stomach**; CC – cardiac crescent; **LPM – lateral plate mesoderm**; **PP – pancreatic primordium**; Δ - deletion; pBS – pBluescript

Generation of the *NGRS-LacZ* construct

The *NGRS* was originally cloned, and the *NGRS-LacZ* construct generated, as part of my Msc (University of Edinburgh, 2003). A BLAST analysis of the murine genome with the *Nkx2-5* sequence (NCBI: AF091351) identified a contig covering the AR7 upstream region reported to confer distal stomach and spleen expression (Reecy et al., 1999). Primers flanking this region were designed based on this contig sequence, using the Primer3 program. A *Hin*dIII recognition site was included at the 5' terminus of each primer to facilitate excision and cloning into the reporter construct. Suitability of this restriction enzyme was confirmed by restriction mapping of the region to be amplified, using Webcutter. The *NGRS* was isolated as a 1956nt fragment from genomic (C57BL/6) mouse DNA by gel extraction of a PCR product generated by high fidelity PCR, and was subcloned into pGEM-T Easy. This construct was used to transform competent DH5α cells. Colony PCR was performed on DNA extracted from white Ampicillin-resistant colonies. Sequencing of gel-extracted PCR products, using vector-based M13 primers, confirmed the identity and integrity of the enhancer fragment. One colony was picked on this basis, and plasmid DNA prepared from this (Miniprep). The *NGRS* was then excised from pGEM-T Easy by *Hin*dIII digestion and isolated by gel extraction. This sticky-ended ~2kb fragment was ligated into p1230, a *LacZ* reporter construct containing a ß-globin promoter (based on pBGZ40). Miniprep DNA from a colony transformed with this construct – as confirmed by colony PCR – was analysed by *Hin*dIII digestion to confirm identity. Identity and sequence integrity of a large-scale (Maxi) preparation of the plasmid DNA was confirmed by restriction digests (*Hin*dIII, *Not*I, *Sal*I, and combinations thereof) and sequence analysis. The *NGRS* in the final construct used for the MSc microinjections lies in a reverse orientation with respect to the promoter and *LacZ*; it still, however, confers the expected expression pattern.

New preparations were used for each microinjection session during my PhD. A ~5.5kb DNA fragment containing the *NGRS*, *LacZ* reporter gene, and ß-globin promoter was excised from the final

NGRS-1230 reporter construct, using *Spe*I and *Sal*I. This fragment was gel-extracted using Agarase - followed by phenol/chloroform extraction, and ethanol precipitation - or by electro-elution from gel slices. Finally, the fragment was resuspended in reduced-EDTA (0.1M) TE buffer, and microinjected into mouse oocytes.

From the original, MSc, microinjection session 5/16 E12.5 embryos were positive for *LacZ* by PCR, and two of these exhibited X-gal staining (spleen, pyloric sphincter, dorsal stomach mesenchyme, thyroid, cardiac outflow tract). Full details were provided in my thesis: Sally Burn, MSc (Res), University of Edinburgh, 2003.

Primer sequences:

Sequences of primers used to amplify the 1956nt *NGRS* region were as follows, orientated 5' to 3':

f: AAGCTTCAGGCATCTTGCTTTCTTCC
r: AAGCTTGCAAAGGCCTGATTTGTGTTC

High fidelity PCR program for initial isolation of *NGRS* from genomic DNA:

1) 3 minutes denaturation at 94°c
2) 94°c for 30s
3) 59°c for 50s
4) 70°c for 120s; back to 2) for 29 cycles
5) 5 minutes at 70°c.

Generation of stable *NGRS-LacZ* transgenic lines

Attempts to generate a transgenic line stably expressing the *NGRS-LacZ* transgene were initially unsuccessful and transgenic mice were only generated in the third round of microinjection sessions. One factor that may have been instrumental in the final success was the use of electro-elution to recover the linearised construct from the agarose gel on which it was separated; standard gel extraction techniques had been used prior to this.

Appendix Table 2 – *NGRS-LacZ* Line 4 plugs

Transgenic parent	Age	Number embryos	Number transgenic
4	E8.5	11	5
F1	E8.5	14	1
F1	E9.0	9	4
4	E9.5	12	7
F1	E9.5	13	8
4	E10.5	12	5
4	E10.5	10	6
4	E11.5	14	9
4	E12.5	15	7
F1	E12.5	15	7
F1	E12.5	11	5
F1	E12.5	13	9
F1	E12.5	12	4
F1	E12.5	12	4
4	E13.5	14	3

Transgenic parents: 4 = founder male; F1 = offspring of male 4.
All matings were with CD1 females/males.
This table does not include mice found not to be pregnant upon dissection.

Appendix Table 3 – *NGRS-LacZ* Line 21 plugs

Transgenic parent	Age	Number embryos	Number transgenic
F1	E8.5	9	5
F1	E9.5	13	7
F1	E9.5	11	3
F1	E10.5	14	5
F1	E11.5	11	4
F1	E11.5	11	6
F1	E12.5	9	4
F1	E12.5	11	5
F1	E13.5	12	3
F1	E13.5	11	3
F3	E13.5	12	6
F3	E13.5	9	3
F3	E13.5	6	1
F1	E14.5	12	7
F1	E15.5	13	6
F1	E16.5	13	5
F1	E17.5	12	6
F1	E18.5	10	4
F1	E18.5	12	5

Transgenic parents: F1 = offspring of female 21, F3 = offspring of F2 generation.
All matings were with CD1 females/males.
This table does not include mice found not to be pregnant upon dissection.

Appendix Table 4 – *NGRS-LacZ* Line 4/*Bapx1*$^{-/-}$ plugs

Age	No. embryos	No. *LacZ+*	No. *Bapx1*$^{-/-}$	No. *LacZ/Bapx1*$^{-/-}$
E9.5	2	0	0	0
E9.5	3	3	0	0
E9.5	8	6	3	1
E10.5	9	4	3	1
E10.5	16	8	2	1
E10.5	8	5	0	0
E11.5	8	2	0	0
E11.5	8	2	1	0
E12.5	7	2	1	0
E12.5	8	4	0	0
E12.5	8	3	1	1

Matings: F1 generation Line 4 males x *Bapx1*$^{+/-}$ females, to generate *LacZ/Bapx1*$^{+/-}$ mice which were then crossed with *Bapx1*$^{+/-}$ mice to produce *LacZ/Bapx1*$^{-/-}$offspring. *Bapx1*$^{+/-}$ mice were stock from the Biomedical Research facility (BRF) and transmitted the *Bapx1* null allele poorly. This table does not include mice found not to be pregnant upon dissection.

Appendix Table 5 – *NGRS-LacZ* Line 21/*Bapx1*$^{-/-}$ plugs

Age	No. embryos	No. *LacZ+*	No. *Bapx1*$^{-/-}$	No. *LacZ/Bapx1*$^{-/-}$
E9.5	6	5	1	1
E9.5	9	5	0	0
E10.5	11	5	2	2
E11.5	10	8	3	3
E11.5	8	3	0	0
E12.5	10	4	2	2
E12.5	7	6	3	3
E16.5	8	4	0	0
E18.5	10	5	0	0
E18.5	6	2	2	0

Matings: F1 generation Line 21 males x *Bapx1*$^{+/-}$ females, to generate *LacZ/Bapx1*$^{+/-}$ mice which were then crossed with *Bapx1*$^{+/-}$ mice to produce *LacZ/Bapx1*$^{-/-}$offspring. *Bapx1*$^{+/-}$ mice were stock from the Transgenic Unit and transmitted the *Bapx1* null allele well. This table does not include mice found not to be pregnant upon dissection.

Appendix: Chapter 3

Generation of the *NGRS-CreERT2* construct

The source of the *intron-CreERT2-poly(A)* DNA fragment was the *pK5-CreERT2* construct, kindly provided by Pierre Chambon. *pK5-CreERT2* was generated by cloning a ~0.85kb *Stu*I-*Sal*I fragment - containing sequences for the rabbit β-globin intron II, a multiple cloning site (MCS), and the SV40 polyadenylation signal – from the *pSG5* vector (Green et al., 1988) into the *Stu*I-*Xho*I sites of pMCS-1 (Feng et al., 1997), to create *pGS*; a ~2kb fragment encoding *CreERT2* (Feil et al., 1997) was then inserted into the *Eco*RI site of the MCS between the intron and poly(A) sequences to generate *pGS-CreERT2*. A ~5.2kb *Sal*I bovine keratin K5 promoter region from *pK18-BK5P* was then placed upstream of the intron, thus creating the final *pK5-CreERT2* construct (Indra et al., 1999). *pK5-CreERT2* was sequenced to facilitate restriction mapping, as suitable sequence data was not available. The *Sal*I K5 promoter fragment was removed and the vector religated to allow excision of the *intron-CreERT2-poly(A)* fragment with *Not*I for use in the *NGRS-CreERT2* construct. This relegated vector is referred to as *pCreERT2*.

To generate *NGRS-CreERT2*, the *pZErO-1* vector was linearised at the MCS *Not*I site and dephosphorylated with Calf Intestinal Phosphatase (CIP) to prevent self-ligation. The *Not*I fragment from *pCreERT2* containing the intron, CreERT2, and SV40 poly(A) sequences was ligated into this site, creating *pZ-ICEA*. Plasmids containing this insert were identified by colony PCR with primers for *Cre* (~1kb product), and positive colonies were cultured overnight in 3ml L-Zeo. *Hin*dIII digestion of Miniprep DNA prepared from these cultures showed the orientation of the insert (one *Hin*dIII site lies 3' with respect to the insert, in the vector, and a second is located between the *Cre* and *ERT2* coding sequences; if the insert is orientated correctly - with respect to the restriction sites needed for subsequent cloning steps – then fragments of ~1.2 and ~4.8kb are generated, whereas incorrectly orientated inserts will produce ~2 and ~4kb fragments). *Sal*I digestion and CIP treatment of a correctly orientated and sequenced *pZ-ICEA* construct was performed in preparation for ligation of the ~2kb *NGRS* and *β-globin promoter* sequences which had been excised as a *Sal*I fragment from a vector in which it was cloned as a *Sal*I-ended PCR product. *Sal*I cuts 5' to the intron in *pZ-ICEA*, and is the cloning site for the original keratin K5 promoter region. Orientation of the *NGRS/β-globin promoter Sal*I fragment was checked using *Not*I digestion (*Not*I restriction sites are located 5' to the *Sal*I insertion site, ~0.3kb from the 3' end of the *NGRS/β-globin promoter* insert, and 3' to the poly(A); a correct orientation will produce approximately 3.3, 1.8, and 2.8kb bands, and incorrect orientation produces approximately 4.8, 0.3, and 2.8kb fragments). This final construct was sequenced and is referred to in this thesis as *NGRS-CreERT2*.

A ~5kb fragment containing the *NGRS, β-globin promoter, rabbit β-globin intron II, Cre, ERT2,* and *SV40 poly(A)* sequences was excised for microinjection using *Nsi*I (*Kpn*I is also a suitable enzyme).

Generation of the *NGRS-LoxSTOPLox-LacZ* construct

To generate the *NGRS-LoxSTOPLox-LacZ* construct, a ~60bp region including the *β-globin* promoter was removed from *NGRS-LacZ* using *Pst*I and the vector was dephosphorylated. The excised region was then replaced by ligation of a sequence identical but for an *Nsi*I site at the 3' end:

CTGCAGCCCGGGCTGGCATAAAAGTCAGGGCAGAGCCATCTATTGCTTACATTTGCTTCTAG
CATGCATCTGCAG

(Blue: *Pst*I recognition site; red: *Nsi*I recognition sequence; underlined: *β-globin* promoter sequence)

The replacement sequence was generated by annealing the following phosphorylated oligos:

OligoF:

GCCCGGGCTGGCATAAAAGTCAGGGCAGAGCCATCTATTGCTTACATTTGCTTCTAGCATGC
ATCTGCA

OligoR:

GATGCATGCTAGAAGCAAATGTAAGCAATAGATGGCTCTGCCCTGACTTTTATGCCAGCCCG
GGCTGCA

Insertion of the double-stranded annealed oligo sequence was verified by colony PCR ("IfOligoIn" PCR program and primers, provided in **Chapter 7**). Miniprep DNA was produced and *Pst*I (analysed on a 3% agarose gel), *Nsi*I, and *Sma*I + *Eco*RI digests performed to confirm correct insertion. A further PCR identified the orientation of the inserted DNA ("OligoOri" PCR program and primers, as described). Sequencing was also performed to ensure the correct sequence was present.

The ~1.4kb *LoxSTOPLox* cassette was amplified by PCR from a host vector (pBS302) using KOD Hi-fidelity *Taq* polymerase and the "LSL" program and primers detailed in **Chapter 7**. The PCR product was gel-extracted and its ends digested with *Nsi*I. Following phenol/chloroform treatment and ethanol precipitation, the *LoxSTOPLox* fragment was subcloned into the *Nsi*I site of pZErO-1 and sequenced. A suitable clone was then digested with *Nsi*I and the released *LoxSTOPLox* DNA was ligated into the *Nsi*I site of the altered *NGRS-LacZ* vector (digested with *Nsi*I and dephosphorylated). Colony PCR was performed to identify clones carrying the *LoxSTOPLox* cassette in the correct orientation ("LSTOPLOri" primers and PCR program), and Miniprep DNA was subjected to restriction digestion to confirm correct cloning of the final construct (*Sal*I, *Spe*I, *Pst*I, *Nsi*I, *Hin*dIII, *Sal*I + *Spe*I).

A ~7kb fragment containing the *NGRS, β-globin* promoter, *LoxSTOPLox*, and *LacZ* sequences was excised for microinjection using *Sal*I + *Spe*I, and electro-eluted from a 1% SEAKEM GTG agarose/MilliQ TAE gel. DNA was then prepared for microinjection as described in **Chapter 7**.

Appendix Table 6 – *NGRS-LoxSTOPLox-LacZ* genotyping results

Mating	#	Blue?	PCR 1: *LacZ*	PCR 2: *STOP*	PCR 3: Recomb.	Conclusion	Genotypes
Male founder x *gl-Cre* #1	1	x	-	-	-	NTG	3/9 NTG 6/9 TG: 5/9 Fragment 1/9 Correct (could also be 3rd defective TG)
	2	x	+	-	No	*LacZ* fragment	
	3	**Yes**	+	-	**Yes**	Correct+recomb	
	4	x	+	-	No	*LacZ* fragment	
	5	x	+	-	No	*LacZ* fragment	
	6	x	-	-	-	NTG	
	7	x	-	-	-	NTG	
	8	x	+	-	No	*LacZ* fragment	
	9	x	+	-	No	*LacZ* fragment	
Male founder x *gl-Cre* #2	1	**Yes**	+	-	**Yes**	Correct+recomb	8/11 NTG 3/11 TG: 2/11 Fragment 1/11 Correct (could also be 3rd defective TG)
	2	x	-	-	-	NTG	
	3	x	-	-	-	NTG	
	4	x	-	-	-	NTG	
	5	x	+	-	No	*LacZ* fragment	
	6	x	-	-	-	NTG	
	7	x	+	-	No	*LacZ* fragment	
	8	x	-	-	-	NTG	
	9	x	-	-	-	NTG	
	10	x	-	-	-	NTG	
	11	x	-	-	-	NTG	
Male founder x **CD1** #1	1	x	-	-	-	NTG	6/10 NTG 4/10 TG: 1/10 Fragment 3/10 Correct (could also be 3rd defective TG)
	2	x	-	-	-	NTG	
	3	x	+	-	No	*LacZ* fragment	
	4	x	-	-	-	NTG	
	5	x	-	-	-	NTG	
	6	x	+	+	No *	Correct	
	7	x	+	+	No *	Correct	
	8	x	+	+	No *	Correct	
	9	x	-	-	-	NTG	
	10	x	-	-	-	NTG	

Male founder x CD1 #2	1	x	-	-	-	NTG	8/19 NTG 11/19 TG: 3/19 Fragment 4/19 Correct 4/19 3rd defective TG or leaky
	2	x	-	-	-	NTG	
	3	x	-	-	-	NTG	
	4	x	-	-	-	NTG	
	5	x	-	-	-	NTG	
	6	x	+	-	No	*LacZ* fragment	
	7	**Yes**	+	+	No *	Defective/"leaky"	
	8	**Yes**	+	+	No &	Defective/"leaky"	
	9	x	-	-	-	NTG	
	10	x	-	-	-	NTG	
	11	x	+	-	No	*LacZ* fragment	
	12	**Yes**	+	+	No *	Defective/"leaky"	
	13	x	+	-	No	*LacZ* fragment	
	14	x	+	+	No *	Correct	
	15	x	+	+	No *	Correct	
	16	x	-	-	-	NTG	
	17	**Yes**	+	+	No *	Defective/"leaky"	
	18	x	+	+	No *	Correct	
	19	x	+	+	No *	Correct	
Mating	**#**	**Blue?**	**PCR 1: *LacZ***	**PCR 2: *STOP***	**PCR 3: Recomb.**	**Conclusion**	**Genotypes**
Female line: male#15 x ***gl-Cre*** #62	1	x	+	-	**Yes**	Correct+recomb	3/5 TG
	2	x	+		**Yes**	Correct+recomb	
	3	x	-	-	-	NTG	
	4	x	-	-	-	NTG	
	5	x	+	-	**Yes**	Correct+recomb	
Female line: male #10 **x gl-Cre** #60	6	x	+	-	**Yes**	Correct+recomb	3/9 TG
	7	x	-	-	-	NTG	
	8	x	-	-	-	NTG	
	9	x	+	-	**Yes**	Correct+recomb	
	10	x	-	-	-	NTG	
	11	x	-	-	-	NTG	
	12	x	-	-	-	NTG	
	13	x	-	-	-	NTG	
	14	x	+	-	**Yes**	Correct+recomb	
Female	1	x	+	+	No *	Correct	9/17 TG
	2	x	+	+	No *	Correct	
	3	x	-	-	-	NTG	
	4	x	-	-	-	NTG	
	5	x	+	+	No *	Correct	

line: male #15 x **CD1**	6	x	+	+	No *	Correct	
	7	x	+	+	No *	Correct	
	8	x	+	+	No *	Correct	
	9	x	-	-	-	NTG	
	10	x	-	-	-	NTG	
	11	x	-	-	-	NTG	
	12	x	+	+	No *	Correct	
	13	x	+	+	No &	Correct	
	14	x	+	+	No *	Correct	
	15	x	-	-	-	NTG	
	16	x	-	-	-	NTG	
	17	x	-	-	-	NTG	
Female line: male #10 x **CD1**	18	x	+	+	No &	Correct	7/13 TG
	19	x	+	+	No *	Correct	
	20	x	-	-	-	NTG	
	21	x	+	+	No *	Correct	
	22	x	+	+	No &	Correct	
	23	x	-	-	-	NTG	
	24	x	-	-	-	NTG	
	25	x	+	+	No &	Correct	
	26	x	-	-	-	NTG	
	27	x	+	+	No &	Correct	
	28	x	-	-	-	NTG	
	29	x	-	-	-	NTG	
	30	x	+	+	No &	Correct	

The presence of X-gal staining is indicated by "**Yes**" in the "Blue?" column. Absence of staining is denoted by "**x**".
The PCR assays are depicted in **Figure 3.5.**
PCR 1 – *LacZ*: *LacZ*+ = "**+**", *LacZ*- = "**-**"
PCR 2 – *STOP*: The presence of a product (**+**) indicated that the *STOP* sequence was present and not therefore recombined out of the genome. The absence of a PCR product (**-**) meant either a) the embryo had never carried the *STOP* sequence, or b) that the *STOP* sequence had been recombined out of the genome by Cre. These possibilities were distinguished between by the third PCR, which tested for recombination.
PCR 3 – Recombination: successful recombination of the *LoxSTOPLox* sequence resulted in a 0.23kb PCR product ("**Yes**"). If recombination had not occurred, a 1.6kb product was produced; this was, however, often not amplifiable from the yolk sac DNA. Failure to amplify the large non-recombined band is denoted by "**No ***". "**No &**" signifies that a band was amplified.
The conclusions are explained fully in **Chapter 3** and in **Figure 3.7**.

Appendix: Chapter 4

Experimental notes

Matings:

It should be noted that whilst a greater number of *NGRS-LacZ*-positive embryos could have been obtained from each litter had two transgenic parents been mated – as opposed to a transgenic male with a CD1 female – this was not the general procedure, but for valid reasons. Firstly, there were not enough transgenic females of breeding age in the *NGRS-LacZ* colony when the culture studies were performed. Secondly, the expression pattern in embryos homozygous for the transgene had not been studied sufficiently at the start of these experiments (though this was later tested and the pattern found to be the same as in those with one CD1 parent; data not shown). Finally, on the occasions when a transgenic with transgenic mating was used, the number of embryos recovered was significantly less than when mating involved a CD1 mouse.

Genotyping:

A genotyping step was not included as gathering tissue for this would have slowed the progress of getting explants rapidly from the uterus into culture and at least the first two days of culture would still need to be undertaken before a genotyping result was obtained. Similarly, X-gal staining of the cardiac outflow tract or thyroid primordium (*LacZ*-positive sites in the E11.5 *NGRS-LacZ* embryo) would not give a result until after the labour-intensive part of the culture process (dissection, introduction to culture, initial photography) had already been performed.

Controls:

A recommendation for whole embryo cultures is that 15-25% of the embryos are used as non-manipulated cultured controls (Klug, 1991). By the end of the studies discussed in this thesis, the standard practice was to keep ~25% of a litter as uncultured controls (to monitor the extent of staining and spleen development at t0), and to use 50% of the remaining guts as non-manipulated cultured controls.

Deviations from the described protocol:

In the culture experiment described in **Section 4.7.2**, and shown in **Figure 4.10**, the explants were cultured for 48 hours as per the standard protocol, with the exception that the culture medium was changed at 24 hours in an attempt to counteract the poor health of the explants. This did not however seem to benefit the guts and may have been detrimental as the microenvironment of growth factors established around the explants will have been removed. Media renewal was thus not repeated in any other culture experiment.

References

Abel,R.M. (2000). Hunterian Lecture. The ontogeny of the peptide innervation of the human pylorus with special reference to understanding the aetiology and pathogenesis of infantile hypertrophic pyloric stenosis. Ann. R. Coll. Surg. Engl. *82*, 371-377.

Abel,R.M., Dore,C.J., Bishop,A.E., Facer,P., Polak,J.M., and Spitz,L. (2004). A histological study of the hph-1 mouse mutant: an animal model of phenylketonuria and infantile hypertrophic pyloric stenosis. Anat. Histol. Embryol. *33*, 125-130.

Ahlgren,U., Jonsson,J., and Edlund,H. (1996). The morphogenesis of the pancreatic mesenchyme is uncoupled from that of the pancreatic epithelium in IPF1/PDX1-deficient mice. Development *122*, 1409-1416.

Ahn,S. and Joyner,A.L. (2004). Dynamic changes in the response of cells to positive hedgehog signaling during mouse limb patterning. Cell *118*, 505-516.

Akazawa,H., Komuro,I., Sugitani,Y., Yazaki,Y., Nagai,R., and Noda,T. (2000). Targeted disruption of the homeobox transcription factor Bapx1 results in lethal skeletal dysplasia with asplenia and gastroduodenal malformation. Genes Cells *5*, 499-513.

Alanentalo,T., Chatonnet,F., Karlen,M., Sulniute,R., Ericson,J., Andersson,E., and Ahlgren,U. (2006). Cloning and analysis of Nkx6.3 during CNS and gastrointestinal development. Gene Expr. Patterns. *6*, 162-170.

Altmann,G.G. and Quaroni,A. (1990). Behavior of fetal intestinal organ culture explanted onto a collagen substratum. Development *110*, 353-370.

Ang,S.J., Stump,R.J., Lovicu,F.J., and McAvoy,J.W. (2004). Spatial and temporal expression of Wnt and Dickkopf genes during murine lens development. Gene Expr. Patterns. *4*, 289-295.

Apelqvist,A., Ahlgren,U., and Edlund,H. (1997). Sonic hedgehog directs specialised mesoderm differentiation in the intestine and pancreas. Curr. Biol. *7*, 801-804.

Asayesh,A., Sharpe,J., Watson,R.P., Hecksher-Sorensen,J., Hastie,N.D., Hill,R.E., and Ahlgren,U. (2006). Spleen versus pancreas: strict control of organ interrelationship revealed by analyses of Bapx1-/- mice. Genes Dev. *20*, 2208-2213.

Aubin,J., Dery,U., Lemieux,M., Chailler,P., and Jeannotte,L. (2002). Stomach regional specification requires Hoxa5-driven mesenchymal-epithelial signaling. Development *129*, 4075-4087.

Austin,T.W., Solar,G.P., Ziegler,F.C., Liem,L., and Matthews,W. (1997). A role for the Wnt gene family in hematopoiesis: expansion of multilineage progenitor cells. Blood *89*, 3624-3635.

Aylsworth,A.S. (2001). Clinical aspects of defects in the determination of laterality. Am. J. Med. Genet. *101*, 345-355.

Azpiazu,N. and Frasch,M. (1993). tinman and bagpipe: two homeo box genes that determine cell fates in the dorsal mesoderm of Drosophila. Genes Dev. *7*, 1325-1340.

Azpiazu,N., Lawrence,P.A., Vincent,J.P., and Frasch,M. (1996b). Segmentation and specification of the Drosophila mesoderm. Genes Dev. *10*, 3183-3194.

Azpiazu,N., Lawrence,P.A., Vincent,J.P., and Frasch,M. (1996a). Segmentation and specification of the Drosophila mesoderm. Genes Dev. *10*, 3183-3194.

Bae,Y.K., Shimizu,T., Muraoka,O., Yabe,T., Hirata,T., Nojima,H., Hirano,T., and Hibi,M. (2004). Expression of sax1/nkx1.2 and sax2/nkx1.1 in zebrafish. Gene Expr. Patterns. *4*, 481-486.

Baekvad-Hansen,M., Tumer,Z., Delicado,A., Erdogan,F., Tommerup,N., and Larsen,L.A. (2006). Delineation of a 2.2 Mb microdeletion at 5q35 associated with microcephaly and congenital heart disease. Am. J. Med. Genet. A *140*, 427-433.

Baena-Lopez,L.A., Baonza,A., and Garcia-Bellido,A. (2005). The orientation of cell divisions determines the shape of Drosophila organs. Curr. Biol. *15*, 1640-1644.

Barrow,J.R., Thomas,K.R., Boussadia-Zahui,O., Moore,R., Kemler,R., Capecchi,M.R., and McMahon,A.P. (2003). Ectodermal Wnt3/beta-catenin signaling is required for the establishment and maintenance of the apical ectodermal ridge. Genes Dev. *17*, 394-409.

Bartram,U., Wirbelauer,J., and Speer,C.P. (2005). Heterotaxy syndrome -- asplenia and polysplenia as indicators of visceral malposition and complex congenital heart disease. Biol. Neonate *88*, 278-290.

Beis,D. and Stainier,D.Y. (2006). In vivo cell biology: following the zebrafish trend. Trends Cell Biol. *16*, 105-112.

Bellusci,S., Grindley,J., Emoto,H., Itoh,N., and Hogan,B.L. (1997). Fibroblast growth factor 10 (FGF10) and branching morphogenesis in the embryonic mouse lung. Development *124*, 4867-4878.

Bellusci,S., Henderson,R., Winnier,G., Oikawa,T., and Hogan,B.L. (1996). Evidence from normal expression and targeted misexpression that bone morphogenetic protein (Bmp-4) plays a role in mouse embryonic lung morphogenesis. Development *122*, 1693-1702.

Belmont,J.W., Mohapatra,B., Towbin,J.A., and Ware,S.M. (2004). Molecular genetics of heterotaxy syndromes. Curr. Opin. Cardiol. *19*, 216-220.

Benson,D.W., Silberbach,G.M., Kavanaugh-McHugh,A., Cottrill,C., Zhang,Y., Riggs,S., Smalls,O., Johnson,M.C., Watson,M.S., Seidman,J.G., Seidman,C.E., Plowden,J., and Kugler,J.D. (1999). Mutations in the cardiac transcription factor NKX2.5 affect diverse cardiac developmental pathways. J. Clin. Invest *104*, 1567-1573.

Bertrand,J.Y., Desanti,G.E., Lo-Man,R., Leclerc,C., Cumano,A., and Golub,R. (2006). Fetal spleen stroma drives macrophage commitment. Development *133*, 3619-3628.

Bhushan,A., Itoh,N., Kato,S., Thiery,J.P., Czernichow,P., Bellusci,S., and Scharfmann,R. (2001). Fgf10 is essential for maintaining the proliferative capacity of epithelial progenitor cells during early pancreatic organogenesis. Development *128*, 5109-5117.

Biben,C., Hatzistavrou,T., and Harvey,R.P. (1998). Expression of NK-2 class homeobox gene Nkx2-6 in foregut endoderm and heart. Mech. Dev. *73*, 125-127.

Biben,C., Weber,R., Kesteven,S., Stanley,E., McDonald,L., Elliott,D.A., Barnett,L., Koentgen,F., Robb,L., Feneley,M., and Harvey,R.P. (2000). Cardiac septal and valvular dysmorphogenesis in mice heterozygous for mutations in the homeobox gene Nkx2-5. Circ. Res. *87*, 888-895.

Bieberich,C.J., Fujita,K., He,W.W., and Jay,G. (1996). Prostate-specific and androgen-dependent expression of a novel homeobox gene. J. Biol. Chem. *271*, 31779-31782.

Bishopric,N.H. (2005). Evolution of the heart from bacteria to man. Ann. N. Y. Acad. Sci. *1047*, 13-29.

Bitgood,M.J. and McMahon,A.P. (1995). Hedgehog and Bmp genes are coexpressed at many diverse sites of cell-cell interaction in the mouse embryo. Dev. Biol. *172*, 126-138.

Bober,E., Baum,C., Braun,T., and Arnold,H.H. (1994). A novel NK-related mouse homeobox gene: expression in central and peripheral nervous structures during embryonic development. Dev. Biol. *162*, 288-303.

Bodmer,R. (1993). The gene tinman is required for specification of the heart and visceral muscles in Drosophila. Development *118*, 719-729.

Bodmer,R., Jan,L.Y., and Jan,Y.N. (1990). A new homeobox-containing gene, msh-2, is transiently expressed early during mesoderm formation of Drosophila. Development *110*, 661-669.

Bodmer,R. and Venkatesh,T.V. (1998). Heart development in Drosophila and vertebrates: conservation of molecular mechanisms. Dev. Genet. *22*, 181-186.

Boorman,C.J. and Shimeld,S.M. (2002). The evolution of left-right asymmetry in chordates. Bioessays *24*, 1004-1011.

Bort,R., Martinez-Barbera,J.P., Beddington,R.S., and Zaret,K.S. (2004). Hex homeobox gene-dependent tissue positioning is required for organogenesis of the ventral pancreas. Development *131*, 797-806.

Bourdelat,D., Barbet,J.P., and Chevrel,J.P. (1992). Fetal development of the pyloric muscle. Surg. Radiol. Anat. *14*, 223-226.

Brendolan,A., Ferretti,E., Salsi,V., Moses,K., Quaggin,S., Blasi,F., Cleary,M.L., and Selleri,L. (2005). A Pbx1-dependent genetic and transcriptional network regulates spleen ontogeny. Development *132*, 3113-3126.

Brendolan,A., Rosado,M.M., Carsetti,R., Selleri,L., and Dear,T.N. (2007). Development and function of the mammalian spleen. Bioessays *29*, 166-177.

Brinster,R.L., Chen,H.Y., Trumbauer,M.E., Yagle,M.K., and Palmiter,R.D. (1985). Factors affecting the efficiency of introducing foreign DNA into mice by microinjecting eggs. Proc. Natl. Acad. Sci. U. S. A *82*, 4438-4442.

Brown,C.O., III, Chi,X., Garcia-Gras,E., Shirai,M., Feng,X.H., and Schwartz,R.J. (2004). The cardiac determination factor, Nkx2-5, is activated by mutual cofactors GATA-4 and Smad1/4 via a novel upstream enhancer. J. Biol. Chem. *279*, 10659-10669.

Buchberger,A., Pabst,O., Brand,T., Seidl,K., and Arnold,H.H. (1996). Chick NKx-2.3 represents a novel family member of vertebrate homologues to the Drosophila homeobox gene tinman: differential expression of cNKx-2.3 and cNKx-2.5 during heart and gut development. Mech. Dev. *56*, 151-163.

Burns,R.C., Fairbanks,T.J., Sala,F., De Langhe,S., Mailleux,A., Thiery,J.P., Dickson,C., Itoh,N., Warburton,D., Anderson,K.D., and Bellusci,S. (2004). Requirement for fibroblast growth factor 10 or fibroblast growth factor receptor 2-IIIb signaling for cecal development in mouse. Dev. Biol. *265*, 61-74.

Cai,J., Qi,Y., Wu,R., Modderman,G., Fu,H., Liu,R., and Qiu,M. (2001). Mice lacking the Nkx6.2 (Gtx) homeodomain transcription factor develop and reproduce normally. Mol. Cell Biol. *21*, 4399-4403.

Cai,W.Q. and Gabella,G. (1984). Structure and innervation of the musculature at the gastroduodenal junction of the guinea-pig. J. Anat. *139 (Pt 1)*, 93-104.

Capdevila,J., Vogan,K.J., Tabin,C.J., and Izpisua Belmonte,J.C. (2000). Mechanisms of left-right determination in vertebrates. Cell *101*, 9-21.

Carter,C.O., Evans,K., and Warren,J. (1980). The grandchildren of patients with pyloric stenosis. J. Med. Genet. *17*, 411-415.

Carter,C.O. and Evans,K.A. (1969). Inheritance of congenital pyloric stenosis. J. Med. Genet. *6*, 233-254.

Chakraborty,R. (1986). The inheritance of pyloric stenosis explained by a multifactorial threshold model with sex dimorphism for liability. Genet. Epidemiol. *3*, 1-15.

Cheesman,S.E., Layden,M.J., Von Ohlen,T., Doe,C.Q., and Eisen,J.S. (2004). Zebrafish and fly Nkx6 proteins have similar CNS expression patterns and regulate motoneuron formation. Development *131*, 5221-5232.

Chen,J.N. and Fishman,M.C. (1996). Zebrafish tinman homolog demarcates the heart field and initiates myocardial differentiation. Development *122*, 3809-3816.

Chi,X., Chatterjee,P.K., Wilson,W., III, Zhang,S.X., DeMayo,F.J., and Schwartz,R.J. (2005). Complex cardiac Nkx2-5 gene expression activated by noggin-sensitive enhancers followed by chamber-specific modules. Proc. Natl. Acad. Sci. U. S. A *102*, 13490-13495.

Chi,X., Zhang,S.X., Yu,W., DeMayo,F.J., Rosenberg,S.M., and Schwartz,R.J. (2003). Expression of Nkx2-5-GFP bacterial artificial chromosome transgenic mice closely resembles endogenous Nkx2-5 gene activity. Genesis. *35*, 220-226.

Choi,M.Y., Romer,A.I., Hu,M., Lepourcelet,M., Mechoor,A., Yesilaltay,A., Krieger,M., Gray,P.A., and Shivdasani,R.A. (2006). A dynamic expression survey identifies transcription factors relevant in mouse digestive tract development. Development *133*, 4119-4129.

Choi,T., Huang,M., Gorman,C., and Jaenisch,R. (1991). A generic intron increases gene expression in transgenic mice. Mol. Cell Biol. *11*, 3070-3074.

Chong,A.S., Shen,J., Tao,J., Yin,D., Kuznetsov,A., Hara,M., and Philipson,L.H. (2006). Reversal of diabetes in non-obese diabetic mice without spleen cell-derived beta cell regeneration. Science *311*, 1774-1775.

Chung,C.Y., Funamoto,S., and Firtel,R.A. (2001). Signaling pathways controlling cell polarity and chemotaxis. Trends Biochem. Sci. *26*, 557-566.

Chung,E., Coffey,R., Parker,K., Tam,P., Pembrey,M.E., and Gardiner,R.M. (1993). Linkage analysis of infantile pyloric stenosis and markers from chromosome 9q11-q33: no evidence for a major gene in this candidate region. J. Med. Genet. *30*, 393-395.

Chung,E., Curtis,D., Chen,G., Marsden,P.A., Twells,R., Xu,W., and Gardiner,M. (1996). Genetic evidence for the neuronal nitric oxide synthase gene (NOS1) as a susceptibility locus for infantile pyloric stenosis. Am. J. Hum. Genet. *58*, 363-370.

Church,V., Yamaguchi,K., Tsang,P., Akita,K., Logan,C., and Francis-West,P. (2005). Expression and function of Bapx1 during chick limb development. Anat. Embryol. (Berl) *209*, 461-469.

Clark,A.J., Archibald,A.L., McClenaghan,M., Simons,J.P., Wallace,R., and Whitelaw,C.B. (1993). Enhancing the efficiency of transgene expression. Philos. Trans. R. Soc. Lond B Biol. Sci. *339*, 225-232.

Cleaver,O.B., Patterson,K.D., and Krieg,P.A. (1996). Overexpression of the tinman-related genes XNkx-2.5 and XNkx-2.3 in Xenopus embryos results in myocardial hyperplasia. Development *122*, 3549-3556.

Collombat,P., Hecksher-Sorensen,J., Serup,P., and Mansouri,A. (2006). Specifying pancreatic endocrine cell fates. Mech. Dev. *123*, 501-512.

Copp,A.J. and Cockroft,D.L. (1990). Postimplantation mammalian embryos : a practical approach. Oxford : IRL Press at Oxford University Press), pp. 15-40.

Dabdoub,A., Donohue,M.J., Brennan,A., Wolf,V., Montcouquiol,M., Sassoon,D.A., Hseih,J.C., Rubin,J.S., Salinas,P.C., and Kelley,M.W. (2003). Wnt signaling mediates reorientation of outer hair cell stereociliary bundles in the mammalian cochlea. Development *130*, 2375-2384.

Damante,G., Pellizzari,L., Esposito,G., Fogolari,F., Viglino,P., Fabbro,D., Tell,G., Formisano,S., and Di Lauro,R. (1996). A molecular code dictates sequence-specific DNA recognition by homeodomains. EMBO J. *15*, 4992-5000.

Danielian,P.S., Muccino,D., Rowitch,D.H., Michael,S.K., and McMahon,A.P. (1998). Modification of gene activity in mouse embryos in utero by a tamoxifen-inducible form of Cre recombinase. Curr. Biol. *8*, 1323-1326.

Dassule,H.R. and McMahon,A.P. (1998). Analysis of epithelial-mesenchymal interactions in the initial morphogenesis of the mammalian tooth. Dev. Biol. *202*, 215-227.

Daudet,N., Ripoll,C., Moles,J.P., and Rebillard,G. (2002). Expression of members of Wnt and Frizzled gene families in the postnatal rat cochlea. Brain Res. Mol. Brain Res. *105*, 98-107.

Davies,J.A., Ladomery,M., Hohenstein,P., Michael,L., Shafe,A., Spraggon,L., and Hastie,N. (2004). Development of an siRNA-based method for repressing specific genes in renal organ culture and its use to show that the Wt1 tumour suppressor is required for nephron differentiation. Hum. Mol. Genet. *13*, 235-246.

de Santa,B.P., van den Brink,G.R., and Roberts,D.J. (2002). Molecular etiology of gut malformations and diseases. Am. J. Med. Genet. *115*, 221-230.

Dear,T.N., Colledge,W.H., Carlton,M.B., Lavenir,I., Larson,T., Smith,A.J., Warren,A.J., Evans,M.J., Sofroniew,M.V., and Rabbitts,T.H. (1995). The Hox11 gene is essential for cell survival during spleen development. Development *121*, 2909-2915.

Dear,T.N. and Rabbitts,T.H. (1994). A Drosophila melanogaster homologue of the T-cell oncogene HOX11 localises to a cluster of homeobox genes. Gene *141*, 225-229.

Dear,T.N., Sanchez-Garcia,I., and Rabbitts,T.H. (1993). The HOX11 gene encodes a DNA-binding nuclear transcription factor belonging to a distinct family of homeobox genes. Proc. Natl. Acad. Sci. U. S. A *90*, 4431-4435.

Deng,M.Y., Wang,H., Ward,G.B., Beckham,T.R., and McKenna,T.S. (2005). Comparison of six RNA extraction methods for the detection of classical swine fever virus by real-time and conventional reverse transcription-PCR. J. Vet. Diagn. Invest *17*, 574-578.

Dentice,M., Cordeddu,V., Rosica,A., Ferrara,A.M., Santarpia,L., Salvatore,D., Chiovato,L., Perri,A., Moschini,L., Fazzini,C., Olivieri,A., Costa,P., Stoppioni,V., Baserga,M., De Felice,M., Sorcini,M., Fenzi,G., Di Lauro,R., Tartaglia,M., and Macchia,P.E. (2006). Missense mutation in the transcription factor NKX2-5: a novel molecular event in the pathogenesis of thyroid dysgenesis. J. Clin. Endocrinol. Metab *91*, 1428-1433.

Dermitzakis,E.T., Reymond,A., and Antonarakis,S.E. (2005). Conserved non-genic sequences - an unexpected feature of mammalian genomes. Nat. Rev. Genet. *6*, 151-157.

Dormann,D. and Weijer,C.J. (2001). Propagating chemoattractant waves coordinate periodic cell movement in Dictyostelium slugs. Development *128*, 4535-4543.

Duh,G., Mouri,N., Warburton,D., and Thomas,D.W. (2000). EGF regulates early embryonic mouse gut development in chemically defined organ culture. Pediatr. Res. *48*, 794-802.

Durocher,D., Charron,F., Warren,R., Schwartz,R.J., and Nemer,M. (1997). The cardiac transcription factors Nkx2-5 and GATA-4 are mutual cofactors. EMBO J. *16*, 5687-5696.

Edlund,H. (2002). Pancreatic organogenesis--developmental mechanisms and implications for therapy. Nat. Rev. Genet. *3*, 524-532.

Esni,F., Stoffers,D.A., Takeuchi,T., and Leach,S.D. (2004). Origin of exocrine pancreatic cells from nestin-positive precursors in developing mouse pancreas. Mech. Dev. *121*, 15-25.

Evans,S.M., Yan,W., Murillo,M.P., Ponce,J., and Papalopulu,N. (1995). tinman, a Drosophila homeobox gene required for heart and visceral mesoderm specification, may be represented by a family of genes in vertebrates: XNkx-2.3, a second vertebrate homologue of tinman. Development *121*, 3889-3899.

Farge,E. (2003). Mechanical induction of Twist in the Drosophila foregut/stomodeal primordium. Curr. Biol. *13*, 1365-1377.

Faustman,D.L., Tran,S.D., Kodama,S., Lodde,B.M., Szalayova,I., Key,S., Toth,Z.E., and Mezey,E. (2006). Comment on papers by Chong et al., Nishio et al., and Suri et al. on diabetes reversal in NOD mice. Science *314*, 1243.

Feil,R., Brocard,J., Mascrez,B., LeMeur,M., Metzger,D., and Chambon,P. (1996). Ligand-activated site-specific recombination in mice. Proc. Natl. Acad. Sci. U. S. A *93*, 10887-10890.

Feil,R., Wagner,J., Metzger,D., and Chambon,P. (1997). Regulation of Cre recombinase activity by mutated estrogen receptor ligand-binding domains. Biochem. Biophys. Res. Commun. *237*, 752-757.

Feng,X., Peng,Z.H., Di,W., Li,X.Y., Rochette-Egly,C., Chambon,P., Voorhees,J.J., and Xiao,J.H. (1997). Suprabasal expression of a dominant-negative RXR alpha mutant in transgenic mouse epidermis impairs regulation of gene transcription and basal keratinocyte proliferation by RAR-selective retinoids. Genes Dev. *11*, 59-71.

Firtel,R.A. and Chung,C.Y. (2000). The molecular genetics of chemotaxis: sensing and responding to chemoattractant gradients. Bioessays *22*, 603-615.

Fischer,E., Legue,E., Doyen,A., Nato,F., Nicolas,J.F., Torres,V., Yaniv,M., and Pontoglio,M. (2006a). Defective planar cell polarity in polycystic kidney disease. Nat. Genet. *38*, 21-23.

Fischer,S., Ludecke,H.J., Wieczorek,D., Bohringer,S., Gillessen-Kaesbach,G., and Horsthemke,B. (2006b). Histone acetylation dependent allelic expression imbalance of BAPX1 in patients with the oculo-auriculo-vertebral spectrum. Hum. Mol. Genet. *15*, 581-587.

Frasch,M. (1995). Induction of visceral and cardiac mesoderm by ectodermal Dpp in the early Drosophila embryo. Nature *374*, 464-467.

Fried,K., Aviv,S., and Nisenbaum,C. (1981). Probable autosomal dominant infantile pyloric stenosis in a large kindred. Clin. Genet. *20*, 328-330.

Friedman,L. (1987). Teratological research using in vitro systems. II. Rodent limb bud culture system. Environ. Health Perspect. *72*, 211-219.

Fu,M., Lui,V.C., Sham,M.H., Pachnis,V., and Tam,P.K. (2004). Sonic hedgehog regulates the proliferation, differentiation, and migration of enteric neural crest cells in gut. J. Cell Biol. *166*, 673-684.

Fukuda,K. and Yasugi,S. (2005). The molecular mechanisms of stomach development in vertebrates. Dev. Growth Differ. *47*, 375-382.

Funayama,N., Sato,Y., Matsumoto,K., Ogura,T., and Takahashi,Y. (1999). Coelom formation: binary decision of the lateral plate mesoderm is controlled by the ectoderm. Development *126*, 4129-4138.

Gavin,B.J., McMahon,J.A., and McMahon,A.P. (1990). Expression of multiple novel Wnt-1/int-1-related genes during fetal and adult mouse development. Genes Dev. *4*, 2319-2332.

Gehring,W.J. (1987). Homeo boxes in the study of development. Science *236*, 1245-1252.

Godin,I., Garcia-Porrero,J.A., Dieterlen-Lievre,F., and Cumano,A. (1999). Stem cell emergence and hemopoietic activity are incompatible in mouse intraembryonic sites. J. Exp. Med. *190*, 43-52.

Goldmuntz,E., Geiger,E., and Benson,D.W. (2001). NKX2.5 mutations in patients with tetralogy of fallot. Circulation *104*, 2565-2568.

Grapin-Botton,A. and Melton,D.A. (2000). Endoderm development: from patterning to organogenesis. Trends Genet. *16*, 124-130.

Gray,H. and Carter,H.V. (1998). Gray's anatomy - Descriptive and Surgical. (London: Magpie Books).

Green,M.C. (1967). A defect of the splanchnic mesoderm caused by the mutant gene dominant hemimelia in the mouse. Dev. Biol. *15*, 62-89.

Green,S., Issemann,I., and Sheer,E. (1988). A versatile in vivo and in vitro eukaryotic expression vector for protein engineering. Nucleic Acids Res. *16*, 369.

Grove,E.A., Tole,S., Limon,J., Yip,L., and Ragsdale,C.W. (1998). The hem of the embryonic cerebral cortex is defined by the expression of multiple Wnt genes and is compromised in Gli3-deficient mice. Development *125*, 2315-2325.

Grow,M.W. and Krieg,P.A. (1998). Tinman function is essential for vertebrate heart development: elimination of cardiac differentiation by dominant inhibitory mutants of the tinman-related genes, XNkx2-3 and XNkx2-5. Dev. Biol. *204*, 187-196.

Guarino,N., Shima,H., and Puri,P. (2000). Structural immaturity of the pylorus muscle in infantile hypertrophic pyloric stenosis. Pediatr. Surg. Int. *16*, 282-284.

Guo,Q., Loomis,C., and Joyner,A.L. (2003). Fate map of mouse ventral limb ectoderm and the apical ectodermal ridge. Dev. Biol. *264*, 166-178.

Gutierrez-Roelens,I., Roy,L.D., Ovaert,C., Sluysmans,T., Devriendt,K., Brunner,H.G., and Vikkula,M. (2006). A novel CSX/NKX2-5 mutation causes autosomal-dominant AV block: are atrial fibrillation and syncopes part of the phenotype? Eur. J. Hum. Genet.

Gutierrez-Roelens,I., Sluysmans,T., Gewillig,M., Devriendt,K., and Vikkula,M. (2002). Progressive AV-block and anomalous venous return among cardiac anomalies associated with two novel missense mutations in the CSX/NKX2-5 gene. Hum. Mutat. *20*, 75-76.

Hadjantonakis,A.K., Dickinson,M.E., Fraser,S.E., and Papaioannou,V.E. (2003). Technicolour transgenics: imaging tools for functional genomics in the mouse. Nat. Rev. Genet. *4*, 613-625.

Hamada,H., Meno,C., Watanabe,D., and Saijoh,Y. (2002). Establishment of vertebrate left-right asymmetry. Nat. Rev. Genet. *3*, 103-113.

Hargrave,M., Wright,E., Kun,J., Emery,J., Cooper,L., and Koopman,P. (1997). Expression of the Sox11 gene in mouse embryos suggests roles in neuronal maturation and epithelio-mesenchymal induction. Dev. Dyn. *210*, 79-86.

Harvey,R.P. (1996). NK-2 homeobox genes and heart development. Dev. Biol. *178*, 203-216.

Haun,C., Alexander,J., Stainier,D.Y., and Okkema,P.G. (1998). Rescue of Caenorhabditis elegans pharyngeal development by a vertebrate heart specification gene. Proc. Natl. Acad. Sci. U. S. A *95*, 5072-5075.

Hayashi,S. and McMahon,A.P. (2002). Efficient recombination in diverse tissues by a tamoxifen-inducible form of Cre: a tool for temporally regulated gene activation/inactivation in the mouse. Dev. Biol. *244*, 305-318.

He,W.W., Sciavolino,P.J., Wing,J., Augustus,M., Hudson,P., Meissner,P.S., Curtis,R.T., Shell,B.K., Bostwick,D.G., Tindall,D.J., Gelmann,E.P., Abate-Shen,C., and Carter,K.C. (1997). A novel human prostate-specific, androgen-regulated homeobox gene (NKX3.1) that maps to 8p21, a region frequently deleted in prostate cancer. Genomics *43*, 69-77.

Hearn,C.J., Young,H.M., Ciampoli,D., Lomax,A.E., and Newgreen,D. (1999). Catenary cultures of embryonic gastrointestinal tract support organ morphogenesis, motility, neural crest cell migration, and cell differentiation. Dev. Dyn. *214*, 239-247.

Heathcote,K., Braybrook,C., Abushaban,L., Guy,M., Khetyar,M.E., Patton,M.A., Carter,N.D., Scambler,P.J., and Syrris,P. (2005). Common arterial trunk associated with a homeodomain mutation of NKX2.6. Hum. Mol. Genet. *14*, 585-593.

Hecksher-Sorensen,J., Watson,R.P., Lettice,L.A., Serup,P., Eley,L., De Angelis,C., Ahlgren,U., and Hill,R.E. (2004). The splanchnic mesodermal plate directs spleen and pancreatic laterality, and is regulated by Bapx1/Nkx3.2. Development *131*, 4665-4675.

Heller,R.S., Dichmann,D.S., Jensen,J., Miller,C., Wong,G., Madsen,O.D., and Serup,P. (2002). Expression patterns of Wnts, Frizzleds, sFRPs, and misexpression in transgenic mice suggesting a role for Wnts in pancreas and foregut pattern formation. Dev. Dyn. *225*, 260-270.

Herrera,P.L., Huarte,J., Zufferey,R., Nichols,A., Mermillod,B., Philippe,J., Muniesa,P., Sanvito,F., Orci,L., and Vassalli,J.D. (1994). Ablation of islet endocrine cells by targeted expression of hormone-promoter-driven toxigenes. Proc. Natl. Acad. Sci. U. S. A *91*, 12999-13003.

Herzer,U., Crocoll,A., Barton,D., Howells,N., and Englert,C. (1999). The Wilms tumor suppressor gene wt1 is required for development of the spleen. Curr. Biol. *9*, 837-840.

Higgins,M., Hill,R.E., and West,J.D. (1992). Dominant hemimelia and En-1 on mouse chromosome 1 are not allelic. Genet. Res. *60*, 53-60.

Hill,R.E. (2004). 'Gotta pick a megabase or two': in silico routes to gene regulation. Brief. Funct. Genomic. Proteomic. *3*, 12-14.

Hill,R.E., Hall,A.E., Sime,C.M., and Hastie,N.D. (1987). A mouse homeo box-containing gene maps near a developmental mutation. Cytogenet. Cell Genet. *44*, 171-174.

Himmelbauer,H., Harvey,R.P., Copeland,N.G., Jenkins,N.A., and Silver,L.M. (1994). High-resolution genetic analysis of a deletion on mouse chromosome 17 extending over the fused, tufted, and homeobox Nkx2-5 loci. Mamm. Genome *5*, 814-816.

Hirayama-Yamada,K., Kamisago,M., Akimoto,K., Aotsuka,H., Nakamura,Y., Tomita,H., Furutani,M., Imamura,S., Takao,A., Nakazawa,M., and Matsuoka,R. (2005). Phenotypes with GATA4 or NKX2.5 mutations in familial atrial septal defect. Am. J. Med. Genet. A *135*, 47-52.

Hiroi,Y., Kudoh,S., Monzen,K., Ikeda,Y., Yazaki,Y., Nagai,R., and Komuro,I. (2001). Tbx5 associates with Nkx2-5 and synergistically promotes cardiomyocyte differentiation. Nat. Genet. *28*, 276-280.

Hoffman,M.P., Kidder,B.L., Steinberg,Z.L., Lakhani,S., Ho,S., Kleinman,H.K., and Larsen,M. (2002). Gene expression profiles of mouse submandibular gland development: FGFR1 regulates branching morphogenesis in vitro through BMP- and FGF-dependent mechanisms. Development *129*, 5767-5778.

Hogan,B.L. (1999). Morphogenesis. Cell *96*, 225-233.

Hogan,B.L.M. and Zaret,K.S. (2002). Development of the Endoderm and its Tissue Derivatives. In Mouse development : patterning, morphogenesis, and organogenesis, J.Rossant and P.P.L.Tam, eds. San Diego ; London : Academic Press, c2002), pp. 301-330.

Hogers,B., Gross,D., Lehmann,V., Zick,K., De Groot,H.J., Gittenberger-De Groot,A.C., and Poelmann,R.E. (2000). Magnetic resonance microscopy of mouse embryos in utero. Anat. Rec. *260*, 373-377.

Holyoke,E.A. (1936). The role of the primitive mesothelium in the development of the mammalian spleen. Anat. Rec. *65*, 333-349.

Horne-Badovinac,S., Rebagliati,M., and Stainier,D.Y. (2003). A cellular framework for gut-looping morphogenesis in zebrafish. Science *302*, 662-665.

Hosoda,T., Komuro,I., Shiojima,I., Hiroi,Y., Harada,M., Murakawa,Y., Hirata,Y., and Yazaki,Y. (1999). Familial atrial septal defect and atrioventricular conduction disturbance associated with a point mutation in the cardiac homeobox gene CSX/NKX2-5 in a Japanese patient. Jpn. Circ. J. *63*, 425-426.

Huang,P.L., Dawson,T.M., Bredt,D.S., Snyder,S.H., and Fishman,M.C. (1993). Targeted disruption of the neuronal nitric oxide synthase gene. Cell *75*, 1273-1286.

Huelsken,J. and Behrens,J. (2002). The Wnt signalling pathway. J. Cell Sci. *115*, 3977-3978.

Hughes,D.C., Allen,J., Morley,G., Sutherland,K., Ahmed,W., Prosser,J., Lettice,L., Allan,G., Mattei,M.G., Farrall,M., and Hill,R.E. (1997). Cloning and sequencing of the mouse Gli2 gene: localization to the Dominant hemimelia critical region. Genomics *39*, 205-215.

Hulka,F., Campbell,T.J., Campbell,J.R., and Harrison,M.W. (1997). Evolution in the recognition of infantile hypertrophic pyloric stenosis. Pediatrics *100*, E9.

Ikeda,Y., Hiroi,Y., Hosoda,T., Utsunomiya,T., Matsuo,S., Ito,T., Inoue,J., Sumiyoshi,T., Takano,H., Nagai,R., and Komuro,I. (2002). Novel point mutation in the cardiac transcription factor CSX/NKX2.5 associated with congenital heart disease. Circ. J. *66*, 561-563.

Indra,A.K., Dupe,V., Bornert,J.M., Messaddeq,N., Yaniv,M., Mark,M., Chambon,P., and Metzger,D. (2005). Temporally controlled targeted somatic mutagenesis in embryonic surface ectoderm and fetal epidermal keratinocytes unveils two distinct developmental functions of BRG1 in limb morphogenesis and skin barrier formation. Development *132*, 4533-4544.

Indra,A.K., Li,M., Brocard,J., Warot,X., Bornert,J.M., Gerard,C., Messaddeq,N., Chambon,P., and Metzger,D. (2000). Targeted somatic mutagenesis in mouse epidermis. Horm. Res. *54*, 296-300.

Indra,A.K., Warot,X., Brocard,J., Bornert,J.M., Xiao,J.H., Chambon,P., and Metzger,D. (1999). Temporally-controlled site-specific mutagenesis in the basal layer of the epidermis: comparison of the recombinase activity of the tamoxifen-inducible Cre-ER(T) and Cre-ER(T2) recombinases. Nucleic Acids Res. *27*, 4324-4327.

Ivanova,A., Signore,M., Caro,N., Greene,N.D., Copp,A.J., and Martinez-Barbera,J.P. (2005). In vivo genetic ablation by Cre-mediated expression of diphtheria toxin fragment A. Genesis. *43*, 129-135.

Jagla,K., Bellard,M., and Frasch,M. (2001). A cluster of Drosophila homeobox genes involved in mesoderm differentiation programs. Bioessays *23*, 125-133.

Jay,P.Y., Harris,B.S., Maguire,C.T., Buerger,A., Wakimoto,H., Tanaka,M., Kupershmidt,S., Roden,D.M., Schultheiss,T.M., O'brien,T.X., Gourdie,R.G., Berul,C.I., and Izumo,S. (2004). Nkx2-5 mutation causes anatomic hypoplasia of the cardiac conduction system. J. Clin. Invest *113*, 1130-1137.

Jiang,X., Rowitch,D.H., Soriano,P., McMahon,A.P., and Sucov,H.M. (2000). Fate of the mammalian cardiac neural crest. Development *127*, 1607-1616.

Johnson,C.F., Koch,R., Peterson,R.M., and Friedman,E.G. (1978). Congenital and neurological abnormalities in infants with phenylketonuria. Am. J. Ment. Defic. *82*, 375-379.

Jonsson,J., Carlsson,L., Edlund,T., and Edlund,H. (1994). Insulin-promoter-factor 1 is required for pancreas development in mice. Nature *371*, 606-609.

Juriloff,D.M., Harris,M.J., Dewell,S.L., Brown,C.J., Mager,D.L., Gagnier,L., and Mah,D.G. (2005). Investigations of the genomic region that contains the clf1 mutation, a causal gene in multifactorial cleft lip and palate in mice. Birth Defects Res. A Clin. Mol. Teratol. *73*, 103-113.

Kanzler,B. and Dear,T.N. (2001). Hox11 acts cell autonomously in spleen development and its absence results in altered cell fate of mesenchymal spleen precursors. Dev. Biol. *234*, 231-243.

Kapur,R.P., Yost,C., and Palmiter,R.D. (1992). A transgenic model for studying development of the enteric nervous system in normal and aganglionic mice. Development *116*, 167-175.

Kasahara,H., Bartunkova,S., Schinke,M., Tanaka,M., and Izumo,S. (1998). Cardiac and extracardiac expression of Csx/Nkx2.5 homeodomain protein. Circ. Res. *82*, 936-946.

Kasahara,H., Lee,B., Schott,J.J., Benson,D.W., Seidman,J.G., Seidman,C.E., and Izumo,S. (2000). Loss of function and inhibitory effects of human CSX/NKX2.5 homeoprotein mutations associated with congenital heart disease. J. Clin. Invest *106*, 299-308.

Kasahara,H., Wakimoto,H., Liu,M., Maguire,C.T., Converso,K.L., Shioi,T., Huang,W.Y., Manning,W.J., Paul,D., Lawitts,J., Berul,C.I., and Izumo,S. (2001). Progressive atrioventricular conduction defects and heart failure in mice expressing a mutant Csx/Nkx2.5 homeoprotein. J. Clin. Invest *108*, 189-201.

Katoh,M. (2005). Comparative genomics on Wnt3-Wnt9b gene cluster. Int. J. Mol. Med. *15*, 743-747.

Kaufman,T.C., Lewis,R., and Wakimoto,B. (1980). Cytogenetic Analysis of Chromosome 3 in DROSOPHILA MELANOGASTER: The Homoeotic Gene Complex in Polytene Chromosome Interval 84a-B. Genetics *94*, 115-133.

Kawazoe,Y., Sekimoto,T., Araki,M., Takagi,K., Araki,K., and Yamamura,K. (2002). Region-specific gastrointestinal Hox code during murine embryonal gut development. Dev. Growth Differ. *44*, 77-84.

Kemp,C., Willems,E., Abdo,S., Lambiv,L., and Leyns,L. (2005). Expression of all Wnt genes and their secreted antagonists during mouse blastocyst and postimplantation development. Dev. Dyn. *233*, 1064-1075.

Kennedy,M.A., Gonzalez-Sarmiento,R., Kees,U.R., Lampert,F., Dear,N., Boehm,T., and Rabbitts,T.H. (1991). HOX11, a homeobox-containing T-cell oncogene on human chromosome 10q24. Proc. Natl. Acad. Sci. U. S. A *88*, 8900-8904.

Khwaja,M.S., al Arfaj,A.L., and Dawoodu,A.H. (1989). Congenital right-sided diaphragmatic hernia: a heterogeneous lesion. J. R. Coll. Surg. Edinb. *34*, 219-222.

Kim,B.M., Buchner,G., Miletich,I., Sharpe,P.T., and Shivdasani,R.A. (2005a). The stomach mesenchymal transcription factor Barx1 specifies gastric epithelial identity through inhibition of transient Wnt signaling. Dev. Cell *8*, 611-622.

Kim,D.W., Kempf,H., Chen,R.E., and Lassar,A.B. (2003). Characterization of Nkx3.2 DNA binding specificity and its requirement for somitic chondrogenesis. J. Biol. Chem. *278*, 27532-27539.

Kim,J.H., Huang,Z., and Mo,R. (2005b). Gli3 null mice display glandular overgrowth of the developing stomach. Dev. Dyn. *234*, 984-991.

Kim,S.K. and Hebrok,M. (2001). Intercellular signals regulating pancreas development and function. Genes Dev. *15*, 111-127.

Kim,Y. and Nirenberg,M. (1989). Drosophila NK-homeobox genes. Proc. Natl. Acad. Sci. U. S. A *86*, 7716-7720.

Kimmel,R.A., Turnbull,D.H., Blanquet,V., Wurst,W., Loomis,C.A., and Joyner,A.L. (2000). Two lineage boundaries coordinate vertebrate apical ectodermal ridge formation. Genes Dev. *14*, 1377-1389.

Kimura,S., Hara,Y., Pineau,T., Fernandez-Salguero,P., Fox,C.H., Ward,J.M., and Gonzalez,F.J. (1996). The T/ebp null mouse: thyroid-specific enhancer-binding protein is essential for the organogenesis of the thyroid, lung, ventral forebrain, and pituitary. Genes Dev. *10*, 60-69.

Klug,S. (1991). Whole embryo culture: interpretation of abnormal development in vitro. Reprod. Toxicol. *5*, 237-244.

Kodama,S., Davis,M., and Faustman,D.L. (2005). Diabetes and stem cell researchers turn to the lowly spleen. Sci. Aging Knowledge. Environ. *2005*, e2.

Kodama,S., Kuhtreiber,W., Fujimura,S., Dale,E.A., and Faustman,D.L. (2003). Islet regeneration during the reversal of autoimmune diabetes in NOD mice. Science *302*, 1223-1227.

Koehler,K., Franz,T., and Dear,T.N. (2000). Hox11 is required to maintain normal Wt1 mRNA levels in the developing spleen. Dev. Dyn. *218*, 201-206.

Komuro,I. and Izumo,S. (1993). Csx: a murine homeobox-containing gene specifically expressed in the developing heart. Proc. Natl. Acad. Sci. U. S. A *90*, 8145-8149.

Konig,K., Will,J.C., Berger,F., Muller,D., and Benson,D.W. (2006). Familial congenital heart disease, progressive atrioventricular block and the cardiac homeobox transcription factor gene NKX2.5: : identification of a novel mutation. Clin. Res. Cardiol. *95*, 499-503.

Krapp,A., Knofler,M., Ledermann,B., Burki,K., Berney,C., Zoerkler,N., Hagenbuchle,O., and Wellauer,P.K. (1998). The bHLH protein PTF1-p48 is essential for the formation of the exocrine and the correct spatial organization of the endocrine pancreas. Genes Dev. *12*, 3752-3763.

Krude,H., Schutz,B., Biebermann,H., von Moers,A., Schnabel,D., Neitzel,H., Tonnies,H., Weise,D., Lafferty,A., Schwarz,S., DeFelice,M., von Deimling,A., van Landeghem,F., DiLauro,R., and Gruters,A. (2002). Choreoathetosis, hypothyroidism, and pulmonary alterations due to human NKX2-1 haploinsufficiency. J. Clin. Invest *109*, 475-480.

Kudo,T., Shimoda,H., Usui,T., and Uchida,Y. (1998). Organization of nitric oxide-producing nerves in the rat pyloric sphincter. Arch. Histol. Cytol. *61*, 361-372.

Kuhl,M., Sheldahl,L.C., Park,M., Miller,J.R., and Moon,R.T. (2000). The Wnt/Ca2+ pathway: a new vertebrate Wnt signaling pathway takes shape. Trends Genet. *16*, 279-283.

Lamarcq,L., Deeds,J., Ginzinger,D., Perry,J., Padmanabha,S., and Smith-McCune,K. (2002). Measurements of human papillomavirus transcripts by real time quantitative reverse transcription-polymerase chain reaction in samples collected for cervical cancer screening. J. Mol. Diagn. *4*, 97-102.

Lan,Y., Ryan,R.C., Zhang,Z., Bullard,S.A., Bush,J.O., Maltby,K.M., Lidral,A.C., and Jiang,R. (2006). Expression of Wnt9b and activation of canonical Wnt signaling during midfacial morphogenesis in mice. Dev. Dyn. *235*, 1448-1454.

Lecaudey,V. and Gilmour,D. (2006). Organizing moving groups during morphogenesis. Curr. Opin. Cell Biol. *18*, 102-107.

Lee,H.H. and Frasch,M. (2000). Wingless effects mesoderm patterning and ectoderm segmentation events via induction of its downstream target sloppy paired. Development *127*, 5497-5508.

Lee,K.H., Evans,S., Ruan,T.Y., and Lassar,A.B. (2004). SMAD-mediated modulation of YY1 activity regulates the BMP response and cardiac-specific expression of a GATA4/5/6-dependent chick Nkx2.5 enhancer. Development *131*, 4709-4723.

Lee,K.H., Xu,Q., and Breitbart,R.E. (1996). A new tinman-related gene, nkx2.7, anticipates the expression of nkx2.5 and nkx2.3 in zebrafish heart and pharyngeal endoderm. Dev. Biol. *180*, 722-731.

Lettice,L., Hecksher-Sorensen,J., and Hill,R. (2001). The role of Bapx1 (Nkx3.2) in the development and evolution of the axial skeleton. J. Anat. *199*, 181-187.

Lettice,L., Hecksher-Sorensen,J., and Hill,R.E. (1999a). The dominant hemimelia mutation uncouples epithelial-mesenchymal interactions and disrupts anterior mesenchyme formation in mouse hindlimbs. Development *126*, 4729-4736.

Lettice,L.A., Heaney,S.J., Purdie,L.A., Li,L., de Beer,P., Oostra,B.A., Goode,D., Elgar,G., Hill,R.E., and de Graaff,E. (2003). A long-range Shh enhancer regulates expression in the developing limb and fin and is associated with preaxial polydactyly. Hum. Mol. Genet. *12*, 1725-1735.

Lettice,L.A., Purdie,L.A., Carlson,G.J., Kilanowski,F., Dorin,J., and Hill,R.E. (1999b). The mouse bagpipe gene controls development of axial skeleton, skull, and spleen. Proc. Natl. Acad. Sci. U. S. A *96*, 9695-9700.

Liberatore,C.M., Searcy-Schrick,R.D., Vincent,E.B., and Yutzey,K.E. (2002). Nkx-2.5 gene induction in mice is mediated by a Smad consensus regulatory region. Dev. Biol. *244*, 243-256.

Lickert,H., Kispert,A., Kutsch,S., and Kemler,R. (2001). Expression patterns of Wnt genes in mouse gut development. Mech. Dev. *105*, 181-184.

Lien,C.L., McAnally,J., Richardson,J.A., and Olson,E.N. (2002). Cardiac-specific activity of an Nkx2-5 enhancer requires an evolutionarily conserved Smad binding site. Dev. Biol. *244*, 257-266.

Lien,C.L., Wu,C., Mercer,B., Webb,R., Richardson,J.A., and Olson,E.N. (1999). Control of early cardiac-specific transcription of Nkx2-5 by a GATA-dependent enhancer. Development *126*, 75-84.

Lin,C.R., Kioussi,C., O'Connell,S., Briata,P., Szeto,D., Liu,F., Izpisua-Belmonte,J.C., and Rosenfeld,M.G. (1999). Pitx2 regulates lung asymmetry, cardiac positioning and pituitary and tooth morphogenesis. Nature *401*, 279-282.

Lints,T.J., Parsons,L.M., Hartley,L., Lyons,I., and Harvey,R.P. (1993b). Nkx-2.5: a novel murine homeobox gene expressed in early heart progenitor cells and their myogenic descendants. Development *119*, 419-431.

Lints,T.J., Parsons,L.M., Hartley,L., Lyons,I., and Harvey,R.P. (1993a). Nkx-2.5: a novel murine homeobox gene expressed in early heart progenitor cells and their myogenic descendants. Development *119*, 969.

Lioubinski,O., Muller,M., Wegner,M., and Sander,M. (2003). Expression of Sox transcription factors in the developing mouse pancreas. Dev. Dyn. *227*, 402-408.

Litingtung,Y., Lei,L., Westphal,H., and Chiang,C. (1998). Sonic hedgehog is essential to foregut development. Nat. Genet. *20*, 58-61.

Liu,P., Wakamiya,M., Shea,M.J., Albrecht,U., Behringer,R.R., and Bradley,A. (1999). Requirement for Wnt3 in vertebrate axis formation. Nat. Genet. *22*, 361-365.

Lo,P.C. and Frasch,M. (1998). bagpipe-Dependent expression of vimar, a novel Armadillo-repeats gene, in Drosophila visceral mesoderm. Mech. Dev. *72*, 65-75.

Loots,G.G. and Ovcharenko,I. (2004). rVISTA 2.0: evolutionary analysis of transcription factor binding sites. Nucleic Acids Res. *32*, W217-W221.

Lu,J., Chang,P., Richardson,J.A., Gan,L., Weiler,H., and Olson,E.N. (2000). The basic helix-loop-helix transcription factor capsulin controls spleen organogenesis. Proc. Natl. Acad. Sci. U. S. A *97*, 9525-9530.

Lu,J., Richardson,J.A., and Olson,E.N. (1998). Capsulin: a novel bHLH transcription factor expressed in epicardial progenitors and mesenchyme of visceral organs. Mech. Dev. *73*, 23-32.

Lu,M.F., Pressman,C., Dyer,R., Johnson,R.L., and Martin,J.F. (1999). Function of Rieger syndrome gene in left-right asymmetry and craniofacial development. Nature *401*, 276-278.

Luke,G.N., Castro,L.F., McLay,K., Bird,C., Coulson,A., and Holland,P.W. (2003). Dispersal of NK homeobox gene clusters in amphioxus and humans. Proc. Natl. Acad. Sci. U. S. A *100*, 5292-5295.

Lyons,I., Parsons,L.M., Hartley,L., Li,R., Andrews,J.E., Robb,L., and Harvey,R.P. (1995). Myogenic and morphogenetic defects in the heart tubes of murine embryos lacking the homeo box gene Nkx2-5. Genes Dev. *9*, 1654-1666.

MacKenzie,A., Purdie,L., Davidson,D., Collinson,M., and Hill,R.E. (1997). Two enhancer domains control early aspects of the complex expression pattern of Msx1. Mech. Dev. *62*, 29-40.

Mahlapuu,M., Enerback,S., and Carlsson,P. (2001a). Haploinsufficiency of the forkhead gene Foxf1, a target for sonic hedgehog signaling, causes lung and foregut malformations. Development *128*, 2397-2406.

Mahlapuu,M., Ormestad,M., Enerback,S., and Carlsson,P. (2001b). The forkhead transcription factor Foxf1 is required for differentiation of extra-embryonic and lateral plate mesoderm. Development *128*, 155-166.

Maretto,S., Cordenonsi,M., Dupont,S., Braghetta,P., Broccoli,V., Hassan,A.B., Volpin,D., Bressan,G.M., and Piccolo,S. (2003). Mapping Wnt/beta-catenin signaling during mouse development and in colorectal tumors. Proc. Natl. Acad. Sci. U. S. A *100*, 3299-3304.

McAteer,J.A., Cavanagh,T.J., and Evan,A.P. (1983). Submersion culture of the intact fetal lung. In Vitro *19*, 210-218.

McElhinney,D.B., Geiger,E., Blinder,J., Benson,D.W., and Goldmuntz,E. (2003). NKX2.5 mutations in patients with congenital heart disease. J. Am. Coll. Cardiol. *42*, 1650-1655.

Mebius,R.E. and Kraal,G. (2005). Structure and function of the spleen. Nat. Rev. Immunol. *5*, 606-616.

Mehta,A.V. and Ambalavanan,S.K. (1997). Infantile hypertrophic pyloric stenosis and congenital heart disease: an under-recognized association. Tenn. Med. *90*, 496-497.

Metzger,D., Clifford,J., Chiba,H., and Chambon,P. (1995). Conditional site-specific recombination in mammalian cells using a ligand-dependent chimeric Cre recombinase. Proc. Natl. Acad. Sci. U. S. A *92*, 6991-6995.

Meyers,E.N. and Martin,G.R. (1999). Differences in left-right axis pathways in mouse and chick: functions of FGF8 and SHH. Science *285*, 403-406.

Miller,C.T., Yelon,D., Stainier,D.Y., and Kimmel,C.B. (2003). Two endothelin 1 effectors, hand2 and bapx1, pattern ventral pharyngeal cartilage and the jaw joint. Development *130*, 1353-1365.

Miller,J.R. (2002). The Wnts. Genome Biol. *3*, REVIEWS3001.

Minoo,P., Su,G., Drum,H., Bringas,P., and Kimura,S. (1999). Defects in tracheoesophageal and lung morphogenesis in Nkx2.1(-/-) mouse embryos. Dev. Biol. *209*, 60-71.

Mishalany,H., Mahnovski,V., and Woolley,M. (1982). Congenital asplenia and anomalies of the gastrointestinal tract. Surgery *91*, 38-41.

Mitchell,L.E. and Risch,N. (1993). The genetics of infantile hypertrophic pyloric stenosis. A reanalysis. Am. J. Dis. Child *147*, 1203-1211.

Moniot,B., Biau,S., Faure,S., Nielsen,C.M., Berta,P., Roberts,D.J., and de Santa,B.P. (2004). SOX9 specifies the pyloric sphincter epithelium through mesenchymal-epithelial signals. Development *131*, 3795-3804.

Monkley,S.J., Delaney,S.J., Pennisi,D.J., Christiansen,J.H., and Wainwright,B.J. (1996). Targeted disruption of the Wnt2 gene results in placentation defects. Development *122*, 3343-3353.

Moore-Scott,B.A., Gordon,J., Blackburn,C.C., Condie,B.G., and Manley,N.R. (2003). New serum-free in vitro culture technique for midgestation mouse embryos. Genesis. *35*, 164-168.

Morin,B.J., Owen,M.H., Ramamurthy,G.V., and Holmes,L.B. (1999). Pattern of skeletal malformations produced by Dominant hemimelia (Dh). Teratology *60*, 348-355.

Moriyama,A., Kii,I., Sunabori,T., Kurihara,S., Takayama,I., Shimazaki,M., Tanabe,H., Oginuma,M., Fukayama,M., Matsuzaki,Y., Saga,Y., and Kudo,A. (2007). GFP transgenic mice reveal active canonical Wnt signal in neonatal brain and in adult liver and spleen. Genesis. *45*, 90-100.

Morkel,M., Huelsken,J., Wakamiya,M., Ding,J., van de,W.M., Clevers,H., Taketo,M.M., Behringer,R.R., Shen,M.M., and Birchmeier,W. (2003). Beta-catenin regulates Cripto- and Wnt3-dependent gene expression programs in mouse axis and mesoderm formation. Development *130*, 6283-6294.

Moses,K.A., DeMayo,F., Braun,R.M., Reecy,J.L., and Schwartz,R.J. (2001). Embryonic expression of an Nkx2-5/Cre gene using ROSA26 reporter mice. Genesis. *31*, 176-180.

Muller,J.K., Prather,D.R., and Nascone-Yoder,N.M. (2003). Left-right asymmetric morphogenesis in the Xenopus digestive system. Dev. Dyn. *228*, 672-682.

Murtaugh,L.C., Zeng,L., Chyung,J.H., and Lassar,A.B. (2001). The chick transcriptional repressor Nkx3.2 acts downstream of Shh to promote BMP-dependent axial chondrogenesis. Dev. Cell *1*, 411-422.

Mycielska,M.E. and Djamgoz,M.B. (2004). Cellular mechanisms of direct-current electric field effects: galvanotaxis and metastatic disease. J. Cell Sci. *117*, 1631-1639.

Natarajan,D., Grigoriou,M., Marcos-Gutierrez,C.V., Atkins,C., and Pachnis,V. (1999). Multipotential progenitors of the mammalian enteric nervous system capable of colonising aganglionic bowel in organ culture. Development *126*, 157-168.

Nelson,S.B., Janiesch,C., and Sander,M. (2005). Expression of Nkx6 genes in the hindbrain and gut of the developing mouse. J. Histochem. Cytochem. *53*, 787-790.

Newman,C.S., Grow,M.W., Cleaver,O., Chia,F., and Krieg,P. (1997). Xbap, a vertebrate gene related to bagpipe, is expressed in developing craniofacial structures and in anterior gut muscle. Dev. Biol. *181*, 223-233.

Newman,C.S. and Krieg,P.A. (1999). The Xenopus bagpipe-related homeobox gene zampogna is expressed in the pharyngeal endoderm and the visceral musculature of the midgut. Dev. Genes Evol. *209*, 132-134.

Newman,C.S. and Krieg,P.A. (2002). Xenopus bagpipe-related gene, koza, may play a role in regulation of cell proliferation. Dev. Dyn. *225*, 571-580.

Nielsen,C., Murtaugh,L.C., Chyung,J.C., Lassar,A., and Roberts,D.J. (2001). Gizzard formation and the role of Bapx1. Dev. Biol. *231*, 164-174.

Nishijima,E., Meijers,J.H., Tibboel,D., Luider,T.M., Peters-van der Sanden MM, van der Kamp,A.W., and Molenaar,J.C. (1990). Formation and malformation of the enteric nervous system in mice: an organ culture study. J. Pediatr. Surg. *25*, 627-631.

Nishio,J., Gaglia,J.L., Turvey,S.E., Campbell,C., Benoist,C., and Mathis,D. (2006). Islet recovery and reversal of murine type 1 diabetes in the absence of any infused spleen cell contribution. Science *311*, 1775-1778.

Ormestad,M., Astorga,J., Landgren,H., Wang,T., Johansson,B.R., Miura,N., and Carlsson,P. (2006). Foxf1 and Foxf2 control murine gut development by limiting mesenchymal Wnt signaling and promoting extracellular matrix production. Development *133*, 833-843.

Ovcharenko,I., Nobrega,M.A., Loots,G.G., and Stubbs,L. (2004). ECR Browser: a tool for visualizing and accessing data from comparisons of multiple vertebrate genomes. Nucleic Acids Res. *32*, W280-W286.

Pabst,O., Forster,R., Lipp,M., Engel,H., and Arnold,H.H. (2000). NKX2.3 is required for MAdCAM-1 expression and homing of lymphocytes in spleen and mucosa-associated lymphoid tissue. EMBO J. *19*, 2015-2023.

Pabst,O., Herbrand,H., and Arnold,H.H. (1998). Nkx2-9 is a novel homeobox transcription factor which demarcates ventral domains in the developing mouse CNS. Mech. Dev. *73*, 85-93.

Pabst,O., Rummelies,J., Winter,B., and Arnold,H.H. (2003). Targeted disruption of the homeobox gene Nkx2.9 reveals a role in development of the spinal accessory nerve. Development *130*, 1193-1202.

Pabst,O., Schneider,A., Brand,T., and Arnold,H.H. (1997). The mouse Nkx2-3 homeodomain gene is expressed in gut mesenchyme during pre- and postnatal mouse development. Dev. Dyn. *209*, 29-35.

Pabst,O., Zweigerdt,R., and Arnold,H.H. (1999). Targeted disruption of the homeobox transcription factor Nkx2-3 in mice results in postnatal lethality and abnormal development of small intestine and spleen. Development *126*, 2215-2225.

Pandur,P., Maurus,D., and Kuhl,M. (2002). Increasingly complex: new players enter the Wnt signaling network. Bioessays *24*, 881-884.

Panganiban,G.E., Reuter,R., Scott,M.P., and Hoffmann,F.M. (1990). A Drosophila growth factor homolog, decapentaplegic, regulates homeotic gene expression within and across germ layers during midgut morphogenesis. Development *110*, 1041-1050.

Park,M., Lewis,C., Turbay,D., Chung,A., Chen,J.N., Evans,S., Breitbart,R.E., Fishman,M.C., Izumo,S., and Bodmer,R. (1998a). Differential rescue of visceral and cardiac defects in Drosophila by vertebrate tinman-related genes. Proc. Natl. Acad. Sci. U. S. A *95*, 9366-9371.

Park,W.Y., Miranda,B., Lebeche,D., Hashimoto,G., and Cardoso,W.V. (1998b). FGF-10 is a chemotactic factor for distal epithelial buds during lung development. Dev. Biol. *201*, 125-134.

Parr,B.A., Shea,M.J., Vassileva,G., and McMahon,A.P. (1993). Mouse Wnt genes exhibit discrete domains of expression in the early embryonic CNS and limb buds. Development *119*, 247-261.

Pashmforoush,M., Lu,J.T., Chen,H., Amand,T.S., Kondo,R., Pradervand,S., Evans,S.M., Clark,B., Feramisco,J.R., Giles,W., Ho,S.Y., Benson,D.W., Silberbach,M., Shou,W., and Chien,K.R. (2004). Nkx2-5 pathways and congenital heart disease; loss of ventricular myocyte lineage specification leads to progressive cardiomyopathy and complete heart block. Cell *117*, 373-386.

Patterson,K.D., Drysdale,T.A., and Krieg,P.A. (2000). Embryonic origins of spleen asymmetry. Development *127*, 167-175.

Pedersen,J.K., Nelson,S.B., Jorgensen,M.C., Henseleit,K.D., Fujitani,Y., Wright,C.V., Sander,M., and Serup,P. (2005). Endodermal expression of Nkx6 genes depends differentially on Pdx1. Dev. Biol. *288*, 487-501.

Peeters,H. and Devriendt,K. (2006). Human laterality disorders. Eur. J. Med. Genet. *49*, 349-362.

Perea-Gomez,A., Lawson,K.A., Rhinn,M., Zakin,L., Brulet,P., Mazan,S., and Ang,S.L. (2001). Otx2 is required for visceral endoderm movement and for the restriction of posterior signals in the epiblast of the mouse embryo. Development *128*, 753-765.

Petit,A.C., Legue,E., and Nicolas,J.F. (2005). Methods in clonal analysis and applications. Reprod. Nutr. Dev. *45*, 321-339.

Phoon,C.K. and Neill,C.A. (1994). Asplenia syndrome: insight into embryology through an analysis of cardiac and extracardiac anomalies. Am. J. Cardiol. *73*, 581-587.

Pitera,J.E., Smith,V.V., Woolf,A.S., and Milla,P.J. (2001). Embryonic gut anomalies in a mouse model of retinoic Acid-induced caudal regression syndrome: delayed gut looping, rudimentary cecum, and anorectal anomalies. Am. J. Pathol. *159*, 2321-2329.

Price,M. (1993). Members of the Dlx- and Nkx2-gene families are regionally expressed in the developing forebrain. J. Neurobiol. *24*, 1385-1399.

Provot,S., Kempf,H., Murtaugh,L.C., Chung,U.I., Kim,D.W., Chyung,J., Kronenberg,H.M., and Lassar,A.B. (2006). Nkx3.2/Bapx1 acts as a negative regulator of chondrocyte maturation. Development *133*, 651-662.

Qiu,M., Shimamura,K., Sussel,L., Chen,S., and Rubenstein,J.L. (1998). Control of anteroposterior and dorsoventral domains of Nkx-6.1 gene expression relative to other Nkx genes during vertebrate CNS development. Mech. Dev. *72*, 77-88.

Quaroni,A. (1985). Development of fetal rat intestine in organ and monolayer culture. J. Cell Biol. *100*, 1611-1622.

Quinlan,R., Martin,P., and Graham,A. (2004). The role of actin cables in directing the morphogenesis of the pharyngeal pouches. Development *131*, 593-599.

Rackley,R.R., Flenniken,A.M., Kuriyan,N.P., Kessler,P.M., Stoler,M.H., and Williams,B.R. (1993). Expression of the Wilms' tumor suppressor gene WT1 during mouse embryogenesis. Cell Growth Differ. *4*, 1023-1031.

Ramalho-Santos,M., Melton,D.A., and McMahon,A.P. (2000). Hedgehog signals regulate multiple aspects of gastrointestinal development. Development *127*, 2763-2772.

Ramsdell,A.F. (2005). Left-right asymmetry and congenital cardiac defects: getting to the heart of the matter in vertebrate left-right axis determination. Dev. Biol. *288*, 1-20.

Ranganayakulu,G., Elliott,D.A., Harvey,R.P., and Olson,E.N. (1998). Divergent roles for NK-2 class homeobox genes in cardiogenesis in flies and mice. Development *125*, 3037-3048.

Reamon-Buettner,S.M. and Borlak,J. (2004). Somatic NKX2-5 mutations as a novel mechanism of disease in complex congenital heart disease. J. Med. Genet. *41*, 684-690.

Reecy,J.M., Li,X., Yamada,M., DeMayo,F.J., Newman,C.S., Harvey,R.P., and Schwartz,R.J. (1999). Identification of upstream regulatory regions in the heart-expressed homeobox gene Nkx2-5. Development *126*, 839-849.

Reecy,J.M., Yamada,M., Cummings,K., Sosic,D., Chen,C.Y., Eichele,G., Olson,E.N., and Schwartz,R.J. (1997). Chicken Nkx-2.8: a novel homeobox gene expressed in early heart progenitor cells and pharyngeal pouch-2 and -3 endoderm. Dev. Biol. *188*, 295-311.

Riazi,A.M., Lee,H., Hsu,C., and Van Arsdell,G. (2005). CSX/Nkx2.5 modulates differentiation of skeletal myoblasts and promotes differentiation into neuronal cells in vitro. J. Biol. Chem. *280*, 10716-10720.

Ricken,A., Lochhead,P., Kontogiannea,M., and Farookhi,R. (2002). Wnt signaling in the ovary: identification and compartmentalized expression of wnt-2, wnt-2b, and frizzled-4 mRNAs. Endocrinology *143*, 2741-2749.

Rinkwitz-Brandt,S., Justus,M., Oldenettel,I., Arnold,H.H., and Bober,E. (1995). Distinct temporal expression of mouse Nkx-5.1 and Nkx-5.2 homeobox genes during brain and ear development. Mech. Dev. *52*, 371-381.

Roberts,C.W., Shutter,J.R., and Korsmeyer,S.J. (1994). Hox11 controls the genesis of the spleen. Nature *368*, 747-749.

Roberts,C.W., Sonder,A.M., Lumsden,A., and Korsmeyer,S.J. (1995a). Development expression of Hox11 and specification of splenic cell fate. Am. J. Pathol. *146*, 1089-1101.

Roberts,D.J. (1999). Embryology of the Gastrointestinal Tract. In Development of the Gastrointestinal Tract, I.R.Sanderson and W.A.Walker, eds. Hamilton, Ont., London : B C Decker), pp. 1-12.

Roberts,D.J. (2000). Molecular mechanisms of development of the gastrointestinal tract. Dev. Dyn. *219*, 109-120.

Roberts,D.J., Johnson,R.L., Burke,A.C., Nelson,C.E., Morgan,B.A., and Tabin,C. (1995b). Sonic hedgehog is an endodermal signal inducing Bmp-4 and Hox genes during induction and regionalization of the chick hindgut. Development *121*, 3163-3174.

Roberts,D.J., Smith,D.M., Goff,D.J., and Tabin,C.J. (1998). Epithelial-mesenchymal signaling during the regionalization of the chick gut. Development *125*, 2791-2801.

Rodrigo,I., Hill,R.E., Balling,R., Munsterberg,A., and Imai,K. (2003). Pax1 and Pax9 activate Bapx1 to induce chondrogenic differentiation in the sclerotome. Development *130*, 473-482.

Roelink,H., Wagenaar,E., Lopes,d.S., and Nusse,R. (1990). Wnt-3, a gene activated by proviral insertion in mouse mammary tumors, is homologous to int-1/Wnt-1 and is normally expressed in mouse embryos and adult brain. Proc. Natl. Acad. Sci. U. S. A *87*, 4519-4523.

Rudnick,A., Ling,T.Y., Odagiri,H., Rutter,W.J., and German,M.S. (1994). Pancreatic beta cells express a diverse set of homeobox genes. Proc. Natl. Acad. Sci. U. S. A *91*, 12203-12207.

Saito,M., Iwawaki,T., Taya,C., Yonekawa,H., Noda,M., Inui,Y., Mekada,E., Kimata,Y., Tsuru,A., and Kohno,K. (2001). Diphtheria toxin receptor-mediated conditional and targeted cell ablation in transgenic mice. Nat. Biotechnol. *19*, 746-750.

Sander,M., Sussel,L., Conners,J., Scheel,D., Kalamaras,J., Dela,C.F., Schwitzgebel,V., Hayes-Jordan,A., and German,M. (2000). Homeobox gene Nkx6.1 lies downstream of Nkx2.2 in the major pathway of beta-cell formation in the pancreas. Development *127*, 5533-5540.

Sarkozy,A., Conti,E., Neri,C., D'Agostino,R., Digilio,M.C., Esposito,G., Toscano,A., Marino,B., Pizzuti,A., and Dallapiccola,B. (2005). Spectrum of atrial septal defects associated with mutations of NKX2.5 and GATA4 transcription factors. J. Med. Genet. *42*, e16.

Saur,D., Vanderwinden,J.M., Seidler,B., Schmid,R.M., De Laet,M.H., and Allescher,H.D. (2004). Single-nucleotide promoter polymorphism alters transcription of neuronal nitric oxide synthase exon 1c in infantile hypertrophic pyloric stenosis. Proc. Natl. Acad. Sci. U. S. A *101*, 1662-1667.

Scherrer,L.C., Picard,D., Massa,E., Harmon,J.M., Simons,S.S., Jr., Yamamoto,K.R., and Pratt,W.B. (1993). Evidence that the hormone binding domain of steroid receptors confers hormonal control on chimeric proteins by determining their hormone-regulated binding to heat-shock protein 90. Biochemistry *32*, 5381-5386.

Schipani,E. (2002). Conditional gene inactivation using cre recombinase. Calcif. Tissue Int. *71*, 100-102.

Schneider,A., Brand,T., Zweigerdt,R., and Arnold,H. (2000). Targeted disruption of the Nkx3.1 gene in mice results in morphogenetic defects of minor salivary glands: parallels to glandular duct morphogenesis in prostate. Mech. Dev. *95*, 163-174.

Schneider,A., Mijalski,T., Schlange,T., Dai,W., Overbeek,P., Arnold,H.H., and Brand,T. (1999). The homeobox gene NKX3.2 is a target of left-right signalling and is expressed on opposite sides in chick and mouse embryos. Curr. Biol. *9*, 911-914.

Schott,J.J., Benson,D.W., Basson,C.T., Pease,W., Silberbach,G.M., Moak,J.P., Maron,B.J., Seidman,C.E., and Seidman,J.G. (1998). Congenital heart disease caused by mutations in the transcription factor NKX2-5. Science *281*, 108-111.

Schubert,F.R., Fainsod,A., Gruenbaum,Y., and Gruss,P. (1995). Expression of the novel murine homeobox gene Sax-1 in the developing nervous system. Mech. Dev. *51*, 99-114.

Schultheiss,T.M., Xydas,S., and Lassar,A.B. (1995). Induction of avian cardiac myogenesis by anterior endoderm. Development *121*, 4203-4214.

Schulze-Delrieu,K. and Shirazi,S.S. (1983). Neuromuscular differentiation of the human pylorus. Gastroenterology *84*, 287-292.

Schwartz,R.J. and Olson,E.N. (1999). Building the heart piece by piece: modularity of cis-elements regulating Nkx2-5 transcription. Development *126*, 4187-4192.

Scott,I.C. and Stainier,D.Y. (2003). Developmental biology: twisting the body into shape. Nature *425*, 461-463.

Searcy,R.D., Vincent,E.B., Liberatore,C.M., and Yutzey,K.E. (1998). A GATA-dependent nkx-2.5 regulatory element activates early cardiac gene expression in transgenic mice. Development *125*, 4461-4470.

Sharpe,J., Ahlgren,U., Perry,P., Hill,B., Ross,A., Hecksher-Sorensen,J., Baldock,R., and Davidson,D. (2002). Optical projection tomography as a tool for 3D microscopy and gene expression studies. Science *296*, 541-545.

Shima,H., Ohshiro,K., and Puri,P. (2000). Increased local synthesis of epidermal growth factors in infantile hypertrophic pyloric stenosis. Pediatr. Res. *47*, 201-207.

Shima,H. and Puri,P. (1999). Increased expression of transforming growth factor-alpha in infantile hypertrophic pyloric stenosis. Pediatr. Surg. Int. *15*, 198-200.

Shiojima,I., Komuro,I., Mizuno,T., Aikawa,R., Akazawa,H., Oka,T., Yamazaki,T., and Yazaki,Y. (1996). Molecular cloning and characterization of human cardiac homeobox gene CSX1. Circ. Res. *79*, 920-929.

Shiratori,H., Sakuma,R., Watanabe,M., Hashiguchi,H., Mochida,K., Sakai,Y., Nishino,J., Saijoh,Y., Whitman,M., and Hamada,H. (2001). Two-step regulation of left-right asymmetric expression of Pitx2: initiation by nodal signaling and maintenance by Nkx2. Mol. Cell *7*, 137-149.

Slack,J.M. (1995). Developmental biology of the pancreas. Development *121*, 1569-1580.

Small,E.M., Vokes,S.A., Garriock,R.J., Li,D., and Krieg,P.A. (2000). Developmental expression of the Xenopus Nkx2-1 and Nkx2-4 genes. Mech. Dev. *96*, 259-262.

Smith,B.R. (2001). Magnetic resonance microscopy in cardiac development. Microsc. Res. Tech. *52*, 323-330.

Smith,D.M., Grasty,R.C., Theodosiou,N.A., Tabin,C.J., and Nascone-Yoder,N.M. (2000a). Evolutionary relationships between the amphibian, avian, and mammalian stomachs. Evol. Dev. *2*, 348-359.

Smith,D.M., Nielsen,C., Tabin,C.J., and Roberts,D.J. (2000b). Roles of BMP signaling and Nkx2.5 in patterning at the chick midgut-foregut boundary. Development *127*, 3671-3681.

Smith,D.M. and Tabin,C.J. (1999). BMP signalling specifies the pyloric sphincter. Nature *402*, 748-749.

Smith,S.T. and Jaynes,J.B. (1996). A conserved region of engrailed, shared among all en-, gsc-, Nk1-, Nk2- and msh-class homeoproteins, mediates active transcriptional repression in vivo. Development *122*, 3141-3150.

Sock,E., Rettig,S.D., Enderich,J., Bosl,M.R., Tamm,E.R., and Wegner,M. (2004). Gene targeting reveals a widespread role for the high-mobility-group transcription factor Sox11 in tissue remodeling. Mol. Cell Biol. *24*, 6635-6644.

Sohal,D.S., Nghiem,M., Crackower,M.A., Witt,S.A., Kimball,T.R., Tymitz,K.M., Penninger,J.M., and Molkentin,J.D. (2001). Temporally regulated and tissue-specific gene manipulations in the adult and embryonic heart using a tamoxifen-inducible Cre protein. Circ. Res. *89*, 20-25.

Soriano,P. (1999). Generalized lacZ expression with the ROSA26 Cre reporter strain. Nat. Genet. *21*, 70-71.

Spann,P., Ginsburg,M., Rangini,Z., Fainsod,A., Eyal-Giladi,H., and Gruenbaum,Y. (1994). The spatial and temporal dynamics of Sax1 (CHox3) homeobox gene expression in the chick's spinal cord. Development *120*, 1817-1828.

Sparrow,D.B., Cai,C., Kotecha,S., Latinkic,B., Cooper,B., Towers,N., Evans,S.M., and Mohun,T.J. (2000). Regulation of the tinman homologues in Xenopus embryos. Dev. Biol. *227*, 65-79.

Srinivas,S., Goldberg,M.R., Watanabe,T., D'Agati,V., al Awqati,Q., and Costantini,F. (1999). Expression of green fluorescent protein in the ureteric bud of transgenic mice: a new tool for the analysis of ureteric bud morphogenesis. Dev. Genet. *24*, 241-251.

Staehling-Hampton,K., Hoffmann,F.M., Baylies,M.K., Rushton,E., and Bate,M. (1994). dpp induces mesodermal gene expression in Drosophila. Nature *372*, 783-786.

Stainier,D.Y. (2005). No organ left behind: tales of gut development and evolution. Science *307*, 1902-1904.

Stanley,E.G., Biben,C., Elefanty,A., Barnett,L., Koentgen,F., Robb,L., and Harvey,R.P. (2002). Efficient Cre-mediated deletion in cardiac progenitor cells conferred by a 3'UTR-ires-Cre allele of the homeobox gene Nkx2-5. Int. J. Dev. Biol. *46*, 431-439.

Stennard,F.A., Costa,M.W., Elliott,D.A., Rankin,S., Haast,S.J., Lai,D., McDonald,L.P., Niederreither,K., Dolle,P., Bruneau,B.G., Zorn,A.M., and Harvey,R.P. (2003). Cardiac T-box factor Tbx20 directly

interacts with Nkx2-5, GATA4, and GATA5 in regulation of gene expression in the developing heart. Dev. Biol. *262*, 206-224.

Suri,A., Calderon,B., Esparza,T.J., Frederick,K., Bittner,P., and Unanue,E.R. (2006). Immunological reversal of autoimmune diabetes without hematopoietic replacement of beta cells. Science *311*, 1778-1780.

Sussel,L., Kalamaras,J., Hartigan-O'Connor,D.J., Meneses,J.J., Pedersen,R.A., Rubenstein,J.L., and German,M.S. (1998). Mice lacking the homeodomain transcription factor Nkx2.2 have diabetes due to arrested differentiation of pancreatic beta cells. Development *125*, 2213-2221.

Tabin,C. (2005). Do we know anything about how left-right asymmetry is first established in the vertebrate embryo? J. Mol. Histol. *36*, 317-323.

Takamoto,N., You,L.R., Moses,K., Chiang,C., Zimmer,W.E., Schwartz,R.J., DeMayo,F.J., Tsai,M.J., and Tsai,S.Y. (2005). COUP-TFII is essential for radial and anteroposterior patterning of the stomach. Development *132*, 2179-2189.

Tanaka,H., Hataba,Y., Saito,S., Fukushima,O., and Miyasaka,M. (1996). Phenotypic characteristics and significance of reticular meshwork surrounding splenic white pulp of mice. J. Electron Microsc. (Tokyo) *45*, 407-416.

Tanaka,M., Chen,Z., Bartunkova,S., Yamasaki,N., and Izumo,S. (1999a). The cardiac homeobox gene Csx/Nkx2.5 lies genetically upstream of multiple genes essential for heart development. Development *126*, 1269-1280.

Tanaka,M., Kasahara,H., Bartunkova,S., Schinke,M., Komuro,I., Inagaki,H., Lee,Y., Lyons,G.E., and Izumo,S. (1998b). Vertebrate homologs of tinman and bagpipe: roles of the homeobox genes in cardiovascular development. Dev. Genet. *22*, 239-249.

Tanaka,M., Kasahara,H., Bartunkova,S., Schinke,M., Komuro,I., Inagaki,H., Lee,Y., Lyons,G.E., and Izumo,S. (1998a). Vertebrate homologs of tinman and bagpipe: roles of the homeobox genes in cardiovascular development. Dev. Genet. *22*, 239-249.

Tanaka,M., Lyons,G.E., and Izumo,S. (1999b). Expression of the Nkx3.1 homobox gene during pre and postnatal development. Mech. Dev. *85*, 179-182.

Tanaka,M., Wechsler,S.B., Lee,I.W., Yamasaki,N., Lawitts,J.A., and Izumo,S. (1999c). Complex modular cis-acting elements regulate expression of the cardiac specifying homeobox gene Csx/Nkx2.5. Development *126*, 1439-1450.

Tanaka,M., Yamasaki,N., and Izumo,S. (2000). Phenotypic characterization of the murine Nkx2.6 homeobox gene by gene targeting. Mol. Cell Biol. *20*, 2874-2879.

Tannour-Louet,M., Porteu,A., Vaulont,S., Kahn,A., and Vasseur-Cognet,M. (2002). A tamoxifen-inducible chimeric Cre recombinase specifically effective in the fetal and adult mouse liver. Hepatology *35*, 1072-1081.

Tarlinton,D., Light,A., Metcalf,D., Harvey,R.P., and Robb,L. (2003). Architectural defects in the spleens of Nkx2-3-deficient mice are intrinsic and associated with defects in both B cell maturation and T cell-dependent immune responses. J. Immunol. *170*, 4002-4010.

Thaung,C., West,K., Clark,B.J., McKie,L., Morgan,J.E., Arnold,K., Nolan,P.M., Peters,J., Hunter,A.J., Brown,S.D., Jackson,I.J., and Cross,S.H. (2002). Novel ENU-induced eye mutations in the mouse: models for human eye disease. Hum. Mol. Genet. *11*, 755-767.

Theodosiou,N.A. and Tabin,C.J. (2003). Wnt signaling during development of the gastrointestinal tract. Dev. Biol. *259*, 258-271.

Theodosiou,N.A. and Tabin,C.J. (2005). Sox9 and Nkx2.5 determine the pyloric sphincter epithelium under the control of BMP signaling. Dev. Biol. *279*, 481-490.

Thiel,G.A. and Downey,H. (1921). The development of the mammalian spleen, with special reference to its hematopoietic activity. Am. J. Anat. *28*, 279-339.

Tissier-Seta,J.P., Mucchielli,M.L., Mark,M., Mattei,M.G., Goridis,C., and Brunet,J.F. (1995). Barx1, a new mouse homeodomain transcription factor expressed in cranio-facial ectomesenchyme and the stomach. Mech. Dev. *51*, 3-15.

Tonissen,K.F., Drysdale,T.A., Lints,T.J., Harvey,R.P., and Krieg,P.A. (1994). XNkx-2.5, a Xenopus gene related to Nkx-2.5 and tinman: evidence for a conserved role in cardiac development. Dev. Biol. *162*, 325-328.

Tribioli,C., Frasch,M., and Lufkin,T. (1997). Bapx1: an evolutionary conserved homologue of the Drosophila bagpipe homeobox gene is expressed in splanchnic mesoderm and the embryonic skeleton. Mech. Dev. *65*, 145-162.

Tribioli,C. and Lufkin,T. (1997). Molecular cloning, chromosomal mapping and developmental expression of BAPX1, a novel human homeobox-containing gene homologous to Drosophila bagpipe. Gene *203*, 225-233.

Tribioli,C. and Lufkin,T. (1999). The murine Bapx1 homeobox gene plays a critical role in embryonic development of the axial skeleton and spleen. Development *126*, 5699-5711.

Tseng,H.T., Shah,R., and Jamrich,M. (2004). Function and regulation of FoxF1 during Xenopus gut development. Development *131*, 3637-3647.

Tucker,A.S., Watson,R.P., Lettice,L.A., Yamada,G., and Hill,R.E. (2004). Bapx1 regulates patterning in the middle ear: altered regulatory role in the transition from the proximal jaw during vertebrate evolution. Development *131*, 1235-1245.

Turnbull,D.H., Bloomfield,T.S., Baldwin,H.S., Foster,F.S., and Joyner,A.L. (1995). Ultrasound backscatter microscope analysis of early mouse embryonic brain development. Proc. Natl. Acad. Sci. U. S. A *92*, 2239-2243.

Valasek,P., Evans,D.J., Maina,F., Grim,M., and Patel,K. (2005). A dual fate of the hindlimb muscle mass: cloacal/perineal musculature develops from leg muscle cells. Development *132*, 447-458.

Vallstedt,A., Muhr,J., Pattyn,A., Pierani,A., Mendelsohn,M., Sander,M., Jessell,T.M., and Ericson,J. (2001). Different levels of repressor activity assign redundant and specific roles to Nkx6 genes in motor neuron and interneuron specification. Neuron *31*, 743-755.

Vanderwinden,J.M., Liu,H., De Laet,M.H., and Vanderhaeghen,J.J. (1996). Study of the interstitial cells of Cajal in infantile hypertrophic pyloric stenosis. Gastroenterology *111*, 279-288.

Vanderwinden,J.M., Mailleux,P., Schiffmann,S.N., Vanderhaeghen,J.J., and De Laet,M.H. (1992). Nitric oxide synthase activity in infantile hypertrophic pyloric stenosis. N. Engl. J. Med. *327*, 511-515.

Wang,C.C., Biben,C., Robb,L., Nassir,F., Barnett,L., Davidson,N.O., Koentgen,F., Tarlinton,D., and Harvey,R.P. (2000a). Homeodomain factor Nkx2-3 controls regional expression of leukocyte homing coreceptor MAdCAM-1 in specialized endothelial cells of the viscera. Dev. Biol. *224*, 152-167.

Wang,J. and Shackleford,G.M. (1996). Murine Wnt10a and Wnt10b: cloning and expression in developing limbs, face and skin of embryos and in adults. Oncogene *13*, 1537-1544.

Wang,W., Lo,P., Frasch,M., and Lufkin,T. (2000b). Hmx: an evolutionary conserved homeobox gene family expressed in the developing nervous system in mice and Drosophila. Mech. Dev. *99*, 123-137.

Wardemann,H., Boehm,T., Dear,N., and Carsetti,R. (2002). B-1a B cells that link the innate and adaptive immune responses are lacking in the absence of the spleen. J. Exp. Med. *195*, 771-780.

Warren,N. and Price,D.J. (1997). Roles of Pax-6 in murine diencephalic development. Development *124*, 1573-1582.

Watanabe,Y., Benson,D.W., Yano,S., Akagi,T., Yoshino,M., and Murray,J.C. (2002). Two novel frameshift mutations in NKX2.5 result in novel features including visceral inversus and sinus venosus type ASD. J. Med. Genet. *39*, 807-811.

Watson,R.P., De Angelis,C., Ahlgren,U., Hecksher-Sorensen,J., Wright,A., Burn,S., and Hill,R.E. (2007). Bapx1 in the Splanchnic Mesoderm Regulates Organ Dimensions and Boundary Formation in the Developing Foregut. Manuscript in preparation.

Wessells,N.K. and Cohen,J.H. (1967). Early pancreas organogenesis: morphogenesis, tissue interactions and mas effects. Dev. Biol. *15*, 237-270.

Wilm,B., Ipenberg,A., Hastie,N.D., Burch,J.B., and Bader,D.M. (2005). The serosal mesothelium is a major source of smooth muscle cells of the gut vasculature. Development *132*, 5317-5328.

Xiang,X., Qiu,D., Hegele,R.D., and Tan,W.C. (2001). Comparison of different methods of total RNA extraction for viral detection in sputum. J. Virol. Methods *94*, 129-135.

Xu,X., Yin,Z., Hudson,J.B., Ferguson,E.L., and Frasch,M. (1998c). Smad proteins act in combination with synergistic and antagonistic regulators to target Dpp responses to the Drosophila mesoderm. Genes Dev. *12*, 2354-2370.

Xu,X., Yin,Z., Hudson,J.B., Ferguson,E.L., and Frasch,M. (1998a). Smad proteins act in combination with synergistic and antagonistic regulators to target Dpp responses to the Drosophila mesoderm. Genes Dev. *12*, 2354-2370.

Xu,X., Yin,Z., Hudson,J.B., Ferguson,E.L., and Frasch,M. (1998b). Smad proteins act in combination with synergistic and antagonistic regulators to target Dpp responses to the Drosophila mesoderm. Genes Dev. *12*, 2354-2370.

Yajima,I., Belloir,E., Bourgeois,Y., Kumasaka,M., Delmas,V., and Larue,L. (2006). Spatiotemporal gene control by the Cre-ERT2 system in melanocytes. Genesis. *44*, 34-43.

Yamamoto,Y., Oguro,N., Nara,T., Horita,H., Niitsu,N., and Imaizumi,S. (1988). Duplication of part of 9q due to maternal 12;9 inverted insertion associated with pyloric stenosis. Am. J. Med. Genet. *31*, 379-384.

Yasugi,S. (1993). Role of Epithelial-Mesenchymal Interactions in Differentiation of Epithelium of Vertebrate Digestive Organs. Develop. Growth&Differ. *35*, 1-9.

Yin,Z., Xu,X.L., and Frasch,M. (1997). Regulation of the twist target gene tinman by modular cis-regulatory elements during early mesoderm development. Development *124*, 4971-4982.

Yokoyama,T., Copeland,N.G., Jenkins,N.A., Montgomery,C.A., Elder,F.F., and Overbeek,P.A. (1993). Reversal of left-right asymmetry: a situs inversus mutation. Science *260*, 679-682.

Yoshioka,H., Meno,C., Koshiba,K., Sugihara,M., Itoh,H., Ishimaru,Y., Inoue,T., Ohuchi,H., Semina,E.V., Murray,J.C., Hamada,H., and Noji,S. (1998). Pitx2, a bicoid-type homeobox gene, is involved in a lefty-signaling pathway in determination of left-right asymmetry. Cell *94*, 299-305.

Young,H.M., Bergner,A.J., Anderson,R.B., Enomoto,H., Milbrandt,J., Newgreen,D.F., and Whitington,P.M. (2004). Dynamics of neural crest-derived cell migration in the embryonic mouse gut. Dev. Biol. *270*, 455-473.

Young,H.M., Ciampoli,D., Southwell,B.R., and Newgreen,D.F. (1996). Origin of interstitial cells of Cajal in the mouse intestine. Dev. Biol. *180*, 97-107.

Zaffran,S., Kuchler,A., Lee,H.H., and Frasch,M. (2001). biniou (FoxF), a central component in a regulatory network controlling visceral mesoderm development and midgut morphogenesis in Drosophila. Genes Dev. *15*, 2900-2915.

Zaffran,S., Reim,I., Qian,L., Lo,P.C., Bodmer,R., and Frasch,M. (2006). Cardioblast-intrinsic Tinman activity controls proper diversification and differentiation of myocardial cells in Drosophila. Development *133*, 4073-4083.

Zakany,J. and Duboule,D. (1999). Hox genes and the making of sphincters. Nature *401*, 761-762.

Zakin,L.D., Mazan,S., Maury,M., Martin,N., Guenet,J.L., and Brulet,P. (1998). Structure and expression of Wnt13, a novel mouse Wnt2 related gene. Mech. Dev. *73*, 107-116.

Zeng,L., Kempf,H., Murtaugh,L.C., Sato,M.E., and Lassar,A.B. (2002). Shh establishes an Nkx3.2/Sox9 autoregulatory loop that is maintained by BMP signals to induce somitic chondrogenesis. Genes Dev. *16*, 1990-2005.

Zhang,H., Fujitani,Y., Wright,C.V., and Gannon,M. (2005). Efficient recombination in pancreatic islets by a tamoxifen-inducible Cre-recombinase. Genesis. *42*, 210-217.

Zhang,X., Stappenbeck,T.S., White,A.C., Lavine,K.J., Gordon,J.I., and Ornitz,D.M. (2006). Reciprocal epithelial-mesenchymal FGF signaling is required for cecal development. Development *133*, 173-180.

Zhu,W., Shiojima,I., Hiroi,Y., Zou,Y., Akazawa,H., Mizukami,M., Toko,H., Yazaki,Y., Nagai,R., and Komuro,I. (2000). Functional analyses of three Csx/Nkx-2.5 mutations that cause human congenital heart disease. J. Biol. Chem. *275*, 35291-35296.